

The electron transport chains of *Neisseria meningitidis*

A thesis submitted for the degree of
Doctor of Philosophy

Manu Deudom

Supervisor : Dr. James W. B. Moir
Department of Biology, University of York
York, United Kingdom
December 2007

Abstract

Neisseria meningitidis contains *c*-type and *b*-type cytochromes. Oxidation of *c*-type and *b*-type cytochromes by oxygen was observed in both cells grown under aerobic and denitrifying conditions, whereas oxidation of cytochromes by nitrite was only seen in cells grown under denitrifying conditions, and the predominant oxidizable cytochromes were *b*-type. These are likely to be associated with the oxidation of a *b*-haem containing nitric oxide reductase. Nitrite inhibits the oxidation of cytochromes by oxygen in a nitrite reductase-independent manner, indicating that nitrite may inhibit oxidase activity directly, as well as via the intermediate of denitrification, nitric oxide.

Cytochromes *c4* and *c2* are major electron donors to the *cbb₃* oxidase. Both strains deficient in cytochrome *c4* and *c2* exhibits a growth defect under high level of oxygen. These growth defects are linked to their decreased oxygen consumption rate. The growth defect and the decreased oxygen consumption rate indicated that cytochrome *c4* dominates electron transfer to *cbb₃* oxidase.

Cytochrome *c5* is an important electron donor to AniA nitrite reductase. A strain deficient in cytochrome *c5* exhibits a growth defect under microaerobic conditions in the presence of nitrite. The mutant can not reduce nitrite to nitric oxide although AniA is expressed normally. A growth defect during high cell density culture under aerobic conditions suggests that cytochrome *c5* is also an electron donor to *cbb₃* oxidase but to a lesser extents than *c4* or *c2*.

Lipid-modified azurin (Laz) was heterologously expressed and purified. The purified protein contains copper ion and can be oxidized or reduced. When oxidized, Laz exhibits an intense blue colour and absorbs visible light around 626 nm. Laz can be oxidized by membrane extract in the presence of oxygen or nitrite. This is likely to be due to the activity of *cbb₃* oxidase and AniA nitrite reductase, respectively, in membrane extract. However the oxidation rate is very slow. A strain deficient in *laz* exhibits a growth defect during high cell density culture, similarly to that of *c5* mutant. This suggests that Laz might be an electron donor to *cbb₃* oxidase.

Acknowledgements

It has been a wonderful time for me working in the Moir lab through these four years. I have learned many things and gained many valuable experiences. I would like to express my gratitude to every member of my lab. Most of all, I would like to thank my supervisor Dr. James Moir for all his support and guidance throughout my study. My thanks go to Matt, Willa, Jon, Mel, Kristin, Linz, Zhenlian, Karin, Stace for helping, sharing, and discussing all laboratory stuffs. I am lucky to know Di, my Yorkshire lady who is kind, warm, and caring. She always laughed at my silly stories and things. This makes me love Yorkshire more and more. Her banana loaf is the best. I would like to thank Raj, Konrad, and Khedidja for being such good friends, sharing conversations and laugh.

My thanks go to CRN, Royal Thai Government for providing funding and the Department of Biology for offering me a place to study. I am grateful to be here and to study what I like.

My thanks go to Sim, Mee, Bow, Lek, Apichat, Kay, Tao, Shine, Num, Rin, Kriang and Joop for sharing both good time and emotional support with me in York.

I would like to thank John for being a good friend and making my last two years in York happy and memorable.

Finally, the biggest thank you all Mum and Dad for your love. Thank you for believing in me and supporting me in everyway for my every decision.

Contents

Chapter 1 Introduction	1
1.1. Biology of <i>Neisseria meningitidis</i>	1
1.2. Genome of <i>N. meningitidis</i>	4
1.3. Pathogenicity of <i>N. meningitidis</i>	5
1.4. Growth and respiration	8
1.5. The electron transport chain	13
1.5.1. Reduction of ubiquinone	14
1.5.1.1. NADH dehydrogenase	14
1.5.1.2. Succinate dehydrogenase	17
1.5.1.3. Lactate dehydrogenase	19
1.5.1.4. Malate: quinone oxidoreductase	20
1.5.2. Oxidation of ubiquinol	21
1.5.2.1. Cytochrome <i>bc₁</i> complex	21
1.5.3. Oxidation of cytochrome <i>bc₁</i> complex	23
1.5.3.1. Soluble <i>c</i> -type cytochromes	23
1.5.3.2. Lipid-modified azurin	26
1.5.4. Terminal redox proteins	27
1.5.4.1. Cytochrome <i>cbb₃</i> oxidase	27
1.5.4.2. AniA nitrite reductase	34
1.5.4.3. Nitric oxide reductase	36
1.6. Regulation of aerobic respiration and denitrification	38
1.6.1. FNR	38
1.6.2. NarQ/P	41
1.6.3. NsrR	42
1.7. Aims and objectives of this work	43

Chapter 2 Materials and Methods	44
2.1. Bacterial strains and plasmids used in this work	44
2.1.1. Bacterial strains used in this work	44
2.1.2. Plasmids used in this work	45
2.2. Growth of cells	46
2.2.1. Growth of <i>N. meningitidis</i>	46
2.2.2. Growth of <i>Escherichia coli</i>	46
2.2.3. Preparation of bacterial frozen stocks	47
2.2.4. Preparation of antibiotic selective media	47
2.3. Fractionation of cells	48
2.3.1. Preparation of whole cell lysate	48
2.3.2. Preparation of periplasm, membranes, and cytoplasm	49
2.3.3. Preparation of outer membrane blebs	49
2.4. Genetic techniques	50
2.4.1. Preparation of plasmid DNA	50
2.4.2. Preparation of chromosomal DNA	50
2.4.3. The polymerase chain reaction	51
2.4.4. Preparation of competent cells of <i>E. coli</i> DH5 α	52
2.4.5. TOPO cloning	52
2.4.6. Transformation of <i>E. coli</i> DH5 α	53
2.4.7. Transformation of <i>E. coli</i> BL21 λ DE3	53
2.4.8. Transformation of <i>N. meningitidis</i> MC58	54
2.4.9. Restriction digestion	54
2.4.10. Purification of DNA fragments and PCR products	54
2.4.11. Ligation of DNA fragments	55
2.4.12. pET-22b (+) cloning	55
2.4.13. Agarose gel electrophoresis	55
2.5. Protein purification procedures	56
2.5.1. Extraction of periplasmic proteins from <i>E. coli</i> BL21 λ DE3	56
2.5.2. Anion exchange column chromatography	57
2.5.3. Concentration, desalting and buffer exchange of protein samples	58
2.6. Protein determination	58

2.7. Analysis of protein samples	58
2.7.1. SDS-PAGE	58
2.7.2. Coomassie stain	59
2.7.3. Haem stain	60
2.7.3.1. Colorimetric method	60
2.7.3.2. Chemiluminescent method	60
2.7.4. Spectra of protein samples	61
2.7.5. Raising antibodies to <i>Laz</i>	61
2.7.6. Western Blot	61
2.7.7. Dot Blot	63
2.7.8. Electrospray mass spectrophotometry	63
2.7.9. Protein fingerprinting	64
2.8. <i>In vivo</i> assays with <i>N. meningitidis</i>	64
2.8.1. Measurement of oxygen uptake	64
2.8.2. Measurement of nitric oxide	65
2.8.3. Assay for nitrite	65
2.8.4. Spectra measurement of intact cells	66
Chapter 3 Cytochromes of <i>Neisseria meningitidis</i>	67
3.1. Introduction	67
3.1.1. Types of cytochromes in <i>N. meningitidis</i>	68
3.1.2. Spectral feature of cytochromes	69
3.2. Results	71
3.2.1. Visualization of cytochromes in by western blot and ECL chemiluminescence	71
3.2.2. Spectroscopic analysis of cytochromes in intact cells	72
3.2.2.1. Oxidation by oxygen	73
3.2.2.2. Oxidation by nitrite	79
3.2.2.3. Oxidation by nitrite and oxygen	84
3.2.2.4. Oxidation of cytochrome by nitric oxide	88
3.2.2.5. Nitrite inhibits cytochrome oxidation by oxygen in <i>aniA</i> mutant	91
3.3. Discussion	95

Chapter 4 Mutagenesis of <i>c</i>-type cytochromes and lipid-modified azurin	98
4.1. Introduction	98
4.2. Construction of cytochrome <i>c2</i> mutant	99
4.3. Construction of cytochrome <i>c4</i> mutant	105
4.4. Construction of cytochrome <i>c5</i> mutant	110
4.5. Construction of cytochrome <i>c2/c4</i> double mutant	116
4.6. Construction of <i>laz</i> mutant	116
4.7. Construction of <i>nsrR/laz</i> double mutant	124
Chapter 5 Cytochromes <i>c2</i> and <i>c4</i> are major electron donors to <i>cbb₃</i> oxidase	126
5.1. Introduction	126
5.1.1. Structure of cytochrome <i>c2</i>	127
5.1.2. Structure of cytochrome <i>c4</i>	130
5.2. Results	133
5.2.1. Visualization of cytochromes by western blot and ECL chemiluminescence	133
5.2.2. Growth under aerobic conditions	134
5.2.3. Growth under microaerobic conditions	136
5.2.4. Growth under microaerobic conditions with nitrite	136
5.2.5. Oxygen reduction rate in cytochrome <i>c2</i> , <i>c4</i> , and <i>c2/c4</i> mutants	138
5.2.6. Nitrite reduction of cytochrome <i>c2</i> , <i>c4</i> , and <i>c2/c4</i> mutant	140
5.2.7. Production of nitric oxide by <i>c2/c4</i> mutant	141
5.2.7.1. Cell preparations for nitric oxide accumulation assay	142
5.2.7.2. Nitric oxide accumulation assay	142
5.2.8. Nitrite inhibits aerobic growth of <i>N. meningitidis</i>	145
5.2.9. Nitrite reduction does not occur under aerobic conditions	146
5.2.10. Spectra of <i>c2</i> , <i>c4</i> , and <i>c2/c4</i> mutants	146
5.3. Discussion	150

Chapter 6 Cytochrome <i>c5</i> is an electron donor to AniA nitrite reductase	155
6.1. Introduction	155
6.1.1. Structure of cytochrome <i>c5</i>	155
6.2. Results	159
6.2.1. Visualization of cytochrome <i>c5</i> by western blot and ECL chemiluminescence	159
6.2.2. Growth under aerobic conditions	159
6.2.3. Growth under microaerobic conditions	160
6.2.4. Growth under microaerobic conditions with nitrite	161
6.2.5. Nitrite reduction	162
6.2.6. Production of nitric oxide by <i>c5</i> mutant	163
6.2.7. Nitric oxide accumulation assay	163
6.2.8. Expression of AniA nitrite reductase in <i>c5</i> mutant	165
6.2.9. Spectra of <i>c5</i> mutant	166
6.2.9.1. Cell oxidation by oxygen	166
6.2.9.2. Cell oxidation by nitrite	170
6.2.9.3. H ₂ O ₂ can oxidize <i>c</i> -type cytochromes directly, not via AniA	173
6.3. Discussion	176
Chapter 7 Characterization of lipid-modified azurin	179
7.1. Introduction	179
7.2. Results	185
7.2.1. Overexpression and characterization of Laz	185
7.2.2. Interaction of Laz with meningococcal membrane extract	192
7.2.3. Expression of Laz under different growth conditions	194
7.2.4. Laz expression in <i>c</i> -type cytochrome mutants	196
7.2.5. Growth of <i>laz</i> mutant under aerobic conditions	196
7.2.6. Growth of <i>laz</i> mutant under microaerobic conditions	197
7.2.7. Growth of <i>laz</i> mutant under microaerobic conditions with nitrite	198
7.2.8. Nitrite reduction	199
7.2.9. Expression of AniA nitrite reductase in <i>laz</i> mutant	200

7.2.10. Production of nitric oxide by <i>laz</i> mutant	201
7.2.10.1. Nitric oxide accumulation assay	201
7.2.11. Spectra of <i>laz</i> mutant	203
7.2.11.1. Cell oxidation by oxygen	203
7.2.11.2. Cell oxidation by H ₂ O ₂	206
7.2.12. Cellular localization of Laz	210
7.2.13. Discussion	213
Chapter 8 General Discussion and Conclusions	218
References	223

Tables and Illustrations

Chapter 1 General Introduction

- Table 1.1 List of genes involved in the electron transports in *Meningitidis*.
- Figure 1.1 Environmental denitrification.
- Figure 1.2 Proposed electron transport chains in *N. meningitidis*.
- Table 1.2 Characteristics of NADH dehydrogenases in bacteria.
- Figure 1.3 Cartoon of mitochondrial complex I structure and functions.
- Figure 1.4 Structure of hydrophilic domain of NDH from *Thermus thermophilus*.
- Figure 1.5 Structure of SQR and FQR in *E. coli*.
- Figure 1.6 Scheme showing electron transfer pathway in SQR and QFR of *E. coli*.
- Table 1.3 Subunit composition of the *bc₁* complex from *Rhodobacter sphaeroides*.
- Figure 1.7 The structure of the *bc₁* complex and the oxidation of ubiquinol in Q-cycle.
- Figure 1.8 Haem types according to structure and mode of binding of the haem prosthetic group.
- Figure 1.9 Structure of cytochrome *c₅₅₂* from *Paracoccus denitrificans*.
- Table 1.4 Reduction potentials of haems in the cytochrome *cbb₃* oxidase from *P. stutzeri*.
- Figure 1.10 Proposed organization of the *fixNOQP* operon in *N. meningitidis*.
- Figure 1.11 Comparison of primary structure of meningococcus FixP and gonococcus CcoP.
- Figure 1.12 Pairwise alignment of cytochrome *c5* protein sequence of NMB1677 and protein sequence of NMB1722.
- Figure 1.13 Structure of soluble AniA nitrite reductase from *N. gonorrhoeae*.
- Figure 1.14 Type I and type II copper sites in AniA.

Chapter 2 Materials and Methods

- Table 2.1 Antibiotic concentration used in this work.
- Table 2.2 Standard PCR protocols used in this work.
- Table 2.3 The PCR reaction cycles used in this work.
- Table 2.4 Protocol for preparation of SDS-PAGE gel.

Chapter 3 Cytochromes of *Neisseria meningitidis*

- Table 3.1 List of genes encoding for cytochromes in *N. meningitidis*.
- Table 3.2 Difference spectra from reduced minus oxidized spectra.
- Figure 3.1 Cytochrome profiles of *fnr* mutant and wild type meningococcus under different growth conditions.
- Figure 3.2 The spectral features of cytochromes in *N. meningitidis* cells grown under aerobic conditions.
- Figure 3.3 The spectral features of cytochromes in *N. meningitidis* cells grown under denitrifying conditions.
- Figure 3.4 Comparison of difference spectra between reduced and oxygen oxidized spectra from cells grown under aerobic conditions (blue) and denitrifying conditions (pink).
- Figure 3.5A Double derivatives of oxidized minus reduced spectra from cells grown under aerobic conditions and denitrifying conditions.
- Figure 3.5B The α features of cells grown under aerobic and denitrifying conditions.
- Figure 3.6 Nitrite can not oxidize cytochromes in cells grown under aerobic conditions.
- Figure 3.7 Reduced minus nitrite-oxidized difference spectra of cells grown under aerobic conditions.
- Figure 3.8 The spectral features of cytochromes in intact cells of *N. meningitidis* grown under denitrifying conditions oxidized by nitrite.
- Figure 3.9 Oxidation of *b*-type cytochrome in cells grown under denitrifying conditions by nitrite.
- Figure 3.10 Nitrite inhibits oxidation of cells grown under denitrifying conditions by oxygen.
- Figure 3.11 Comparison of cytochrome oxidation by different oxidants.
- Figure 3.12 Double derivative difference spectra showing cytochrome oxidation by different oxidants.
- Figure 3.13 Oxidation of cytochromes in cells grown under denitrifying conditions by nitric oxide.
- Figure 3.14 Comparison of difference spectra of cells oxidized by nitrite and by nitric oxide.
- Figure 3.15 Nitrite inhibits cytochrome oxidation by oxygen in *aniA* mutant cells.

- Figure 3.16 Reduced minus oxidized spectra of *aniA* mutant cells grown under aerobic conditions.
- Figure 3.17 Double derivative of oxidized minus reduced spectra of *aniA* mutant cells.

Chapter 4 Mutagenesis of *c*-type cytochromes and lipid-modified azurin

- Figure 4.1 The cytochrome *c2* gene with flanking region used for constructing mutant.
- Figure 4.2 Pfu PCR product of cytochrome *c2* gene with flanking region.
- Figure 4.3 Colony PCR screen for pCR-Blunt II TOPO plasmid with insertion of cytochrome *c2* gene.
- Figure 4.4 *EcoRI* digested products of pCR-Blunt II TOPO plasmid with insertion of cytochrome *c2* gene.
- Figure 4.5A *BsgI* digested products of pCR-Blunt II TOPO + *c2* plasmid.
- Figure 4.5B Spectinomycin resistance gene cassette or Ω cassette.
- Figure 4.6 Colony PCR screen of *E. coli* DH5 α transformants for *c2* gene with Ω cassette insert.
- Figure 4.7 *EcoRI* digest screen for *c2* gene with Ω cassette insert in constructed plasmid from *E. coli* DH5 α transformants.
- Figure 4.8. Colony PCR screen for *c2* gene with Ω cassette insert in *N. meningitidis* MC58 transformants.
- Figure 4.9 The cytochrome *c4* gene with flanking region used for constructing mutant.
- Figure 4.10 Colony PCR screen for pCR-Blunt II TOPO plasmid with insertion of cytochrome *c4* gene.
- Figure 4.11 *EcoRI* digested screen for pCR-Blunt II TOPO plasmid with cytochrome *c4* gene insert.
- Figure 4.12 *Bsu36I* digested products of pCR-Blunt II TOPO + *c4* plasmid.
- Figure 4.13 Pfu PCR products of *ery^r* cassette exhibits size of 1.2 kb.
- Figure 4.14 Colony PCR screen of *c4* gene with *ery^r* insert in *E. coli* DH5 α transformants.
- Figure 4.15 *EcoRI* digest screen of *c4* gene with *ery^r* insert for recombinant plasmids

in *E. coli* DH5 α transformants.

- Figure 4.16 Colony PCR screen of disrupted *c4* gene in MC58 transformants.
- Figure 4.17 The cytochrome *c5* gene with flanking region used for constructing mutant.
- Figure 4.18 Colony PCR screen of pCR-Blunt II TOPO plasmid with insertion of cytochrome *c5* gene from *E. coli* DH5 α transformants.
- Figure 4.19 *Eco*RI digested products of pCR-Blunt II TOPO plasmid with insertion of cytochrome *c5* gene.
- Figure 4.20 Pfu PCR product of *tet*^r cassette exhibits size of 2.7 kb.
- Figure 4.21 Colony PCR screen of *c5* gene with *tet*^r insert in *E. coli* DH5 α transformants.
- Figure 4.22 *Eco*RI digest screen of *c5* gene with *tet*^r insert.
- Figure 4.23 Colony PCR screen of disrupted *c5* gene in MC58 transformants.
- Figure 4.24 Colony PCR screen for double disrupted *c2* and *c4* gene in MC58 transformants.
- Figure 4.25 The cytochrome *c5* gene with flanking region used for constructing mutant.
- Figure 4.26 Pfu PCR product of *laz* gene with flanking region exhibit size of 1.7 kb.
- Figure 4.27 Colony PCR screen for *laz* gene insert in pCR-Blunt II TOPO plasmid.
- Figure 4.28 *Eco*RI digested products of pCR-Blunt II TOPO plasmid with insertion of *laz* gene.
- Figure 4.29 PFU PCR products of *chl*^r gene from pST2 plasmid.
- Figure 4.30 Expanded PFU PCR of pCR-Blunt II TOPO + *laz* plasmid.
- Figure 4.31 Pfu expanded PCR products of pCR-Blunt II TOPO + *laz* plasmid.
- Figure 4.32 Colony PCR screen of *laz* gene with *chl*^r cassette insert.
- Figure 4.33 *Eco*RI digest screen of *laz* gene with *chl*^r insert.
- Figure 4.34 Colony PCR screen of disrupted and partially deleted *laz* gene in MC58 transformants.
- Figure 4.35 Colony PCR screen for combined disrupted *nsrR* gene and *laz* gene in MC58 transformants.

Chapter 5 Cytochromes *c2* and *c4* are major electron donors to *cbb₃* oxidase

- Figure 5.1 Primary sequence of cytochrome *c2* from *N. meningitidis* strain MC58.
- Figure 5.2 Multiple alignment of cytochrome *c2* homologs.
- Figure 5.3 Methionine in the N-terminal region is predicted to be the sixth ligand for haem in cytochrome *c2* (NMB0717) of the meningococcus.
- Figure 5.4 Primary sequence of cytochrome *c4*.
- Figure 5.5 Cytochrome *c4* is extremely conserved among *N. meningitidis* serogroup A, B and C and *N. gonorrhoeae*.
- Figure 5.6 Cytochrome profiles of respiratory mutants.
- Figure 5.7 Growth of *c*-type cytochrome mutants under aerobic conditions.
- Figure 5.8 Microaerobic growth of *c2* and *c4* mutant.
- Figure 5.9 Growth of *c2*, *c4*, and *c2/c4* mutants under denitrifying conditions.
- Figure 5.10 Oxygen reduction rate of *c4* mutant, *c2* mutant, and WT.
- Figure 5.11 Oxygen reduction rate of *c2/c4* double mutant.
- Figure 5.12 The *c2* mutant, *c4* mutant, and *c2/c4* double mutant can reduce nitrite during microaerobic growth.
- Figure 5.13 NO accumulation between cell grown under denitrifying conditions and cells grown under microaerobic conditions.
- Figure 5.14 NO production in WT (A) and *c2/c4* double mutant.
- Figure 5.15 Nitrite inhibits aerobic growth of WT and *c2/c4* double mutant.
- Figure 5.16 WT strain and *c2/c4* mutant did not utilize nitrite under aerobic conditions.
- Figure 5.17A Double derivatives of oxidized minus reduced difference spectra of mutants.
- Figure 5.17B Mutant strains exhibited different absorption at α band.
- Figure 5.18A Lost peaks of respiratory mutants. Light absorption at Soret and α peak can distinguish different *c*-type cytochrome.
- Figure 5.18B Lost peak at α band of cytochrome mutant represents actual absorption of that cytochrome.
- Figure 5.19 In *N. meningitidis*, electron flow from *bc₁* complex to *cbb₃* oxidase depends on periplasmic *c*-type cytochromes.

Chapter 6 Cytochrome *c5* is an electron donor to AniA nitrite reductase

- Figure 6.1 Primary structure of cytochrome *c5*.
- Figure 6.2 Primary structure comparison of cytochrome *c5* of serogroup B and its homologs in serogroup C, serogroup A, and *N. gonorrhoeae*.
- Figure 6.3 Methionine as the sixth haem ligand of cytochrome *c5*.
- Figure 6.4 Domain repeats in cytochrome *c5* structure.
- Figure 6.5 Growth of *c5* mutant under aerobic conditions.
- Figure 6.6 Growth of *c5* mutant under microaerobic conditions without nitrite.
- Figure 6.7 Growth of *c5* mutant under microaerobic conditions with 5 mM nitrite.
- Figure 6.8 The *c5* mutant showed decreased ability to utilize nitrite under microaerobic growth conditions.
- Figure 6.9 The *c5* mutant can not generate and accumulate NO.
- Figure 6.10 AniA expressions in respiratory mutants.
- Figure 6.11A Double derivatives of oxidized minus reduced difference spectra of mutants.
- Figure 6.11B Mutant strains exhibited different absorption at α band.
- Figure 6.12A Lost absorptions of respiratory mutants.
- Figure 6.12B Lost peak at α band of cytochrome mutant represents actual absorption of that cytochrome.
- Figure 6.13A Nitrite can not oxidize cytochromes in *c5* mutant.
- Figure 6.13B Difference spectra of wild type oxidized by nitrite gives α peak at 560 nm indicating oxidation of *b*-haem or *b*-type cytochrome.
- Figure 6.14A Oxidation of *c5* mutant cells by hydrogen peroxide.
- Figure 6.14B Difference spectra of wild type cells oxidized by hydrogen peroxide.

Chapter 7 Characterization of lipid-modified azurin

- Figure 7.1 Predicted secondary structure of Laz protein with three domains.
- Figure 7.2 Homologs of Laz in other organisms.
- Figure 7.3 Predicted tertiary structure of Laz.
- Figure 7.4 Paralogs of Laz linker region.
- Figure 7.5 Alignment of Laz linker region and Lip.
- Figure 7.6 Predicted cellular localization of Laz.

- Figure 7.7 Partial FNR box upstream of *laz* gene compared to FNR box in *P. denitrificans*.
- Figure 7.8 Expression of meningococcal Laz protein in *E. coli*.
- Figure 7.9 Purified Laz from DEAE-sepharose anion exchange chromatography.
- Figure 7.10 Molecular mass of Laz detected by electrospray mass spectroscopy.
- Figure 7.11 Spectral feature of oxidized Laz by UV-VIS spectroscopy and effect of copper chelating agent diethyldithiocarbamate (DDC).
- Figure 7.12 Difference spectra of the meningococcal membrane extract.
- Figure 7.13 Interaction of Laz with meningococcal membrane extract.
- Figure 7.14 The expression of Laz under different growth conditions.
- Figure 7.15 Laz expression in respiratory mutants.
- Figure 7.16 Growth of *laz* mutant under microaerobic conditions.
- Figure 7.17 Growth of *laz* mutant under microaerobic conditions with nitrite.
- Figure 7.18 Nitrite reduction of *laz* mutant.
- Figure 7.19 AniA expression in *laz* mutant.
- Figure 7.20 NO generation in *laz* mutant.
- Figure 7.21A Spectra of *laz* mutant.
- Figure 7.21B The α peak of *laz* mutant.
- Figure 7.22A Lost absorptions of respiratory mutants.
- Figure 7.22B Lost peak at α band of *laz* mutant represents actual absorption of cytochromes.
- Figure 7.23A Difference spectra of *laz* mutant cells oxidized by hydrogen peroxide.
- Figure 7.23B The α features of difference spectra of *laz* mutant cells oxidized by hydrogen peroxide.
- Figure 7.24 Localization of Laz in the outer membrane.
- Figure 7.25 Outer membrane bleb proteins of *N. meningitidis*.

Chapter 8 Discussion and Conclusions

- Figure 8.1 New proposed electron transport chains in *N. meningitidis*.

Abbreviations

ADH	alcohol dehydrogenase
APS	ammonium persulphate
BSA	bovine serum albumin
CSF	cerebrospinal fluid
DUS	DNA uptake signal sequence
DDC	diethyldithiocarbamate
EDTA	ethylenediaminetetraacetic acid
FNR	fumarate nitrate reduction regulator
FRD	fumarate reductase
HCO	haem-copper oxidases
IHT	islands of horizontal DNA transfer
IPTG	isopropyl β -D-1-thiogalactopyranoside
LB	Lysogeny broth
LDH	lactate dehydrogenase
MHB	Mueller-Hinton broth
MQO	malate: quinone oxidaoreductase
NDH	NADH dehydrogenase
OMV	outer membrane vesicle
PBS	Phosphate buffer saline
QFR	quinol: fumarate reductase
SDH	succinate dehydrogenase
SDS PAGE	sodium dodecyl sulphate polyacrylamide gel electrophoresis
SQR	succinate: quinone oxidoreductase
SQ	semiquinone
TBE	Tris-borate-EDTA buffer

Chapter 1

General Introduction

1.1 Biology of *Neisseria meningitidis*

N. meningitidis is a Gram-negative coccus bacterium in the family *Neisseriaceae*. It is a non-spore forming and non-motile bacterium. While many organisms in this family are part of normal flora of mammals including human, two species of the genus *Neisseria* can cause human diseases. *N. meningitidis*, the meningococcus, is one of the most common causes of bacterial meningitis and the causative agent of meningococcal septicaemia. *Neisseria gonorrhoea* is the causative agent of the sexually transmitted disease gonorrhoea. *Neisseria* are in a group of β -proteobacteria which also includes the human pathogens *Burkholderia* and *Bordetella*, the nitrifying bacteria *Nitrosomonas*, purple phototrophic bacteria *Rhodocyclus*, sulfur-oxidizing bacteria *Thiobacillus*, and hydrogen-oxidizing bacteria *Ralstonia* (Madigan and Martinko, 2006). The natural habitat of *N. meningitidis* is only in the human nasopharynx and oropharynx. The majority of *Neisseria* species that colonize the nasopharynx are non-pathogenic, including *N. lactamica*, *N. mucosa*, *N. sicca*, *N. flavescens*, and *N. subflava*. *Neisseria* have evolved a symbiotic lifestyle with human host and established itself as flora of the upper respiratory system. Approximately 5% to 10% of human population harbours *N. meningitidis* as a part of the normal flora of the nasopharynx. These carriers do not exhibit clinical symptoms, which maybe due to the successful competition for resources between all resident commensal organisms. The competition may limit the growth of pathogenic strains. Secretory IgA in the respiratory tract also plays a crucial role for controlling the growth of pathogenic bacteria. However, occasionally infection of *N. meningitidis* can lead to invasive disease. The

organism can enter the bloodstream, cross the blood-brain barrier, and invade the meninges leading to meningitis or septicaemia. However, CSF absorption from nasal lymphatic vessels is a characteristic feature of all mammals including human (Johnston *et al*, 2004). The infection and inflammation of nasopharynx might cause tissue damage and provide opportunity for the organism to gain entry into CSF via these lymphatic vessels. Other bacterial meningitis, including those by *Streptococcus* and *Haemophilus*, might also gain entry into CSF by this route. The host factors that induce susceptibility and trigger the invasive meningococcal disease are not defined yet. The prevalence of meningitis is low but the percent of people that die when they contract clinical disease is high. Life-threatening meningitis remains a significant problem in many countries, especially in Africa, Europe and North America.

Community-acquired meningitis often occurs among small children and young adults where close and prolonged contact is required for transmission. The group of highest risk is children between the ages of 6 months and 6 years. The incidence of disease drops with increasing age due to the development of acquired immunity in the nasopharyngeal mucosa (Frasch, 2001). Although the group of highest risk is children as the acquired immunity is not fully developed yet, university students are also at greater risk of meningococcal disease than other people at the same age. In the United Kingdom, it has been found that the carriage rate of meningococci among university first year undergraduate students increased rapidly in the first week of term. The rate was further increased during the term probably due to social mixing (Neal *et al*, 2000). The university undergraduate students have higher rate of invasive meningococcal disease than adults of the same age who are not attending university (Neal *et al*, 1999), supporting the notion that the outbreak of meningococcal diseases can be community-acquired. Alcohol consumption may affect the interaction between the bacteria and

human host due to the change of bacterial profiles in nasopharynx, body homeostasis and immune integrity. Alcohol might be one of many factors that influence host susceptibility to meningococcal infection. Studies in the United States suggested that alcohol consumption and additional factors common to campus bar environments enhances transmission of *N. meningitidis* (Imrey *et al*, 1995; Imrey *et al*, 1996). Studies of short-term effect of ethanol on bacterial composition of human oral microflora revealed that ethanol ingestion increased counts of *Neisseria* (Muto *et al*, 2000). *Neisseria* are capable of producing acetaldehyde from ethanol in the oral cavity as they have high alcohol dehydrogenase (ADH) activity and can tolerate high ethanol concentrations (Muto *et al*, 2000). When incubated in medium containing ethanol, *Neisseria* produced more than 100 times greater level of acetaldehyde than did other organisms isolated from mouth. It is likely that alcohol consumption can suppresses the growth of ADH-negative bacteria and give a growth advantage to *Neisseria* (Muto *et al*, 2000). Maltose content in certain alcoholic beverage, such as beers, might promote further growth of *N. meningitidis* on nasopharyngeal mucosa. Level of lactate might be another factor involved with virulence of diseases. Alcohol consumption causes high blood lactate (Sarkola *et al*, 2002). It is interesting that CSF of meningitis patients, not specifically meningococcal meningitis, contains high level of lactate (Martin, 1983). These high level of lactate, mainly L-lactate, are generated by human host, not by bacteria (Wellmer *et al*, 2001). CSF lactate might promote growth of *N. meningitidis* during infection as the mutant strain lacking lactate permease, encoded by *lctP* gene, had a reduced growth rate in CSF (Exley *et al*, 2005 A). The *lctP* mutant was also attenuated during bloodstream infection through loss of resistance against complement (Exley *et al*, 2005 B). It is likely that during septicaemic infection *N. meningitidis* grows under low level of free oxygen in blood circulation system by fermentation and

anaerobic respiration. It has been shown that the growth of a *fnr* mutant strain was attenuated in a mouse model of meningococcal bacteremia (Bartolini *et al*, 2006). FNR is well characterized as a regulator of gene expression for anaerobiosis. Though the notion that during infection of the blood system the meningococci might survive by fermentation and anaerobic respiration, oxygen is still required for synthesis of nucleic acid (Rock *et al*, 2005) and possibly other cellular reactions.

1.2 Genome of *N. meningitidis*

There are complete genome sequences of *N. meningitidis* serogroup A (Strain Z2491), serogroup B (Strain MC58) and more recently serogroup C (Strain FAM18). The serogroup C genome contains 2,194,961 basepairs with 51.62 % G + C content, and 1,976 predicted coding sequences of which 60 do not match those in the serogroup A or B strain (Bentley *et al*, 2007). The sequence of serogroup A has 2,184,406 base pairs. It contains G + C content of 51.81 %, and contains 2,121 predicted coding sequences. There are many hundreds of repetitive elements, ranging from short repeats to insertion sequences and gene duplications of one kilobase or more. These repeats might be involved in genome fluidity and antigenic variation (Parkhill *et al*, 2000). Serogroup B has a genome size of 2,272,351 base pairs with 51.53 % G + C content. The genome contains 2,158 predicted coding regions. However, only 1,158 (53.7%) coding regions (ORFs) were assigned a biological role. 345 (16%) ORFs matched gene products of unknown function from other species and 532 (24.7%) ORFs had no database match. There are 1,910 DNA uptake signal sequences (DUS) distributed throughout the genome. The DNA uptake sequence is a conserved 10-bp repeat required for efficient genetic transformation in meningococcus and gonococcus (Ambur *et al*, 2006). The consensus motif of neisserial DNA uptake sequence is GCCGTCTGAA or TTCAGACGGC. The neisserial DUS is believed to help the bacterial cells to uptake

recognizable DNA fragments in their natural environment with strong preference of their own species. The receptor for DUS is unknown.

There are three major islands of horizontal DNA transfer (IHT). Two of them contains genes encoding proteins involved in pathogenicity, one contains the gene cluster of encapsulation and another contains 30 genes that may involved with virulence, such as those encoded for toxins and immunogenic proteins. The third island contains 24 hypothetical proteins. None of these IHTs is characterized as classical “pathogenicity islands” as transposase gene flank only one IHT, other regions are not flanked by inverted repeats, and none is adjacent to tRNA genes (Tetelin *et al*, 2000). *N. meningitidis* contains more genes that undergo phase variation than any pathogens. Phase variation may be an important strategy to adapt to changing environment of human host and facilitate invasive infection eventually, both to overcome immune response and to grow. Many genes encoding for cell surface proteins contain homopolymeric tracts. Slippage of the DNA replication machinery at these homopolymeric tracts can result in epigenetic mutation and antigenic variation giving advantage to survive humoral immune surveillance.

Genome sequence analysis revealed that *N. meningitidis* strain MC58 (serogroup B) has only about 10% of the genome differing from that of serogroup A (Tetelin *et al*, 2000). This may account for different spreading pattern through human population.

1.3 Pathogenicity of *N. meningitidis*

Cell adhesion of *N. meningitidis* is crucial for colonizing nasopharyngeal mucosa. Biofilm formation might be important for meningococcal colonization. It has been shown that 30% of carriage isolates can form a biofilm on a polystyrene surface and they lack capsule (Yi *et al*, 2004). Only 12% of invasive-disease isolates formed biofilms. Expression of capsule is down regulated upon contact with the host epithelium

(Deghmane *et al*, 2002), possibly to promote adhesion of the organism. Biofilm were also observed in a standardized flow system. Interestingly, only acapsulate meningococci can form biofilm under these conditions (Lappann *et al*, 2006). Meningococcal exopolysaccharides have not been identified and there is no gene homologous to the genes encoding alginate of *P. aeruginosa* (Yi *et al*, 2005).

During growth in liquid culture, cells release some part of the outer membrane to form small outer membrane vesicles (OMV) called “blebs” (Devoe, 1973). These outer membrane blebs are commonly found among Gram-negative bacteria. It is proposed to be a result of cell wall turnover. The peptidoglycan turnover causes turgor pressure on the outer membrane leading to bulging and finally blebbing (Doyle *et al*, 1998). The outer membrane contains many proteins that can interact with host cells. These include well known opacity proteins Opa and Opc which are important to bacterial adhesion and invasion of host cells (Virji *et al*, 1992).

The polysaccharide capsule is essential for pathogenicity as it confers resistance to phagocytosis and complement-mediated lysis (Frosch *et al*, 1999; Frasch and Pollard, 2001). The structure of the capsular polysaccharides has been used to distinguish serogroup of meningococci. They are classified into many serogroups but only five serogroups are pathogenic, namely serogroup A, B, C, Y and W135. The serogroup A is widespread in the sub-Saharan belt whereas serogroups B and C are more prevalent in Europe and the United States. Strains of serogroup B are of particular interest because of the lack of a vaccine due to capsule having sialic acid which is similar to that of humans. Since *N. meningitidis* is a strict human pathogen and most patients have not been in contact with other cases, asymptomatic carriers are presumably the major source of the pathogenic strains. Most carrier isolates are shown to lack capsule production.

The capsule deficient state of meningococcal strains in the nasopharynx may be crucial for colonization of nasopharyngeal mucosa (Yazdankhah and Caugant, 2004).

The meningococci express type IV pili which play an important role in adhesion to host cell. Strains that do not express pilin protein cannot bind erythrocytes (Stephen *et al*, 1991). Pili are essential for meningococcal interactions with host cells in both capsulate and acapsulate strains whereas Opc-mediated invasion was observed only in acapsulate strains (Virji *et al*, 1995).

How the organism gain entry to host tissue, bloodstream or CSF is still not well characterized. Meningococcal internalization to nasopharyngeal epithelial cells are related to switching of multiple phase-variable bacterial surface components, including many opacity proteins, but the series of expression of those genes are not well understood yet (de Vries *et al*, 1996). Opc-dependent internalization is facilitated by host fibronectin (Unkmier *et al*, 2002).

It has been demonstrated that the capsule which prevents bacterial adhesion and entry is crucial for intracellular survival in macrophage. In vitro assays suggest that the encapsulate strain can resist killing by cationic antimicrobial peptides (CAMPs) in macrophages. Acapsulated meningococci were more susceptible to well known antimicrobial peptides defensins, cathelicidins, protegrins and to polymyxin B. Capsular genes (*siaD*, *lipA*) and those encoding an efflux pump involved in resistance to CAMPs were up-regulated during the intracellular infection (Spinosa *et al*, 2007). The capsule maybe less negatively charged than LPS and hence decrease the binding of cationic antimicrobial peptide on the meningococcal cell surface.

The enzyme NorB nitric oxide reductase conferred resistance to killing by nitric oxide released in endolysosome of macrophage and nasopharyngeal epithelial cells. This enzyme enhanced intracellular survival of the meningococci (Stevanin *et al*, 2005).

Quorum sensing might also be important for meningococcal pathogenesis. *N. meningitidis* contains a functional copy of *luxS* that is necessary for full meningococcal virulence. LuxS is involved in autoinducer 2 (AI-2) synthesis. It was demonstrated that strains with a *luxS* deletion are defective for bacteremia in mouse model (Winzer *et al*, 2002). Production of signalling molecule AI-2 has been found in *N. meningitidis* (Dove *et al*, 2003) but its role in regulation of other virulence genes are not characterized. There is no exotoxin detected in the meningococci.

1.4 Growth and respiration

The ability to obtain and utilize nutrients is crucial for adaptation during colonization and disease. Carbon source and energy source are very important for survival. Glucose and maltose, are the only sugars utilized for carbon and energy by *N. meningitidis* (Larson *et al*, 1968 and Leighton *et al*, 2001). The meningococci grow well on peptide-based media such as Columbia agar or Mueller Hinton broth. However, when glucose is present, it can promote much more *in vitro* growth than in the absence of glucose. Growth in the presence of combined glucose with lactate was only marginally better than glucose alone (Exley *et al*, 2005). In human host, high level of blood glucose and lactate might promote meningococcal growth upon entry to blood circulation. However, most of blood oxygens are bound to haemoglobins, only 1.5% is freely dissolved in blood serum. Since the level of free oxygen in blood is very low, the growth of meningococcus might rely more on anaerobic respiration, such as nitrite respiration, than aerobic respiration, unless they can scavenge oxygen from haemoglobin. In bacterial meningitis patients, level of CSF lactate is increased from 1.4 mM to at least 3.5 mM (Komorowski *et al*, 1978; Lindquist *et al*, 1988; Hutchesson *et al*, 1997). CSF glucose level is generally up to 300 mg/dl (16.7 mM) regardless of serum level (Dougherty *et al*, 1986). In case of bacterial meningitis, level of CSF

glucose is decreased to less than 1.9 mM (Spanos *et al*, 1989). It is not known whether the decreased CSF glucose is due to the glucose utilization by the meningitis bacteria or not. The meningococcus utilizes glucose via central metabolism including Entner-Doudoroff (ED) pathway, pentose phosphate (PP) pathway, but not Embden-Meyerhof-Parnas (EMP) glycolytic pathway. The gene for phosphofructokinase is not present for functional set of EMP pathway. Glucose is mainly catabolized by the ED pathway and to a lesser extent by the PP pathway (Jyssum, 1962). Major part of pyruvate (67-87%) is synthesized through ED pathway and the rest through PP pathway (Jyssum, 1963). This proportion was found to be similar in gonococcus (Morse *et al*, 1974). Pyruvate can be oxidized to acetyl CoA and enter TCA cycle if enough external electron acceptor present. Lactate is proposed to donate electrons to ubiquinone pool of the respiratory chain (Erwin and Gotschlich, 1993 and 1996) and is also used assimilatively to enhance sialylation of capsule polysaccharide. The infection of the meninges, more specifically CSF, progresses rapidly indicating that the organism grows very quickly under the conditions in CSF. The level of oxygen in CSF might be high enough to allow aerobic respiration in the organism.

In *N. meningitidis*, oxygen is more favorable source of terminal electron acceptor than nitrite. At the level of physiology, electron flow to oxygen generates more energy than that of flow to nitrite. Electron flow to oxygen can generate more proton translocation along the transport chain, which in turn, generates more ATP. Upon oxidation of one NADH, electrons flow to oxygen can induce translocation of total protons at NDH (NADH dehydrogenase), *bc₁* complex, and *cbb₃* oxidase. Meanwhile, electron flow to nitrite induces translocation of protons only at NDH and *bc₁* complex. The reduction of nitrite by AniA nitrite reductase, possibly in periplasm or outer membrane, does not translocate any protons from cytoplasm to periplasm. Furthermore,

the higher positive redox potential of oxygen reduction than nitrite reduction favors oxygen reduction, electrochemically. The redox potential of $O_2/2H_2O$ is +820 mV whereas that of NO_2^-/NO is about +348 mV. Therefore, O_2 has higher tendency to acquire electrons than that of NO_2^- . Therefore, it is likely that when both oxygen and nitrite present, electrons will flow more to oxygen than to nitrite. Reverse electron flows from H_2O to cbb_3 also requires more energy to drive than that from NO to nitrite reductase. Therefore, the equilibrium of $O_2 \leftrightarrow H_2O$ will shift closer toward H_2O than that of $NO_2^- \leftrightarrow NO$ toward NO .

The meningococcus has a large number of genes devoted to electron transport systems (Tettelin *et al*, 2000)(Table 1.1). The organism is likely to derive more energy through elaborate branched electron transport systems than through substrate level phosphorylation. Nasopharyngeal mucosa is the natural habitat for *N. meningitidis*'s adapted and evolved symbiotic lifestyle. The varying conditions in the nasopharynx might pressure the organism to be flexible to the availability of respiratory substrates, oxygen and nitrite. They might employ aerobic respiration, anaerobic respiration, and fermentation to supplement growth where fluctuation of oxygen and nitrite occur. The flexibility of its respiratory metabolism probably, in part, contributes to adaptability and pathogenic behavior during invasive infection.

N. meningitidis can grow under both aerobic and microaerobic conditions. Under aerobic conditions, it uses molecular oxygen (O_2) as a terminal electron acceptor. The reduction of oxygen is catalyzed by the cytochrome cbb_3 oxidase encoded by the *fixNOQP* genes. When oxygen is limited, it can use nitrite (NO_2^-) as an alternative terminal electron acceptor, resulting in reduction of nitrite to nitric oxide (NO). This reaction is proposed to be catalyzed by a copper-containing nitrite reductase (Cu-NiR) encoded by the *aniA* gene. It can also use nitric oxide as a terminal electron acceptor,

resulting in reduction of nitric oxide to nitrous oxide (N₂O). Ecologically, microbial reduction of nitrate (NO₃⁻) to nitrogen gas (N₂) is termed denitrification (Figure 1.1). However, *N. meningitidis* can only reduce nitrite to nitrous oxide which we refer to as “partial denitrification”. The electron transport chain in this organism is proposed as shown (Figure 1.2). The reduction of nitric oxide is catalyzed by a predicted quinol-oxidizing nitric oxide reductase encoded by the *norB* gene (Anjum *et al*, 2002). This raises the question if removal of nitric oxide can provide the meningococcus with the ability to resist to killing by nitric oxide produced by macrophage upon respiratory burst. It has been shown that *norB* and *cycP*, which encodes cytochrome *c*’, to lesser extent, enhanced survival of the organism in macrophages (Stevanin *et al*, 2005). It was also demonstrated that *norB* prevents macrophage apoptosis upon internalization (Tunbridge *et al*, 2006), suggesting that the organism might survive and grow in macrophage by utilizing nitric oxide as a respiratory substrate in the hypoxic environment. The spreading of the meningococcus from the primary site of infection to CSF might be shuttled by the infected neutrophils and macrophages.

Locus	Gene Symbol	Common Name	EC Number
NMB_0434		putative AcnD-accessory protein PrpF	
NMB_0564	nqrF	Na(+)-translocating NADH-quinone reductase, subunit F	
NMB_0565	nqrE	Na(+)-translocating NADH-quinone reductase, subunit E	1.6.5.-
NMB_0566	nqrD	Na(+)-translocating NADH-quinone reductase, subunit D	1.6.5.3
NMB_0567	nqrC	Na(+)-translocating NADH-quinone reductase, subunit C	
NMB_0568	nqrB	Na(+)-translocating NADH-quinone reductase, subunit B	1.6.5.-
NMB_0569	nqrA	Na(+)-translocating NADH-quinone reductase, subunit A	
NMB_1533	laz	Lipid-modified azurin	
NMB_1622	norB	nitric oxide reductase	1.7.99.-
NMB_1623	aniA	Copper-containing nitrite reductase	
NMB_0123		ferredoxin, 4Fe-4S bacterial type	
NMB_0208		ferredoxin, 4Fe-4S bacterial type	
NMB_0241	nuoA	NADH dehydrogenase I, A subunit	1.6.5.3
NMB_0242	nuoB	NADH dehydrogenase I, B subunit	1.6.5.3
NMB_0243	nuoC	NADH dehydrogenase I, C subunit	1.6.5.3
NMB_0244	nuoD	NADH dehydrogenase I, D subunit	1.6.5.3
NMB_0245	nuoE	NADH dehydrogenase I, E subunit	1.6.5.3
NMB_0246	nuoF	NADH dehydrogenase I, F subunit	1.6.5.3
NMB_0249	nuoG	NADH dehydrogenase I, G subunit	1.6.5.3
NMB_0250	nuoH	NADH dehydrogenase I, H subunit	1.6.5.3
NMB_0251	nuoI	NADH dehydrogenase I, I subunit	1.6.5.3

NMB_0253	nuoJ	NADH dehydrogenase I, J subunit	1.6.5.3
NMB_0254	nuoK	NADH dehydrogenase I, K subunit	1.6.5.3
NMB_0257	nuoL	NADH dehydrogenase I, L subunit	1.6.5.3
NMB_0258	nuoM	NADH dehydrogenase I, M subunit	1.6.5.3
NMB_0259	nuoN	NADH dehydrogenase I, N subunit	1.6.5.3
NMB_0564	nqrF	Na(+)-translocating NADH-quinone reductase, subunit F	
NMB_0565	nqrE	Na(+)-translocating NADH-quinone reductase, subunit E	1.6.5.-
NMB_0566	nqrD	Na(+)-translocating NADH-quinone reductase, subunit D	1.6.5.3
NMB_0567	nqrC	Na(+)-translocating NADH-quinone reductase, subunit C	
NMB_0568	nqrB	Na(+)-translocating NADH-quinone reductase, subunit B	1.6.5.-
NMB_0569	nqrA	Na(+)-translocating NADH-quinone reductase, subunit A	
NMB_0581		electron transfer flavoprotein-ubiquinone oxidoreductase	1.5.5.1
NMB_0717		putative cytochrome	
NMB_0923		cytochrome c	
NMB_0978	pntB	NAD(P) transhydrogenase, beta subunit	1.6.1.1
NMB_0980	pntA	NAD(P) transhydrogenase, alpha subunit	1.6.1.1
NMB_0993		rubredoxin	
NMB_1044	fpr-1	ferredoxin--NADP reductase	1.18.1.2
NMB_1134	fdx-1	ferredoxin, 2Fe-2S type	
NMB_1158		nickel-dependent hydrogenase, b-type cytochrome subunit	
NMB_1172	fdx-2	ferredoxin, 2Fe-2S type	
NMB_1196		nickel-dependent hydrogenase, b-type cytochrome subunit	
NMB_1287		putative ferredoxin	
NMB_1324	trxB	thioredoxin reductase	1.6.4.5
NMB_1366		thioredoxin	
NMB_1450	fpr-2	ferredoxin--NADP reductase	1.18.1.2
NMB_1454		ferredoxin, 4Fe-4S bacterial type	
NMB_1677		cytochrome c5	
NMB_1722		cytochrome C555, truncation	
NMB_1723	fixP	cytochrome c oxidase, subunit III	1.9.3.1
NMB_1724	fixO	cytochrome c oxidase, subunit II	1.9.3.1
NMB_1725	fixN	cytochrome c oxidase, subunit I	1.9.3.1
NMB_1734	grx	glutaredoxin	
NMB_1790	grxC	glutaredoxin 3	
NMB_1803		putative cytochrome c-type biogenesis protein	
NMB_1804		putative cytochrome c-type biogenesis protein	
NMB_1805		cytochrome c4	
NMB_1845		thioredoxin	
NMB_1958		putative thioredoxin	
NMB_2051	petC	ubiquinol--cytochrome c reductase, cytochrome c1	1.10.2.2
NMB_2052	petB	ubiquinol--cytochrome c reductase, cytochrome b	1.10.2.2
NMB_2053	petA	ubiquinol--cytochrome c reductase, iron-sulfur subunit	1.10.2.2
NMB_2154	etfA	electron transfer flavoprotein, alpha subunit	
NMB_2155	etfB	electron transfer flavoprotein, beta subunit	

Table 1.1 List of genes involved in the electron transports in *N. meningitidis*.



Figure 1.1 Environmental denitrification. Denitrification is the process in which bacteria use nitrate as a terminal electron acceptor and convert it through a series of intermediates to nitrogen gas.

1.5 The electron transport chain

It is proposed that *N. meningitidis* can utilize three different respiratory substrates, which are oxygen, nitrite, and nitric oxide. The proposed electron transport chain in *N. meningitidis* is shown (Figure 1.2). *N. meningitidis* is predicted to contain ubiquinone in the cytoplasmic membrane. Major electron sources include NADH, succinate, malate, lactate, and pyruvate from the cytoplasm. Reduction of ubiquinone by each of these substrates is catalyzed by specific enzymes in the cytoplasmic membrane. This generates electron flow into the ubiquinone pool. The ubiquinol in ubiquinone pool is then oxidized, predominantly, by the cytochrome bc_1 complex in the cytoplasmic membrane. The bc_1 complex is oxidised by periplasmic c -type cytochromes and a cupredoxin Laz. Then, these periplasmic proteins are oxidized by terminal reductases including cbb_3 oxidase in cytoplasmic membrane and AniA nitrite reductase in outer membrane. The cbb_3 oxidase reduces oxygen to water whereas AniA reduce nitrite to nitric oxide. NorB nitric oxide reductase reduces nitric oxide to nitrous oxide. It is predicted that NorB can oxidize ubiquinol directly based on its homolog of quinol-oxidizing NorB found in *Ralstonia eutropha* (Cramm *et al*, 1999).

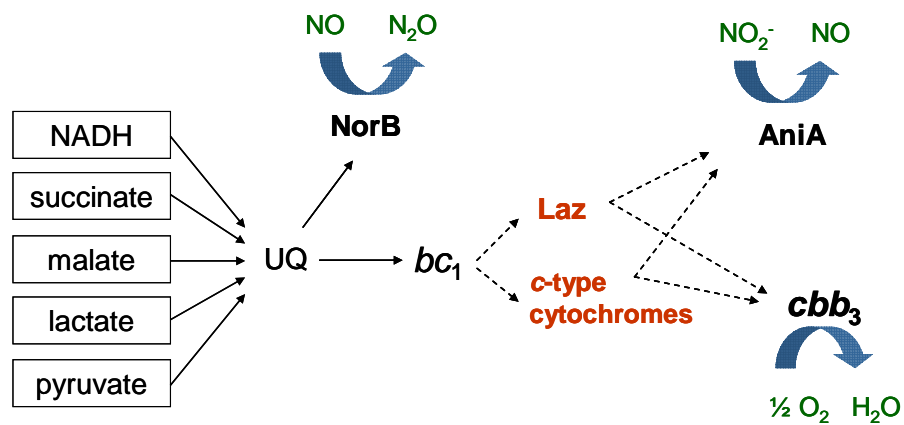


Figure 1.2 Proposed electron transport chain in *N. meningitidis*. The dotted arrow lines present possible electron transport pathways at the level of cytochrome c .

1.5.1 Reduction of Ubiquinone

N. meningitidis is predicted to contain ubiquinone as the sole quinone source because the genome lacks menaquinone synthetic pathway. The ubiquinone pool of *N. meningitidis* may receive electrons from many donors. From genome analysis, there are many potential enzymes that could catalyze reduction of ubiquinone. These include NADH dehydrogenase, succinate dehydrogenase, malate: quinone oxidoreductase, lactate dehydrogenase, electron transferring flavoprotein (ETF), glyceraldehyde 3-phosphate dehydrogenase, and proline dehydrogenase. This may demonstrate the high level of flexibility of the respiratory chain at the level of electron inputs.

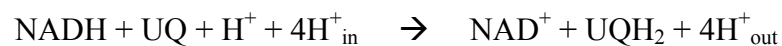
1.5.1.1 NADH dehydrogenase

There are three types of NADH dehydrogenases in bacteria depending on whether they contain an energy-coupling site (Table 1.2). The first type is the proton-translocating NADH: quinone oxidoreductase (NDH-1). The NDH-1 is similar to the complex I of mitochondria but has a relatively simpler structure as it is made up of 14 different subunits instead of 46 subunits (Weiss *et al*, 1991 ; Carroll *et al*, 2003; Friedrich and Bottcher, 2004). It pumps protons from the cytosolic side to the periplasmic side (Figure 1.3). The second type is the NADH: quinone oxidoreductase that lacks an energy coupling site (NDH-2). The NDH-2 is a single subunit enzyme that contains non-covalently bound FAD and has no Fe-S clusters (Yagi, 1991). The third type is Na⁺-translocating NADH: quinone oxidoreductase (Na⁺-NDH). The Na⁺-NDH is made up of 6 different subunits and contains two covalently bound FMN and one noncovalently bound FAD and possibly one binuclear Fe-S cluster (Steuber *et al*, 2002).

	NDH-1	NDH-2	Na⁺-NDH
Ion-pump	H ⁺ (and Na ⁺ ?)	not a pump	Na ⁺
Cofactors	one noncovalent FMN 2 [2Fe-2S] 6 - 8 [4Fe-4S]	one noncovalent FAD	one noncovalent FAD two covalent FMN 1 [2Fe-2S]
Subunit Composition	13-14	1	6
Inhibitors	Rotenone Piericidin A Capsaicin Acetogenins Pyridaben Fenpyroximate	Flavone (?)	Ag ⁺ HQNO Korormicin
Organisms	<i>Paracoccus denitrificans</i> <i>Rhodobacter capsulatus</i> <i>Escherichia coli</i> <i>Synechocystis PCC6803</i> <i>Thermus thermophilus</i> <i>Klebsiella pneumoniae</i>	many Gram-positive bacteria many archaea <i>Vibrio</i> <i>Haemophilus influenzae</i> <i>Escherichia coli</i>	<i>Vibrio</i> <i>Haemophilus influenzae</i> <i>Pseudomonas aeruginosa</i> <i>Klebsiella pneumoniae</i>

Table 1.2 Characteristics of NADH dehydrogenases in bacteria (modified from <http://www.scripps.edu/mem/biochem/CI/bactNDH.html>).

The mitochondrial complex I, with characteristic L-shape, contains a hydrophilic arm protruding into cytoplasm and a hydrophobic arm embedded within the membrane (Figure 1.3) (Friedrich and Bottcher, 2004). The majority of electrons enter the respiratory chain through this complex. It catalyses the oxidation of NADH, the reduction of ubiquinone, and the transfer of 4H⁺/NADH across the membrane (Figure 1.3) as the following reaction:



In *Thermus thermophilus*, the hydrophilic arm of complex I contains the NADH-binding site, the flavin-mononucleotide (FMN), and eight or nine iron-sulfur (Fe-S) clusters (Figure 1.4) (Sazanov and Hinchliffe, 2006). FMN transfers electrons from NADH to ubiquinone through a cascade of Fe-S clusters (Figure 1.4).

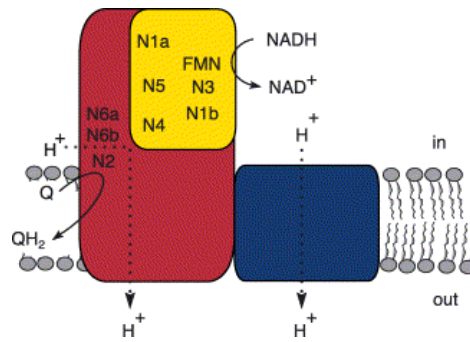


Figure 1.3 Cartoon of mitochondrial complex I structure and functions. There are three modules. The NADH dehydrogenase module (in yellow) and the hydrogenase module (in red) are part of hydrophilic arm whereas the transporter module (in blue) is the hydrophobic arm or transmembrane arm. The Fe-S clusters are denoted as N1a, N1b, N2, N3, N4, N5, N6a, and N6b. The two proposed coupling sites are indicated (Based on Friedrich and Bottcher, 2004).

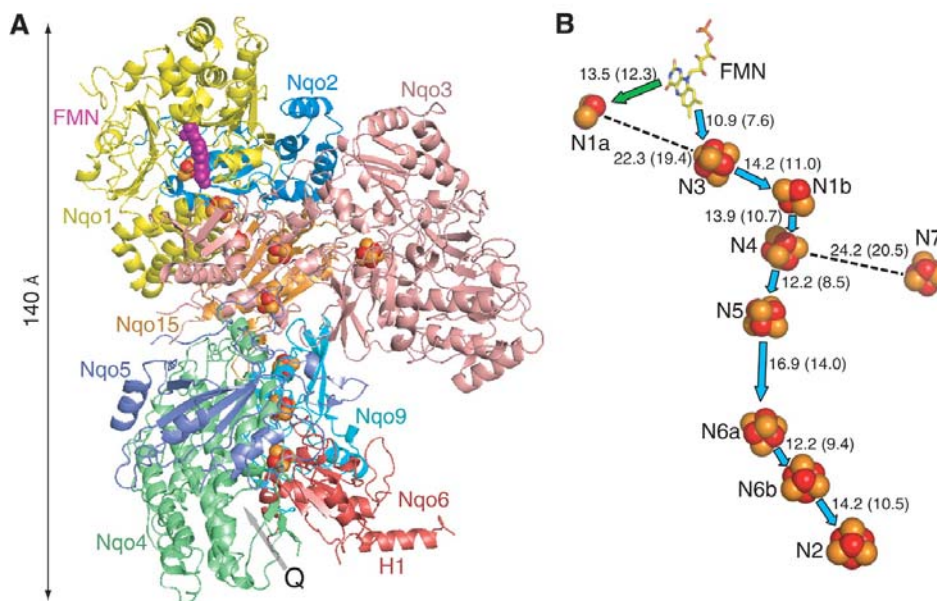
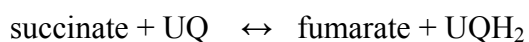


Figure 1.4 Structure of hydrophilic domain of NDH from *Thermus thermophilus*, showing Nqo subunits (each in different colour, Nqo = NADH: quinone oxidoreductase) and electron transfers through redox centers, Fe-S clusters (Fe in red sphere, S in yellow sphere) (Based on Sazanov and Hinchliffe, 2006). (A) Side view, with the membrane arm likely to be beneath and extending to the right. FMN is shown as magenta spheres. A possible quinone-binding site (Q) is indicated by an arrow. (B) Arrangement of redox centers. Cluster N1a is in subunit Nqo2; N3 and FMN in Nqo1; N1b, N4, N5, and N7 in Nqo3; N6a/b in Nqo9; and N2 in Nqo6. The main pathway of electron transfer is indicated by blue arrows, and a diversion to cluster N1a by a green arrow. The distances between the centers given in angstroms were calculated both center-to-center and edge-to-edge (shown in parentheses)(Based on Sazanov and Hinchliffe, 2006).

NADH dehydrogenase of *N. meningitidis* strain MC58 is a predicted NDH-1 encoded by the *nuoABCDEFGHIJKLMN* genes cluster (*nuo*, NADH: ubiquinone oxidoreductase). It is predicted to pump protons while transferring electrons to ubiquinone. From genome analysis, it consists of 14 subunits (A to N) encoded by the *nuo* operon and contains FMN and Fe-S clusters. It is not known whether there is a formation of a sodium motive force that could drive ATP synthesis by a Na⁺ dependent F₁F₀ ATP synthase. However, the meningococcus has *nqrABCDEF* gene cluster (*nqr*, NADH-quinone reductase) that is predicted to encode 6 subunits that compose Na⁺ translocating NADH: quinone reductase complex.

1.5.1.2 Succinate dehydrogenase

Succinate dehydrogenase (SDH) or succinate: quinone oxidoreductase (SQR) is known as complex II of electron transport in mitochondria. It consists of 4 subunits, two hydrophilic proteins and two transmembrane proteins. The hydrophobic transmembrane proteins are a membrane anchor protein and a cytochrome *b₅₆₀*. The hydrophilic proteins are a flavoprotein and an iron-sulfur protein (Sun *et al*, 2005). It oxidizes succinate into fumarate and transfers electrons to FAD which then is reduced to FADH₂. Electrons from FADH₂ then are transferred through Fe-S centers of the complex into ubiquinone. The oxidation of succinate to fumarate is a part of TCA cycle. The complex II catalyses the following reaction:



In *E. coli*, two distinct membrane-bound enzyme complexes are responsible for the interconversion of succinate and fumarate. Succinate dehydrogenase (SDH or SQR) is employed in aerobic growth whereas fumarate reductase (FRD or QFR, quinol: fumarate reductase) is employed in anaerobic growth (Cecchini *et al*, 2002). They are encoded by different gene sets. Both complexes consist of four main components,

similarly to the mitochondrial complex II (Figure 1.5). The catalytic site, at which succinate is oxidized, is on the flavoprotein subunit. The bound FAD acts as electron acceptor. The flavin semiquinone, and the Fe-S centers in the Fe-S protein subunit act to transfer electrons to the ubiquinone reductase site. *E. coli* QFR lacks *b* haem (Cecchini *et al*, 2003). No proton translocation is associated with reactions in *E. coli* SQR and QFR but it was observed in *Bacillus subtilis* (Cecchini *et al*, 2003) (Figure 1. 6).

N. meningitidis strain MC58 has genes for all 4 subunits, *sdhC* encoding cytochrome *b*556 subunit, *sdhD* encoding hydrophobic membrane anchor protein, *sdhA* encoding flavoprotein subunit, and *sdhB* encoding Fe-S protein. This might predict that SDH complex of the organism could have function/activity for supplying electrons into ubiquinone pool as well as taking a part in TCA cycle, similar to *E. coli* SQR.

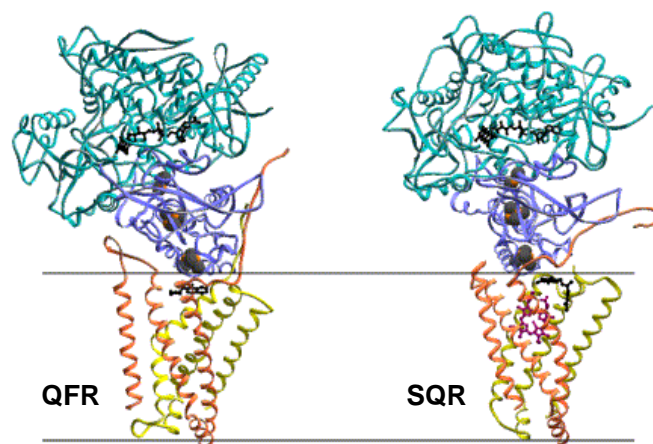


Figure 1.5 Structure of SQR and FQR in *E. coli*. Flavoprotein subunit is in blue, Fe-S protein subunit in purple with Fe-S clusters in red and black spheres, two transmembrane subunits in orange and yellow, haem *b* in magenta. QFR lacks haem *b* in transmembrane subunits whereas SQR contains haem *b* in transmembrane subunits (Based on Cecchini *et al*, 2003).

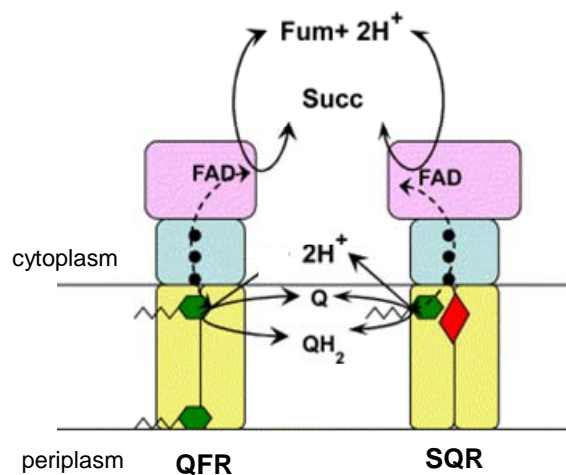


Figure 1.6 Scheme showing electron transfer pathway in SQR and QFR of *E. coli*. The reactions catalyzed by *E. coli* QFR and SQR shown do not induce proton translocation to periplasm. The Fe–S clusters of the enzymes are in the dark closed circles. The position of quinone molecules are in green hexagons. The position of the *b* haem is in red diamond (Based on Cecchini *et al*, 2003).

1.5.1.3 Lactate dehydrogenase

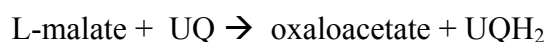
There are two types of lactate dehydrogenases (LDH) in bacteria, the cytoplasmic and the membrane bound. The cytoplasmic lactate dehydrogenase catalyses the interconversion of pyruvate and lactate with interconversion of NADH and NAD⁺. The membrane bound lactate dehydrogenase is involved with electron donation from lactate to ubiquinone pool. It catalyzes the one-way conversion of lactate to pyruvate and couples electron donation to ubiquinone (shown below). Its activity is NAD⁺ independent (Bhatanagar *et al*, 1989; Hendry *et al*, 1990; Fischer *et al*, 1994). Oxidation of lactate coupled with energy transduction has been described in many bacteria (Ingledeew and Poole, 1984). *N. meningitidis* contain two D-lactate dehydrogenases, *ldhA* (NMB1685) and *dld* (NMB0997) and one L-lactate dehydrogenase, *lldD* (NMB1377). *Dld* is more specific for D-lactate, with low-affinity activity for L-lactate (Erwin and Gotschlich, 1993). The enzyme lactate dehydrogenase catalyze the following reaction:



L-lactate-oxidizing activity was detected in both wild type strain and *dld* mutant strains (Erwin and Gotschlich, 1993). *E. coli* has only a single L-LDH gene (*lldD*) and the activity is only induced in medium with L-lactate as the carbon source. However, in *N. meningitidis*, there is probably more than one L-LDH. The activity of these enzymes are not dependent on growth in L-lactate. The deletion mutant of *lldD* gene (NMB1377) has reduced L-LDH activity but still grow on L-lactate. This suggests another L-LDH might exist (Erwin and Gotschlich, 1993) or that activity is due to Dld enzyme (NMB0997).

1.5.1.4 Malate: quinone oxidoreductase

Malate: quinone oxidoreductase (MQO) is a membrane bound protein that catalyzes the conversion of L-malate to oxaloacetate and transfers electrons to ubiquinone (Molenaar *et al*, 1998). This enzyme is an alternative to NAD-dependent malate dehydrogenase, in the cytoplasm, as a part of TCA cycle. The protein sequence is similar to hypothetical proteins from *Escherichia coli*, *Klebsiella pneumoniae*, *Corynebacterium glutamicum* and *Mycobacterium tuberculosis* (Molenaar *et al*, 1998). The enzyme catalyses the following reaction:



Unlike most bacteria, *N. meningitidis* appears not to encode a cytoplasmic malate dehydrogenase enzyme. The gene product of NMB2096 (*yojH*) is similar to the membrane bound malate: quinone oxidoreductase enzyme identified in *Corynebacterium glutamicum*. Thus, it appears likely that the meningococcus oxidizes malate at the expense of ubiquinone, not NADH.

1.5.2 Oxidation of Ubiquinol

In general, ubiquinol can be oxidized by cytochrome bc_1 complex. In *N. meningitidis*, it is predicted that ubiquinol can also be oxidized by nitric oxide reductase.

1.5.2.1 Cytochrome bc_1 complex

The cytochrome bc_1 complex, ubiquinol: cytochrome c oxidoreductase or complex III, is membrane protein that catalyzes the oxidation of ubiquinol in membrane and reduces c -type cytochromes in the periplasm. It also uses the free energy change to translocate protons across the membrane from cytoplasm into periplasm. The reaction is as follow:
$$QH_2 + 2 \text{ ferricyt } c^{3+} + 2H^+_N \rightleftharpoons Q + 2 \text{ ferrocyt } c^{2+} + 4H^+_P$$

The reactions are catalyzed by three subunits (Table 1.3); cytochrome b , containing two b -type haems, b_L (lower potential haem) and b_H (higher potential haem); cytochrome c_1 containing haem c_1 ; and the iron-sulfur protein (ISP) containing an 2Fe-2S center. Quinol is oxidized at the Q_o -site of the complex. Quinol oxidation is divided into two chains of reaction, in which one electron is transferred to a high potential chain and the other to a low potential chain at the same time. The high potential chain consists of the ISP and cytochrome c_1 . The initial acceptor of the first electron from quinol is the 2Fe-2S cluster of the Rieske iron sulfur protein, which transfers electron to cytochrome c_1 and leave a semiquinone at the Q_o -site (Figure 1.5). The semiquinone is unstable and the reaction at the Q_o -site appears to be a concerted electron transfer to cytochrome b . The chain serves as a pathway through which electrons are transferred across the coupling membrane from semiquinone to the Q_i -site where quinone is reduced to quinol. The Q_o -site oxidizes two equivalents of quinol in succession to provide the two electrons at the Q_i -site required for reduction of quinone.

The first electron at the Q_i-site generates a relatively stable semiquinone which is reduced to quinol by the second electron (Berry *et al*, 2000; Croft, 2004).

Subunit	Redox centers	MW (kDa)	Function
Cytochrome <i>b</i>	haem <i>b_H</i>	50	Donor to Q _i -site Acceptor of electrons from heme <i>b_L</i>
	haem <i>b_L</i>		Acceptor from SQ at Q _o -site Transmembrane electron transfer
Cytochrome <i>c</i> ₁	haem <i>c</i> ₁	28.6	Donor to periplasmic cytochrome <i>c</i>
Rieske	2Fe-2S center	19.9	Acceptor from Q _o H ₂ Donor to cytochrome <i>c</i> ₁
Subunit IV	none	14.4	May contribute to Q _o -site

Table 1.3 Subunit composition of the *bc*₁ complex from *Rhodobacter sphaeroides*. SQ = semiquinone (Reproduced from http://www.life.uiuc.edu/crofts/bioph354/bc-complex_summary.html).

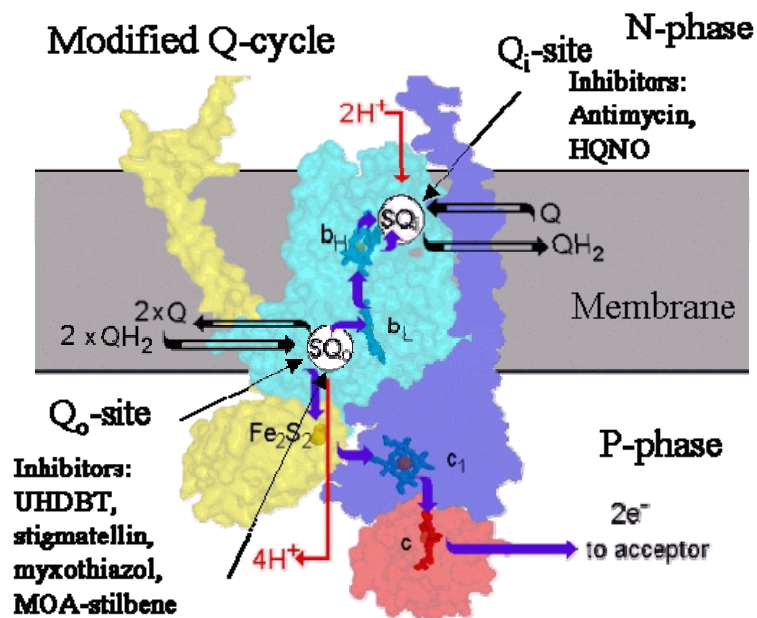


Figure 1.7 The structure of the *bc*₁ complex and the oxidation of ubiquinol in Q-cycle. (Based on Berry *et al*, 2000).

In *N. meningitidis*, the cytochrome *bc₁* complex is encoded by the *petABC* gene cluster. It is predicted to transfer electrons from ubiquinone to *c*-type cytochromes and a cupredoxin Laz. In other bacteria, the cytochrome *bc₁* complex is shown to be very important and cannot be substituted by other ubiquinone oxidation pathways. The cytochrome *bc₁* complex deletion mutant of *Corynebacterium glutamicum* showed a severe growth defect (Bott and Niebisch, 2003) and the cytochrome *c₁* mutant of *Pseudomonas aeruginosa* also grew poorly under aerobic conditions (Igarashi *et al*, 2003).

1.5.3 Oxidation of Cytochrome *bc₁* complex

Generally, the bacterial cytochrome *bc₁* complex can be oxidized by *c*-type cytochromes in periplasm. In *N. meningitidis*, the *bc₁* complex is proposed to be oxidized by periplasmic *c*-type cytochromes and a cupredoxin Laz.

1.5.3.1 Soluble *c*-type cytochromes

In proteobacteria, some soluble *c*-type cytochromes are found in the periplasm and loosely associated with cytoplasmic membrane. These soluble *c*-type cytochromes are usually involved with both aerobic respiration and denitrification. They act as electron transfer proteins that carry electrons from *bc₁* complex to terminal reductases. Their function is similar to cytochrome *c* in mitochondria which transfers electrons from the *bc₁* complex to cytochrome *c* oxidase. In *P. denitrificans*, both cytochrome *c₅₅₂* and *c₅₅₀* accept electrons from *bc₁* complex. *c₅₅₂* donates electrons to cytochrome *aa₃* oxidase while *c₅₅₀* donates electrons to both *aa₃* oxidase and *cbb₃* oxidase (Otten *et al*, 2001). *c₅₅₀* also donates electrons to *cd₁* nitrite reductase (Pearson *et al*, 2003). *Pseudomonas aeruginosa* cytochrome *c₅₅₁* functions as an electron donor to nitrite reductase. *c*-type cytochromes are characterized by the covalent attachment of haem to a

polypeptide chain via, usually, two thioether bonds involving sulfhydryl groups of cysteine residues (Figure 1.8 and 1.9). The conserved haem binding site is C-XX-CH where histidine provides an axial ligand, the fifth ligand, to its iron. In terms of haem structure, haems of *c*-type cytochrome and *b*-type cytochromes are not different from each other. These two cytochrome types can only be distinguished by the mode of binding of haem to apoprotein, as haem of *b*-type cytochrome is not covalently bound to apoprotein. There is no conserved motif of haem binding site for *b*-type cytochrome. The difference in haem-iron coordination makes cytochromes exhibit different electron spin. Low spin haem typically has hexacoordination with two axial iron ligands which normally are His-Fe-His or His-Fe-Met. High spin haem usually has pentacoordination with one axial ligand which usually is histidine of the C-XX-CH motif. The remaining axial coordination site can be occupied by small molecules such as oxygen or nitric oxide.

N. meningitidis strain MC58 has 3 genes that encode for 3 different putative soluble *c*-type cytochromes. NMB0717 is predicted to encode for periplasmic monohaem cytochrome *c*₂. NMB1677 is predicted to encode for a periplasmic dihaem cytochrome *c*₅ with a transmembrane domain and a cytoplasmic domain. NMB1805 is predicted to encode for periplasmic dihaem cytochrome *c*₄. These *c*-type cytochromes are predicted to transfer electrons from the *bc*₁ complex to *cbb*₃ oxidase and AniA nitrite reductase. Roles of these *c*-type cytochromes in aspects of electron transport, respirations and growth of *N. meningitidis* will be investigated in this thesis.

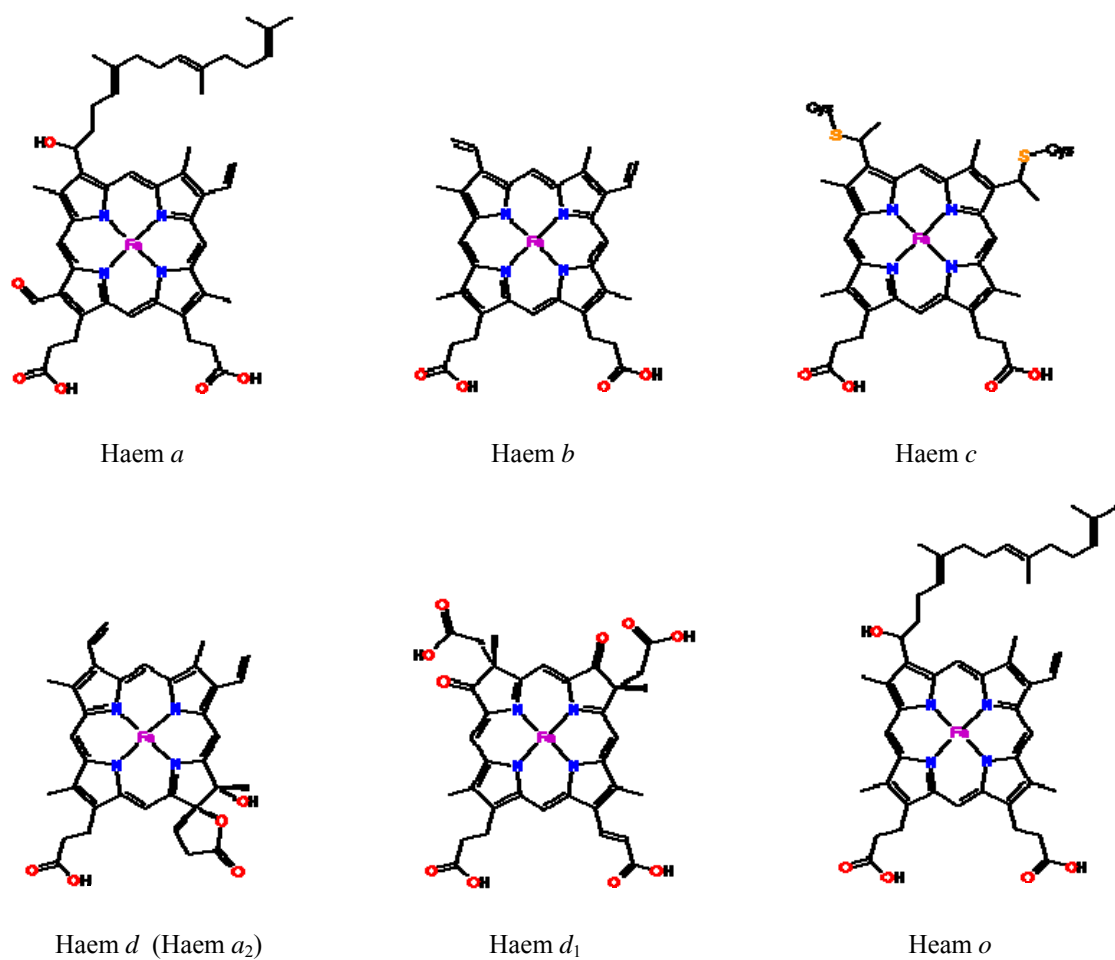


Figure 1.8 Haem types according to structure and mode of binding of the haem prosthetic group (Reproduced from <http://metallo.scripps.edu/PROMISE/CYTC.html>).

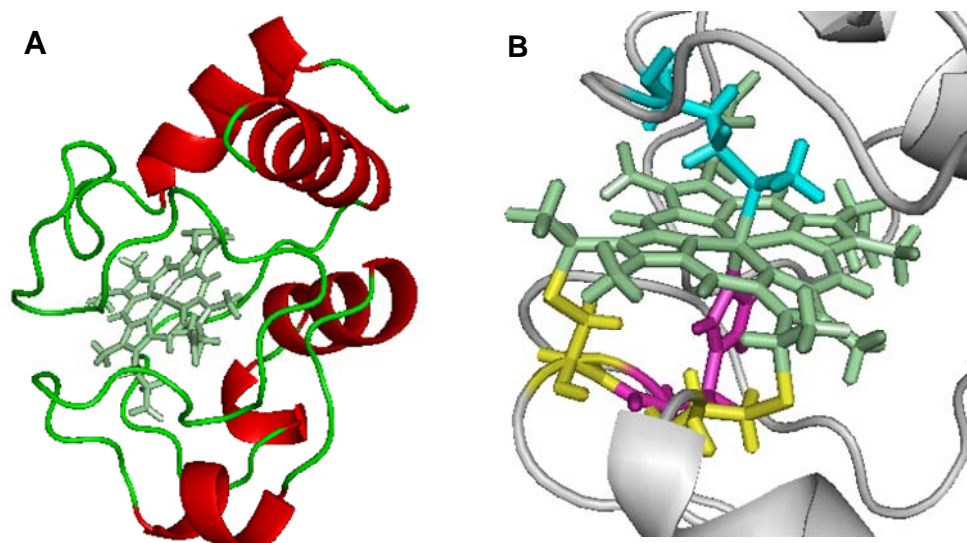


Figure 1.9 Structure of cytochrome c_{552} from *Paracoccus denitrificans*. (A) Tertiary structure of cytochrome c_{552} contains c -haem. (B) Haem center has hexacoordination with axial ligands His18 (purple) and Met78 (blue). Methionine is often found, in C-terminal region, as the sixth ligand of haem. Haem is covalently attached to two cysteines (yellow) of the C-XX-CH motif.

1.5.3.2 Lipid-modified azurin

Gene NMB1533 of *N. meningitidis* is predicted to encode for Lipid-modified azurin (Laz). Laz is a blue copper protein in the cupredoxin family. Members of cupredoxin include azurin, pseudoazurin, plastocyanin, amicyanin, rusticyanin, and stellacyanin. Some cupredoxins are found to be involved in respiratory chains. *P. denitrificans* pseudoazurin is an electron donor to cytochrome cd_1 nitrite reductase (Pearson *et al*, 2003). Spinach plastocyanin donates electrons to Photosystem I (Haehnel *et al*, 1994; Hippler *et al*, 1996). *Thiobacillus ferrooxidans* uses rusticyanin as an electron transfer protein in the aerobic respiratory chain (Cobley and Haddock, 1975; Blake *et al*, 1991). Amicyanin of *Methylomonas spp.*, a methylotroph, accepts electrons from methylamine dehydrogenase (Tobari and Harada, 1981; Dinarieva and Netrusov,

1989). However, *Pseudomonas aeruginosa* azurin does not play obligatory role in denitrification (Vijgenboom *et al*, 1997).

Laz contains a predicted globular azurin domain, similar to azurin in *Methylobacillus* and *Pseudomonas*. However, it contains an extra N-terminal linker domain predicted to allow attachment to outer membrane while azurin domain is exposed in periplasm. This linker domain contains AAEAP repeats. The structure and functions of linker region is unknown. It is predicted that Laz functions as an electron transfer protein in respiratory chains of *N. meningitidis*. Details of Laz will be further discussed in Chapter 7. Roles of Laz in aspects of electron transport, respirations and growth of *N. meningitidis* will be investigated in this thesis.

1.5.4 Terminal redox proteins

The predicted terminal redox proteins in *N. meningitidis* are the cytochrome *cbb₃* oxidase, copper-containing AniA nitrite reductase, and NorB nitric oxide reductase. The cytochrome *cbb₃* oxidase and nitrite reductase are predicted to accept electron from *c*-type cytochromes or Laz, whereas the nitric oxide reductase is predicted to accept electron directly from ubiquinol. Proposed respiratory chains were described earlier in section 1.5.

1.5.4.1 Cytochrome *cbb₃* oxidase

Cytochrome *cbb₃* oxidases are commonly found among proteobacteria, such as *Rhodobacter capsulatus*, *Campylobacter jejuni*, *Helicobacter pylori*, *Neisseria gonorrhoeae*, *Vibrio cholerae*, *Ralstonia solanacearum*, *Pseudomonas aeruginosa*, *Pseudomonas stutzeri*. They are most studied in *Rhodobacter*, *Pseudomonas*, *Bradyrhizobium*, and *Paracoccus*. These cytochromes belong to the haem–copper oxidases (HCO) superfamily. Haem-copper oxidases (HCO) are enzymes that couple

the reduction of dioxygen to water with translocation of protons across the membrane. There are two types of HCO categorized by types of the electron donors. One type is the cytochrome *c* oxidases which accept electrons from *c*-type cytochromes. Another type is quinol oxidases which accept electrons from ubiquinol. Quinol oxidases do not contain Cu_A. There are diverse types of cytochrome *c* oxidases, especially in bacteria. Cytochrome oxidases can also be classified on the basis of haem types. Cytochrome *c* oxidases of mitochondria are *aa*₃ type (Keilin and Hartree, 1939). There are reports of cytochrome *ba*₃, *bb*₃, *bo*₃, *caa*₃, *cao*₃, *cbb*₃, *cbo*₃, and *oo*₃ oxidases in bacteria. The *bd* oxidases have unique structure not related to any haem-copper oxidases, suggesting that they may have different evolutionary origin from other (Junemann, 1997).

Cytochrome *cbb*₃ oxidases have been proposed to have very high affinity for oxygen. *Bradyrhizobium japonicum cbb*₃ oxidase exhibited K_m value for oxygen at 7 nM (Preisig *et al*, 1996). This is at least sevenfold lower than that by mitochondrial *aa*₃ oxidase and is the lowest K_m value reported so far. As *cbb*₃ oxidases are found in respiratory chains of many human pathogens and this type of cytochrome complex has high oxygen affinity we could hypothesize they may play an important role to allow many human pathogens colonise and grow in hypoxic environments (Preisig *et al*, 1996a). In general, cytochrome *cbb*₃ oxidases are often found among proteobacteria. This group of bacteria might employ this type of cytochromes for adapting to live in the low oxygen environment. For example, *Bradyrhizobium japonicum* lives under an extremely low level of oxygen in root nodule of soy bean where nitrogen fixation takes place. Low oxygen is required to protect nitrogen fixing enzyme nitrogenase while *cbb*₃ oxidase still catalyze reduction of oxygen to supplement growth by aerobic respiration (Preisig *et al*, 1996a, 1996b). *cbb*₃ oxidases are strongly expressed under microaerobic conditions in some bacteria, such as *B. japonicum* (Preisig *et al*, 1996) and *Brucella*

suis (Loisel-Meyer *et al*, 2005), However, *cbb*₃ oxidases are equally expressed under both aerobic and microaerobic conditions in some bacteria such as *P. aeruginosa* (Comoli and Donohue, 2004), and *Rhodobacter capsulatus* (Thorny-Meyer *et al*, 1994).

The *cbb*₃ oxidases catalyse the reduction of dioxygen to water and translocate protons across the cytoplasmic membrane to periplasm (Garcia-Horsman *et al*, 1998 ; van der Oost *et al*, 1996). They terminate the electron transport chain and function for energy conservation similar to the cytochrome *c* oxidase in mitochondria. Cytochrome *cbb*₃ oxidase utilizes *c*-type cytochromes, and not quinol, as electron donors (Gray *et al*, 1994). This type of cytochrome oxidase does not contain Cu_A (Gray *et al*, 1994). The *cbb*₃ oxidase catalyzes the following reaction:



In *P. stutzeri*, cytochrome *cbb*₃ genes are assigned as *ccoNOQP*. They encode for four proteins. CcoN is a dihaem cytochrome of b-type. It contains two *b*-haems, *b* and *b*₃, and one copper ion which is Cu_B. CcoN is catalytic center of oxygen reduction. It has highest reduction potential among cytochromes in the complex (Table 1.4). CcoO is a monohaem cytochrome of *c*-type. It contains one *c*-haem. CcoO is redox center that accepts electrons from *c*-type cytochrome and transfer to catalytic subunit CcoN. CcoP is a dihaem cytochrome of *c*-type. It contains two *c*-haems. CcoP and CcoO have similar reduction potentials (Table 1.6). CcoQ is a predicted small membrane bound protein. Its function is unknown. It is not present in *cbb*₃ complex purified from *P. stutzeri* (Saraste and Castresana, 1994). FixQ is also not found in *cbb*₃ complex purified from *B. japonicum* (Preisig *et al*, 1996).

Subunit	Redox center	Haem axial ligands	Midpoint reduction potentials
CcoN	haem <i>b</i>	His-Fe-His	+310 mV, +265 mV
	haem <i>b</i> ₃	n.d.	+225 mV
CcoO	haem <i>c</i>	His-Fe-Met	+245 mV, +215 mV
CcoP	haem <i>c</i>	His-Fe-Met	+245 mV, +205 mV
	haem <i>c</i>	His-Fe-His	+185 mV, +105 mV

Table 1.4 Reduction potentials of haems in the cytochrome *cbb*₃ oxidase from *P. stutzeri* (Based on Pitcher and Watmough, 2004).

Cytochrome *cbb*₃ complex is the only oxidase found in *N. meningitidis*. The *cbb*₃ subunits are encoded by four genes of the operon *fixNOQP*. The locus number for each gene is as follow, *fixN* (NMB1725), *fixO* (NMB1724), and *fixP* (NMB1723). The *fixQ* gene is present downstream of *fixO* but it is not assigned the locus number yet (CMR, TIGR). The organization of the operon and the proposed structural complex is shown (Figure 1.10). Protein sequence analysis revealed that the C-terminal region of meningococcus FixP (NMB1723) is shorter than its counterpart gonococcus CcoP (NGO1371) (Figure 1.11). The meningococcus FixP lacks the third haem domain present in N-terminus of gonococcus CcoP (Figure 1.11). The gonococcus CcoP is a trihaem cytochrome whereas the meningococcus FixP is a dihaem cytochrome. However, the DNA sequence downstream of *fixP*, the NMB1722 region, is almost identical to that in 3' region of CcoP. Comparison of combined NMB1723 and NMB1722 continuous DNA sequence to NGO1371 DNA sequence revealed that a point mutation, CAG→TAG, substitutes glutamine with stop codon in the meningococcus (Figure 1.11) exactly the position between the last amino acid residue of NMB1723 and the first residue of NMB1722. It is likely that the ancestor protein of meningococcus FixP contains three haem domains like that in gonococcus CcoP. Protein sequence of NMB1722 is very similar to the second haem domain of

cytochrome c_5 (NMB1677) (Figure 1.12). The functions of FixP or CcoP is unclear because the CcoNO subcomplex purified from *B. japonicum* (Zufferey *et al*, 1996) and *P. denitrificans* (de Gier *et al*, 1996) are catalytically active in oxygen reduction. It is not known under what circumstances FixP or CcoP is required for respiration.

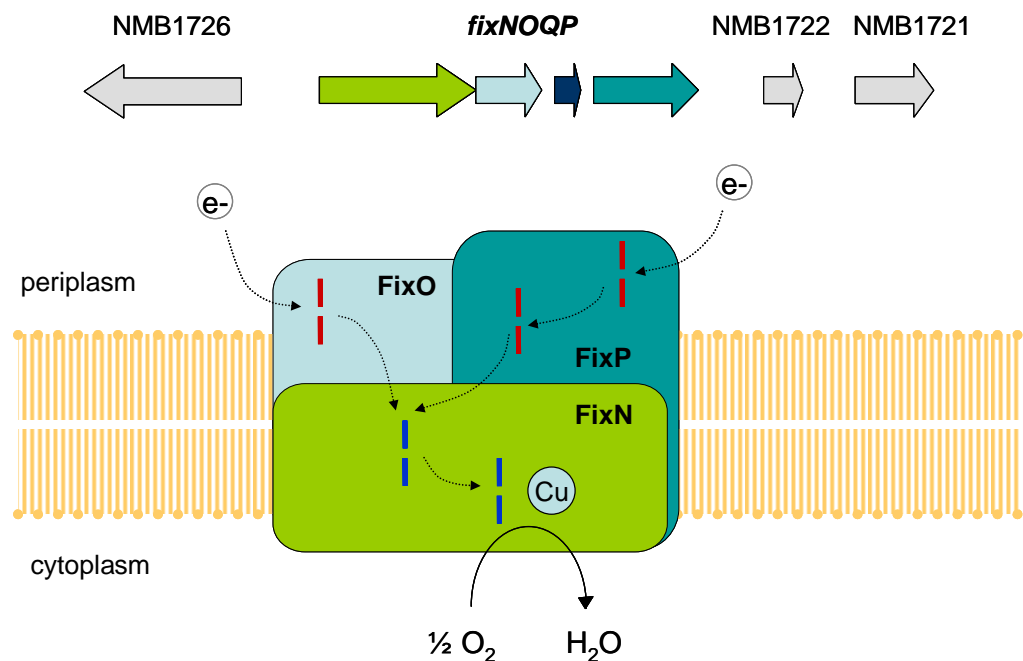
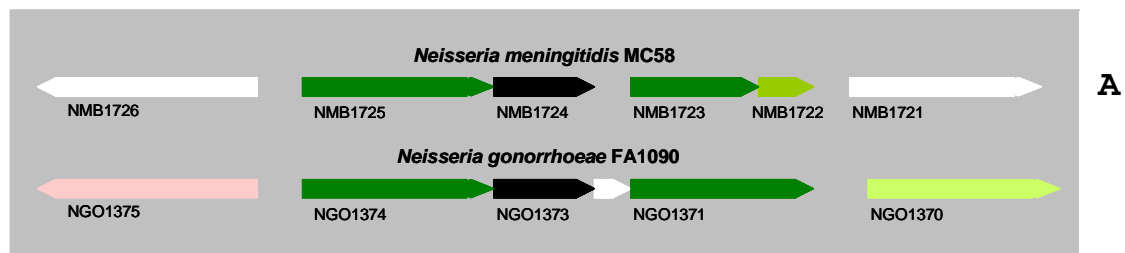


Figure 1.10 Proposed organization of the *fixNOQP* operon in *N. meningitidis*. The *fixNOQP* operon of *N. meningitidis* encodes the three structural proteins that comprises the cytochrome *cbb3* oxidase complex. FixQ is predicted not to be associated with the complex. In this scheme, *b*-type haems are coloured blue whereas *c*-type haems red. (Modified from Pitcher and Watmough, 2004).



A

NMB1723	MNTTSQFTSNFWNIYIAVIVLLSFIALAWLLLSQNVVVKRPKKGEEVQTTGHEWDGIAEYD	60
NGO1371	MNATSQFTSNFWNIYIAVIVLLSFIALAWLLLSQNVVVKRPKKGEEVQTTGHEWDGIAEYD	60
	.**	
NMB1723	NPLPRWWFWL CVL TWLFGIGYLVMPGVGDYKGLLKWTS HNQYEKVEKKADEQY GKLYAK	120
NGO1371	NPLPRWWFWL CVL TWLFGIGYLVMPGVGDYKGLLKWTS HNQYEKVEKKADEQY GKLYAK	120

NMB1723	FADMP IEK VAKDPQAKQIAQNLFNTY CIQCH GSDAKGSKGF PNL TDS DWLWGGDPDKIHE	180
NGO1371	FADMP IEK VAKDPQAKQIAQNLFNTY CIQCH GSDAKGSKGF PNL TDS DWLWGGDPDKIHE	180

NMB1723	TIEKGRVATMPAWGPALGEEGVKDV AHYVMSLSKPEGQYDEERAARGQALFSGPPAN CFT	240
NGO1371	TIEKGRVATMPAWGPALGEEGVKDV AHYVMSLSKPKGQYDEERAARGQALFSGPPAN CFT	240
	*****.*****	
NMB1723	CHGDKGQGIQGLGPNLTDDVWLWGGTQKSI IETITNGRSSQMPAWGHFLDKDKLHIMTAY	300
NGO1371	CHGDKGQGIQGLGPNLTDDVWLWGGTQKSI IETITNGRSSQMPAWGHFLDKDKLHIMTAY	300

NMB1723	VWGLSDKDGKAPVKAEPAPT PAPA AEA PAASAPAEAAQAVSEAKPAAAEPKAE EKAAPAA	360
NGO1371	VWGLSNKDGKAPVKAEPAP ---AAEPAPSAPAEAAQAASEAKPAAAEPKAE EKAAPAA	356
	*****.*****	
NMB1723	KADGK VYETVCAACHGNAIPGIPHVGIKADWADRIKKGKDTLHKHAI EGFNTMPAKGGR	419
NGO1371	KADGKQVYETV CAACHGNAIPGIPHV GTKADWADRIKKGKDTLHKHAI EGFNTMPAKGGR	416

NMB1723	GDLSDDEVKAAVDYMNQSGGKF	442
NGO1371	GDLSDDEVKAAVDYMNQSGGKF	439

B

Figure 1.11 Comparison of the *cbb₃* gene cluster structure in meningococcus and gonococcus and the difference between primary structure of the meningococcus FixP and the gonococcus CcoP. (A) The gonococcus *ccoP* gene (NGO1371) is longer than the meningococcus *fixP* gene (NMB1723). The gonococcus CcoP contains three haem binding sites (yellow highlight) while the meningococcus FixP is shorter and contains only two haem binding sites. It is hypothesized that pseudogene NMB1722 downstream of *fixP* gene once used to be a part of *fixP* gene. The sequence in blue letter is the truncated protein NMB1722 downstream of FixP protein. Point mutation, CAG→TAG, introduces stop codon and substitutes Gln366 residue.

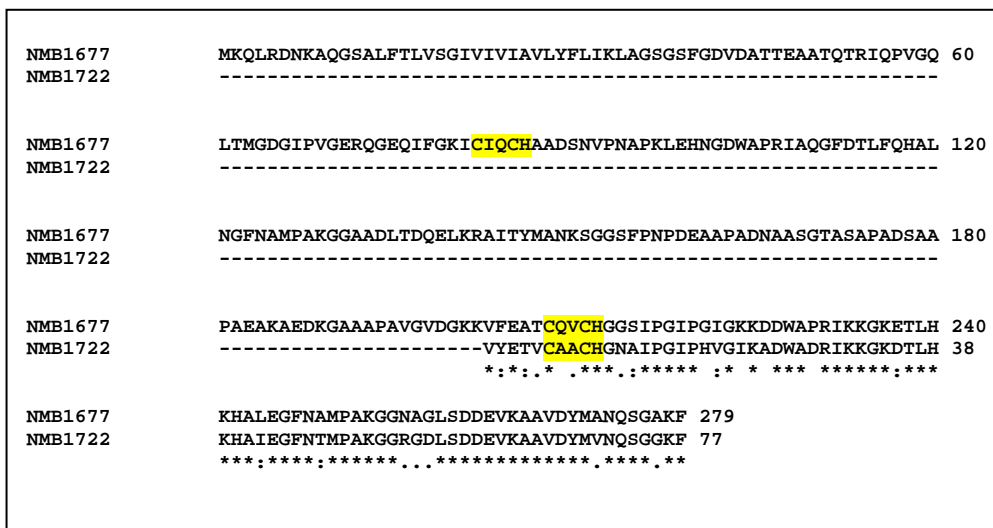


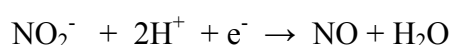
Figure 1.12 Pairwise alignment of cytochrome *c5* protein sequence of NMB1677 (279 amino acid residues) and protein sequence of NMB1722 (77 amino acid residues). Protein sequence of NMB1722 is very similar to the second haem binding domain of cytochrome *c5*. They share 75 % sequence identity.

As the cytochrome *cbb₃* oxidase has high affinity to oxygen, this might suggest that *N. meningitidis* has adapted to live in low oxygen environment in human host. The high affinity to oxygen of *cbb₃* oxidase may play an important role for its successful colonization of the nasopharynx and oropharynx. In terms of phylogenetic distribution, aerobic respiration is one of the most common respiratory mechanisms (Castresana, 2001). The *cbb₃* oxidases have evolved for respiration under very low level of oxygen (Preisig *et al*, 1993). It has been widely claimed that the aerobic respiration arose late in evolution as early atmosphere did not contain enough oxygen to drive aerobic respiration. However, some geological studies revealed that early atmosphere might contain at least 1.5% of the present level (Ohmoto, 1996). Many bacteria supplement growth by aerobic respiration under very low level of oxygen (0.3-0.5%) and use hydrogen as electron donor (Huber *et al*, 1992). This respiratory metabolism is present in many hyperthermophiles that may include the earliest diverging bacteria (Reysenbach

and Shock, 2002). Based on subunits composition comparison between *cbb₃* oxidases and cytochrome *cb*-type NO reductases, it has been suggested that *cbb₃* oxidase was evolved from the enzyme of the nitrogen metabolism (Saraste and Castresana, 1994; Castresana *et al*, 1995). It is possible that the ancestral function of this enzyme was nitric oxide reduction before it evolved to have oxidase activity (Castresana, 2004).

1.5.4.2 AniA nitrite reductase

AniA nitrite reductase is a copper-containing protein found in many denitrifying proteobacteria, including *Neisseria gonorrhoeae*, *Burkholderia pseudomallei*, *Pseudomonas aeruginosa*, *Rhodobacter sphaeroides*, *Alcaligenes faecalis*, *Bradyrhizobium japonicum*, and *Nitrosomonas europaea*. In *N. gonorrhoeae*, this protein is not expressed under aerobic growth. It can be induced under anaerobic conditions using nitrite as an electron acceptor and it was found to be associated with the outer membrane (Clark *et al*, 1987). Hence, it was named AniA for anaerobically induced protein A. The crystal structure of gonococcus AniA revealed that monomers are organized into a homotrimer. Each monomer contains two core cupredoxin folds and two copper atoms (Figure 1.13) (Boulanger and Murphy, 2002). The cupredoxin fold, an eight-stranded Greek key β -barrel, is conserved among proteins containing type I copper center (Murphey *et al*, 1997). Copper I ligands are two histidine residues, a cysteine residue, and a methionine residue whereas copper II ligands are three histidine residues and one water molecule (Figure 1.14). Copper I accepts electrons from donors whereas copper II is the catalytic site for nitrite reduction. Data from crystal structure showed that ligand water of copper II is displaced in favour of nitrite. In *Alcaligenes faecalis*, copper I accepts electrons from pseudoazurin and transfers to copper II where nitrite is reduced to nitric oxide (Kukimoto *et al*, 1994). The reaction is as below:



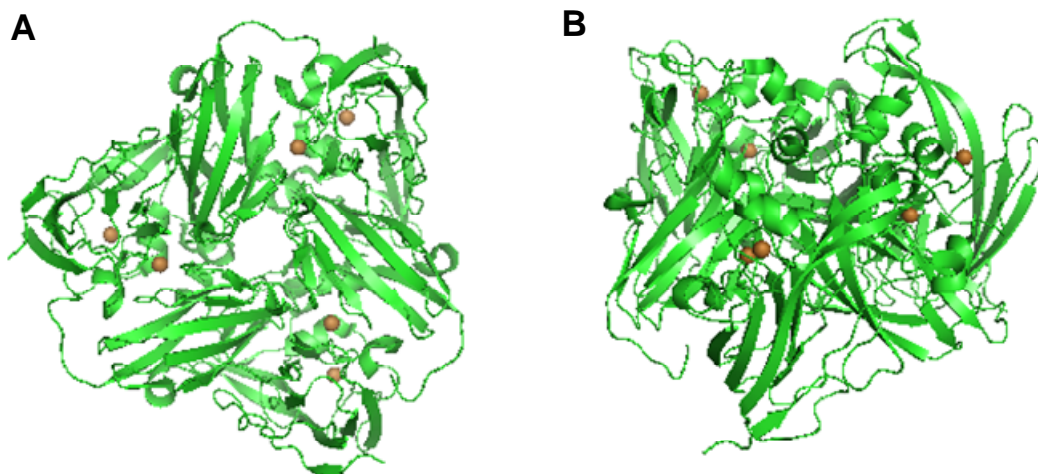


Figure 1.13 Structure of soluble AniA nitrite reductase from *N. gonorrhoeae*. Trimer of AniA which each monomer contains two copper ion. (A) Top view. (B) Side view. The pictures are from PDB file (PDB ID 1kbw).

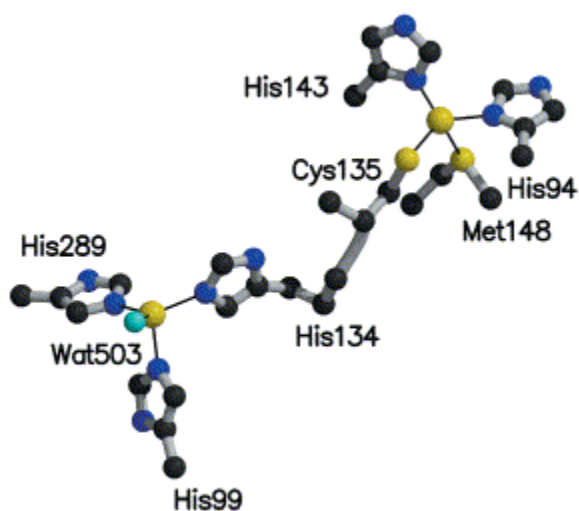


Figure 1.14 Type I and type II copper sites in AniA. The copper sites are depicted as balls and sticks showing the covalent linkage between them. Copper I ligands are two histidines, one cysteine and one methionine. Copper II ligands are three histidines and one water molecule (blue sphere). Nitrite binds copper II by displacing the water molecule (Based on Boulanger and Murphy, 2002).

There are two classes of nitrite reductases in denitrifying bacteria, the haem enzymes and copper (Cu) enzymes. The copper enzymes are more commonly found than the haem enzymes. The haem enzyme most studied is cytochrome *cd₁* nitrite reductase. This cytochrome is found in *Pseudomonas aeruginosa*, *Paracoccus denitrificans*, and *Paracoccus pantotrophus*. In *P. denitrificans*, *cd₁* nitrite reductase can accept electrons from both *c*-type cytochromes and pseudoazurin (Ferguson *et al*, 2003).

Gene *aniA* (NMB1623) in *N. meningitidis* is predicted to encode AniA nitrite reductase. The protein is predicted to be attached to the outer membrane with linker region at the N-terminus similar to that of Laz (see section 1.5.3.2). It is predicted to have two bound copper ions not far from each other (Figure 1.13 and 1.14). The copper I site on the side of the globular domain is predicted to accept electrons from donor proteins such as *c*-type cytochromes and /or cupredoxin. After the reduction of copper I, electrons are transferred to the copper II at the deeper groove. The copper II is reduced and electrons are finally passed to nitrite leading to reduction of nitrite to nitric oxide. The AniA nitrite reductase of *N. meningitidis* catalyzes the reduction of nitrite to nitric oxide and play an important role in microaerobic respiration and growth as during the oxygen limitation the organism supplemented growth by denitrification and it was linked to the expression of the enzyme (Rock *et al*, 2005).

1.5.4.3 Nitric oxide reductase

In bacteria, nitric oxide reductase is an integral membrane protein complex that catalyzes reduction of nitric oxide (NO) to nitrous oxide (N₂O). It belongs to the haem-copper oxidase family. There are three types of NOR identified so far. One is cytochrome *bc* type complex (cNOR) that receives electrons from soluble redox protein donors, such as *c*-type cytochromes or pseudoazurin. Another is cytochrome *b* type

complex that lack cytochrome *c* component (qNOR) and receive electrons from quinol. Another one is qNOR that contains a Cu_A at the electron entry site (qCu_ANOR) (Hendriks *et al*, 2000; de Vries and Schroder, 2002). In *Pseudomonas stutzeri*, nitric oxide reductase is a cytochrome *bc* type complex of NorB and NorC protein. NorC is small subunit of membrane anchored *c*-type cytochrome whereas NorB is a large subunit of 12 transmembrane helices of cytochromes with 2 haems of *b*-type (Hendriks *et al*, 2000). Nitric oxide reductase catalyzes the reduction of nitric oxide to nitrous oxide.

The meningococcus nitric oxide reductase (NorB) encoded by *norB* gene (NMB1622) is predicted to be a *b*-type cytochrome of the qNOR type. NorB is very similar to those of the gonococcus (Householder *et al*, 2000) and *Ralstonia eutropha* (Cramm *et al*, 1997). Nitric oxide reductase in the meningococcus contains a homologous region similar to that found in other quinol oxidizing enzymes. This homology is in an N-terminal region predicted to contain two putative membrane spans and a quinol binding site. NorB plays an important role in denitrifying growth as a *norB* mutant of *N. meningitidis* was unable to grow microaerobically in the presence of nitrite (Anjum *et al*, 2002). It was shown that under oxygen-limited conditions the meningococcus reduced nitrite to support growth and this caused the accumulation of nitric oxide (Rock *et al*, 2005). Nitric oxide inhibits oxygen respiration by competitive binding to *cbb*₃ oxidase. The rapid removal of nitric oxide was observed approximately one hour after the accumulation whereas this rapid removal did not occur in the *norB* mutant strain. This suggests that NorB is required for removal of endogenous free radical nitric oxide accumulated from nitrite reduction in order to maintain denitrifying growth. NorB may be important for maintaining growth and colonization of the

nasopharynx as the organism possibly grows in mixed species biofilm where fluctuation of oxygen and nitrite occurs.

1.6 Regulation of aerobic respiration and denitrification

The availability of respiratory substrates is crucial for regulation of gene expressions. In many bacteria, oxygen starvation can induce gene expression involved in fermentation and anaerobic respiration, including the enzymes for denitrification. Denitrification in bacteria is often involved with anaerobic respiration. *N. meningitidis* utilizes three respiratory substrates which are oxygen, nitrite, and nitric oxide. The regulation of gene expression to respond to availability of respiratory substrates is crucial for maintaining growth. The concentrations of these respiratory substrates are sensed by multiple sensors/regulators that act simultaneously to maintain growth and keep the toxic intermediates below deleterious levels. In the meningococcus, there is evidence demonstrating that some proteins play an important regulatory role in response to level of oxygen, nitrite, and nitric oxide. These proteins are FNR, NarQ/P, and NsrR.

1.6.1 FNR

FNR (fumarate-nitrate reduction regulator) protein is both an oxygen sensor and transcription regulator. It is localized in cytoplasm and acts as a global activator of transcription initiation in response to oxygen starvation. When oxygen level is low, FNR increases the expression of proteins involved in fermentation and anaerobic respiration (Li *et al*, 1998). FNR and Crp (cAMP receptor protein) are believed to have similar structures and to have evolved from a common origin (Li *et al*, 1998). Early studies in *E. coli* suggested that under anaerobic conditions FNR is a dimer and active for DNA binding whereas under aerobic conditions, FNR is inactivated by conversion to a monomer (Lazazzera *et al*, 1993). It has been shown later that anaerobically

purified FNR contains a $[4\text{Fe-4S}]^{2+}$ cluster which is unstable toward oxygen. The presence of the $[4\text{Fe-4S}]^{2+}$ cluster increases dimerization of FNR which is correlated with an increase in site-specific DNA binding. According to Mossbauer spectroscopy on purified FNR and cells containing overexpressed FNR, the $[4\text{Fe-4S}]^{2+}$ cluster is converted by oxygen to a $[2\text{Fe-2S}]^{2+}$. The $[2\text{Fe-2S}]^{2+}$ cluster can be reconverted to the $[4\text{Fe-4S}]^{2+}$ cluster on reduction with dithionite *in vitro* (Kiley and Beinert, 1998). This suggests that level oxygen might be directly sensed by the Fe-S clusters of FNR. Later, it is suggested that the sensing mechanism involves the transformation of a $[4\text{Fe-4S}]^{2+}$ cluster into a $[2\text{Fe-2S}]^{2+}$ cluster on reaction with oxygen (Crack *et al*, 2004). It is proposed that FNR carries a sensory domain, remote from the DNA binding helix-turn-helix motif, which responds to oxygen.

FNR dimer can bind DNA target at consensus specific palindromic sequence of palindromic 5'-TTGATNNNNATCAA-3' (FNR box) in the promoter region of a target gene. FNR dimer mediates transcription regulation by direct contact of FNR-RNA polymerase. It was demonstrated that approximately two Fe^{2+} ions are released from the reaction of oxygen with the $[4\text{Fe-4S}]^{2+}$ cluster. It was also found that there was no detectable difference in the rate of oxygen-induced cluster conversion for FNR free in solution compared to its DNA-bound form. The rate of FNR inactivation was monitored *in vivo* by measuring the rate at which transcriptional regulation by FNR is lost upon the exposure of cells to oxygen. A comparison of the *in vitro* and *in vivo* rates of conversion suggests that oxygen-induced cluster conversion is sufficient to explain FNR inactivation in cells (Sutton *et al*, 2004).

In *E. coli*, FNR acts as both an activator and repressor involved in the control of more than 100 genes for adaptation from aerobiosis to anaerobiosis. Chromatin immunoprecipitation (ChIP) and high-density microarrays have shown the distribution

of FNR across the entire *Escherichia coli* chromosome in exponentially growing cells. Sixty-three binding targets, each located at the 5' end of a gene, were identified. In stationary phase, the distribution of FNR was largely unchanged. FNR distribution is little altered when cells enter stationary phase, while RNA polymerase undergoes a complete redistribution (Grainger *et al*, 2007).

In gonococcus, FNR activated nitrite reductase (*aniA*) and cytochrome *c* peroxidase gene (*ccp*) (Lissenden *et al*, 2000). DNA microarray has shown that FNR controls a much smaller regulon of meningococcus than its *E. coli* counterpart. It activated *aniA* and *nosR*. *nosR* is gene that encodes for a putative nitrous oxide reductase regulator protein but there is a frameshift causing truncated protein in the meningococcus. FNR also activated twelve other genes including a gene for iron uptake outer membrane protein. Meanwhile, it repressed six genes that include *norB* (Whitehead *et al*, 2007). As described earlier that NorB functions to remove toxic nitric oxide upon nitrite reduction by *aniA*. This contradicts the evidence that FNR activated AniA expression and nitrite reduction.

N. meningitidis FNR protein regulates gene expression involved in fermentation and anaerobic respiration (Bartolini *et al*, 2006). DNA microarray showed that FNR activated the expression of GTP binding protein (NMB1806), maltosephosphorylase(NMB0390), β -phosphoglucomutase (NMB0391), sugar transporter (NMB0388), aldose-1-epimerase (NMB0389), hypothetical protein (NMB0363), cytochrome *c4* (NMB1805), NosR nitrous oxide reductase regulator (NMB0577), cytochrome *c5* (NMB1677), AniA nitrite reductase (NMB1623), and hypothetical protein (NMB1870). Analysis of *aniA* and *norB* DNA sequence revealed that the promoter region of *aniA* (-94 to -81) and *norB* (-290 to -277) contains FNR box. This is the same sequence as *aniA* and *norB* are divergently transcribed. It was

shown that FNR is required for activation of *aniA* gene (Rock *et al*, 2005). AniA expression was very low during aerobic growth whereas it was increased fivefold under oxygen-limited conditions. A strain defective in FNR grew poorly under oxygen-limited conditions in the presence of nitrite and can not utilize nitrite. AniA expression was not detectable (Rock *et al*, 2005). This suggests a crucial role of FNR in activation of denitrification in this organism.

1.6.2 NarQ/P

In *E. coli*, gene expression in response to level of nitrite is regulated by two component NarQ/P signal transduction (Robin *et al*, 1997). The NarQ sensor protein is an inner membrane protein while NarP is a cytoplasmic soluble protein. NarQ contains three modules which are the sensory module, the central module, and the transmitter module (Stewart, 2003; Stewart *et al*, 2003). The sensory module comprises a periplasmic ligand binding domain with “P Box”, which is similar to CheY protein in chemotaxis, and a linker domain that mediates signal to transmitter module. Upon receiving signal and becoming phosphorylated, NarP binds target DNA sequences and activates expression of target genes. NarP functions as a transcription activator and also as a global repressor (Constantinidou *et al*, 2006). NarP activated 14 genes and repressed 37 genes in *E. coli*.

It was found that a *N. gonorrhoeae narP* mutant grew more slowly than wild type under oxygen-limited conditions in the presence of nitrite (Overton *et al*, 2006). It is presumed that the slow growth was due to the decreased ability to express *aniA* and to reduce nitrite. It was shown that the level of mRNA transcript of *aniA* in wild type was threefold more than that in *narP* mutant. This suggests that NarP is involved in activation of *aniA* gene in response to nitrite.

As discussed earlier that the absence of oxygen can induce *aniA* expression in *N. meningitidis*. However, it was found that inclusion of nitrite in growth media can increase AniA expression in *N. meningitidis* grown microaerobically by further tenfold (Rock *et al*, 2005), suggesting that the availability of nitrite substrate is more powerful for activation of *aniA*. However, FNR is a pre-requisite for activation of *aniA* by NarQ/P as an *fnr* mutant grown under microaerobic conditions in the presence of nitrite failed to activate *aniA* and failed to reduce nitrite (Rock *et al*, 2005). Without FNR, NarQ/P itself cannot activate *aniA*. This might suggest that the absence of oxygen is crucial for activation of nitrite reduction. Oxygen respiration in this organism is favored over nitrite respiration even under oxygen-limited conditions. The organism will not utilize nitrite unless oxygen level becomes extremely low. It is not known what the lowest concentration of oxygen that allows the organism to utilize an alternative respiratory substrate nitrite. The utilization of these two respiratory substrates is tightly regulated by interplay between FNR and NarQ/P system. This is predicted to be the characteristic of microaerophiles which prefer to maintain aerobic respiration under a wide range of physiological oxygen, even under submicromolar dissolved oxygen tension. In facultative anaerobes, it is not known whether FNR is required for activation of nitrite reduction by NarQ/P.

1.6.3 NsrR

In denitrifying bacteria, nitric oxide is a product of nitrite reduction. This endogenous nitric oxide is usually further reduced to nitrous oxide by nitric oxide reductase. One of the regulators of gene expression in response to nitric oxide that has been studied is NsrR protein. NsrR was first identified in a nitrifying bacterium *Nitrosomonas eutropha* (Beaumont *et al*, 2004). However, that study proposed NsrR to be a nitrite sensitive transcription repressor that plays an important role in the regulation

of nitrite reduction. Later, the homologs of NsrR found in *E.coli* (Bodenmiller and Spiro, 2006) and in *Bacillus subtilis* (Nakamoto *et al*, 2006) were shown to be involved in control of gene expression in response to nitric oxide. The homologous gene is also found in *N. meningitidis* genome. It was shown that the meningococcus NsrR is a repressor of both *aniA* gene and *norB* gene (Rock *et al*, 2007). The *nsrR* mutant grew more rapidly and utilized nitrite at more rapid rate than wild type when grown under oxygen-limited conditions in the presence of nitrite (Rock *et al*, 2007). AniA and NorB in *nsrR* mutant were upregulated under both oxygen limited conditions in the presence of nitrite and under aerobic conditions in the absence of nitrite. The repression of *norB* was lifted only in the presence of nitric oxide, not nitrite. Hence, NsrR functions as a repressor of *aniA* and *norB* gene and that it senses nitric oxide. However, the repression of *aniA* was not lifted in the presence of nitric oxide. It might be possible that the meningococcus NsrR functions to prevent FNR-dependent *aniA* expression under aerobic conditions (Rock *et al*, 2007).

1.7 Aims and objectives of this work

The aims of this work are to identify the roles of periplasmic cytochrome *c2*, cytochrome *c4*, cytochrome *c5*, and Laz in electron transport, respiration, and growth of *N. meningitidis*. Ultimately, this work aims to gain insight of organization of respiratory chains in this important human pathogen. Two approaches will be employed, the use of genetics and biochemistry to study the importance of these electron transfer proteins. One approach will involve with construction of bacterial strains defective in these electron transfer proteins and characterization of mutants using various microbiological and biochemical techniques. Another approach will involve with heterologous expression of an electron transfer protein and identification of its functions using various biochemical techniques.

Chapter 2

Materials and Methods

2.1 Bacterial strains and plasmids used in this work

2.1.1 Bacterial strains used in this work

Name	Genotype and Description	Source
<i>Escherichia coli</i> DH5 α	General cloning strain carries F ϕ 80 <i>lacZ</i> Δ M15 (<i>lacZYA-argF</i>) U169 <i>recA1 endA1 hsdR17</i> (r _k ⁻ , m _k ⁺) <i>phoA supE44 - thi-1 gyrA96 relA1</i>	Invitrogen
<i>Escherichia coli</i> BL21 λ DE3	Expression strain for cloning of Laz protein carries F ⁻ <i>ompT hsdS_B</i> (r _B ⁻ m _B ⁻) <i>gal dcm</i> (DE3)	Invitrogen
<i>Escherichia coli</i> BL21 λ DE3-laz	Containing plasmid borne copy of meningococcal <i>laz</i> gene for expression of Laz protein	This work
<i>Neisseria meningitidis</i> MC58	Wild type	McGuinness <i>et al</i> , 1991
<i>N. meningitidis</i> <i>c2::spc^f</i>	Containing disrupted chromosomal copy of <i>c2</i> gene	This work
<i>N. meningitidis</i> <i>c4::ery^f</i>	Containing disrupted chromosomal copy of <i>c4</i> gene	This work
<i>N. meningitidis</i> <i>c5::tet^f</i>	Containing disrupted chromosomal copy of <i>c5</i> gene	This work
<i>N. meningitidis</i> Δ <i>laz::chl^f</i>	Containing partially deleted and disrupted chromosomal copy of <i>laz</i> gene	This work
<i>N. meningitidis</i> <i>c2::spc^f c4::ery^f</i>	Containing disrupted chromosomal copy of <i>c2</i> and <i>c4</i> genes	This work
<i>N. meningitidis</i> <i>nsrR::spc^f laz::chl^f</i>	Containing disrupted chromosomal copy of <i>nsrR</i> and <i>laz</i> genes	This work

2.1.2 Plasmids used in this work

Name	Description	Source
pCR-Blunt II TOPO	Linearized plasmid cloning vector for blunt end cloning of PCR products	Invitrogen
pET22-b(+)	Cloning/Expression vector carries N-terminal <i>pelB</i> signal sequence for potential periplasmic localization, plus optional C-terminal HisTag sequence.	Novagen
pCR-Blunt II TOPO- <i>lazP</i>	pCR-Blunt II TOPO containing a copy of <i>laz</i> gene without lipoprotein signal sequence region	This work
pET22-b(+)- <i>lazP</i>	pET22-b(+) containing a copy of <i>laz</i> gene (without lipoprotein signal sequence)for protein expression	This work
pCR-Blunt II TOPO- <i>c2</i>	pCR-Blunt II TOPO containing a chromosomal copy of <i>c2</i> gene with flanking sequence	This work
pCR-Blunt II TOPO- <i>c4</i>	pCR-Blunt II TOPO containing a chromosomal copy of <i>c4</i> gene with flanking sequence	This work
pCR-Blunt II TOPO- <i>c5</i>	pCR-Blunt II TOPO containing a chromosomal copy of <i>c5</i> gene with flanking sequence	This work
pCR-Blunt II TOPO- <i>lazM</i>	pCR-Blunt II TOPO containing a chromosomal copy of <i>laz</i> gene with flanking sequence	This work
pHP45Ω	pHP45 plasmid containing spectinomycin resistance (<i>spc^r</i>) cassette, a.k.a. Ω cassette	Prentki and Krisch, 1984
pTOPO- <i>ery^r</i>	pCR-Blunt II TOPO plasmid containing erythromycin resistance gene (<i>ery^r</i>) cassette derived from pKErmC' plasmids	Zhou and Apicella, 1996
pGEM T-easy <i>sodC::tet^r</i>	pGEM T-easy plasmid containing <i>sodC::tet^r</i> (<i>tet^r</i> cassette was excised from pGEM-tetM plasmid)	Seib <i>et al</i> , 2004
pST2	plasmid containing chloramphenicol resistance gene (<i>ccm</i> or <i>chl^r</i>) cassette, derived from pACYC184 plasmid	Turner <i>et al</i> , 2005
pCR-Blunt II TOPO- <i>c2::spc^r</i>	Containing a disrupted chromosomal copy of <i>c2</i> gene by spectinomycin resistance gene cassette	This work
pCR-Blunt II TOPO- <i>c4::ery^r</i>	Containing a disrupted chromosomal copy of <i>c4</i> gene by erythromycin resistance gene cassette	This work
pCR-Blunt II TOPO- <i>c5::tet^r</i>	Containing a disrupted chromosomal copy of <i>c5</i> gene by tetracycline resistance gene cassette	This work
pCR-Blunt II TOPO- <i>lazM::chl^r</i>	Containing a disrupted chromosomal copy of <i>laz</i> gene by chloramphenicol resistance gene cassette	This work

2.2 Growth of cells

2.2.1. Growth of *N. meningitidis*

N. meningitidis strain MC58 was obtained from Prof. Robert Read, University of Sheffield. *fnr*⁻, *nsrR*⁻ and *aniA*⁻ strain were derived within the Moir lab as described in the literature (Rock *et al*, 2005). *laz*⁻, *c2*⁻, *c4*⁻, *c5*⁻, *c2/c4*⁻, *laz*⁻/*nsrR*⁻, and *aniA*⁻/*nsrR*⁻ disruption mutant strains were generated in this study.

These strains were grown in Columbia-Blood Agar or Muller-Hinton Broth (MHB). Using Muller-Hinton broth, aerobic growth was obtained in 5 ml of the media in plastic McCartney tube shaken at 200 rpm. Microaerobic growth was obtained in 20 ml of MHB in plastic McCartney tube shaken at 90 rpm. Denitrifying growth was obtained in 20 ml of MHB supplemented with 5 mM sodium nitrite in plastic McCartney tube shaken at 90 rpm. Growth of all strains were at 37°C .

For growth on Columbia-Blood Agar plates, 5% horse blood was added to Columbia Agar and 25-30 ml of this suspension was poured into plastic petri dishes with 85 mm diameters. All neisserial plate cultures were incubated under 5% carbon dioxide atmosphere to enhance growth.

2.2.2. Growth of *Escherichia coli*

E. coli strain DH5- α and BL21 λ -DE3 were used in this work. *E. coli* was grown in Lysogeny Broth (LB) at 37°C. *E. coli* was grown aerobically in 5 ml in McCartney tube or 500 ml in 2 L conical flask at 37 °C. *E. coli* was also grown on agar plates using 25-40 ml of LB agar suspension in petri dishes with 85 mm diameter, and streaking *E. coli* onto these plates once they had set. For protein expression, however, they were grown at 25°C to increase yield of soluble protein.

LB medium

	Concentration (g/l)
Tryptone	10
Yeast extract	5
NaCl	5

Add water to make 1000 ml. The pH of dissolved medium was adjusted to 7.5.

For making agar medium, 3 g of agar was added to each 200 ml of liquid medium.

2.2.3 Preparation of bacterial frozen stocks

All bacterial strains were grown in liquid to late log phase or for overnight on agar plate before harvesting cells for making stocks. Bacterial cells grown on agar plate can be directly stocked in 50 % glycerol and 50 % LB broth. Liquid culture was centrifuged at 4000 g for 5 minutes and cell pellets were resuspended in 50 % glycerol and 50 % LB broth. For neisserial cell stocks, 50% glycerol and 50% MHB were used instead. Then, bacterial stocks were frozen at -80 °C. The frozen stocks to be used for culturing were streaked on solid agar plate to check for purity/contaminations prior to further use.

2.2.4 Preparation of antibiotic selective media

To prepare selective media with antibiotic(s), antibiotic(s) in liquid solution was added to liquid media or molten agar at temperature around 55-60°C. The final concentration of antibiotics used for *E. coli* and *N. meningitidis* are shown in Table 2.1.

Antibiotic	<i>Escherichia coli</i>	<i>Neisseria meningitidis</i>
Ampicillin	50 µg/ml	50 µg/ml
Kanamycin	50 µg/ml	50-80 µg/ml
Erythromycin	50 µg/ml	50 µg/ml
Chloramphenicol	25 µg/ml	25 µg/ml
Tetracycline	20 µg/ml	5-20 µg/ml
Spectinomycin	50 µg/ml	50µg/ml

Table 2.1 Antibiotic concentration used in this work.

2.3 Fractionation of cells

2.3.1 Preparation of whole cell lysate

N. meningitidis was grown to late log phase and harvested. Each 1 ml of culture was centrifuged in 1.5 ml eppendorf tube at 4°C and 4000 g for 15 minutes. Cell pellet was resuspended in 500 ul of 30 mM Tris buffer pH 8.0 with 1% dodecyl maltoside. n-Dodecyl-β-D-maltoside maltoside is a water soluble nonionic detergent often used in the isolation of membrane proteins. Multiple studies have shown that n-Dodecyl-b-D-maltoside is a gentle detergent that is often able to preserve enzyme activity better than many commonly used detergents. Cell suspension, then, was frozen at -70° C. To lyse cells, cell suspension were frozen and thawed for more 8-10 cycles. 1 mg/ml of lysozyme and DNase were added to achieve the lysis.

2.3.2 Preparation of periplasm, membranes, and cytoplasm

N. meningitidis was grown to late log phase and harvested by centrifugation at 4°C and 4000 g for 15 minutes. The periplasm was obtained by using osmotic shock as follows. The supernatant was discarded and the pellet was resuspended in 1 ml of 20% (w/v) sucrose, 100 mM TrisHCl (pH 8.0) for 10 minutes on ice. Normally, 1 ml of the resuspension buffer was used for an initial culture volume of 5 ml. This suspension was centrifuged at 6000 g for 10 minute. The supernatant was discarded. The pellet was resuspended in 1 ml of ice-cold 0.5 mM MgCl₂ for 10 minute on ice with occasional gentle mixing to release periplasmic content. The suspension was centrifuged at 6000 g to separate periplasm from cells. The supernatant after centrifugation contains periplasmic content. To obtain cytoplasmic content, cell pellet was resuspended in 1 ml of 1.0 mM Tris pH 8.0 with 0.2 mg/ml lysozyme and a few grains of DNase I. This suspension was incubated at 30 °C for 30 minutes. Under this hypotonic environment cells were lysed and the cytoplasmic contents were released into suspension. DNase I was included to degrade nucleic acid in order to reduce viscosity of cell lysate. Suspension of cell lysate was centrifuged at 12000 g for 30 minutes. The pellet was total membrane and the supernatant was cytoplasm. The pellet was resuspended in 1 ml of 30 mM Tris pH 8.0 with 1 % dodecyl maltoside.

2.3.3. Preparation of outer membrane blebs

N. meningitidis was grown to late log phase and harvested by centrifugation at 4°C and 4000 g for 15 minutes. Then, the culture supernatant was centrifuge at 100,000 X g for 1 hour using ultracentrifuge. The supernatant was discarded. The glassy pellet, the outer membrane blebs, was resuspended and solubilized in 30 mM Tris pH 8.0 with 1 % dodecyl maltoside.

2.4 Genetic techniques

2.4.1 Preparation of plasmid DNA

To prepare plasmid DNA, *E. coli* cells were grown in 5 ml of LB broth in McCartney tube. The antibiotic(s) were added into LB to allow selection of cells containing desired plasmid. Liquid culture was grown aerobically by shaking at 200 rpm at 37° C until reaching late log phase. The culture could also be grown for 12-15 hours. Cells were harvested in a microfuge at 10000 g for one minute. Plasmid DNA were extracted using Qiagen Plasmid Miniprep Kit. Extraction protocols were followed the manufacturer's instructions. Plasmids were stocked at -20°C until used.

2.4.2 Preparation of chromosomal DNA

This protocol is simple and rapid for extraction of bacterial genomic DNA (Chen and Kuo, 1993). The DNA was extracted as follows. To separate chromosomal DNA, 1 ml of late-log culture was centrifuged in benchtop microfuge at 12000 rpm for 3 minute. Cell pellet was resuspended and lysed in lysis buffer (40 mM Tris acetate pH 7.8, 20 mM sodium acetate, 1 mM EDTA, 1% SDS) by vigorous pipetting. Then, 66 µl of 5M NaCl solution was added to precipitate proteins. The mixture was mixed well and centrifuged at 12000 rpm for 10 minutes. Supernatant was collected and transferred into another eppendorf tube. An equal volume of chloroform was added. The tube was gently inverted at least 50 times until a milky solution was completely formed. The mixture was centrifuged at 12000 rpm for 3 minutes. The supernatant was transferred to another tube. The DNA was precipitated with 100% EtOH, washed twice with 70% EtOH, and air dried. The dried DNA pellet was dissolved in 50 ul sterile water.

2.4.3 The polymerase chain reaction

The polymerase chain reaction (PCR) was used throughout this work to amplify desired DNA fragments and to screen constructs. For PCR screenings when the DNA were not required for further works, Taq polymerase (Promega) was used. For amplifications to produce DNA for use in further works, Pfu polymerase (Promega) was used, as this enzyme has a proofreading function which reduces errors in final product. Template DNA was obtained from plasmid DNA or chromosomal DNA preparation. For colony PCR, cells were sampled from a single bacterial colony, using micropipette tip, and suspended directly in reaction mixture. Two standard PCR reaction mixtures were used through this work, shown in Table 2.2. The PCR cycles were carried out as shown in Table 2.3.

Components	Standard Taq	Standard Pfu
Buffer	5 μ l	5 μ l
Template DNA	1 μ l	1 μ l
Forward primer (100 pmoles/ μ l)	1 μ l	1 μ l
Reverse primer (100 pmoles/ μ l)	1 μ l	1 μ l
1.25 mM dNTPs	8 μ l	8 μ l
25 mM MgCl ₂	2.5 μ l	-
Polymerase	1 μ l	1 μ l
Sterile water	30.5 μ l	33 μ l
Total	50 μ l	50 μ l

Table 2.2. Standard PCR protocols used in this work. Concentration of template DNA can be variable but generally used at 50 ng/ μ l.

	Taq polymerase	Pfu polymerase
Initial denaturation	94 °C 5min	94 °C 5 min
35 cycles Denaturation Annealing* Extension	94 °C 30 sec X °C 30 sec 72 °C 1 min/kb	94 °C 30 sec X °C 30 sec 72 °C 2 min/kb
Final Extention	72 °C 5 min	-
Storage	16 °C	16 °C

Table 2.3. The PCR reaction cycles used in this work. Annealing temperature depends on the length and GC content of the primers.

2.4.4 Preparation of competent cells of *E. coli* DH5 α

Chemically competent cells of *E. coli* DH5 α were used to allow uptake of TOPO plasmid containing cloned gene or mutant construct. Competent cells were prepared using method of Hanahan ,1983 (Sambrook *et al*, 1989) and stored at -80°C.

2.4.5 TOPO cloning

pCR Blunt II-TOPO plasmid (Zero Blunt TOPO Cloning Kit, Invitrogen) was used throughout this study for cloning genes of interest. The orientation of inserted gene is not certain as this is blunt end cloning. The cloning reaction was set up following the manufacturer instructions. The reaction mixture consists of 4.5 μ l of Pfu PCR products, 1.0 μ l of Salt solution, and 0.5 μ l of TOPO vector. The mixture was incubated for ten minutes at room temperature to allow ligation. Then, competent cells of *E. coli* DH5 α was transformed by the cloned plasmids.

2.4.6 Transformation of *E. coli* DH5 α

To introduce plasmid DNA into competent *E. coli* DH5 α cells, 200 μ l of cells were thawed on ice. On ice, 200 μ l of competent cells were added to 2 μ l of plasmid in an eppendorf tube. The mixture was incubated on ice for 45 minutes and heat shocked at 42°C for 45 seconds. The mixture was placed on ice for 5 minute and 800 μ l of LB broth was added to the mixture. The mixture was incubated at 37°C for 1 hour with shaking at 200 rpm. Each 100-200 μ l of mixture was spread on selective agar plate.

2.4.7 Transformation of *E. coli* BL21 λ DE3

E. coli BL21 λ DE3 (Novagen) strain was used for expressing Laz protein in this study. Transformation of this organism was done using electroporation. *E. coli* BL21 λ DE3 were grown on agar plate for overnight. All colonies were scraped off and resuspended in 10% glycerol. The suspension was centrifuged to remove glycerol. This washing was repeated for 5-6 times. The cell pellet was resuspended in 10% glycerol. Each 50 μ l of cell suspension was mixed with 1.5 μ l of plasmid DNA. The mixture was incubated on ice for 45 minutes. The transformation mixture was put into electroporation cuvette and cell suspension was electroporated. Set the resistance on the Voltage Booster to 4 k Ω ; set the Pulse Control unit to LOW and 330 μ F. Charge the Pulse Control unit by setting the CHARGE ARM switch on the Pulse Control unit to CHARGE and then pressing the UP voltage control button until the voltage reading is 5 to 10 volts higher than the desired discharge voltage. For *E. coli*, the standard conditions are 2.4 kv, which means setting the Pulse Control unit to 405 volts (400 volts is the desired discharge voltage + 5). The voltage booster amplifies the volts by sixfold such that the total discharge voltage is 2400 volts, or 2.4 kv. Set the CHARGE/ARM switch to the ARM position. The green light indicates that the unit is ready to deliver a DC

pulse. Depress the pulse discharge TRIGGER button and hold for 1 second. Then, 1 ml of LB was added into cuvetted immediately after electric shock. Transformants were transferred into an eppendorf tube and incubated at 37°C for 1 hour. Each 100 µl of culture was spread on a selective agar plate.

2.4.8 Transformation of *N. meningitidis* MC58

N. meningitidis is a naturally competent cell. Transformation of the meningococcus follows the method of Bogdan *et al*, 2002. The organism was grown on agar plate for overnight at 37°C with 5% CO₂. A loopful of cells were suspended in 1 ml of ice-cold Transformation Solution (TS) consisting of LB broth with 10% (w/v) PEG 8000, 5% (v/v) DMSO and 50 mM Mg²⁺ (MgCl₂) at a final pH of 6.5. Then, 190 µl of suspension was transferred into a 15 ml Falcon tube. 10 µl of plasmid DNA or PCR product was added. The mixture was incubated at 37°C for 1-2 hours with shaking at 200 rpm. Each 100-200 µl of mixture was spread on selective agar plate.

2.4.9 Restriction digestion

All restriction digestions were done using protocols following the manufacturers instructions. All restriction enzymes used are from Promega and New England Biolabs.

2.4.10 Purification of DNA fragments and PCR products

Desired DNA fragments from restriction digest or PCR products were purified using agarose gel electrophoresis. The band of interest was excised from the gel using a clean scalpel and placed into an eppendorf tube. The DNA was then extracted using QIAEX II Gel Extraction Kit (Qiagen) following the manufacturer instructions.

2.4.11 Ligation of DNA fragments

Blunt end ligation and cohesive end ligation of DNA fragment with linearized plasmid were done using T4 DNA ligase (Promega) following the manufacturer instructions. Normally ligation reaction was allowed at room temperature for overnight.

2.4.12 pET-22b (+) cloning

The pET-22b(+) plasmid vector (Novagen) was used as an expression vector of *laz* gene. It carries N-terminal pelB signal sequence for potential periplasmic localization. The cloning region carries restriction sites for NcoI and EcoRI. Double digestion of vector plasmid was done and dephosphorylation of plasmid by alkali phosphatase was followed. The PCR fragment of *laz* gene was designed to carry NcoI site on one end and EcoRI site on the other end. After restriction digestion, compatible cohesive ends allows specific-orientation ligation with plasmid vector. The ligation mixture consists of 6 μ l of pET-22b(+) plasmid, 2 μ l of insert DNA, 1 μ l of ligase buffer, and 1 μ l of T4 DNA ligase. The, mixture was incubated at room temperature for 18 hours. Then, competent cells of *E. coli* DH5 α was transformed by the cloned plasmids.

2.4.13 Agarose gel electrophoresis

This method was used for separation of DNA fragments by size. Preparation of 0.8% agarose gel is as follows. 0.48 g of Agarose (electrophoresis grade, Invitrogen) was dissolved in 60 ml TBE buffer (90 mM Tris, 90 mM boric acid, 2 mM EDTA). The mixture was heated using microwave at medium power for a few minutes to completely dissolve. The heated agarose was cooled down to 60°C. One drop of 1.25 mg/ml of ethidium bromide was added and mixed well. Agarose was poured into gel tray (size of 10 cm X 9 cm) with a comb in. The agarose gel was completely formed after 15-20

minutes. DNA samples were mixed 5:1 with agarose gel loading buffer (0.25% bromophenol blue, 30% glycerol). Sample was slowly added to each well in which the agarose gel must be completely under the 0.5X TBE buffer level. Gels were run at room temperature at 100 V for 90 minutes. The DNA was visualized by UV illumination.

5X TBE buffer stock	
Tris base	54.0 g
Boric Acid	27.5 g
EDTA	2.92 g
Add water to 1000 ml.	

2.5 Protein purification procedures

2.5.1 Extraction of periplasmic proteins from *E. coli* BL21 λ DE3

Laz protein was expressed in *E. coli* BL21 λ DE3. The extraction of Laz protein was done using osmotic shock. Laz-expressing strain was grown in liquid medium for protein expression. Cells were grown in 1000 ml of LB containing ampicillin and copper chloride at 37°C to optical density of 0.6 at 600 nm. IPTG was added to induce Laz expression and the culture was incubated at 25°C for 3 hours.

Cells were harvested by centrifugation at 4°C and 4000 g for 15 minutes. The periplasm was obtained by using osmotic shock as follows. The supernatant was discarded and the pellet was resuspended in 100 ml of 20% (w/v) sucrose, 100 mM TrisHCl (pH 8.0) for 10 minutes on ice. This suspension was centrifuged at 6000 g for 10 minute. The supernatant was discarded. The pellet was resuspended in 100 ml of ice-cold 0.5 mM MgCl₂ for 10 minute on ice with occasional gently mixing to release periplasmic content. The suspension was centrifuged at 6000 g to separate periplasm from cells. The supernatant after centrifugation contains periplasmic content.

2.5.2 Anion exchange column chromatography

Laz protein, with predicted pI of 4.6, was separated on the basis of interaction of negatively charged amino acid residues with the anion exchange resin DEAE Sepharose Fast Flow (Amersham Biosciences). This resin was packed into C16/40 Column (Amersham Biosciences) to final bed volume of 60 ml and was equilibrated with 150 ml (2.5X column volume) of 100 mM Tris/HCl (pH 8). Then, 100 ml of periplasmic extract with 0.01 % potassium ferricyanide was loaded onto column followed by 150 ml of 100 mM Tris/HCl (pH 8). A gradient of 0-500 mM NaCl in the same buffer, volume of 200 ml, was used to elute bound protein. The separation was carried out at flow rate of 1 ml/min and 4 ml fractions were collected. The blue fractions containing Laz were pooled and desalted using Amicon Ultra-15 Centrifugal Filter Unit (Millipore). The desalted protein was further purified by anion exchange column chromatography using second mobile phase with lower pH. The column was equilibrated with 150 ml of 25 mM HEPES (pH 7). Then, Laz protein was loaded followed by 150 ml of 25 mM HEPES (pH 7). A gradient of 0-500 mM NaCl in the same buffer, volume of 200 ml, was used to elute bound protein. The separation was carried out at flow rate of 1 ml/min and 4 ml fractions were collected. The blue fractions containing Laz were pooled and desalted using Amicon Ultra-15 Centrifugal Filter Unit (Millipore).

2.5.3 Concentration, desalting and buffer exchange of protein samples

Protein samples were concentrated using Amicon Ultra-15 Centrifugal Filter Unit (Millipore) for volume under 15 ml or Centricon Centrifugal Filter Unit for volume under 2 ml. PD10 column was also used for desalting of protein with small volume of 1-2 ml.

2.6 Protein determination

Protein concentration in column fractions, total cell lysate, and subcellular fraction were measured using Bio-Rad Protein Assay, based on method of Bradford (Bradford, 1976). It involves the addition of an acidic dye to protein solution, and subsequent measurement at 595 nm with a spectrophotometer. Comparison to a standard curve provides a relative measurement of protein concentration. Bovine serum albumin (BSA) was used for standard curve. The linear range of assay for BSA is 0.2 to 0.9 mg/ml. One part of dye reagent concentrate was diluted with four part of distilled deionized water. 20 µl of protein sample was mixed with 1 ml of diluted dye reagent by vortexing. The mixture was incubated at room temperature for 10 minutes and the absorption was measured at 595 nm. The absorbance will increase over time. The mixture should not be incubated more than 1 hour.

2.7 Analysis of protein samples

2.7.1 SDS-PAGE

SDS-PAGE was used for analysis of protein samples for their molecular weights, relative concentrations, the presence of haem, or their immunological response to antibodies. Gel equipments from Biorad were used throughout this study. Acrylamide gel stock (Protogel) contains 30% acrylamide, 0.8% bis-acrylamide (37.5:1) from National Diagnostics. Gels were prepared as below protocol (Table 2.4) with resolving gel size of 10 x 6 cm. The sample loading buffer and running buffer were prepared as followings. Protein samples were mixed 3:1 with sample loading buffer and boiled at 95°C for 5 minutes. Then, protein samples were loaded into set gel and analyzed using the method of Laemmli (1970). Gels were run at 100 V for about two hours.

Components	Resolving Gel (15%)	Stacking Gel (5%)
Water	2.54 ml	5.49 ml
1.5 M Tris Buffer pH 8.8	2.50 ml	-
0.5 M Tris Buffer pH 6.8	-	2.50 ml
30% Acrylamide	4.75 ml	1.70 ml
10% SDS	0.10 ml	0.10 ml
Mix together. Add APS and TEMED just before casting gel.		
10% APS	0.10 ml	0.10 ml
TEMED	0.01 ml	0.01 ml
Total volume	10 ml	10 ml

Table 2.4 Protocol for preparation of SDS-PAGE gel.

4X Sample loading buffer		10X Running buffer	
1M Tris/HCl pH 6.8	2.4 ml	Tris	30.3 g
20% SDS	3.0 ml	Glycine	144 g
Glycerol (100%)	3.0 ml	SDS	10 g
Bromophenol blue	0.006 g		
Make to 10 ml with water and store 4°C.		Make to 1000 ml with water.	

2.7.2 Coomassie stain

SDS/PAGE gels were stained for protein using Coomassie Brilliant Blue. After the electrophoresis the gels were soaked in an aqueous solution of 0.5 % (w/v) Coomassie Brilliant Blue, 50% methanol, and 10% acetic acid for 2 hours at room temperature with gentle shaking. The Coomassie binds preferentially to positively charged amino acid side chains but can also bind to the acrylamide gel itself. Destaining is required to remove non-specific bound Coomassie. The gels were rinsed with water and destained in aqueous solution of 10% acetic acid, 10% methanol with gentle shaking until protein bands could be clearly visualized.

2.7.3 Haem stain

2.7.3.1. Colorimetric method (Goodhew *et al*, 1986)

Haem staining relies on peroxidase activity of the haem moiety. The SDS-PAGE gel was equilibrated in 30 ml of 0.25 M sodium acetate/acetic acid (pH 5) for 15 minutes at room temperature. Then, 20 mg of light-sensitive 3,3',5,5'-Tetramethyl benzidine (3,3',5,5'-TMBZ) was dissolved in 20 ml methanol and added to the acetate buffer containing the gel. The container was wrapped in aluminum foil and incubated at room temperature for 15 minutes with gentle shaking. 150 μ l of 30% H₂O₂ was added to start the peroxidase reaction and the green stain was allowed to develop fully for 15 minute or maybe overnight. After staining gels were stored in water to resume regular size.

2.7.3.2 Chemiluminescent method (Vargas *et al*, 1993)

A rapid, nontoxic enhanced chemiluminescence (ECL) was used for staining haem *c* on nitrocellulose membrane. This method also relies on detection of peroxidase activity of haem moiety. Proteins from SDS-PAGE gels were transferred to nitrocellulose by blotting method described earlier. The membrane was stained with Ponceau S to check the efficiency of protein transfer and destained with water. 500 μ l of chemiluminescence agents (SuperSignal West Dura Substrate, Pierce) were mixed and spread across the membrane for 5 minutes. The membrane was sandwiched inside clear plastic and exposed to X-ray film for various durations (5 seconds– 5 minutes) to achieve an optimum luminescence signal. The protein bands containing haem *c* were clearly visualized upon film developing.

2.7.4 Spectra of protein samples

The spectra of protein sample such as Laz or membrane extract were measured by using UV-Visible spectrophotometry. Generally, the range of spectra measurement is from 250 nm to 800 nm. The Jasco V550 UV/VIS spectrophotometer and integrating reflective sphere ISV-469 were used throughout this study. The reflective sphere helps to compensate light scattering in experiments with membrane extract.

Spectra measurement of 1 ml of cell protein was done in 1.4 ml quartz cuvette with sealed cap (117.100F-QS, Hellma). Each measurement was undertaken in 5 repeats to achieve accumulated spectra or average spectra. The measurement was done under different redox state of proteins, reduced and oxidized by various reductant and oxidants.

2.7.5 Raising antibodies to Laz

Polyclonal antibodies specific to Laz was raised in rabbit. After immunizing, the rabbit sera were collected at Day 0, Day 35, Day 49, and Day 56. The production of polyclonal antibodies was done by Charles River Laboratories, France.

2.7.6 Western Blot

In this study, western blot was used to detect Laz protein and AniA protein under different growth conditions and among respiratory mutant strains. In order to detect specific protein, the proteins from SDS/PAGE were transferred onto nitrocellulose membrane and detected with antibodies specific to Laz or AniA. Blotting of protein was done using tank transfer system (Mini-Trans-Blot Cell) from Bio-Rad. The method details are as follows.

The SDS/PAGE gel was rinsed thoroughly in water and equilibrated in blotting buffer for 5 minutes. All components of blotting cassette, including fiber pads, filter

papers, and membrane were soaked and equilibrated in blotting buffer prior to use. The gel was placed onto nitrocellulose membrane (Hybond ECL, Amersham). The assembly should be done carefully to avoid air bubble trapped between gel and membrane. Filter papers and fiber pads were used to hold the gel and nitrocellulose together in a blotting cassette. In tank (or wet) transfer systems, the gel and membrane sandwich is held within a gel holder cassette and submerged entirely under blotting/transfer buffer. Proteins were transferred at 4°C at 100 V for one hour or at 30 V for overnight. The efficiency of transfer was checked by using prestained protein markers or staining blotted membrane with Ponceau S solution (0.1% w/v in 5% acetic acid) for 5-10 minutes. Ponceau was rinsed off and the membrane was blocked in PBS-Tween + 3% skimmed milk at room temperature for 1 hour with gentle shaking. To probe specific protein by antibodies, the membrane was transferred into PBS-Tween + 1% skimmed milk + 0.005% α Laz antibodies. The membrane was incubated at 4°C for 1 hour with gentle shaking. The membrane was washed with PBS-Tween for 20 minutes once and for 5 minute four times with fast shaking. To probe the primary antibody, the membrane was put into PBS-Tween + 1% skimmed milk + 0.01% secondary antibody (α Rabbit IgG-HRP) and incubated at room temperature for 1 hour with slow shaking. The membrane was washed with PBS-Tween for 20 minutes once and for 5 minute four times with fast shaking. 500 μ l of chemiluminescence agents (SuperSignal West Dura Substrate, Pierce) were mixed and spread across the membrane for 5 minutes. The membrane was sandwiched inside clear plastic and exposed to X-ray film for various durations (5 seconds – 5 minutes) to achieve an optimum luminescence signal.

<p>25X Tris/Glycine stock</p> <p>Tris 18.2 g Glycine 90.0 g Make to 1000 ml in water.</p>	<p>10X PBS-Tween stock (1000 ml)</p> <p>NaCl 80 g KCl 2 g KH₂PO₄ 2 g Anhydrous Na₂HPO₄ 11.5 g Tween 20 30 ml</p> <p>Make to 1000 ml in water.</p>
<p>Blotting buffer (1000 ml)</p> <p>25X Tris/Glycine stock 40 ml Methanol 200 ml Water 760 ml</p>	

2.7.7 Dot Blot

Laz was also detected by dot blot. Total cell extracts were prepared in 50 mM Tris pH 8. Total protein contents were equalized to 0.25 mg/ml. Series of 2 fold dilution of protein samples were made. 5 µl of each protein sample was dotted onto nitrocellulose membrane and the dots were allowed to dry in air. The detection of Laz on membrane using αLaz antibodies and αRabbit IgG-HRP was similar to the method described earlier in Western Blot.

2.7.8 Electrospray mass spectrophotometry

This technique was used for identifying and characterizing purified meningococcus Laz protein heterologously expressed in *E. coli*. It was done by Molecular Interaction Laboratory, Technology Facility, Biology Department. Laz protein samples in various solvents such as 20% methanol, acetonitrile, or acidic solvent were sprayed from a fine electrically charged nozzle. This created droplets from which the solvent evaporates leaving the protein molecules as charged particles. These droplets were introduced into a mass analyser which measures their mass/charge ratio (m/z). As m/z can be measured to high accuracy (1 part in 10000 or better) the mass of the protein molecules can be determined. The resolution is much better than any other physical technique, allowing tiny changes such as mutation of a single amino acid

residue or addition of a modifying group to be detected, where this might be difficult or impossible e.g. by gel electrophoresis or activity measurements.

2.7.9 Protein fingerprinting

Protein fingerprinting was used for identifying major membrane proteins in the outer membrane vesicles of the meningococcus. It was done by the Proteomics and Analytical Biochemistry Laboratory, Technology Facility, Biology Department. Briefly, protein samples on SDS-PAGE gel were cut and digested by trypsin. The absolute masses of peptide were then measured by matrix assisted laser ionization mass spectrometry (MALDI-MS). Detected masses are then compared with a database of known proteins to find the best match.

2.8 *In vivo* assays with *N. meningitidis*

2.8.1 Measurement of oxygen uptake

The measurement of oxygen uptake by intact cell was used to determine the rate of oxygen respiration in this organism. The measurement was done using a Clark electrode (Clark *et al*, 1953). The electrode was supplied by Rank Brothers, Cambridge, UK. The electrode consisted of a silver anode and a platinum cathode set in well filled with saturated KCl as an electrolyte. The electrode compartment is isolated from the reaction chamber by a thin teflon membrane which permeably allows molecular oxygen reach the cathode, where it is electrolytically reduced. 3 ml of cell suspension was added in the electrode chamber and was stirred with a magnetic flea to maintain equilibrium of oxygen concentration. The chamber was sealed with an adjustable cap with narrow entry port through which additions were made or NO probe was inserted. The temperature of the chamber was controlled through an external circulating

waterbath. The reduction of oxygen allows a current to flow and a potential difference was recorded on a chart recorder (Graphic1002, Seatallan Ltd) over time course.

2.8.2 Measurement of nitric oxide

Nitric oxide concentration in bacterial suspension was measured using nitric oxide sensor (ISO-NOP 2mm) connected with isolated nitric oxide meter (ISO-NO Mark II, World Precision Instruments). This nitric oxide sensor probe was inserted through an entry port of the sealed cap of oxygen electrode chamber to immerse 2-3 mm in cell suspension. Once nitrite was added, through another port, to final concentration of 5 mM in cell suspension, nitric oxide was generated through nitrite reduction by intact cells. A current was shown on the nitric oxide meter and was recorded on a chart recorder. The measurement of nitric oxide and oxygen can be undertaken simultaneously.

2.8.3 Assay for nitrite

The ability to utilize nitrite as respiratory substrate was measured in bacterial growing culture using the colorimetric assay described by Nicholas and Nason (1957). The reaction involves conversion of nitrite into nitrous acid in acidic medium followed by diazotization of sulphanilic acid and formation of a diazonium salt. The diazonium salt is then combined with naphthylethylenediamine to form an azo pink dye which intensity can be determined by absorbance at 540 nm. Each 50 μ l of sample was added to 850 μ l of 1% sulphanilamide in 1M HCl. Then, 100 μ l of 0.02% N-naphthylethylenediamine in 1M HCl. The mixture was measured for absorbance at 540 nm and compared to standard curve.

2.8.4 Spectra measurement of intact cells

The spectra of intact cells were measured by using UV-Visible spectrophotometry. Generally, the range of spectra measurement is from 350 nm to 800 nm. Spectra of bacterial intact cell are predominantly of cytochromes. The Jasco V550 UV/VIS spectrophotometer and integrating reflective sphere ISV-469 were used throughout this study. The reflective sphere helps to compensate light scattering in a very high cell density bacterial suspension.

Bacterial cultures were grown to late log phase, harvested, and resuspended in 25 mM HEPES pH 7 with 5 mM glucose. Glucose was used to generate reducing equivalents, such as NADH, in intact cells. The optical density of bacterial suspension was adjusted to 1.0-1.2 at 600 nm. Spectra measurement of 1 ml of cell suspension was done in 1.4 ml quartz cuvette with sealed cap (117.100F-QS, Hellma). Each measurement was undertaken in 5 repeats to achieve accumulated spectra or average spectra. The measurement was done under different redox state of cells, reduced and oxidized. Normally, cell suspension at this high optical density becomes reduced quickly. Upon adding oxygen by strong shaking of cuvette, cells become temporarily oxidized and return to reduced state. Both reduced spectra and oxidized spectra were measured and recorded. Nitrite and hydrogen peroxide were also used for oxidation of cells. Only small volume, 5 μ l, of nitrite or hydrogen oxide solution was injected into the cuvette to prevent drastic change in total volume of cell suspension.

Chapter 3

Cytochromes of *N. meningitidis*

3.1 Introduction

Genome analysis of the meningococcus with respect to respiratory chains has revealed the possibility that there are three terminal reductases. First, an oxidase of the cytochrome *cbb₃*-type which utilizes oxygen as respiratory substrate. Second, a nitrite reductase of the copper-containing protein AniA which utilizes nitrite. Third, a single subunit nitric oxide reductase of the *b* haem-containing protein NorB which utilizes nitric oxide. It has been shown that *N. meningitidis* is able to use oxygen for aerobic respiration to support growth under aerobic conditions and nitrite as an alternative terminal electron acceptor for anaerobic respiration to support growth under microaerobic conditions (Rock *et al*, 2005). The reduction of nitric oxide is predicted to be directly dependent on the quinone pool, not the cytochrome *bc₁* complex. Beyond the detoxifying role of NorB, the reduction of nitric oxide also takes part in the electron transport chains. The reduction of nitric oxide, therefore, is an energy-transducing process. The reduction of *cbb₃* oxidase and AniA nitrite reductase is predicted to be dependent on *bc₁* complex and small periplasmic *c*-type cytochromes. In general, cytochromes are major components of respiratory chains and play a crucial role in growth.

Cytochromes display strong absorption of visible light. Different redox state of cytochromes show different absorption features. This property of light absorption can be used to study the organization of respiratory chains using intact cell suspension. This chapter will investigate the organization of the respiratory chains using the oxidation of

cytochromes in intact cells of *N. meningitidis* by three different respiratory substrates, oxygen, nitrite, and nitric oxide

3.1.1 Types of cytochromes in *N. meningitidis*

Genome sequence analysis revealed that the predicted cytochromes in *N. meningitidis* are *b*-type and *c*-type. In respect of structure, there is no structural difference between *b*-haem and *c*-haem in *b*-type cytochromes and *c*-type cytochromes, respectively. The only difference is that in *c*-type cytochrome haem is covalently bound to protein while haem in *b*-type cytochrome is not covalently bound. *N. meningitidis* contains predicted 55 genes involved in electron transport. There are 5 genes encoding for *b*-type cytochromes and 7 genes encoding for *c*-type cytochromes (Table 3.1). Two of *b*-type cytochromes are identical (NMB1158 and NMB 1196, Table 3.1). The genes flanking these *b*-type cytochromes are also identical suggesting that they originated from gene cluster region duplication. The regulation of cytochrome expressions in *N. meningitidis* is not well understood. In gonococcus, the components of *bc₁* complex and *cbb₃* oxidase are predicted to be constitutively expressed. Periplasmic cytochromes involved in respiratory metabolism are also predicted to be constitutively expressed (Turner *et al*, 2005). It might be possible that most of the meningococcal cytochromes are also constitutively expressed.

N. meningitidis lacks cytochrome *c* peroxidase that is present in *N. gonorrhoea* (Turner *et al*, 2003). Another *c*-type cytochrome in the meningococcus is cytochrome *c'*. It has been demonstrated that the cytochrome *c'* has a role in nitric oxide detoxification (Anjum *et al*, 2002; Huston *et al* 2005).

Locus	Gene Symbol	Common Name
NMB_0717		cytochrome <i>c2</i>
NMB_0923		cytochrome <i>c'</i>
NMB_1158		nickel-dependent hydrogenase, <i>b</i> -type cytochrome subunit
NMB_1196		nickel-dependent hydrogenase, <i>b</i> -type cytochrome subunit
NMB_1622	<i>norB</i>	nitric oxide reductase
NMB_1677		cytochrome <i>c5</i>
NMB_1723	<i>fixP</i>	cytochrome oxidase, subunit III cytochrome <i>c</i>
NMB_1724	<i>fixO</i>	cytochrome oxidase, subunit II cytochrome <i>c</i>
NMB_1725	<i>fixN</i>	cytochrome oxidase, subunit I cytochrome <i>b</i>
NMB_1805		cytochrome <i>c4</i>
NMB_2051	<i>petC</i>	ubiquinol--cytochrome <i>c</i> reductase, cytochrome <i>c₁</i>
NMB_2052	<i>petB</i>	ubiquinol--cytochrome <i>c</i> reductase, cytochrome <i>b</i>

Table 3.1 List of genes encoding for cytochromes in *N. meningitidis*. The NMB1158 and NMB1196 genes are identical. Their flanking genes are also identical. They are probably the result of gene cluster duplication.

3.1.2 Spectral feature of cytochromes

Since most cytochromes exhibit strong absorption of visible light (wavelength of 350-700 nm), visible light spectra of cytochromes is a very useful characteristic used for investigating organization of respiratory chains. Absorption of light in the range of 350-700 nm by cytochromes occurs differently depending on the redox state of cytochrome and structure of cytochromes. At reduced state, cytochromes exhibit light absorption around three bands, α , β , and Soret. Upon oxidation, the absorption in α and β bands are decreased while absorption in Soret band is blue-shifted. In general, the reduced minus oxidized difference spectra of a cytochrome exhibits three major absorption bands, the α band (545-650 nm), the β -band (520-530 nm), and the γ -band or Soret band (410-450 nm) (Jones and Poole, 1985). The structure of cytochromes shows different spectral features, especially at area of α band (Table 3.2). The proteins

predicted to be *c*-type cytochromes contain conserved amino acid motif of C-XX-CH while this motif is not found in *b*-type cytochromes.

Cytochrome	Wavelength (nm)	Source
<i>aa</i> ₃	605-630	<i>Paracoccus denitrificans</i>
<i>b</i>	560-575 563-577	<i>Escherichia coli</i> Beef heart mitochondria
<i>b</i> haem	562-580	<i>Escherichia coli</i> <i>bd</i> complex
<i>c</i>	550-540	Beef heart mitochondria
<i>c</i> ₁	552-540	Beef heart mitochondria
<i>d</i>	630-655	<i>Escherichia coli</i>
<i>d</i> haem	628-608	<i>Escherichia coli</i> <i>bd</i> complex
<i>o</i>	553-571	<i>Vitreoscilla</i>

Table 3.2 Difference spectra from reduced minus oxidized spectra. Selected wavelengths are spectral features of the alpha band of each type of cytochrome (modified from Jones and Poole, 1985).

In this chapter, these aspects will be studied. 1) Spectral features of cytochromes in intact cells of *N. meningitidis*. 2) The involvement of cytochromes in different branches of respiratory chains. Three different respiratory substrates of the meningococcus will be used as oxidants of intact cells. 3) The influence of oxygen and nitrite on expression of cytochromes. 4) Role of FNR in regulation of cytochrome expression. 5) The interplay between these respiratory substrates with respect of regulation of respiration.

3.2 Results

3.2.1 Visualization of cytochromes in by western blot and ECL chemiluminescence

The purpose was to characterize *c*-type cytochromes of the meningococcus by SDS-PAGE and to investigate the effect of oxygen and nitrite level on expression of *c*-type cytochromes. The role of FNR in regulation of *c*-type cytochromes was also investigated. Wild type strain and *fnr* mutant strain were grown under three different growth conditions, aerobic, microaerobic, and denitrifying conditions. In this investigation, soluble fraction of whole cell extracts were prepared and solubilized in 25 mM HEPES pH 7.0 with 1% dodecyl maltoside to give better resolution of cytochrome profiles. After solubilization, soluble fractions were separated and used for SDS-PAGE. The haem group of *c*-type cytochromes is covalently linked to the protein polypeptide. It is quite stable and can be characterized using haem-staining on SDS-PAGE gel by the method of Goodhew (Goodhew *et al*, 1986). Alternatively, it can be visualized by detecting peroxidase activity using chemiluminescence after blotting gels onto nitrocellulose membrane (Vargas *et al*, 1993). Since the haem group has peroxidase activity, it can be detected by using hydrogen peroxide substrate with chemiluminescence. The chemiluminescent signal is then detected by exposure on X-ray film. Then, the signal is visualized upon developing the film. However, this method does not represent the absolute amount of cytochrome but the peroxidase activity of the cytochrome.

There are 4 *c*-type cytochromes detected by this ECL chemiluminescence staining (Figure 3.1). One having MW of 48 kDa is predicted to be FixP (NMB1723), a cytochrome subunit of *cbb*₃ oxidase. The one having MW of 35 kDa is predicted to be cytochrome *c*5 (NMB1677), while that having MW of 28 kDa is predicted to be PetC or cytochrome *c*₁ (NMB2051) subunit of the *bc*₁ complex. The protein with 23 kDa is

predicted to be cytochrome *c4*. The smear below *c4* band might be degradation products of cytochrome *c4*. All detectable *c*-type cytochromes are constitutively expressed under different level of oxygen and nitrite. Neither level of oxygen nor nitrite affects the expression of *c*-type cytochromes. The expressions of these *c*-type cytochromes in the meningococcus are not regulated by FNR as *fnr* mutant showed no differences from wild type. However, FixP subunit of *cbb₃* oxidase expression appeared to be slightly increased under microaerobic conditions. The expressions of these cytochromes were not altered under different growth conditions.

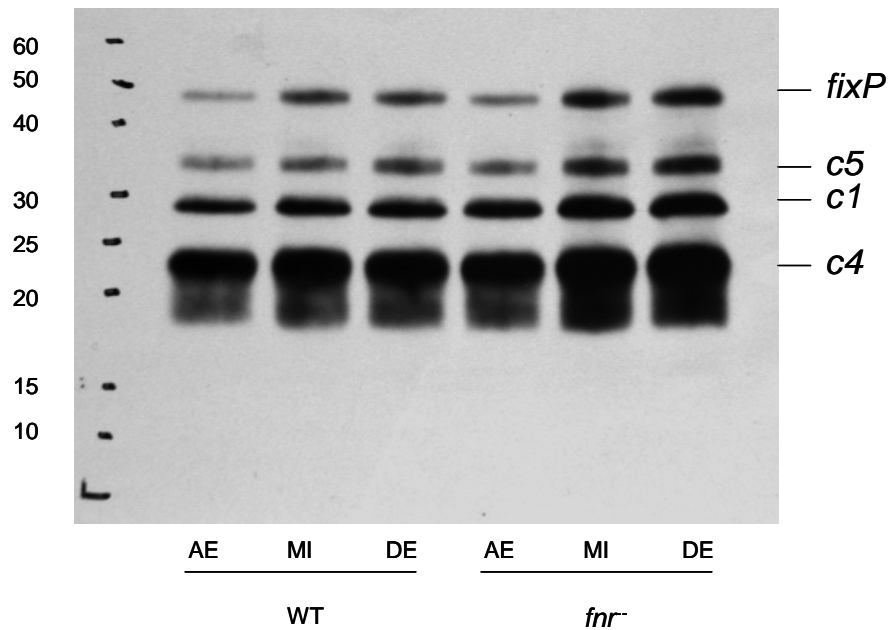


Figure 3.1 Cytochrome profiles of *fnr* mutant and wild type meningococcus under different growth conditions. Extracts were separated by SDS-PAGE, blotted and stained for haem. The amount of protein loaded in each lane is 10 µg. AE = aerobic conditions, MI = microaerobic conditions, DE = denitrifying conditions which is microaerobic conditions with nitrite.

3.2.2 Spectroscopic analysis of cytochromes in intact cells

In order to investigate the organization of cytochromes in the respiratory chain in *N. meningitidis*, spectroscopy of intact cells was used. *N. meningitidis* was grown in

MHB with 5 mM glucose to induce the expression of machinery for utilizing glucose as another carbon source. Glucose was used as sole carbon source later in cell suspension as a physiological electron donor into the respiratory chain following the catabolic production of reducing equivalents (NADH, etc.) during spectra measurement. *N. meningitidis* was grown aerobically on Columbia agar supplemented with 5% horseblood at 37 °C in an air atmosphere supplemented with 5% CO₂. Under this condition, it might not be fully aerobic. For liquid culture, *N. meningitidis*, was grown in Mueller-Hinton broth supplemented with 10 mM NaHCO₃ and sometimes supplemented with 5 mM glucose. For aerobic growth, 6 ml of the medium was incubated in 25 ml McCartney flasks shaken at 200 rpm. For denitrifying growth, 20 ml of cultures supplemented with 5mM NaNO₂ in 25 ml McCartney flasks were shaken at 90 rpm. Cultures were incubated at 37 °C for about 12-14 hours. After that, cells were separated and resuspended in 25 mM HEPES with 5 mM glucose to optical density 600 nm above 1.0. Then, 1 ml of cell suspensions was transferred into a 1.5 ml quartz cuvette with rubber sealed cap. Cytochrome spectra of intact cells were measured using UV-VIS spectrophotometer fitted with a reflective sphere for collection of light scattered by the highly turbid cell suspensions.

3.2.2.1 Oxidation by oxygen

The purpose was to investigate what type of cytochrome(s) can be oxidized upon exposure of intact cells to oxygen and what growth conditions allow cytochrome oxidation by oxygen. Under anaerobic conditions in cuvettes, cell suspensions supplemented with glucose rapidly became reduced, giving rise to UV–visible spectral features characteristic of *b*- and *c*-type cytochromes. (Figures 3.2 and 3.3). Following the addition of oxygen to these cell suspensions, the spectral features due to reduced α - and β -bands disappear and the Soret peak is blue-shifted, indicating oxidation of

cytochromes (Figure 3.2 and 3.3). Difference spectra (Figure 3.4) show that the oxygen-dependent oxidation is characterized by the disappearance of a major α -feature at 552 nm. This feature is presumably made up of a number of *c*-type cytochromes that are found in the electron transport pathway to oxygen, and fewer *b*-type cytochromes as indicated by the slight shoulder on the α -band around 560 nm, especially in cells grown under denitrifying conditions. Oxygen can oxidize both cells grown under aerobic conditions and denitrifying conditions (Figure 3.4). Interestingly, oxidation of cells grown in denitrifying conditions exhibited small absorption at 560 nm in alpha band while this absorption was not found in that from cells grown under aerobic conditions (Figure 3.5A and 3.5B).

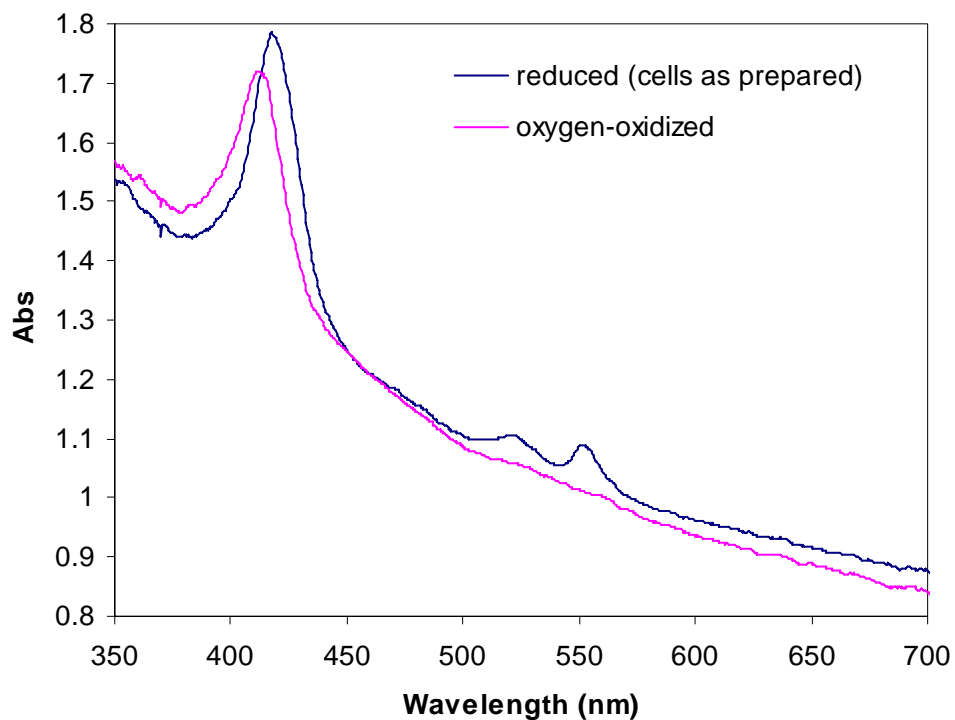


Figure 3.2 The spectral features of cytochromes in *N. meningitidis* cells grown under aerobic conditions. The reduced spectra showed absorption in three areas around 416 nm, 520 nm, and 551nm. The oxygen oxidized spectra showed absorption shift from 416 nm to 411 nm (blue shift) while the absorption around 520 and 551 nm disappeared.

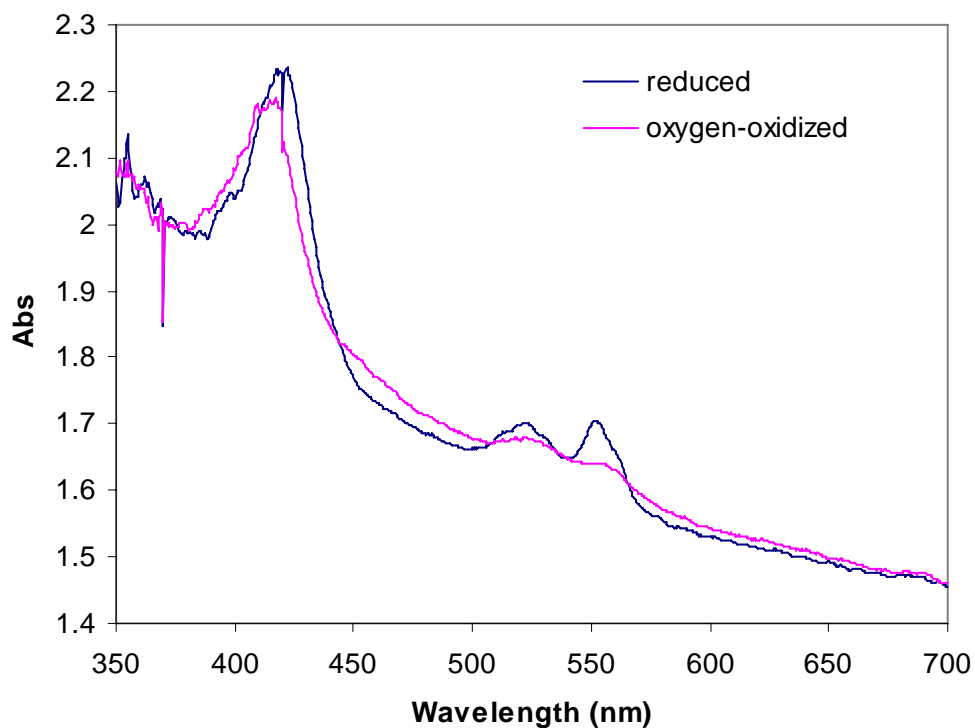


Figure 3.3 The spectral features of cytochromes in *N. meningitidis* cells grown under denitrifying conditions. The reduced spectra showed absorption in three areas around 416 nm, 520 nm, and 551nm. The alpha peak exhibits noticeable shoulder around 560 nm while this shoulder is lacking in aerobic preculture cells (Figure 3.2). The oxygen oxidized spectra showed absorption shift from 416 nm to 411 nm (blue shift) while the absorption around 520 and 551 nm decreased.

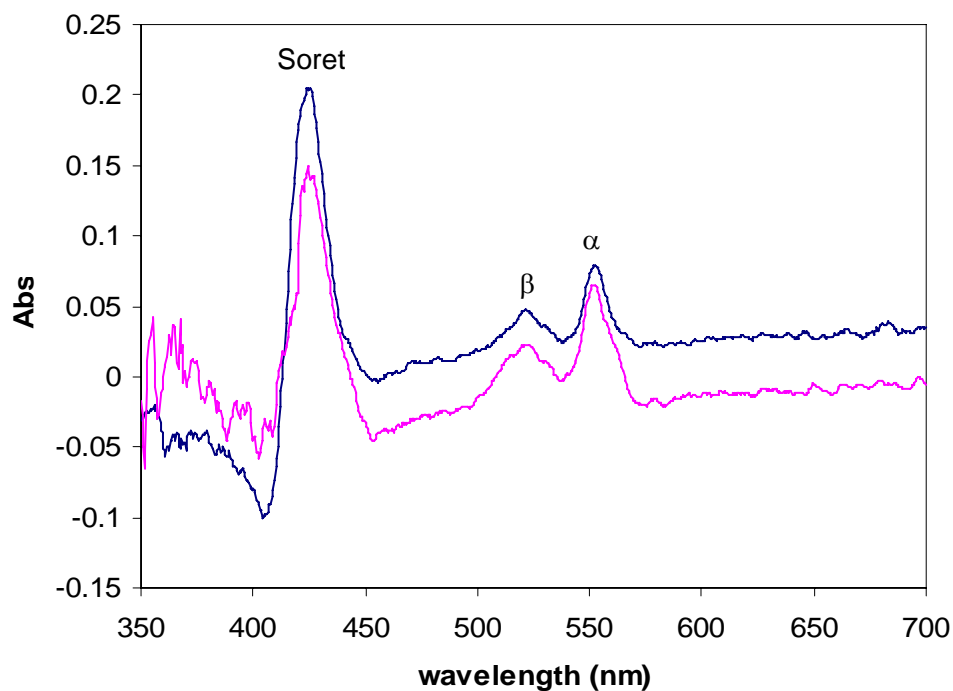


Figure 3.4 Comparison of difference spectra between reduced and oxygen oxidized spectra from cells grown under aerobic conditions (blue) and denitrifying conditions (pink). In general, the reduced minus oxidized difference spectra of a cytochrome exhibits three major absorption bands, the α band (545-650 nm), the β band (520-530 nm), and the γ band or Soret band (410-450 nm). The α peak of both type of cells are similarly at 552-553 nm. Interestingly, the alpha band of cells grown under denitrifying conditions exhibits more absorption around 560 nm than that from aerobic preculture cells.

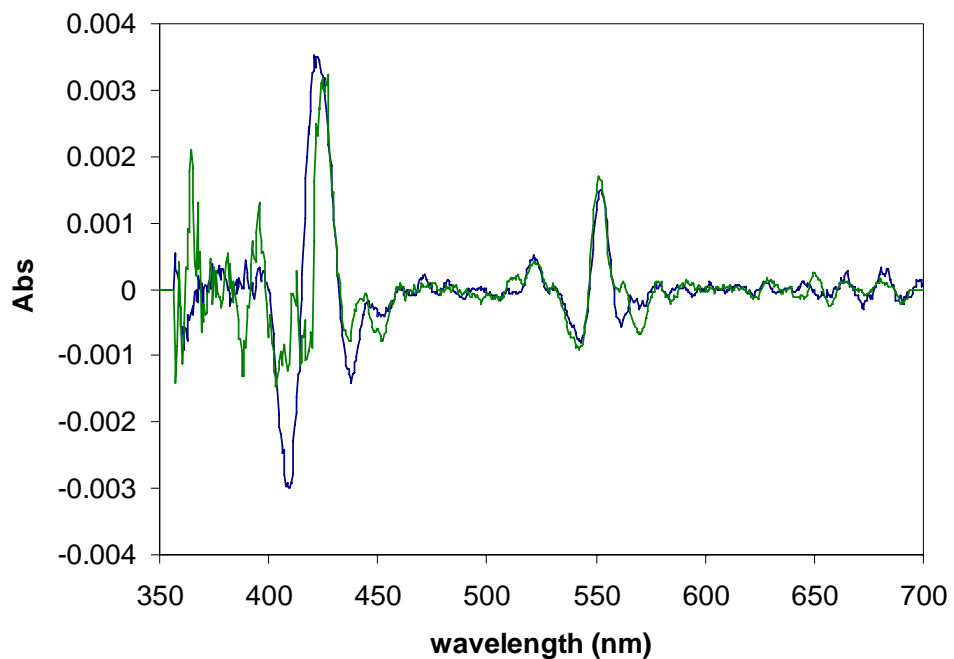


Figure 3.5A Double derivatives of oxidized minus reduced spectra from cells grown under aerobic conditions and denitrifying conditions. Oxygen can oxidize *c*-type and *b*-type cytochromes in cells grown under denitrifying condition (green) whereas there was no oxidizable *b*-type cytochrome present in cells grown under aerobic conditions (blue). This indicates that cells grown under denitrifying conditions can produce particular *b*-type cytochrome while cells grown under aerobic conditions can not. This *b*-type cytochrome can be oxidized by oxygen.

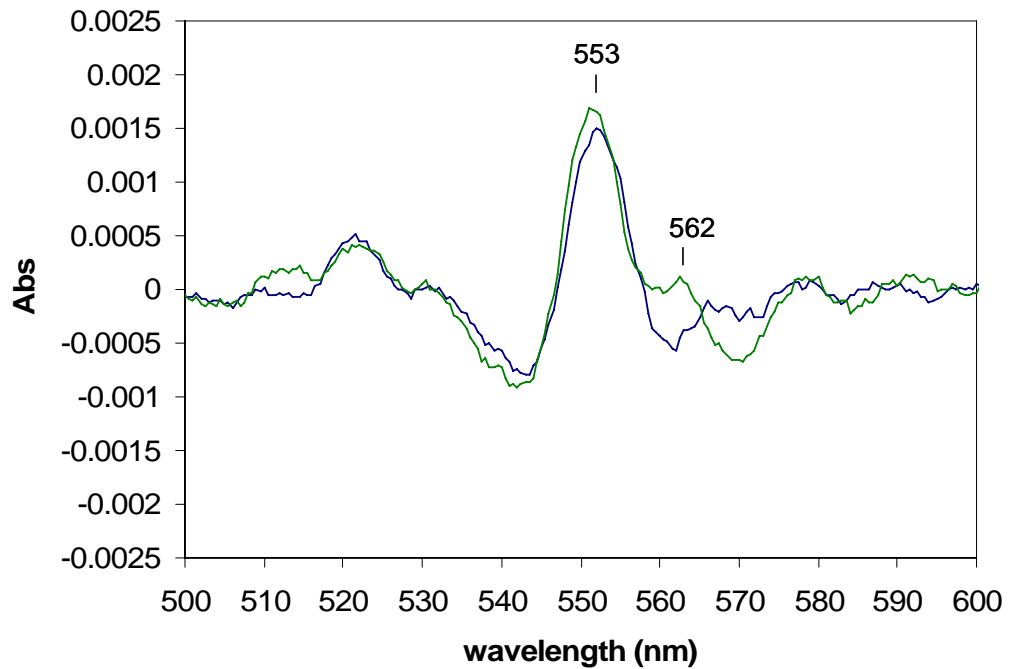


Figure 3.5B The α features of cells grown under aerobic and denitrifying conditions. Double derivative of oxidized minus reduced spectra is used to resolve alpha features of *c*- and *b*-type cytochromes. The derivative revealed that the oxidation by oxygen in cells grown under aerobic conditions (blue) exhibits only alpha band of *c*-type cytochromes. In cells grown under denitrifying condition (green), however, oxidation by oxygen produced two alpha peaks at 553 and 560 nm, indicating oxidation of both *c*-type and *b*-type cytochromes.

3.2.2.2 Oxidation by nitrite

The purpose was to investigate what type of cytochrome(s) that can be oxidized upon exposure of intact cells to nitrite and what growth conditions allow cytochrome oxidation by nitrite. Under anaerobic conditions in cuvettes, cell suspensions supplemented with glucose rapidly became reduced, giving rise to UV-visible spectral features characteristic of *c*-type cytochromes (Figure 3.6). In cells grown under aerobic conditions, following the addition of 5 mM nitrite to these cell suspensions, the spectral features due to reduced α - and β -bands and the Soret peak are not altered (Figure 3.6). Difference spectra (Figure 3.7) show that nitrite can not oxidize any cytochromes. However, the oxidation of cells grown under denitrifying conditions by nitrite show only decreased absorption at 560 nm in α area (Figure 3.8 and 3.9) while absorption in Soret area and β area were less than observed after oxidation by oxygen. The decreased absorption at 560 nm suggests the oxidation of *b*-type cytochrome(s). From the experiment, nitrite can only oxidize cells grown under denitrifying conditions and oxidizable cytochromes are *b*-type.

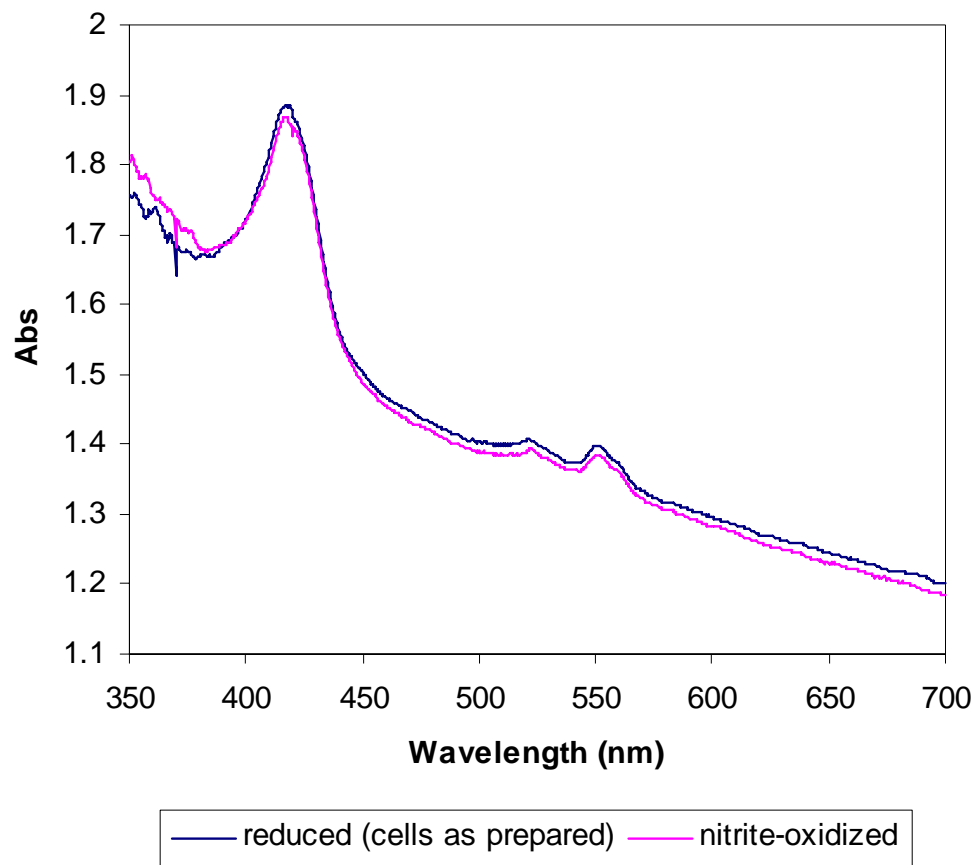


Figure 3.6 Nitrite can not oxidize cytochromes in cells grown under aerobic conditions.

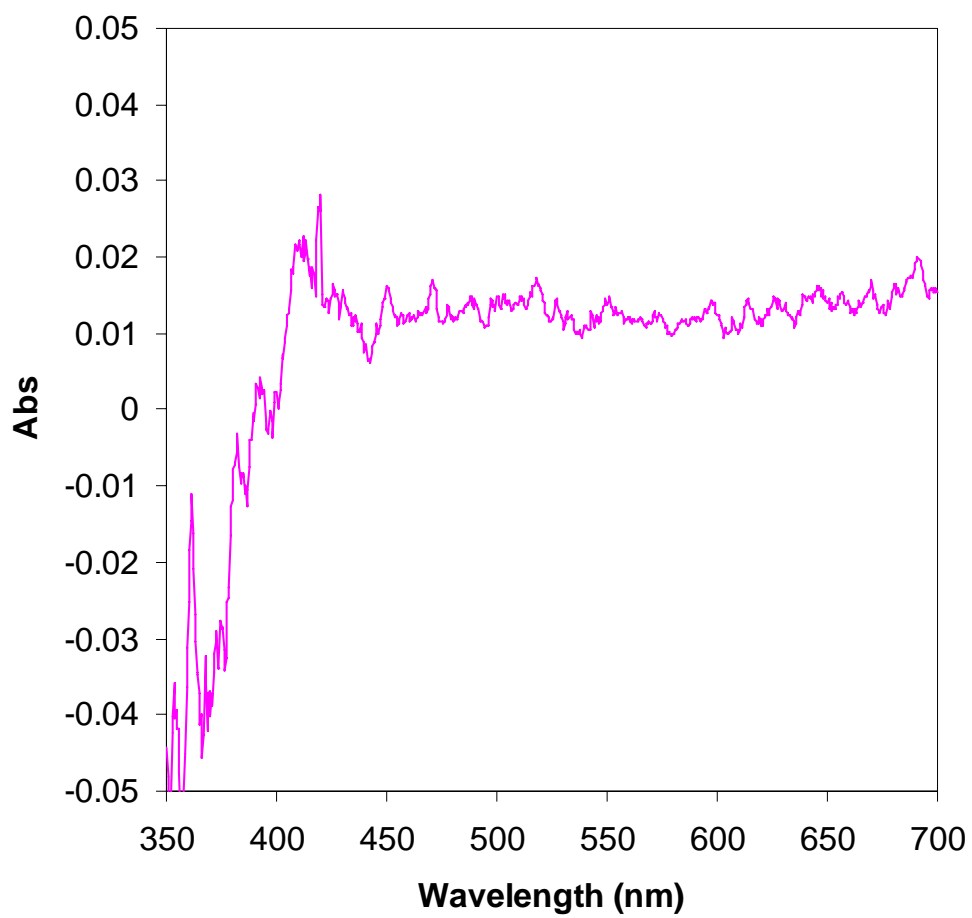


Figure 3.7 Reduced minus nitrite-oxidized difference spectra of cells grown under aerobic conditions. Nitrite can not oxidize cytochromes in cells grown under aerobic conditions.

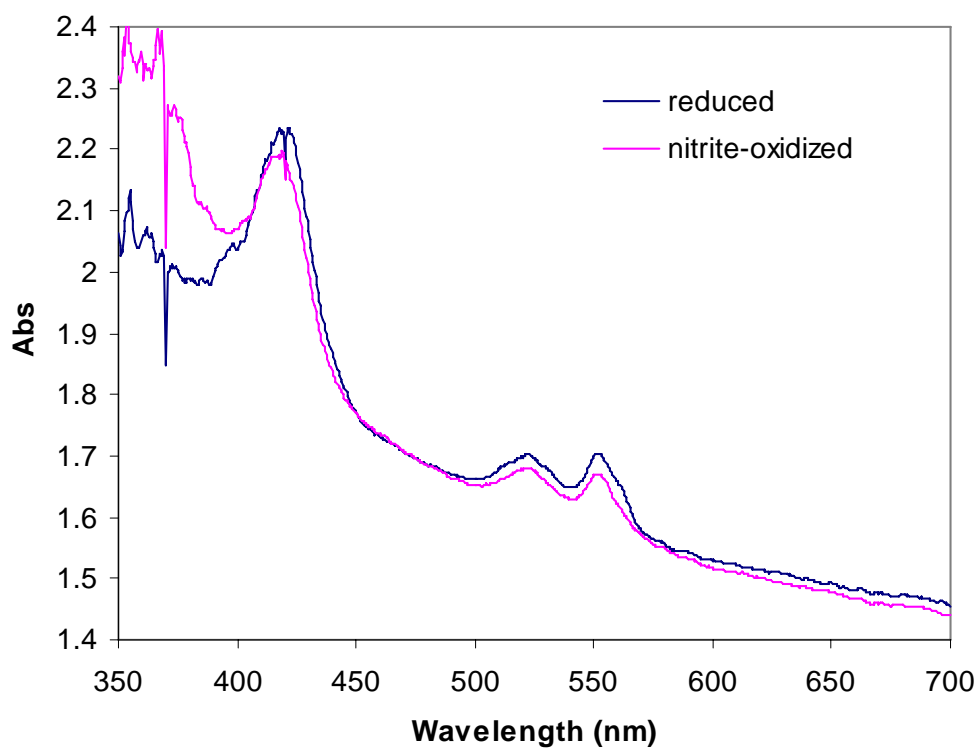


Figure 3.8 The spectral features of cytochromes in intact cells of *N. meningitidis* grown under denitrifying conditions oxidized by nitrite. The reduced spectra showed absorption in three areas around 416 nm, 520 nm, and 551nm. The nitrite oxidized spectra showed very low absorption shift from 416 nm (blue shift) while the absorption around 520 and 551 nm also decreased very little.

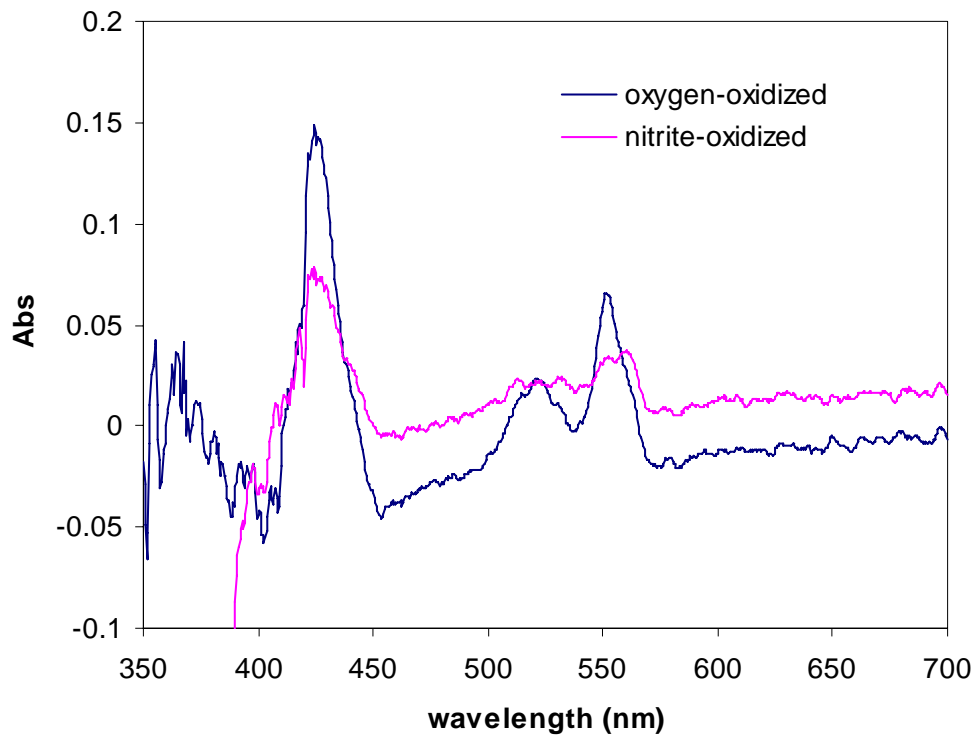


Figure 3.9 Oxidation of *b*-type cytochrome in cells grown under denitrifying conditions by nitrite. In cells grown under denitrifying conditions, cytochrome oxidation by nitrite produced α peak at 560nm indicating oxidation of *b*-type cytochrome. This is likely to be oxidation of *b*-haem in NorB nitric oxide reductase as denitrifying preculture cell can express AniA which reduces nitrite to nitric oxide. The oxidation by oxygen showed that oxidizable cytochromes are predominantly *c*-type cytochromes. Low levels of oxidation of *b*-type cytochrome by oxygen are also seen, as shoulder around 560 nm, but not predominant feature of the α band.

3.2.2.3 Oxidation by nitrite and oxygen

The meningococcus can utilize two terminal electron acceptors, oxygen and nitrite, as respiratory substrates to support growth (Rock *et al*, 2005). In term of redox potential energy, electron flow is more likely to favor oxygen over nitrite. It was assumed that in the presence of both respiratory substrates, electrons will flow more to oxygen. The purpose of this experiment was to investigate the interplay of these two respiratory substrate in controlling electron flow at a metabolic level. Denitrifying preculture cells were used in this experiment as the cytochromes can be oxidized by either oxidant. First, cells were oxidized by oxygen. Then cells were allowed to re-reduced for a few minutes before being oxidized by both nitrite and oxygen at the same time. It was found that oxidation by nitrite plus oxygen gave different spectra from those by either oxygen or nitrite alone (Figure 3.10 and 3.11). The oxidation of cytochromes by nitrite plus oxygen is intermediate between that by oxygen and that by nitrite (Figure3.11 and 3.12). The level of *c*-type cytochrome oxidation is lower than that by oxygen and the level of *b*-type cytochrome oxidation is also lower than that by nitrite alone.

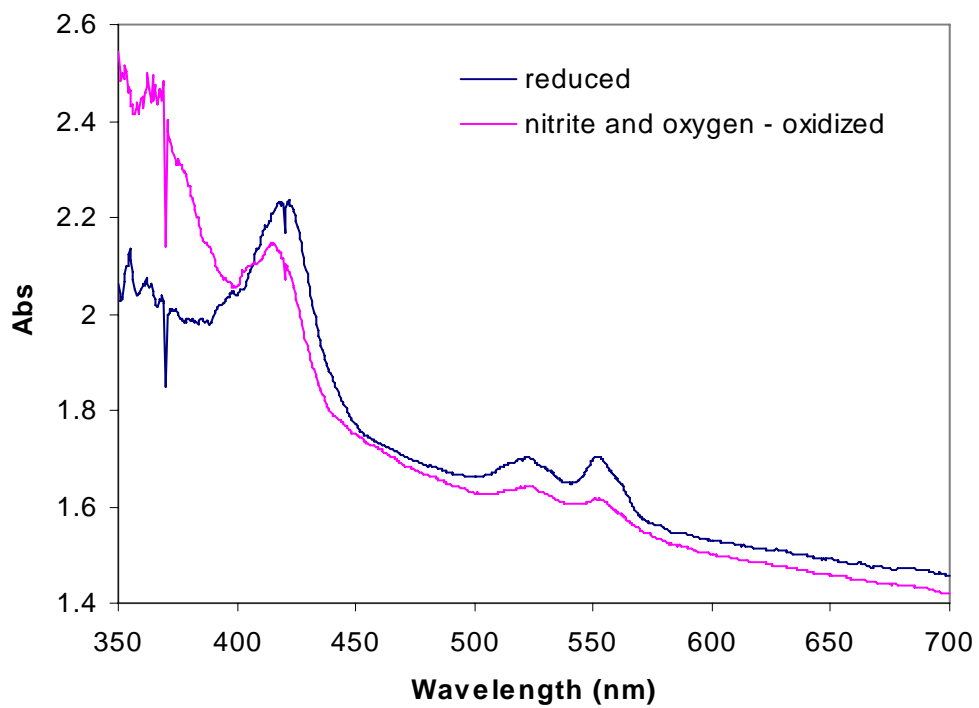


Figure 3.10 Nitrite inhibits oxidation of cells grown under denitrifying conditions by oxygen. Cells grown under denitrifying conditions were exposed to nitrite first and then were exposed to oxygen immediately after. Nitrite was shown to inhibit oxidation of cytochrome by oxygen.

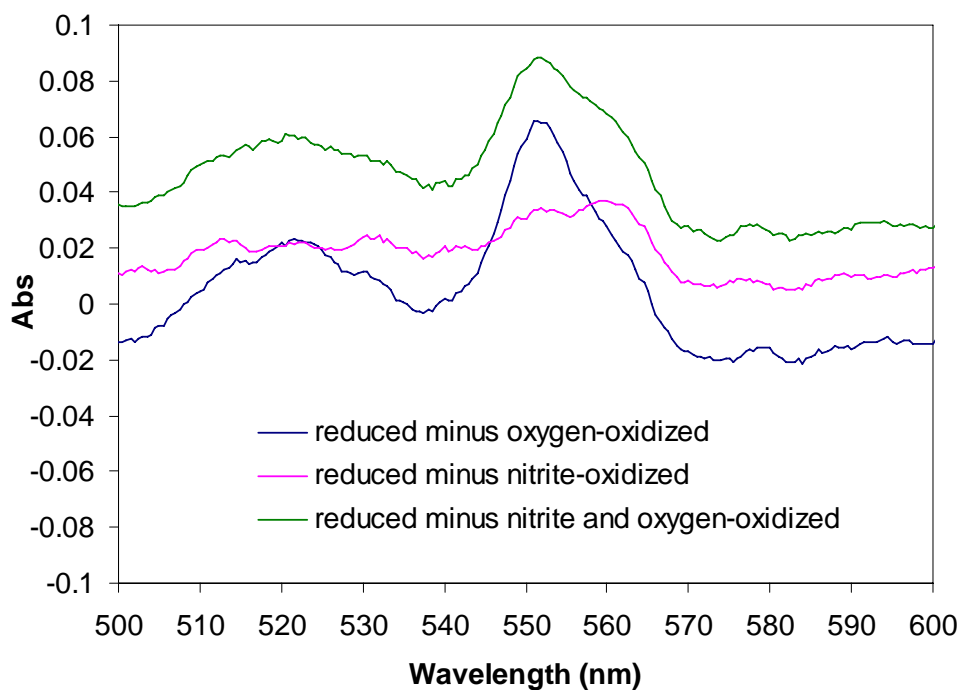
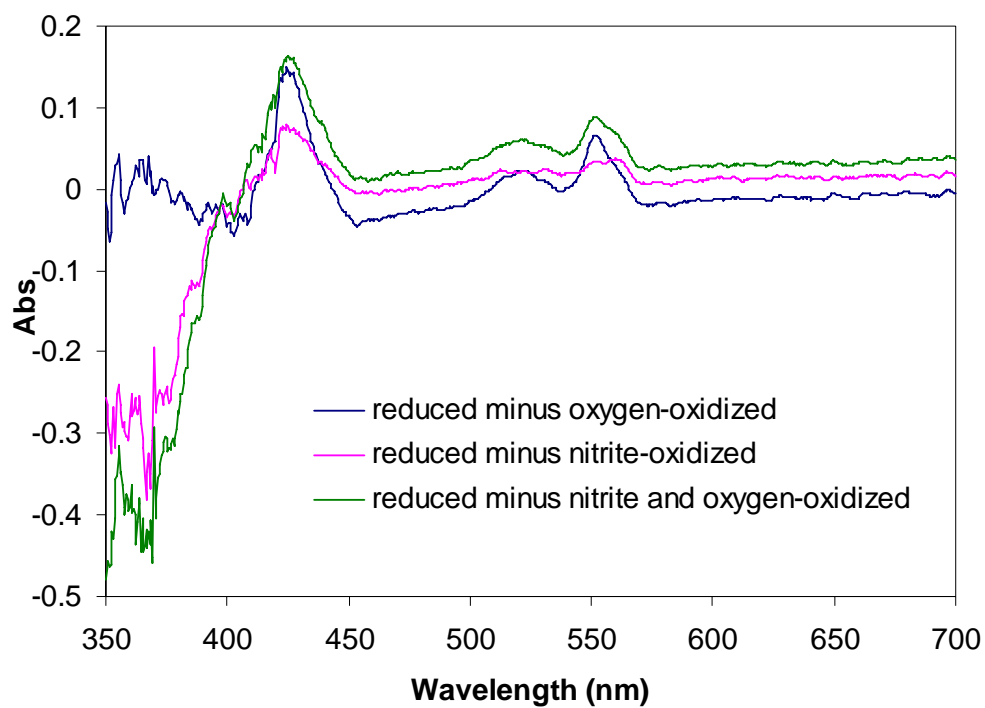


Figure 3.11 Comparison of cytochrome oxidation by different oxidants. The level of cytochrome oxidation by nitrite plus oxygen is intermediate between that by oxygen and that by nitrite.

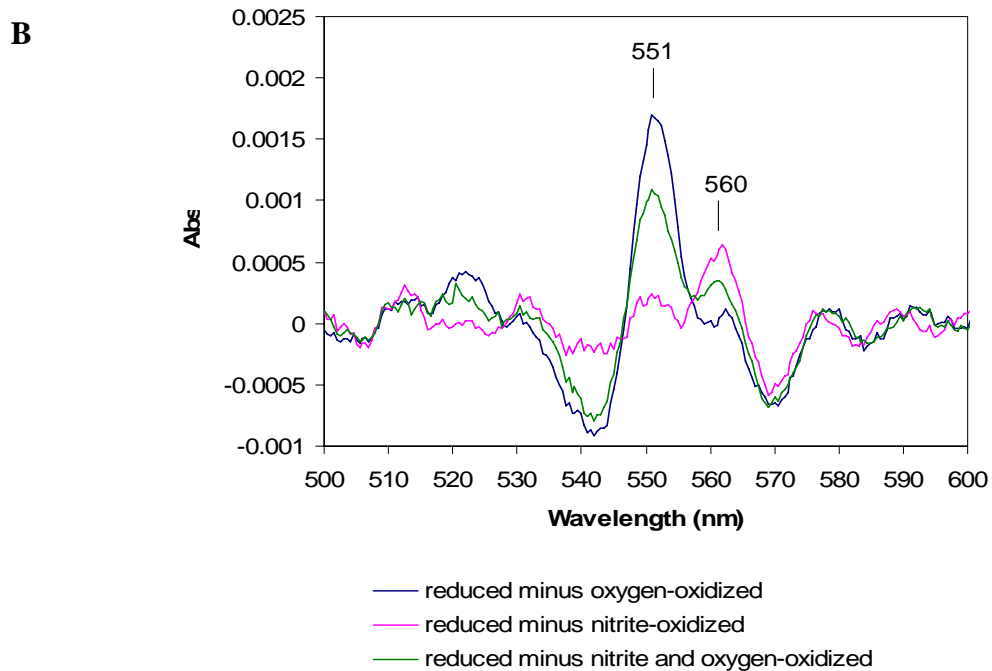
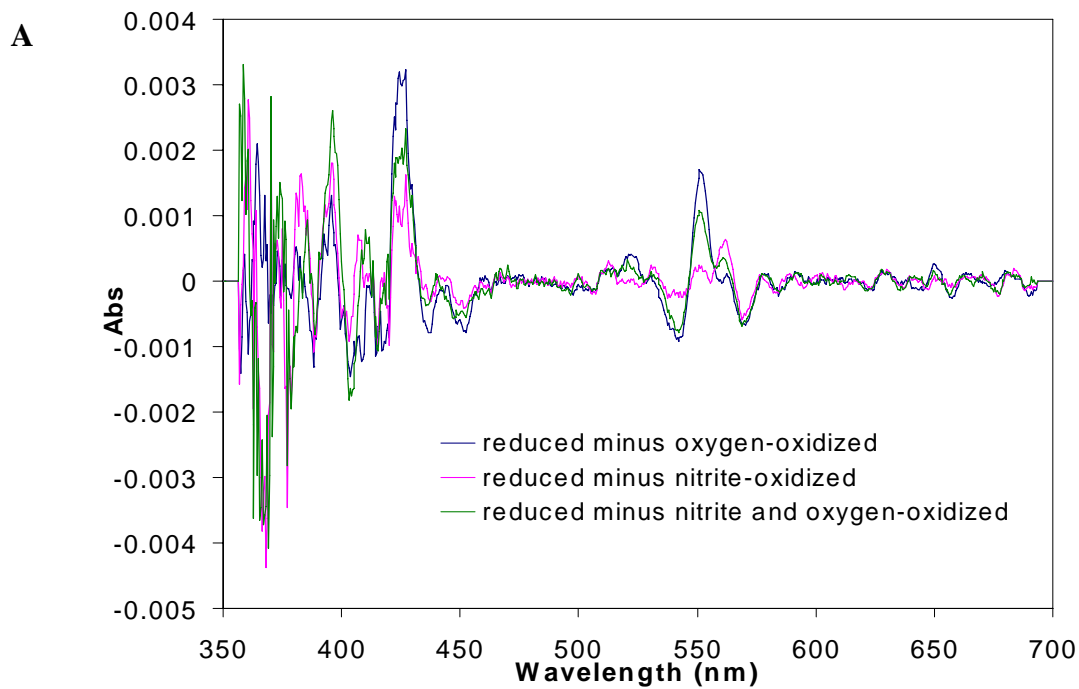


Figure 3.12 (Previous page) Double derivative difference spectra showing cytochrome oxidation by different oxidants. Double derivative of oxidized minus reduced difference spectra is used to resolve α features. Oxidation by oxygen shows that predominantly oxidizable cytochromes are *c*-type, α peak at 552 nm, though there is low level of *b*-type cytochrome oxidation, α peak at 560 nm. This might suggest that oxygen is able to oxidize *b*-haem in NorB to a lesser extent. The oxidation by nitrite shows that predominantly oxidizable cytochromes are *b*-type, α peak at 560 nm. The oxidation by nitrite plus oxygen show intermediate level of oxidation both in *c*-type and *b*-type cytochromes, suggesting that nitrite can inhibit *c*-type cytochrome oxidation by oxygen.

3.2.2.4 Oxidation of cytochrome by nitric oxide

The nitric oxide radical causes nitrosative stress to the meningococcus. The organism employs NorB to reduce nitric oxide to nitrous oxide as a means of neutralizing toxicity of this free radical. The removal of nitric oxide by NorB is predicted to be quinol dependent, based on homologs of NorB in other organism. Therefore, this process could possibly as well benefit the organism energetically, though to lesser extent than oxygen and nitrite. The purpose was to investigate the spectral features of cytochrome(s) upon oxidation by nitric oxide. As previously shown that oxidation of cytochromes by nitrite gave alpha peak at 560 nm suggesting oxidation of *b*-type cytochrome. This is likely to be an oxidation of NorB by nitric oxide generated from nitrite reduction. This experiment aimed to investigate if there is an evidence to support that notion. Denitrifying cells were exposed to 200 nM NONOate which released nitric oxide gradually. It was found that oxidation by NONOate gave similar spectra to that by nitrite (Figure 3.13 and Figure 3.14). It gave α peak at 560 nm.

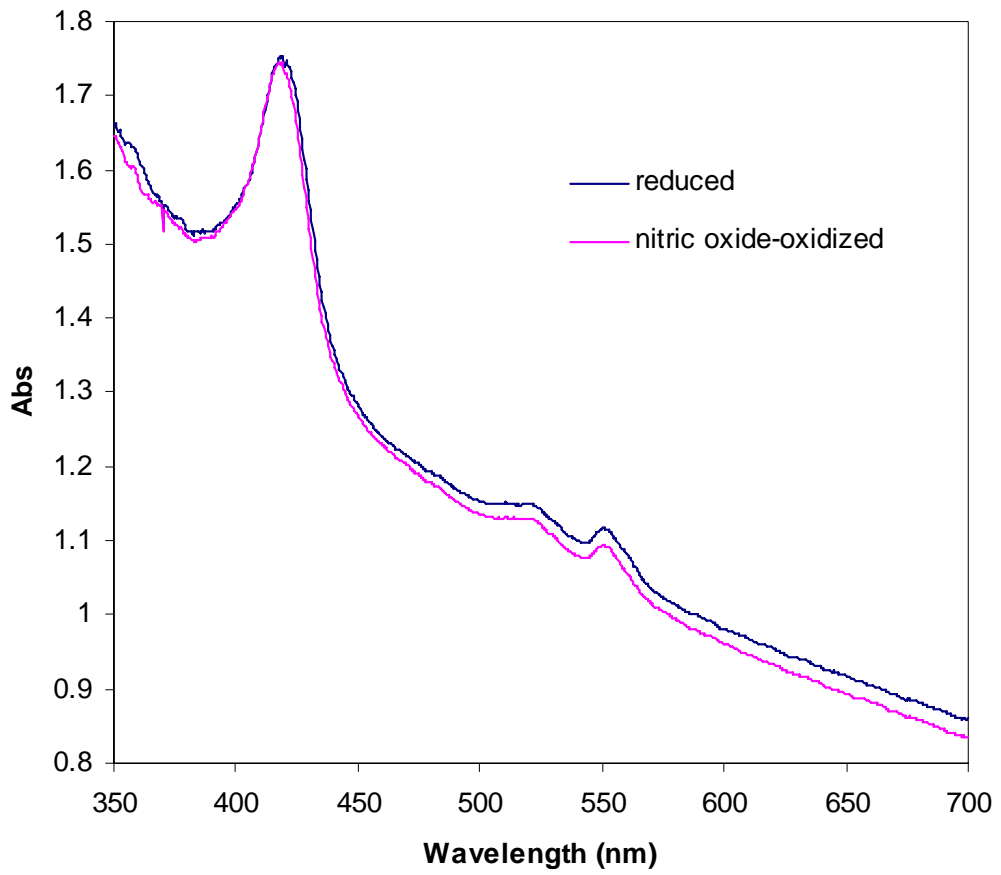


Figure 3.13 Oxidation of cytochromes in cells grown under denitrifying conditions by nitric oxide.

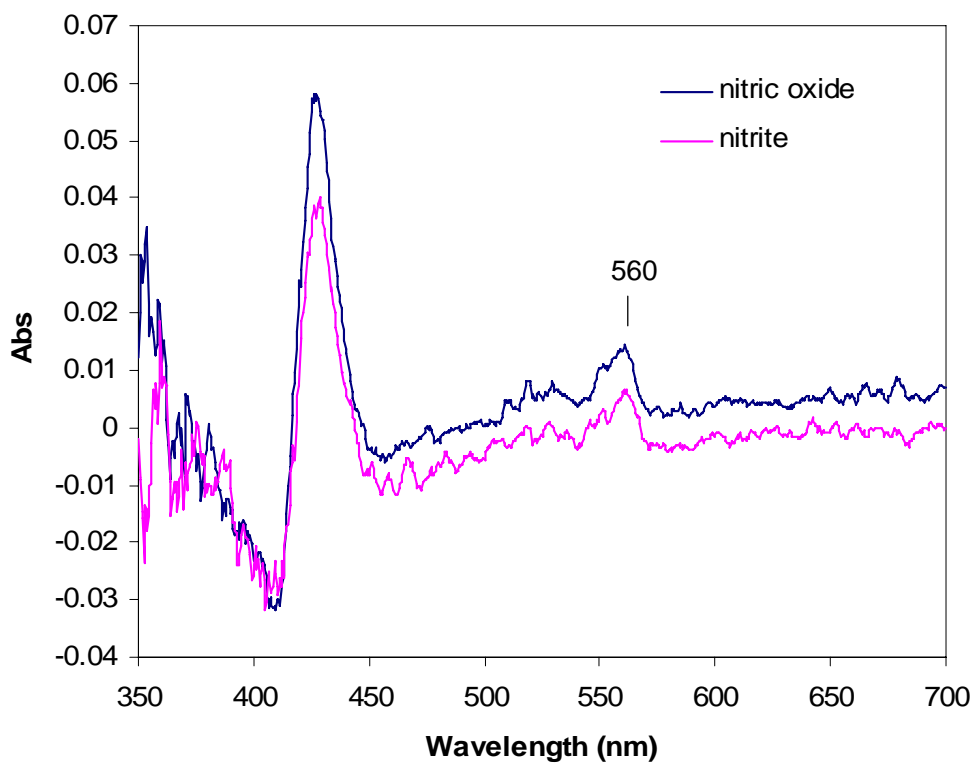


Figure 3.14 Comparison of difference spectra of cells oxidized by nitrite and by nitric oxide. Oxidation by nitric oxide exhibited alpha peak at 560 nm suggesting oxidation of *b*-type cytochrome. This cytochrome is likely to be NorB nitric oxide reductase which contains *b*-haem. The spectra are similar to that by nitrite suggesting that nitrite might be reduced to NO and, consequently, NO oxidizes NorB.

3.2.2.5 Nitrite inhibits cytochrome oxidation by oxygen in *aniA* mutant

It was shown earlier (section 3.2.2.3) that nitrite inhibits cytochrome oxidation by oxygen. This section aims to investigate whether this inhibition could be due directly to nitrite or whether it is due to the formation of nitric oxide during denitrification. AniA is the only protein predicted to have nitrite reductase activity in *N. meningitidis*, so the strain deficient in AniA was used to check if nitrite can still inhibit cytochrome oxidation by oxygen when it is not being metabolized to nitric oxide. The *aniA* mutant cells were grown aerobically for 8-12 hours. Then cells were harvested and resuspended. The cell suspension was allowed to reach a reduced state then exposed to oxygen. After oxidation by oxygen, cells were allowed to become re-reduced before exposure to nitrite. After exposure to nitrite, cells were exposed to oxygen in the presence of nitrite. It was found that oxygen can normally oxidize *aniA* mutant cells while nitrite can not (Figure 3.15 and Figure 3.16). Interestingly, though exposure to nitrite can not produce alpha peak at 560 nm, oxidation of *c*-type cytochrome by oxygen was still inhibited (Figure 3.15-3.17). Difference spectra of reduced minus oxidised shows that alpha peak from oxidation by nitrite plus oxygen was much smaller than that by oxygen alone.

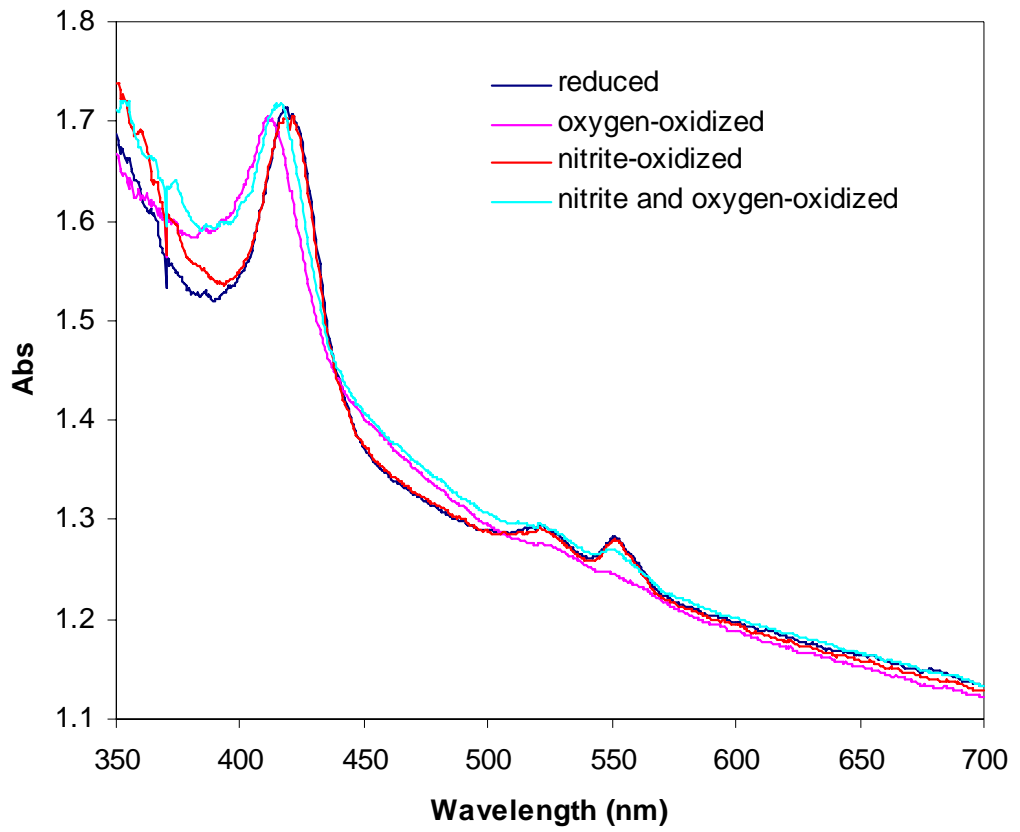


Figure 3.15 Nitrite inhibits cytochrome oxidation by oxygen in *aniA* mutant cells.

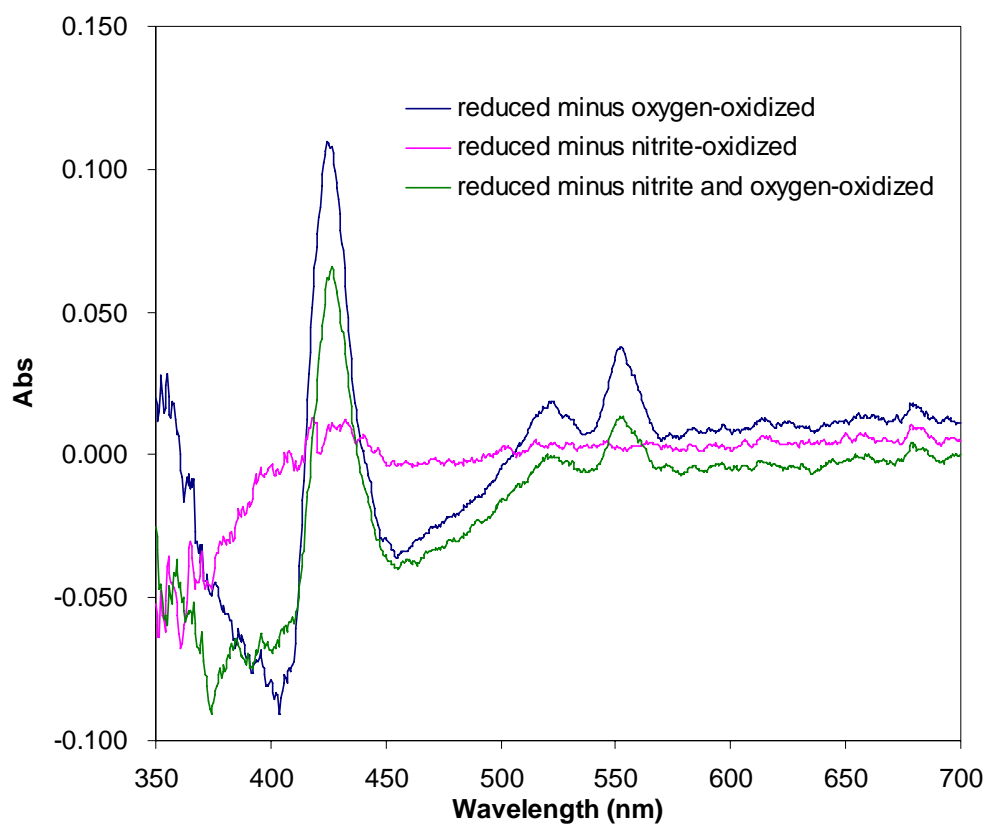


Figure 3.16 Reduced minus oxidized spectra of *aniA* mutant cells grown under aerobic conditions. Nitrite inhibits cytochrome oxidation by oxygen in the absence of AniA. The *aniA* mutant was grown aerobically and then cells were exposed to oxygen, nitrite, and nitrite plus oxygen. Nitrite can not oxidize any cytochromes but it still can inhibit cytochrome oxidation by oxygen.

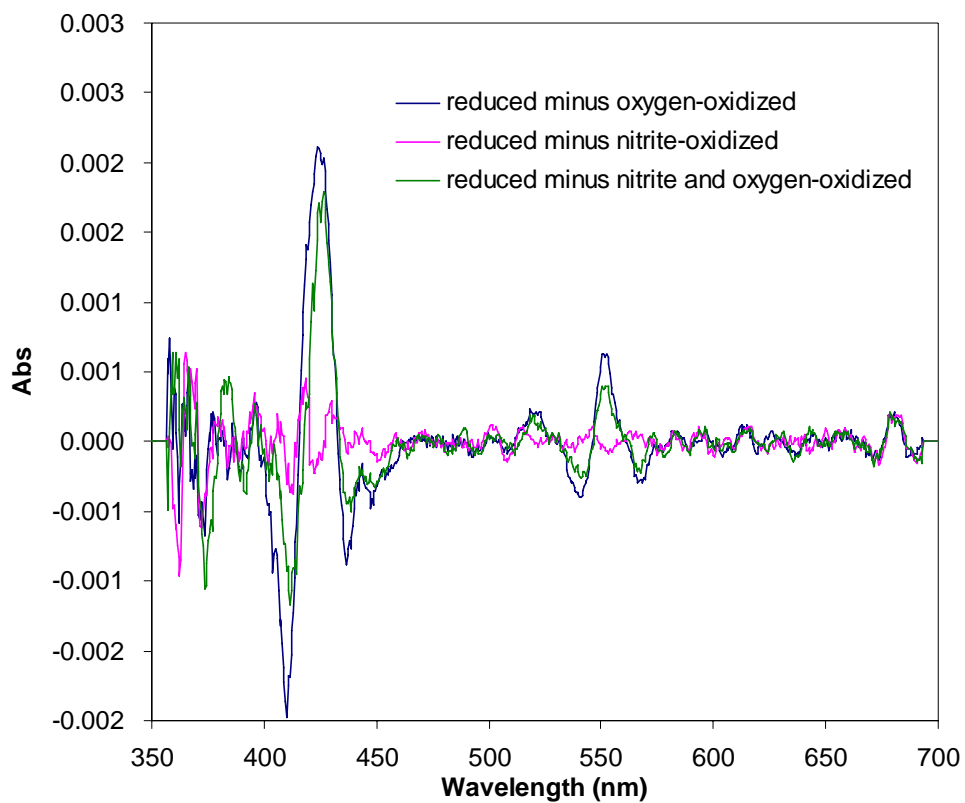


Figure 3.17 Double derivative of oxidized minus reduced spectra of *aniA* mutant cells. In *aniA* mutant cells grown under aerobic conditions, nitrite can not oxidize any *b*-type cytochromes but still inhibited oxidation of *c*-type cytochrome by oxygen. This might suggest a direct inhibitory effect of nitrite on cytochrome oxidation by oxygen.

3.3 Discussion

The expression of most *c*-type cytochromes detected in this organism appeared to be constitutive. These cytochromes are predicted to be FixP (NMB1723) which is a cytochrome subunit of *cbb₃* oxidase, cytochrome *c5* (NMB1677), PetC or cytochrome *c1* (NMB2051) subunit of the *bc₁* complex and cytochrome *c4* (NMB1805). However, expression of FixP was slightly increased under microaerobic conditions both in the presence and in the absence of nitrite. This might suggest a role of FixP for aerobic respiration under low level of oxygen. There are three more *c*-type cytochromes that can not be detected by this chemiluminescence staining. These cytochromes might include cytochrome *c2* (NMB0717), cytochrome *c'* (NMB0923) and FixO (NMB1724). All detectable *c*-type cytochromes are constitutively expressed under different level of oxygen and nitrite. Moreover, the expressions of these *c*-type cytochromes are not regulated by FNR. In addition, cytochrome spectra of *fnr* mutant cells grown under various growth conditions should have been done to observe the effect of FNR on cytochrome expression. Interestingly, the expression of these cytochromes are not affected by either level of oxygen or nitrite though all of these cytochromes are most likely to be components of respiratory chains. It may be possible that these *c*-type cytochromes are involved in electron transport chain to oxygen (see later chapters). The constitutive expression of these *c*-type cytochromes may be important for maintaining oxygen respiration, suggesting oxygen respiration as major energy-transducing mean for maintaining metabolism and growth of this organism under wide range of physiological oxygen. Microaerophilic bacteria such as *N. meningitidis* may be adapted to respond to changes in physiological oxygen relatively rapidly compared to aerobic, anaerobic, or facultative bacteria (Ludwig, 2004).

It was shown that glucose can be used successfully as a physiological reductant in this organism for preparation of cell suspension for spectrophotometry. Glucose has been used throughout the experiments here to induce highly reduced state of cells under anaerobic conditions via the production of reducing equivalent, such as NADH. Under anaerobic conditions, cell suspensions supplemented with glucose rapidly became reduced, giving rise to UV-visible spectral features characteristic of *b*- and *c*-type cytochromes. Following the addition of oxygen to these cell suspensions, the spectral features due to reduced α - band and β -band disappear and the Soret peak is blue-shifted, indicating oxidation of cytochromes.

Difference spectra showed that the oxygen-dependent oxidation is characterized by disappearance of a major α -feature at 552-553 nm. This feature is presumably made up of a number of *c*-type cytochromes that are found in the electron transport pathway to oxygen, and fewer *b*-type cytochromes as indicated by the slight shoulder on the α -band around 560 nm. Oxidation of *c*-type cytochromes in denitrifying preculture cells is not different from that seen in aerobic preculture cells, suggesting that machinery for aerobic respiration were not down regulated or repressed. The very low level of oxygen did not repressed expression of these cytochromes, which may include both *cbb*₃ oxidase and upstream cytochromes of the respiratory chains. Low degree of oxidation of *b* haem was seen in denitrifying preculture cells. This may be due to the oxidation of NorB by oxygen. It is possible that oxygen can oxidize NorB as NorB and *cbb*₃ oxidase are closely related in the course of evolution (Saraste and Castresana, 1994).

With aerobically cultured *N. meningitidis*, nitrite has no effect on the spectra of cell suspensions, but following culturing under conditions to allow expression of denitrification machinery, the oxidation by nitrite causes predominantly the oxidation of *b*-type cytochrome. This is most likely to be due to the oxidation of reduced NorB by

the nitric oxide generated by nitrite reduction, and this is confirmed by oxidizing intact cells with nitric oxide by treating cells with 1 mM DEA-NONOate [2-(N,N-diethylamino)-diazonolate-2-oxide diethylammonium salt] as a source of NO.

It is observed that there are *c*-type cytochromes in the respiratory chain of the meningococcus that are oxidized by oxygen but not nitrite. It is not yet clear whether these oxygen-specific cytochromes are part of the *cbb₃* oxidase itself or *c*-type cytochromes that are involved in shuttling electrons to the oxidase. Interestingly, there is no spectrum of cytochromes oxidized directly due to nitrite. Oxidation of *c*-type cytochrome on pathway to nitrite reductase was not observed despite the fact that majority of nitrite reduction in this organism depends on the *bc₁* complex (Deeudom *et al.*, 2006). Some *c*-type cytochrome is required for transferring electrons from *bc₁* to AniA. It is proposed that because nitrite reduction turnover is slow, electron transfer into the respiratory chain exceeds the rate of removal of electrons by oxidation via nitrite.

In order to characterize further the interplay of the oxidants oxygen and nitrite on the respiratory components, the effect of oxygen plus nitrite on the spectra of cytochromes in intact cells were investigated. It was found that the degree of oxidation by nitrite plus oxygen was intermediate between the oxidation by nitrite alone and oxygen alone. It was initially considered that this would be due to the production of nitric oxide from nitrite, which in turn partially inhibits oxidase activity under these experimental conditions. However, it was found that the inhibition by nitrite is also observed in a mutant deficient in the nitrite reductase, which is unable to synthesize NO from nitrite. This indicates that nitrite may also have a direct effect on oxygen metabolism in this bacterium, rather than just inhibiting via the production of the nitric oxide radical.

Chapter 4

Mutagenesis of *c*-type cytochromes and Laz

4.1 Introduction

Gene disruptions were employed to achieve mutant strains deficient in cytochrome *c2*, *c4*, *c5*, *c2* and *c4*, and a cupredoxin Laz. Allelic exchanges or homologous recombinations were done to replace wild type allele with mutant allele. The genetic transformations of the wild type strain by mutant plasmids were done using natural transformation. *N. meningitidis* and *N. gonorrhoea* are naturally competent bacteria. Their genome contains a large number, nearly 2000, of distributed copies of short DNA sequence called DNA uptake sequence (DUS) (Ambur *et al* 2007). The consensus motif of neisserial DNA uptake sequences are GCCGTCTGAA or TTCAGACGGC. This 10-bp repeat is important for efficient genetic transformation in these bacteria. The neisserial DUS is believed to help the bacterial cells to uptake recognizable DNA fragments in their natural environment with strong preference of their own species. A potential DUS-specific binding receptor is yet to be identified. The plasmid vector used for construction of all respiratory mutants is pCR-Blunt II TOPO plasmid. Disruption marker genes used in this work are all antibiotic resistance genes, including spectinomycin resistance gene (*spc^r*), erythromycin resistance gene (*ery^r*), tetracycline resistance gene (*tet^r*), and chloramphenicol resistance gene (*chl^r*). The purpose is to generate strains deficient in *c*-type cytochrome(s) or cupredoxin in order to be able to characterize the roles of these proteins in respects of electron transport, respiration and growth in *N. meningitidis*.

4.2 Construction of cytochrome *c2* mutant

Gene NMB0717 of *N. meningitidis* strain MC58 is predicted to encode a small periplasmic *c*-type cytochrome. This cytochrome is designated cytochrome *c2*. Disruption of the cytochrome *c2* gene was undertaken using a spectinomycin resistance gene cassette insertion as follows. The cytochrome *c2* gene with flanking region containing *N. meningitidis* uptake sequence, GCCGTCTGAA or TTCAGACGGC (Figure 4.1) with size of 1321 bp was amplified by PCR using PFU polymerase (Figure 4.2). The uptake sequence promotes the efficiency of DNA uptake by *N. meningitidis*. Forward primer (22 nucleotides) and reverse primer (22 nucleotides) are as shown respectively.

Forward primer (c552F) 5'-TTG GAA ACC ATG GAA GAA ATC G-3'

Reverse primer (c552R) 5'-GAC AGT ACA AAT AGT ACG GAA C-3'

```
CAGGATTTGTTTCGGCAAACCTGCCCAAACAGGGGGTAACCGAGCTGGACGTATTTTGCCCGGGCTTTTTGGCAGACTGT
TTGGAAACCATGGAAGAAATCGCCCTGATGGGGCGGGAAACAGTTTTATGAAGCAGGCGGCAAAAGCTACCGCTACATC
CCCTGCCTCAACGACAACCCCGACTGGATAGATGCACTCGTCGCACTTGCCGAAGAAAACCTTGGCAGCTGGCGTTGA
AACTGTTTGACCCATGTCTAAAATGCCGTCTGAACCGCGTGTTCAGACGGCATTTCCTCCGCTACTTTAGCGTATGATG
GCATCTATGCTGGACAACAACATCAAGTGCAACCTTATAGTGGATTTAAATTTAAACCAGTACGGCGTTGCCTCGCCTT
GCCGTACTATTTGTACTGTCTGCGGCTTCGTGCGCTTATCCTGATTTTTGTTAATCCACTATACTACTGATTCGGCAA
AAAAATCTTTCACCCGCTACGCAAAATCAACAACAAGTTTTCAAACATGAAGGAAACACCAATGAACACAACCCGACT
GCCGACCGCCCTCGTCTGGGCTGCTTCTGCGCCCGCTTCTGCCGCGGACAACAGCATCATGACAAAAGGGCAAAA
AGTGTACGAATCCAACCTGCGTCGCTGCCACGGCAAAAAGGGCGAAGGCCGCGGAACCATGTTTCCGCGCTCTACCG
CTCCGACTTCATCATGAAAAAACCGCAGGTGCTGCTGCACAGCATGGTCAAAGGCATCAACGGTACAATCAAAGTCAA
CGGCAAAACCTACAACGATTTCATGCCCGCAACCGCCATCAGCGATGCGGACATTGCCGCGCTCGCCACTTATATCAT
GAACGCCTTTGACAACGGCGGCGGAAGCGTTACCGAAAAAGACGTAAACAGGCAAAAAGCAAAAAAACTAAACAGA
CAAAATGCCGTCTGAACCGGCAATCCGGCTTCAGACGGCATTCAAATCAAACCTTTCTAACGCAGCACTTTCAGCCC
CATAGACCCGATATTGCCGCCACCGTCAACCTCCTTTGCGGTGAGCATAAAGCCGCCGATGCAATACGGCCGCCCTC
GACCGGCTCCTGACTATCGGAACGCTTATCGAAAAGCTCGGCAAGGCTCAAACCTCTTCGCCCGCTTCCAGCCTCAA
ACCGTAAGTAAGTGCCAAATCACCCGAACGTGCTGCCGGCAAAACGACAAACTCACCGAAGAAATCAAATGCTCACG
GACGCTAATACCCGTTCTCGGTAAAGTATTTGCCATTTTATAGTGAACATAAATTTAAACCAGTACGGCGTTGCCTCGC
CTTAGCTCAAAGAGAACGATTCTCTAAGGTGCTGAAGCACAAGTGAATCGGTTCCGTACTATTTGTACTGTCGCGG
CTCGCCGCTTGTCTGATTTTTGTTAATTCATAATCG
```

Figure 4.1 The cytochrome *c2* gene with flanking region used for constructing mutant. The cytochrome *c2* gene (blue) with flanking region (black) containing *N. meningitidis* uptake sequences (orange) and primer sequences (yellow highlight) has size of 1321 bp. The *Bsp*I site is in grey highlight. The enzyme cuts between the two A residues shown boldin red) and cut out once in the middle of *c2* gene.

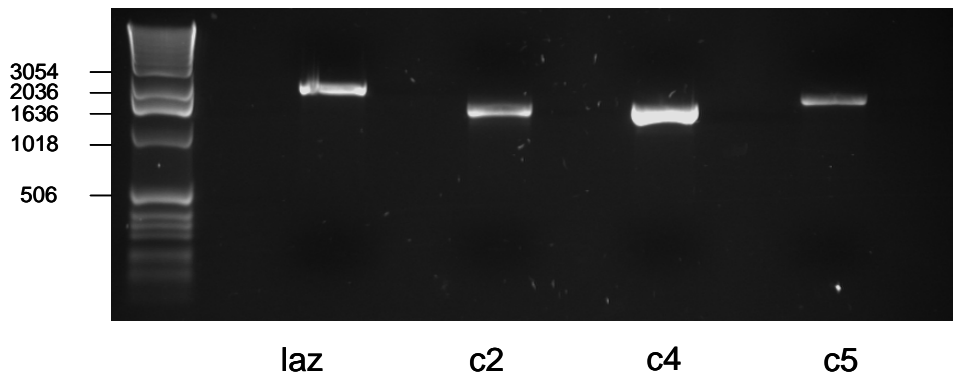


Figure 4.2 PFU PCR product of cytochrome *c2* gene with flanking region. The *c2* fragment exhibits size of 1321 bp. Lane 1 is *laz*, lane 2 is *c2* gene, lane three is *c4* gene and lane 4 is *c5* gene.

Then, blunt end cloning of cytochrome *c2* gene with flanking region from PCR product was undertaken. The blunt end PCR products were inserted into pCR-Blunt II TOPO plasmid. Then the plasmids were transformed into *E. coli* strain DH5- α by heat shock. The transformants were grown on selective agar plate containing kanamycin. Colony PCR was performed to screen for bacterial colonies containing plasmid with inserted cytochrome *c2* gene (Figure 4.3). Then, each of 5 recombinant colonies were individually grown in LB for plasmid propagation for over night. Cells were harvested and the recombinant plasmids were purified with Qiagen Miniprep Kit and digested with *EcoRI*. The digested DNA products showed the right size of 1.3 kb (*c2* gene) and 3.5 kb (pCR-Blunt II TOPO plasmid) (Figure 4.4). pCR-Blunt II TOPO + *c2* plasmid were then digested with *Bsg* I which cut only once in the middle of *c2* gene (Figure 4.5). The ends of *Bsg* I-digested plasmid were blunted using Klenow fragment in order to allow blunt end ligation and insertion of *spc^r* gene cassette.

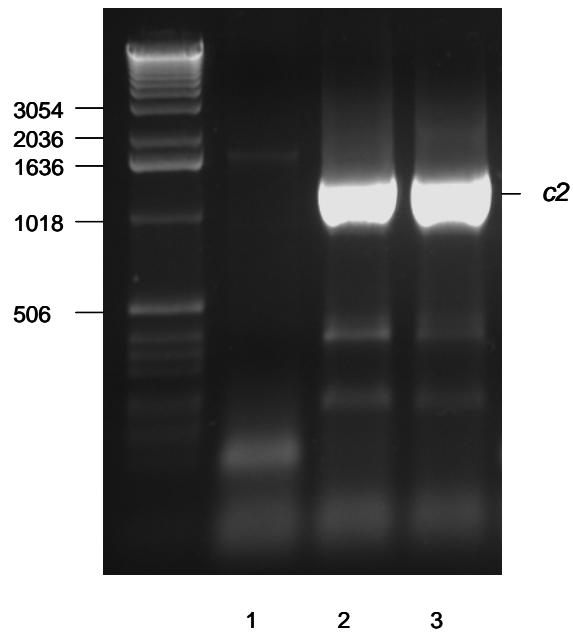


Figure 4.3 Colony PCR screen for pCR-Blunt II TOPO plasmid with insertion of cytochrome *c2* gene. The *c2* fragment exhibits size of 1321 bp found in Lane 2 and 3.

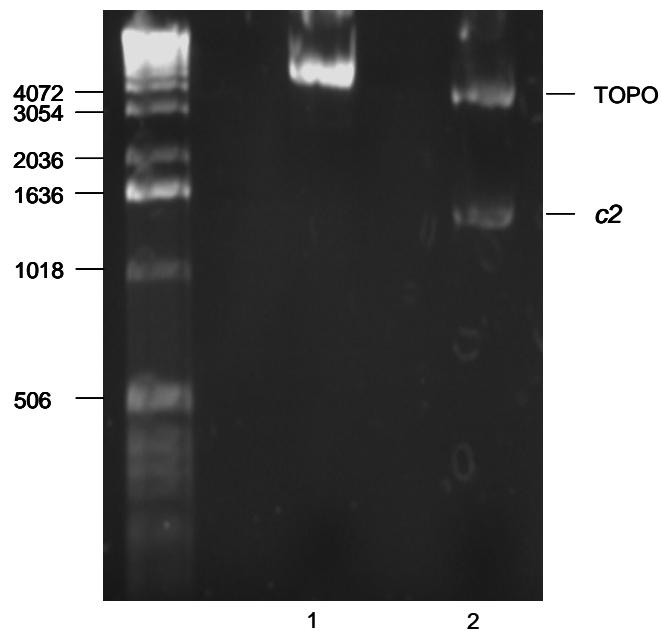


Figure 4.4 *Eco*RI digested products of pCR-Blunt II TOPO plasmid with insertion of cytochrome *c2* gene. The *c2* insert was found in lane 2 with size of 1.3 kb and TOPO vector plasmid with size of 3.5 kb. Lane one is pCR-Blunt II TOPO + *lacZ* plasmid.

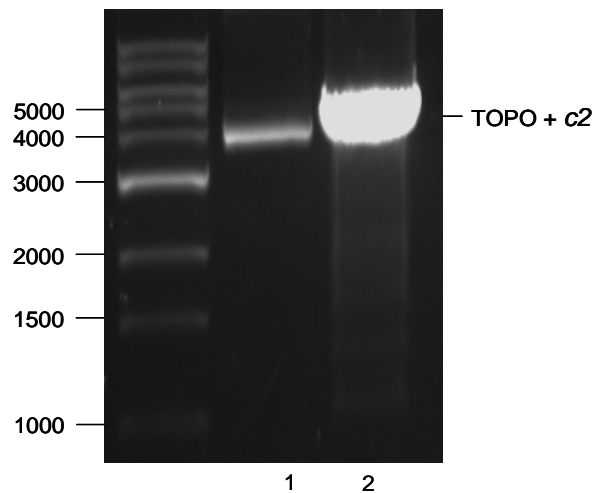


Figure 4.5A *BsgI* digested products of pCR-Blunt II TOPO + *c2* plasmid. Lane 1 is plasmid before digest and lane 2 is plasmid after digested by *BsgI*. The size of pCR-Blunt II TOPO + *c2* plasmid is 4.8 kb.

The spectinomycin resistance gene cassette (*spc^r*) or the Ω cassette is chosen to insert into pCR-Blunt II TOPO + *c2* plasmid in order to disrupt the function of *c2* gene. This gene cassette is obtained by digesting pHP45 Ω plasmid with *SmaI*. The digested plasmid yielded DNA fragments of 2.0 kb corresponding to *spc^r* cassette and DNA fragments of 2.2 kb corresponding to the remainder of the plasmid (Figure 4.5B). The Ω cassette was then ligated with the pCR-Blunt II TOPO + *c2* plasmid. The *E. coli* DH5 α cells were then transformed by the ligation products which contains *c2* gene disrupted with the Ω cassette. The transformants were selected by plating on spectinomycin LB agar. Colony PCR were performed to check if grown colonies contained *c2* gene with Ω cassette insert. Colonies with *c2* gene disrupted by Ω cassette were found (Figure. 4.6). The PCR products exhibit size of 3.3 kb. Recombinant plasmids were extracted and digested by *EcoRI* to confirm the insertion of Ω cassette. The digested plasmids showed DNA fragments with size of 3.3 kb corresponding to *c2* (1.3 kb) with *spc^r* cassette (2.0 kb) (Figure 4.7). *N. meningitidis* strain MC58 was

transformed by plasmid containing *c2* gene disrupted by *spc^r* cassette. The transformants were selected on spectinomycin MH Blood Agar. Colonies grown on selective agar plate were screened for *c2* gene disrupted by *spc^r* cassette by colony PCR. Colony containing disrupted *c2* gene was found (Figure 4.8).

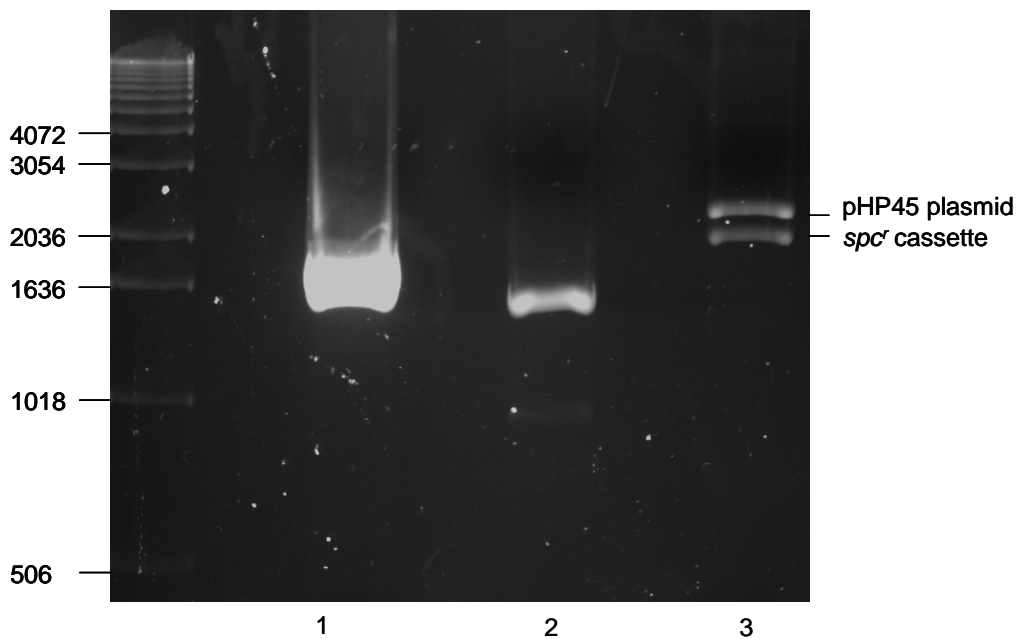


Figure 4.5B Spectinomycin resistance gene cassette or Ω cassette. This gene cassette is obtained by digesting pHP45 Ω plasmid with *Sma*I. The digested plasmid yielded DNA fragments of 2.0 kb (lane 3, lower band) corresponding to *spc^r* cassette while the digested pHP45 plasmid yielded DNA fragments of 2.2 kb (lane 3, upper band). Lane 1 is PCR products of *laz* gene while lane 2 is that of *c5* gene.

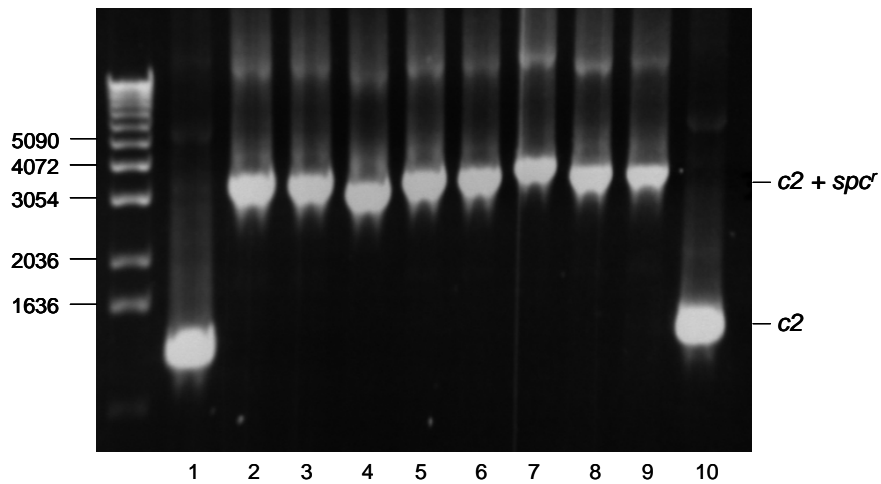


Figure 4.6 Colony PCR screen of *E. coli* DH5 α transformants for *c2* gene with Ω cassette insert. PCR products from colonies containing *c2* gene disrupted by *spc*^r gene exhibit size of 3.3 kb (lanes 2 -9).

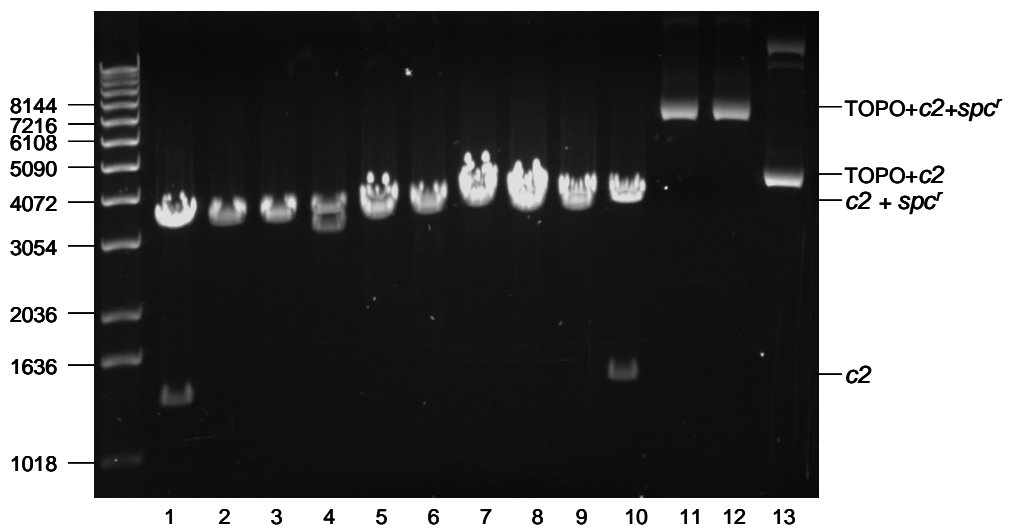


Figure 4.7 *Eco*RI digest screen for *c2* gene with Ω cassette insert in constructed plasmid from *E. coli* DH5 α transformants. The disrupted *c2* gene were found in lanes 1-10. The *c2 + spc*^r fragment exhibits size of 3.3 kb and the remainder vector plasmid exhibits size of 3.5 kb. Lane 11 and 12 are pCR-Blunt II TOPO + *c2 + spc*^r plasmid before digest. Lane 13 is pCR-Blunt II TOPO + *c2* plasmid.

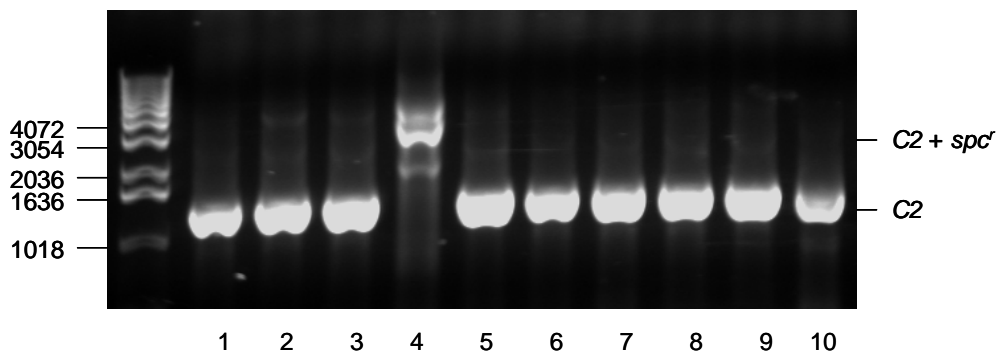


Figure 4.8 Colony PCR screen for *c2* gene with Ω cassette insert in *N. meningitidis* MC58 transformants. The *c2* gene with *spc'* insert, size of 3.3 kb, was found in lane 4.

4.3 Construction of cytochrome *c4* mutant

Cytochrome *c4* (NMB1805) is predicted to function as an electron donor to AniA nitrite reductase and to cytochrome *cbb₃* oxidase in *N. meningitidis*. This gene is very similar to that of *Neisseria gonorrhoea* and contains nucleotide sequence of 624 bp encoding for a sequence of 207 amino acids with molecular weight of 20175 Da. It contains a predicted signal peptide of first 18 amino acid residues and two predicted haem-binding site (CAACH and CMSCH). Therefore it is predicted to be a dihaem cytochrome which is localized in periplasm.

Gene disruption was employed using erythromycin resistance gene cassette as follows. The cytochrome *c4* gene with flanking region containing *N. meningitidis* uptake sequence (Figure 4.9) with size of 1373 bp was amplified by PCR using PFU polymerase (Figure 4.2). The uptake sequence promotes the efficiency of DNA uptake by *N. meningitidis*. Forward primer (22 nucleotides) and reverse primer (22 nucleotides) are as shown respectively.

Forward primer (c554F) 5'-GTT TTT GAA ACG TAG GCA AGA C-3'

Reverse primer (c554R) 5'-CCG AAT TTG ACC AAA TAA TCC G-3'

TGCCGTTTCTGCAGCTCGAAGAAGTTGATATGCTGCGTCCGTCGGGTGTTTTTGAACGTAGGCAAGACGGACATGGTTGGTCAGGGT
 ATTGATGGCACTGGATTTTCCGGCATTGCTCCTGCCGACAAAGGCAATTTTCGAGAGGGGTGTCCGGCAGGTCTTTAAGGTGGTTGATC
 GTCGTGAAGAATTTGGCGTTTGGAAAAAGGTTTCATGGGCATATCCTTGTTCGCCCGCCGTTTGTCCGACAGCAAAAATATGCGGTT
 GGTFTTATGTGAAACACAGTGGTAATTTAATGTAAATTTAGTATAGAAATAACACGTTTACAGAATCATCGGTTTTAATCGGGTCAAAA
 ATCCCGTATTTGAATATAAAAAGAGCATTGTTGCGTTATCCAATGCTGTAATCAGGAGCACTCCATGAAACGATTGACTTTATTGGCC
 TTTGTTTTGGCTGCCGGTGGGTTTCCGCCTCTCCCAAAGCAGAGCTGGAAAAAGGCAACAGGTTGCCGCAACGGTTTTGTCCGGCTT
 GCCATGCAGCAGACGGTAACAGCGGCATTGCGATGTATCCGCGTTTGGCGGCACAGCATACTGCTTACATCTATCATCAAACATTCGG
 CATCCCGACGGTAAACGCACCCACGGTTCGGCAGCTGTGATGAAACCGGTGGTAATGAATTTGAGCGATCAGGATATTTTGAACGTA
 TCCGATTTCTATGCCAAACAGCAGCCAAATCCGGTGAAGCCAATCTAAGGAAAATCCCGAATGGGTGCGAAAATCTATCCGGCG
 GTTTGAGCGATAAAAAAGTGCCGGCGTGTATGTCTGCCACGGTCCGAGCGGTGCGGGTATGCCGGGAGCGGAAGCGAAATTCAGGC
 TTATCCGCGTTTGGCGGTCAGCATCAGGCATATATTGTTGAACAGATGAATGCCTACAAGTCCGGTCAGCGTAAAAATACCATCATG
 GAAGATATTGCAACCGTATGCTGAAGAAGATTGAAAGCGGTCGCCAACTTTATCCAAGGTTTGCCTTAATCCGCAATAGTCTGT
 TTTAGAGGCCGCTGTGAAAGTTTTCAGACGGCTTCAGGCAATTTCTGCGATAAGTTTTTTCAATCGCAACCGTTGGAATCGATGCAGGC
 TGTCTTCATTTGCTTGAATAAAAAGCATCAAGACAGTAGAATCGGGACGTTGTTTTCTGTTTGCCCAATTTCTGCTTTCCCATATTC
 TGATGGCGGAATAAACACACAATGAGTAAATCCCGTAGATCTCCCCACTTCTTTCCCGTCCGTTGCTTTTTTTCAGCTCCATGC
 GCTTTGCACTCGCTTTGCTCAGTCTGCTGGTATTGCATCGGTTATCGGTACGGTGTTCAGCAAAACCAGCCGAGACGGATTATT
 GGTCAAATTCGGATCGTTTTGGGCGCAGATT

Figure 4.9 The cytochrome *c2* gene with flanking region used for constructing mutant. The cytochrome *c4* gene (blue) with flanking regions (black) containing *N. meningitidis* uptake sequences (orange) and primer sequences has size of 1373 bp. Bsu36 I site is in blue highlight. The enzyme cut between C and T residues shown bold in red and cut only once in the middle of *c4* gene.

Then, blunt end cloning of cytochrome *c4* gene with flanking region from PCR product was undertaken. The blunt end PCR product was inserted into pCR-Blunt II TOPO plasmid. Then the plasmids were transformed into *E. coli* strain DH5- α by heat shock. Colony PCR was performed to screen for bacterial colonies containing plasmid with inserted cytochrome *c4* gene (Figure 4.10). Then, each of 5 recombinant colonies was individually grown in LB for plasmid propagation for over night. Cells were harvested and the recombinant plasmids were purified with Qiagen Miniprep Kit and digested with *EcoR* I. The digested DNA products showed the right size of 1373 bp (*c4* gene) and 3519 bp (pCR-Blunt II TOPO plasmid) (Figure 4.11). The pCR-Blunt II TOPO + *c4* plasmid were then digested with Bsu36I which cut only once in the middle of *c4* gene (Figure 4.12)

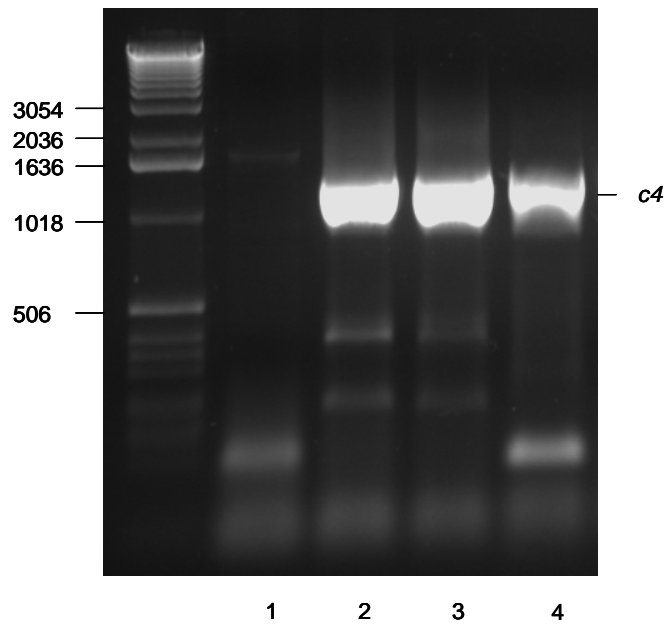


Figure 4.10 Colony PCR screen for pCR-Blunt II TOPO plasmid with insertion of cytochrome *c4* gene. The vector plasmid with *c4* gene insert was found in lane 4. Lane 2 and lane 3 are plasmid with *c2* gene insert.

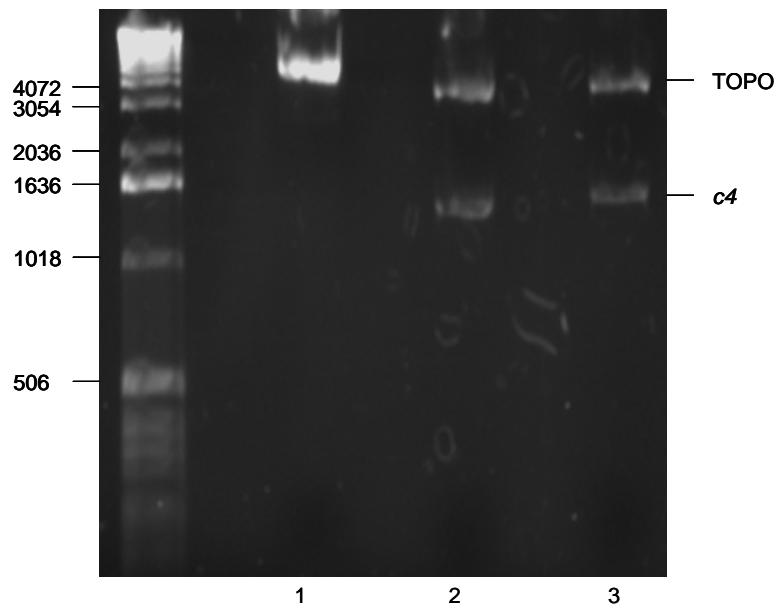


Figure 4.11 *EcoRI* digested screen for pCR-Blunt II TOPO plasmid with cytochrome *c4* gene insert. The plasmid with *c4* gene insert was found in lane 3. The digested products exhibit two bands, one with size of 1.4 kb corresponding to *c4* gene and one with size of 3.5 kb corresponding to pCR-Blunt II TOPO plasmid. Lane 2 is digested products from plasmid with *c2* gene insert.

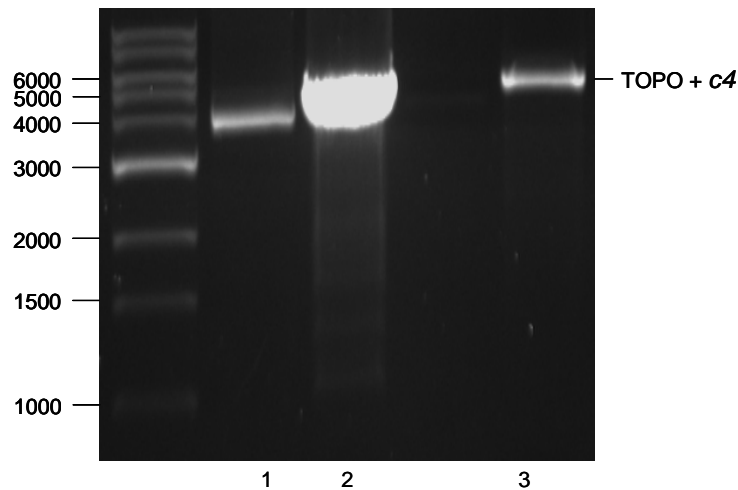


Figure 4.12 *Bsu36I* digested products of pCR-Blunt II TOPO + *c4* plasmid (lane 3). Lane 1 is of pCR-Blunt II TOPO + *c2* plasmid while lane 2 is of pCR-Blunt II TOPO + *c2* plasmid digested by *BsgI*.

The erythromycin resistance gene cassette (*ery^r*) was chosen to insert into pCR-Blunt II TOPO + *c4* plasmid in order to disrupt the function of *c4* gene. This gene cassette is obtained from pTOPOery plasmid by PCR using PFU. PCR products exhibited size of 1.2 kb corresponding to size of *ery^r* cassette (Figure 4.13). Forward primer (31 nucleotides) and reverse primer (33 nucleotides) are as shown respectively.

Forward primer (*eryfwd1*) 5'-TTC CCC GGG CTT AAG AGT GTG TTG ATA GTG CAG-3'

Reverse primer (*eryrev1*) 5'- TTC CCC GGG TCG ATA CAA ATT CCC GTA GGC G-3'

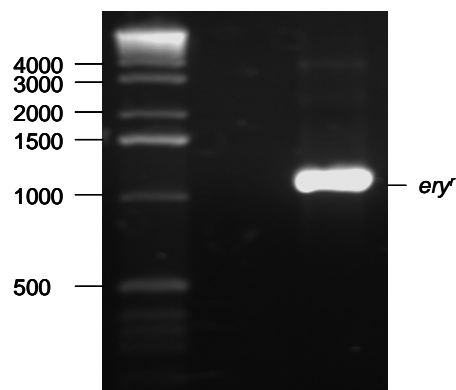


Figure 4.13 PFU PCR products of *ery^r* cassette exhibits size of 1.2 kb.

The pCR-Blunt II TOPO plasmids with *c4* gene insert were digested by *Bsu36* I and the overhang ends were blunted by Klenow fragment (DNA polymerase I). The *ery^r* cassettes were blunt end-ligated with linearized pCR-Blunt II TOPO + *c4* plasmid. The *E. coli* DH5 α was transformed by the ligation products. The transformants were plated and selected on erythromycin LB Agar. Colonies grown on the selective plate were screened for disrupted *c4* gene by colony PCR (Figure 4.14). Then, each of the recombinant colonies was individually grown in LB for plasmid propagation for over night. Cells were harvested and the recombinant plasmids were purified with Qiagen Miniprep Kit and digested with *Eco*RI. The digested DNA products showed the right size of 2.6 kb (*c4* gene + *ery^r* gene) and 3.5 kb (pCR-Blunt II TOPO plasmid) (Figure 4.15). Then MC58 strain was transformed by TOPO plasmid containing disrupted *c4* gene. The transformants were plated and selected on erythromycin Blood Agar plate. Colonies selectively grown were screened for disrupted *c4* gene by colony PCR (Figure 4.16).

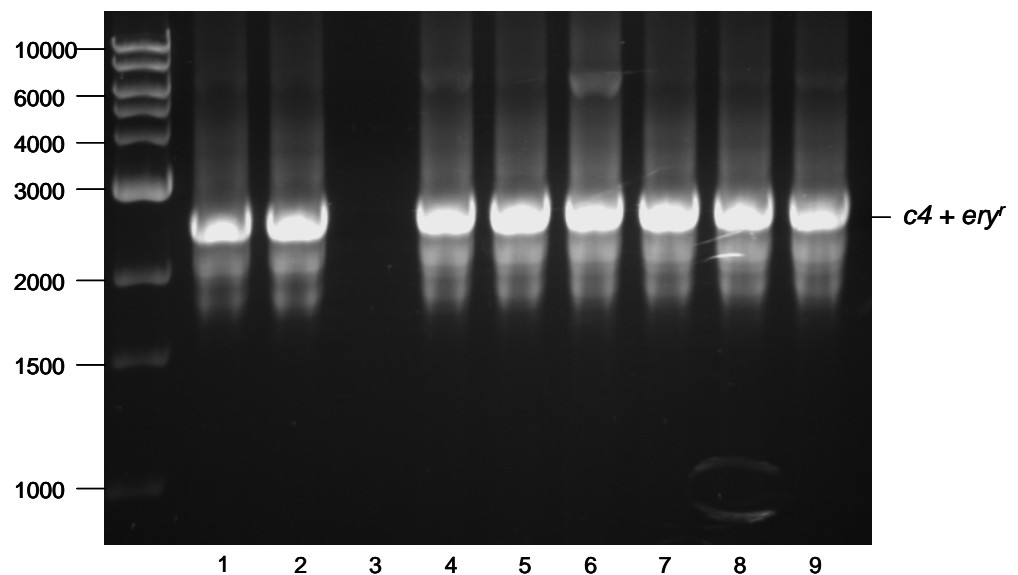


Figure 4.14 Colony PCR screen of *c4* gene with *ery^r* insert in *E.coli* DH5 α transformants. The PCR products exhibit size of 2.5-2.6 kb.

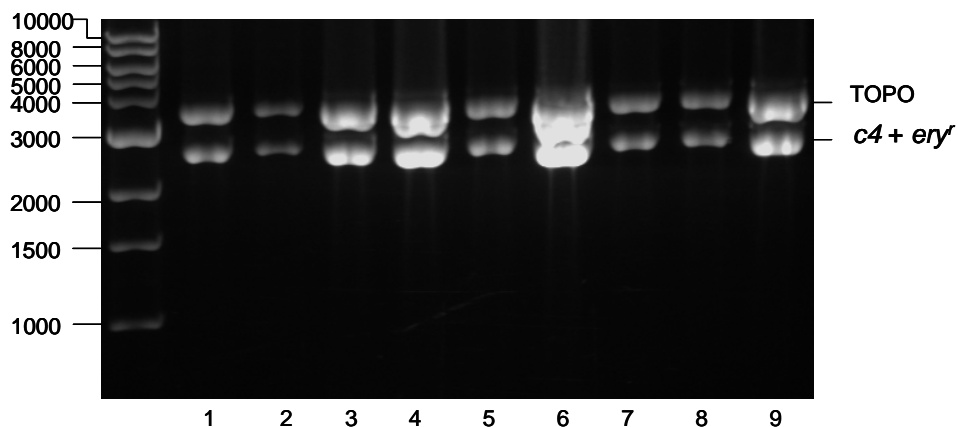


Figure 4.15 *Eco*RI digest screen of *c4* gene with *ery^r* insert for recombinant plasmids in *E. coli* DH5α transformants. The digested products exhibits *c4::ery^r* fragments with size of 2.6 kb and linearized pCR-Blunt II TOPO plasmid vector with size of 3.5 kb.

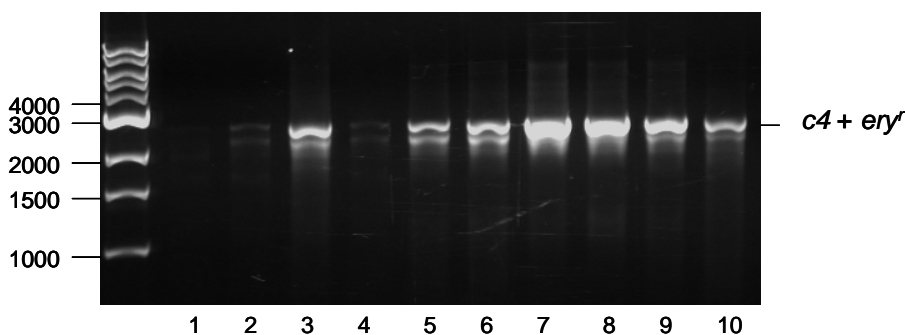


Figure 4.16 Colony PCR screen of disrupted *c4* gene in MC58 transformants. The *c4::ery^r* fragments were found in transformant with size of 2.6 kb. The *c4* gene in the meningococcus was successfully disrupted by *ery^r* gene.

4.4 Construction of cytochrome *c5* mutant

Cytochrome *c5* (NMB1677) is predicted to function as an electron donor to AniA nitrite reductase and an electron donor to cytochrome *cbb₃* oxidase. This gene (NMB1677) is most similar to that of *Neisseria gonorrhoea* and contains nucleotide sequence encoding for a sequence of 138 amino acids with molecular weight of 14715 Da. It contains a predicted cytoplasmic domain, a transmembrane domain and two

predicted haem-binding site. Therefore, it is predicted to be a dihaem cytochrome which is localized in periplasm but with a membrane anchor.

Gene disruption was employed using an antibiotic resistance gene cassette as follows. The cytochrome *c5* gene with flanking region containing *N. meningitidis* uptake sequence (Figure 4.17) with size of 1574 bp was amplified by PCR using PFU polymerase (Figure 4.2). The uptake sequence promotes the efficiency of DNA uptake by *N. meningitidis*. Forward primer (22 nucleotides) and reverse primer (22 nucleotides) are as shown respectively.

Forward primer (c555F) 5'-AAT TGG CAA AGG TTA TCT TGC G-3'

Reverse primer (c555R) 5'-GGA AAA TTA TGA AGA CTG ACT G-3'

```

AAATTCTGCA AATGGCAAAGGTTATCTTGCC CCGGCAGGCGGCGTATGGCGGCATAAGGAGAGTTTTCTTGAGGATAAACAATTATT
TTCAAAGGATTATTTGTTTTATACAGATACCGTTGGCAAATTTTTTCATATTTTCAATGATAGCGATTGGAAAGACCCTGT SAATTC
GTATAATCCAGCAAATAATTGTTAACTGCGTTTTAACACACCAAACCTATAATTTACAGCACAACTAACCTGACGGCGAGGCCTACCAA
ATGAAACAACTCCGCGACAACAAAGCCCAAGGCTTGCAGTGTTCACCTTGTGAGCGGTATCGTTATTGTTATTGCAGTCCTTTATT
TCCTGATTAAGCTGGCGGGCAGCGGCTCGTTTCGGCGATGTCGATGCCACTACGGAAGCAGCAACGCAGACCCGATCCAGCCTGTCCG
ACAATTGACGATGGGCGACGGCATCCCCGTCGGCGAAGCCAAAGCGAACAGATTTTCGGCAAAATCTGTATCCAATGCCACGCGGGC
GACAGCAATGTGCCAAGCCTCCGAACTGGAACACAACGGCGATTGGGCACCGCGTATCGCGCAAGGCTTCGATACCTTGTTCAC
ACGCGCTGAACGGCTTTAACGCCATGCCTGCAAAAGGCGGTGCGGCAGACCTGACCGATCAGGAACTTAAACGGGCGATTACTTACAT
GGCGAACAAAAGCGGCGTTCCTTCCGAATCCTGATGAGGCTGCGCCTGCCGACAATGCCGCTTCAG SAACAGCTTCGCTCCTGCC
GATAGTGCAGCTCCGGCAGAAGCGAAGGCAGAAGACAAGGGTGCAGCCCTGCCGTCGGCGTTGACGGTAAAAAAGTCTTCGAAG
CAACCTGTCAGGTGTGCCACGGCGGTTTCGATTCCCGGTATTCCCGGCATAGGCCAAAAAGACGATTGGGCACCGCGTATCAAAAAAGG
CAAAGAAACCTTGCAAAACACGCCCTTGAAGGCTTTAACGCGATGCCTGCCAAAGGCGCAATGCAGGTTTGAGCGATGACGAAGTC
AAAGCGGCTGTGACTATATGGCAAACCAATCCGGTGCAAAATCTAAATTTAGATTAAAATTTCCGATTAAAATAAAAAACGGGCGAGG
TATCTGCTCCGTTTTTTTTATGGGAATTTATAGTGAATTAACAAAAATCAGGACAAGGCGACGAAGCCGTAGACAGTACAAATAGTACG
GAACCGATTCACTTGGTGCTTGTAGCACCTTAGAGAATCGTTCTCTTTGAGCTAAGGCGAGGCAACGCTGTACTGGTTTTTTGTTAATCC
ACTATATTTGTTTCCGTGTGGAAATGACATCAAAGGTTGTGAATAGGCTTTTCATCTTTGAAATCTGTTTGCACGATCGGATGAAT
AAAAAGTAGGATGATAAAAAAGCTGATGTATGGATACTGGTTAACTCATTTGTTTTAAAGTTATAGTCGAGATACGTGTATTGGTGC
AACTGGTTTGCCTTGATGAAAATGCCGTCTGAAAATGTTCAGACGGCATTTTTTAAGATATCAA CAGTCAGTCTTCATAATTTTCC
ATCGGTGGGCGAG

```

Figure 4.17 The cytochrome *c5* gene (blue) with flanking regions (black) containing *N. meningitidis* uptake sequences (orange) and primer sequences (yellow highlights). *XmnI* site is in blue highlight. This enzyme bluntly cut between the A and G residues shown in bold and red and cut only once in the middle of *c5* gene. The whole size of PCR products is 1574 bp. There is an *EcoR I* site in this fragment (red highlight).

Then, blunt end cloning of cytochrome *c5* gene with flanking region from PCR product was undertaken. The blunt end PCR products were inserted into pCR-Blunt II TOPO plasmid. Then the plasmids were transformed into *E. coli* strain DH5- α by heat shock. Colony PCR was performed to screen for bacterial colonies containing plasmid with inserted cytochrome *c5* gene (Figure 4.18). Then, each of the recombinant colonies was individually grown in LB for plasmid propagation for over night. Cells were harvested and the recombinant plasmids were purified with Qiagen Miniprep Kit and digested with *EcoRI*. The digested DNA products showed the right size of 1574 bp (*c5* gene) and 3519 bp (pCR-Blunt II TOPO plasmid)(Figure 4.19).

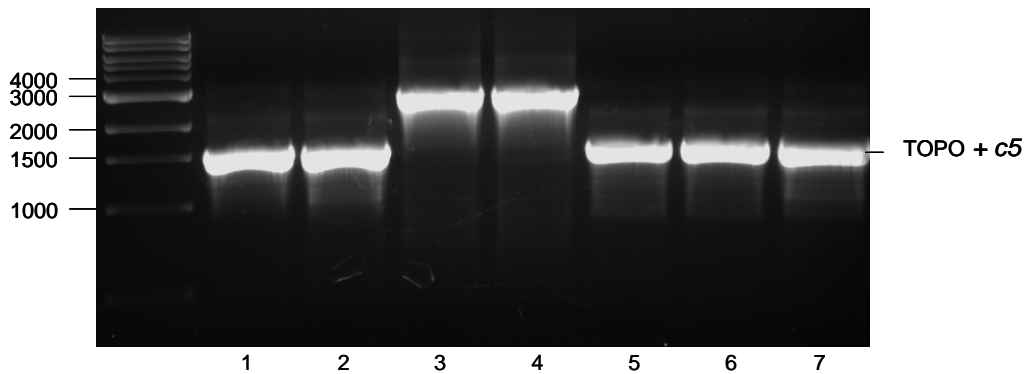


Figure 4.18 Colony PCR screen of pCR-Blunt II TOPO plasmid with insertion of cytochrome *c5* gene from *E.coli* DH5 α transformants.

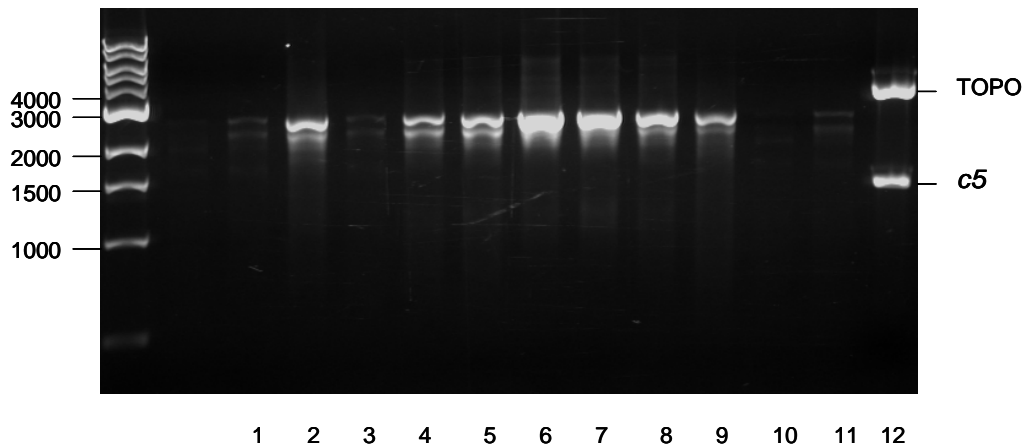


Figure 4.19 *EcoRI* digested products of pCR-Blunt II TOPO plasmid with insertion of cytochrome *c5* gene (lane 12). The *c5* fragment was found with size of 1.6 kb and the fragment of linearized pCR-Blunt II TOPO plasmid with size of 3.5 kb.

The tetracycline resistance gene cassette (*tet^r*) was chosen to insert into pCR-Blunt II TOPO + *c5* plasmid in order to disrupt the function of *c5* gene. This gene cassette is obtained from pGEM-TetM by PCR using PFU. The PCR product showing DNA fragments of 2.7 kb corresponding to *tet^r* cassette, 2758 bp (Figure 4.20). Forward primer (26 nucleotides) and reverse primer (28 nucleotides) are as shown respectively.

Forward primer (HP14) 5'-TTG AAG TCG ACG GGA GTA ATT GGA AG-3'

Reverse primer (HP15) 5'-TAA AAG TCG ACA TAC ATA ACG GAA AGA G-3'

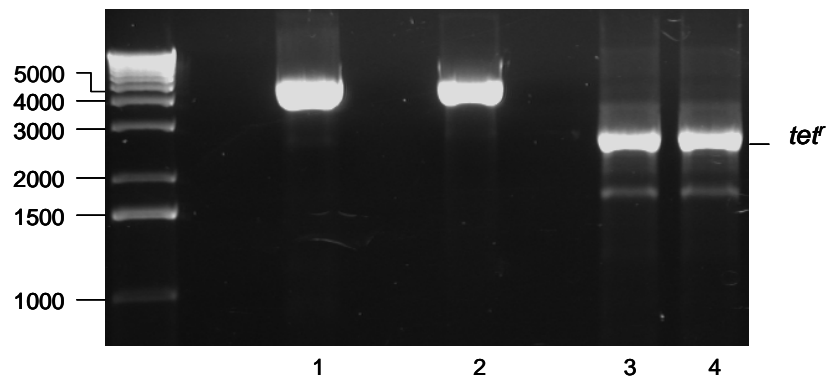


Figure 4.20 PFU PCR product of *tet^r* cassette exhibits size of 2.7 kb.

The pCR-Blunt II TOPO plasmid with *c5* gene insert were bluntly digested by *Xmn*I which cut only once in the middle of *c5* gene. The *tet*^r cassettes were blunt end-ligated with pCR-Blunt II TOPO + *c5* plasmid. The *E. coli* strain DH5 α was transformed by the ligation products. The transformants were plated and selected on tetracycline LB Agar. Colonies grown on the selective plate were screened for disrupted *c5* gene by colony PCR (Figure 4.21). Then, each recombinant colony was individually grown in LB for plasmid propagation for over night. Cells were harvested and the recombinant plasmids were purified with Qiagen Miniprep Kit and digested with *Eco*RI. The digested DNA products showed the right size of 4.1 kb (*c5* gene + *tet*^r gene) and 3.5 kb (pCR-Blunt II TOPO plasmid) (Figure 4.22). Then MC58 strain was transformed by TOPO plasmid containing disrupted *c5* gene. The transformants were plated and selected on tetracycline Blood Agar plate. Colonies selectively grown were screened for disrupted *c5* gene by colony PCR (Figure 4.23).

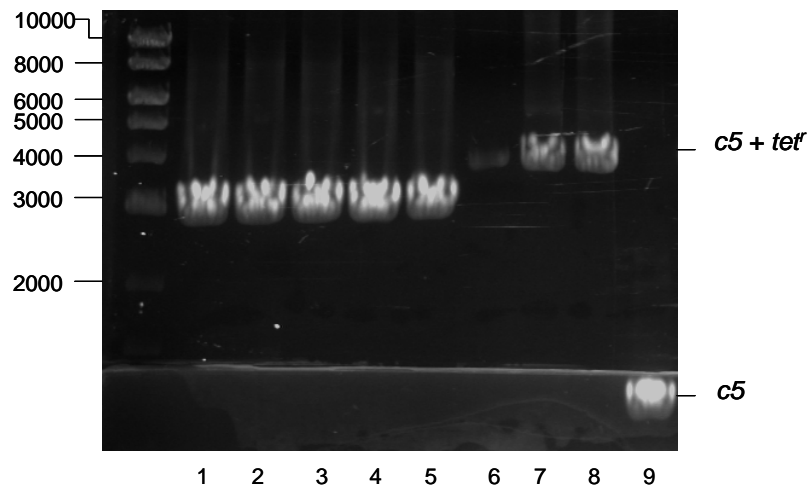


Figure 4.21 Colony PCR screen of *c5* gene with *tet*^r insert in *E. coli* DH5 α transformants. The *c5*::*tet*^r fragment were found in lane 7 and 8 with size of 4.2 kb (1.5 kb of *c5* + 2.7 kb of *tet*^r).

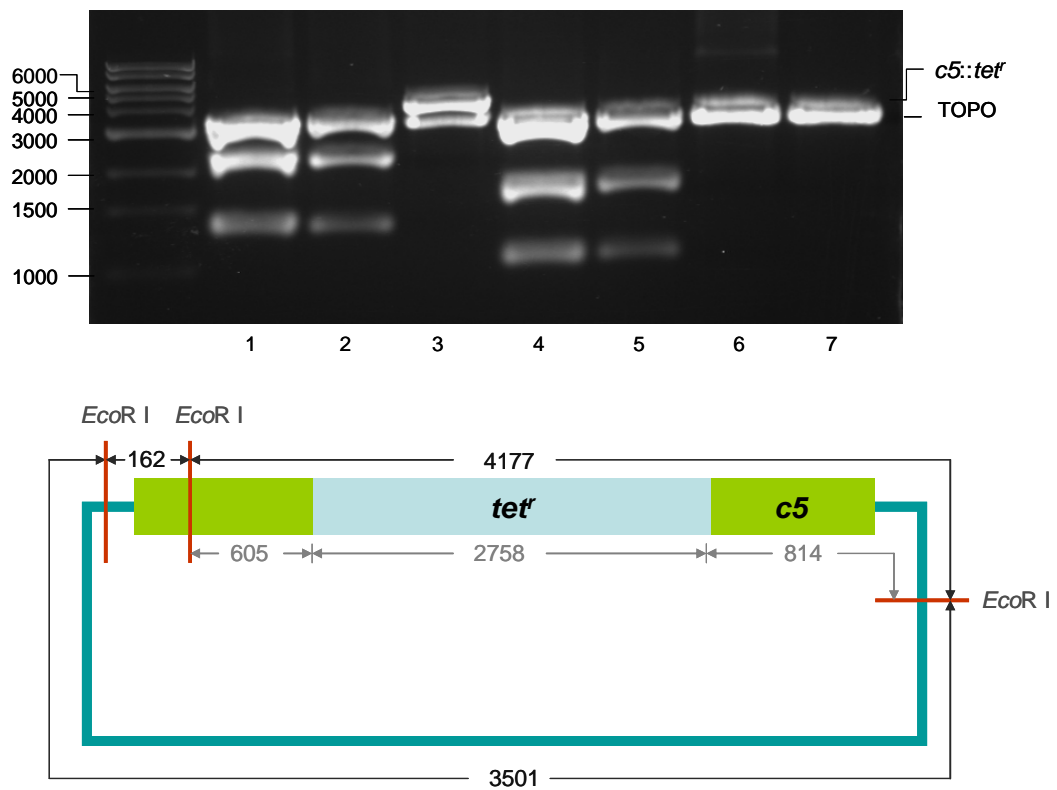


Figure 4.22 *EcoRI* digest screen of *c5* gene with *tet^r* insert. In lane 6 and 7, the digested DNA products showed the right size of 4.1 kb (*c5* gene + *tet^r* gene) and 3.5 kb (linearized pCR-Blunt II TOPO plasmid). Lane 3 is digested products of pCR-Blunt II TOPO + *laz* + *tet^r* plasmid.

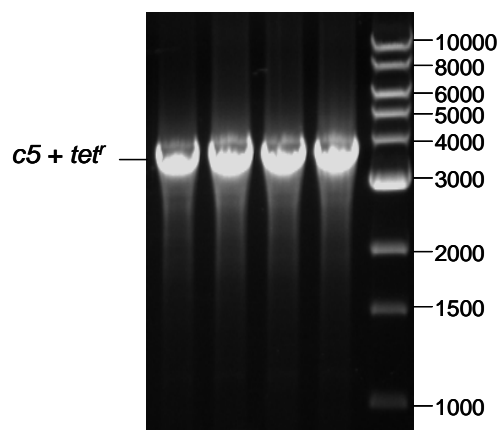


Figure 4.23 Colony PCR screen of disrupted *c5* gene in MC58 transformants. The *c5::tet^r* fragments were found in all lanes with size of 4.1 kb.

4.5 Construction of cytochrome *c2/c4* double mutant

N. meningitidis *c4* mutant strain was transformed by pCR-Blunt II TOPO + *c2* + *spc^r* plasmid. Transformants were plated and selected on combined spectinomycin and erythromycin Blood Agar plate. Colonies grown on the selective agar plate were screened for disrupted *c2* and *c4* genes by colony PCR (Figure 4.24). Colonies containing combined disrupted *c2* and *c4* gene were found.

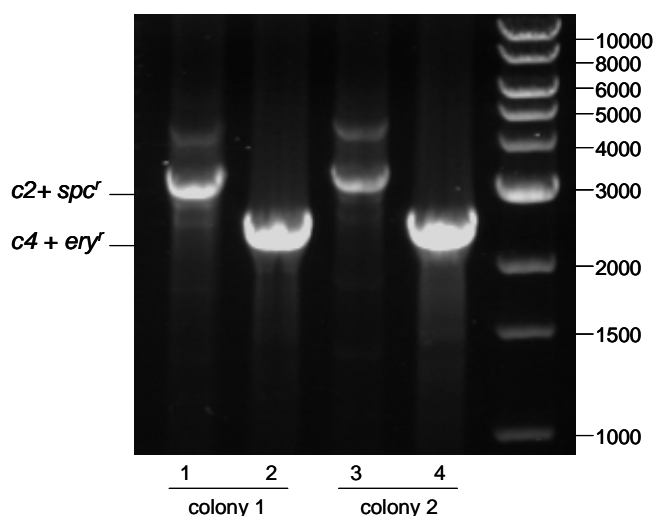


Figure 4.24 Colony PCR screen for double disrupted *c2* and *c4* gene in MC58 transformants. The *c2/c4* double mutant was successfully constructed as *c2::spc^r* (3.3 kb) and *c4::ery^r* fragment (2.6 kb) were found in both colonies 1 and 2.

4.6 Construction of *laz* mutant

Laz (NMB1533) is predicted to function as an electron donor to AniA nitrite reductase and an electron donor to cytochrome *cbb₃* oxidase. The *laz* gene contains nucleotide sequence encoding for a sequence of 182 amino acids with molecular weight of 17045 Da. It contains a predicted lipoprotein signal peptide of first 17 amino acid residues, a linker region (residue 18-62) and a globular azurin domain (residue 63-182). It is predicted to be cupredoxin and is localized in periplasm whilst the linker region is associated with the outer membrane.

Gene disruption was employed using an antibiotic resistance gene cassette as follows. The *laz* gene with flanking region containing *N. meningitidis* uptake sequence (Figure 4.25) with size of 1753 bp was amplified by PCR using PFU polymerase (Figure 4.26). The uptake sequence promotes the efficiency of DNA uptake by *N. meningitidis*. Forward primer (22 nucleotides) and reverse primer (22 nucleotides) are as shown respectively.

Forward primer (LazF) 5'-CAT TTT CAG ACG GCA TGT ATG G-3'

Reverse primer (LazR) 5'-TGT TTC AGA CGG CAT TAT TTG C-3'

```

AAAACTGCTGCCTGCCAACCTGCACCCG CATTTCAGACGGCATGTATCG AAGACGGCAGGCTTGCCTTTGGCGGCAAACAATATG
GCGGCATCGCGCTTGAAAATGATTGCACCGTCGGTATTGCCGCAGTTGGCAGGGCTTGATGCTTCGATACGCTCTGTTTCGGTCAGGC
TGGTCCCGAAACCGGAAAAACCGCCGAAAACCAATACCTGCAATTTAGTAAGGCTGCGCTGGAGAGTTTCGGTTCGGCGGCGGCAAA
GTTGGAAAAACGGCATCCCGAATTGGCGGAGGCATTGGCAAACCTGGTTAGAAGGCATGGCGCATAAAAATGTATACGGGAATTTGTGT
AAACATCCGTTAATATTAAGAAGTAAAGGATAATAGGTCTAATACTAAAGAAAATAGGTTCCGGGTAAAATGCCCCTTTTTGGGTAAA
CGATTGTAAACTTGCAAACAGGC TTTGATTTCAAATGAAATTTGTAGCAAAAATGCCGCTCCGAAACATCTGTTTGTGCAACGGCGCG
AATCTTTTTCAAGGTTTTGTTAATGGCGGTTGCACTTTGATTTCTGTAAAACCGAATATATTTTATCGATTGGAGATTTGTTATGAA
AGCGTATCTGGCTCTGATTTCTGCGCGGTTATCGGTTTGGCTGCCTGCTCTCAAGAACCTGCCGCGCCTGCTGCCGAGGCAACTCCT
GCTGCTGAAGCACCCGCTTCCGAAGCGCCTGCCGCCGAAGCTGCTCCTGCAGATGCTGCCGAAGCCCCTGCTGCCGCAACTGTGCGG
CAACTGTCGAATCCAACGACAATATGCAGTTC AACACCAAGACATCCAAGTCAGCAAAGCATGTAAGAGTTCACCATCACTCTGAA
ACATACCGGTACGCAACCCAAAGCCAGCATGGGTCACAATCTCGTGATTGCCAAAGCTGAAGACATGGACGGCGTATTTAAAGACGGC
GTAGGTGCTGCCGATACCGACTATGTCAAACCTGATGATGCACGCGTGTGTTGCCCATACCAAACCTGATCGGCGGCGGCGAAGAAGCTT
CCCTGACTCTGGATCCTGTCTAAATGGCCGACGGCGAATATAAATTCGCTTGTAACCTCCAGGTCACGGTGCTTTGATGAACGGCAA
AGTGACTTTGGTCGATTAATCCGCTTAAAGTCTCAAAAGACGGACAGCCTGCTTTGTGCAGGCTGTTTTATTATAAAAATGACTGCTTG
AAAAGTGCCTGTTGAGAACGAAAACATGAATCCGTTTGAACCAAAAAGCGTTACCTTTGCCGAACCGATTGAAATGCTGTATGCCTGC
CACGGCAAAGTGCCTGTTTTTGGGACAAGTCGCCATGCTGTGCGACTATATCGCCGAAAACGGCTGCAATCAGATTGTTTTGCAAA
CCATCCGCCAAATCGCCAGTATTTCAACGTTGCCGCGCCTGCACCATGAAGACGAAGAAGAAAACCTTCTCCGCTGCTGCTGCA
ATATGCCCGCAAGCCCAAGAAAGCGTGGACGAGCTTTTGGCCCAACATATCGGGCTGCACGACAACTGGGCGGCTGTTTTCCGCCGAA
TTTGCCAAACTCGAAGCAGACAACGCTTATGTCCCGATGAGGAAGCGTTCAAACGTTTTTGGCGGGATATGATGTTCAATTTGGCGA
TTGAAGAGCCGCTGTTTGTATATGGCAACACCTTTATCCAAAAGAAAACTGACCGAAATCGGCGAAATATGGCGGCGCGCCGGCG
CAAATAATGCCGCTCTGAAACAATCGTCT

```

Figure 4.25 The *laz* gene (blue) with flanking region(black) containing *N. meningitidis* uptake sequences (orange) and primer sequences (yellow highlight).

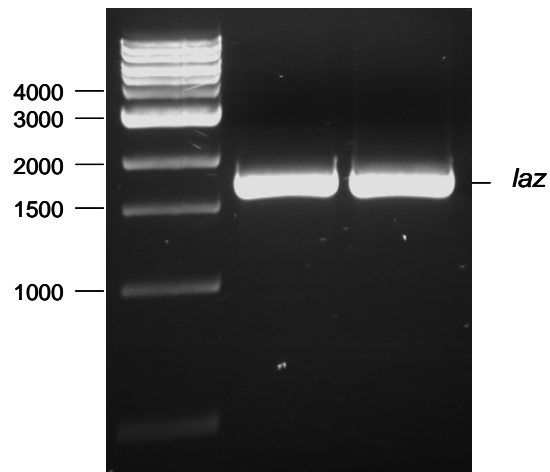


Figure 4.26 PFU PCR product of *laz* gene with flanking region exhibit size of 1.7 kb.

Then, blunt end cloning of *laz* gene with flanking region from PCR product was undertaken. The blunt end PCR product was inserted into pCR-Blunt II TOPO plasmid. Then the plasmids were transformed into *E. coli* strain DH5 α by heat shock. Colony PCR was performed to screen for bacterial colonies containing plasmid with inserted *laz* gene (Figure 4.27). Then, each of the recombinant colonies was individually grown in LB for plasmid propagation for over night. Cells were harvested and the recombinant plasmids were purified with Qiagen Miniprep Kit and digested with *EcoRI*. The digested DNA products showed the right size of 1.7 kb (*laz* gene) and 3.5 kb (pCR-Blunt II TOPO plasmid) (Figure 4.28).

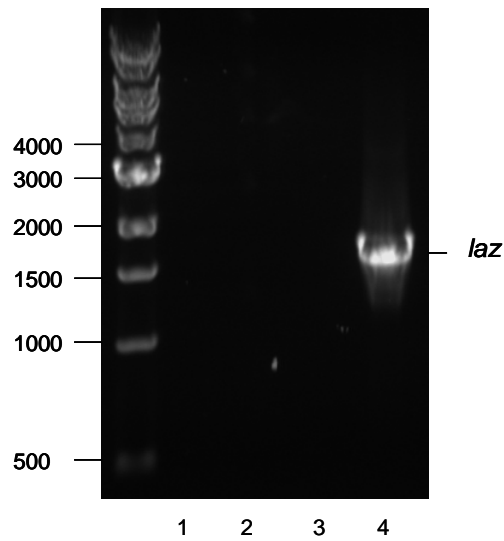


Figure 4.27 Colony PCR screen for *laz* gene insert in pCR-Blunt II TOPO plasmid. Fragment of *laz* gene was found in lane 4 exhibiting size of 1.7 kb.

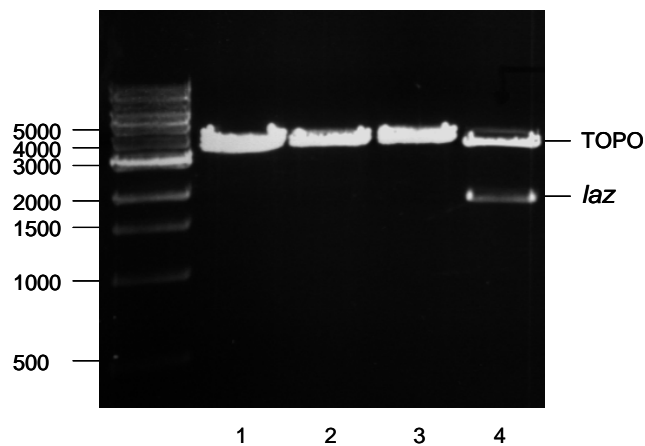


Figure 4.28 *Eco*RI digested products of pCR-Blunt II TOPO plasmid with insertion of *laz* gene.

The chloramphenicol resistance gene cassette (*chl^r*) was chosen to insert into pCR-Blunt II TOPO + *laz* plasmid in order to disrupt the function of *laz* gene. This antibiotic resistance gene cassette is on pST2 plasmid which is a derivative plasmid of pACYC184 plasmid. This gene cassette is obtained by PCR using PFU. The PCR products yielded DNA fragments of 1906 bp corresponding to *chl^r* cassette (Figure 4.29). Forward primer (22 nucleotides) and reverse primer (22 nucleotides) are as shown respectively.

Forward primer (ChloramF) 5'-AAG AAT TGG AGC CAA TCA ATT C-3'

Reverse primer (ChloramR) 5'-TAC ACT AAA TCA GTA AGT TGG C-3'

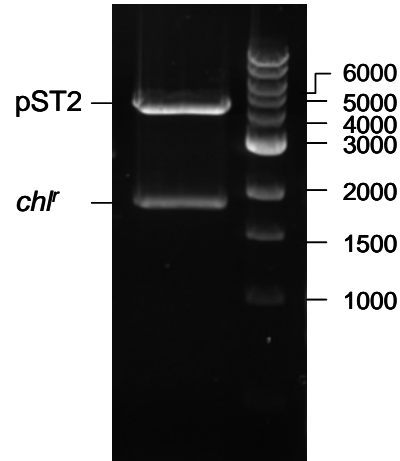


Figure 4.29 PFU PCR products of *chl'* gene from pST2 plasmid exhibits size of 1.9 kb while pST2 plasmid exhibits size of 4.2 kb.

In order to insert *chl'* cassette into the middle of *laz* gene, a small gap in the middle of *laz* gene on pCR-Blunt II TOPO + *laz* plasmid was generated using expanded PFU PCR. The forward and reverse primers are designed to bind and to initiate amplification from the middle of *laz* gene. The positions of the forward primer and the reverse primers are 8 nucleotides away from each other (Figure 4.30) Therefore, 8 nucleotides of *laz* gene were deleted from the PCR products. Forward primer (22 nucleotides) and reverse primer (22 nucleotides) are as shown respectively.

Forward primer (lazTOPO F) 5'-GCA TGG GTC ACA ATC TCG TGA T-3'

Reverse primer (lazTOPO R) 5'-GGT TGC GTA CCG GTA TGT TTC A-3'

AAAACTGCTGCCTGCCAACCTGCACCCG **CATTTTCAGACGGCATGTATCG** AAGACGGCAGGCTTGCCTTTTGGCGGCAAACAATATG
 GCGGCATCGCGCTTGAAAATGATTGCACCGTCGGTATTGCCGCGAGTTGGCAGGGCTTGATGCTTCGATACGCTCTGTTTCGGTCAGGC
 TGGTCCCGAAAACCGGAAAACCGCCGAAAACCAATACCTTGCATTTGAGTAAGGCTGCGCTGGAGAGTTTCGGTTCCGGCGCGGCAAA
 GTTGGAAAAACGGCATCCCGAATTGGCGGAGGCATTGGCAAACCTTGGTTAGAAGGCATGGCGCATAAAAATGTATACGGGAATTTGTGT
 AAACATCCGTTAATATTAAGAAGTAAAGGATAAATAGGTCTAATACTAAAGAAAATAGGTTCCGGGGTAAAAATGCCCTTTTTTGGGTAAA
 CGATTGTAAACTTGCAACAGGCTTTGATTTCAAATGAAATTTGTAGCAAAAATGCCGCTCCGAAACATCTGTTTGTGCAACGCGGCGG
 AATCTTTTTCAAGGTTTTGTTAATGGCGGTTGCACTTTGATTTCTGTAAAACCGAATATATTTTATCGATTGGAGATTGTTA**ATGAA**
AGCGTATCTGGCTCTGATTTCTGCCGCGTATCGGTTTGGCTGCCTCTCAAGAACCTGCCGCGCTGCTGCCGAGGCAACTCCT
GCTGCTGAAGCACCCGCTTCCGAAGCGCTGCCGCCGAAGCTGCTCCTGCAGATGCTGCCGAAGCCCTGCTGCCGCAACTGTGCGG
CAACTGTGCAATCCAACGACAATATGCAGTTCAACACCAAGACATCCAAGTCAGCAAAGCATGTAAAGAGTTCACCATCACTCTGA
TCATACGCTTACGCACT CAAAGCCA **GTATGGGTCAGCAACTGCTCA** TGCCAAGCTGAAGACATGGACGGCGTATTTAAAGACGGC
 GTAGGTGCTGCCGATACCGACTATGTCAAACCTGATGATGCACGCGTTGTTGCCCATACCAAACCTGATCGGGCGGCGGCAAGAAGCTT
 CCTGACTCTGGATCCTGCTAAATGGCCGACGGCGAATATAAAATTCGCTTGTAACCTTCCAGGTCACGGTGCTTTGATGAACGGCAA
 AGTGACTTTGGTCGAT**TAA**TCCGCTTAAAGTCTCAAAGACGGACAGCCTGCTTTGTGCAGGCTGTTTTATTATAAAAATGACTGCTTG
 AAAAGTGCCCGTTGAGAACGAAAACATGAATCCGTTTGAACCAAAAAGCGTTACCTTTGCCGAACCGATTGAAATGCTGTATGCCTGC
 CACGGCAAAGTGCGCCGTTTTTGGCGACAAGTCGCCATGCTGTGCGACTATATCGCCGAAAACGGCTGCAATCAGATTGTTTTGCAAA
 CCATCCGCAAAATCGCCAGTATTCAACGTTGCCGCGCGCTGCACCATGAAGACGAAGAAGAAAACCTTCTCCGCTGCTGCTGCA
 ATATGCCCGCAAGCCCAAGAAAGCGTGGACGAGCTTTTGGCCAAACATATCGGGCTGCACGACAACCTGGGCGGCTGTTTTCCGCCGAA
 TTTGCCAAACTCGAAGCAGACAACGCTTATGTCCCCGATGAGGAAGCGTTCAAACGTTTTGTGGCGGGATATGATGTTCAATTTGGCGA
 TTGAAGAGCCGCTGTTTGTATATGGGCAACACCTTTATCCAAAAGAAAACCTGACCGAAATCGGGCAAAATTATGGCGGCGCGCCGGC**G**
CAAATAATGCCGCTCTGAACAATCGTCT

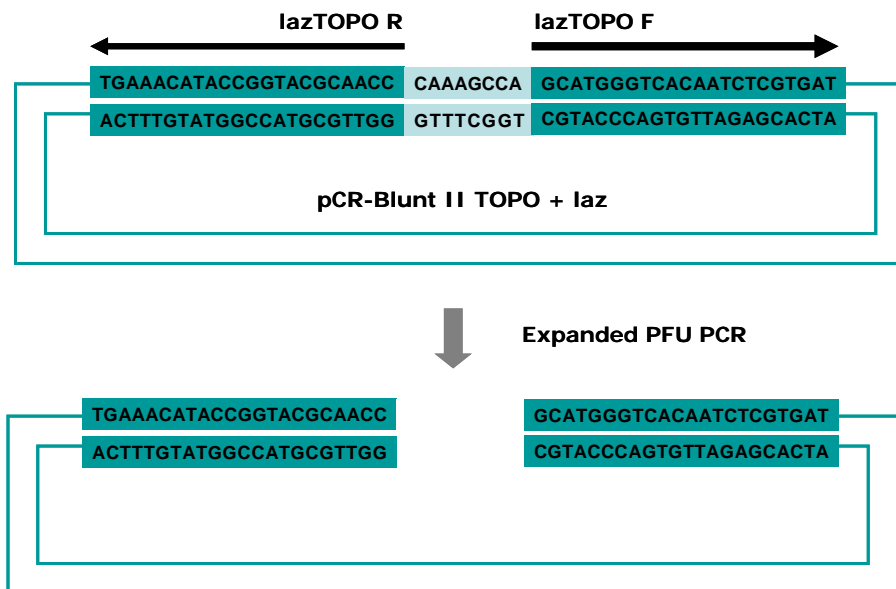


Figure 4.30 Expanded Pfu PCR of pCR-Blunt II TOPO + *laz* plasmid. The positions of primers (red highlight) for expanded PFU PCR of pCR-Blunt II TOPO + *laz* plasmid is indicated. The forward primer *laz*TOPO F is 8 nucleotide away from the reverse primer *laz* TOPO R. The PCR products are linearized pCR-Blunt II TOPO + *laz* plasmid that 8 nucleotides in the middle of the *laz* gene were deleted.

The Pfu expanded PCR products exhibited size of 5.2 kb corresponding to the combined size of *laz* gene (1.7 kb) and pCR-Blunt II TOPO plasmid (3.5 kb) (Figure 4.31).

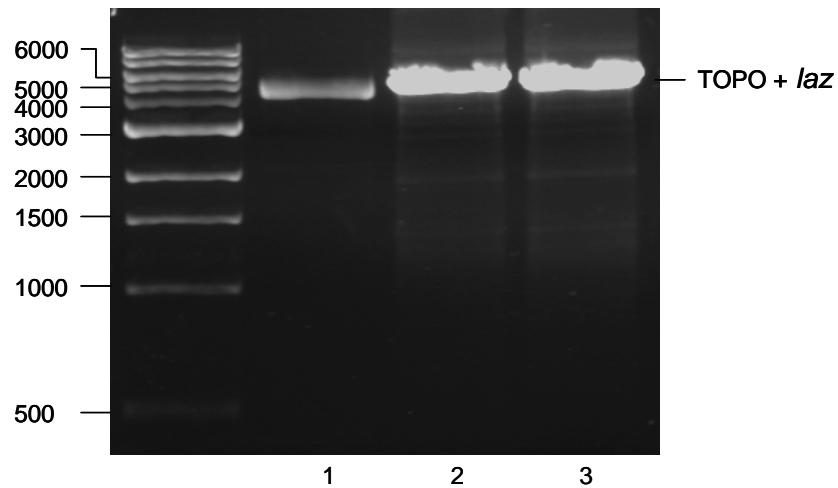


Figure 4.31 Pfu expanded PCR products of pCR-Blunt II TOPO + *laz* plasmid exhibits size of 5.2 kb corresponding to the combined size of *laz* gene (1.7 kb) and pCR-Blunt II TOPO plasmid (3.5 kb).

The PFU expanded PCR products of pCR-Blunt II TOPO + *laz* plasmid were bluntly ligated with *chl*' cassette. The *E. coli* DH5 α cells were then transformed by the ligation products. The transformants were selected by plating out on LB Agar plates containing chloramphenicol. Colonies grown on selective agar were screened for disrupted and partially deleted *laz* gene by colony PCR. Isolates containing copy of *laz* gene with partial deletion and disruption were found (Figure 4.32). Then, each recombinant colony was individually grown in LB with chloramphenicol for plasmid propagation for over night. Cells were harvested and the recombinant plasmids were purified with Qiagen Miniprep Kit and digested with *Eco*RI. *Eco*RI cuts three loci on this recombinant plasmid. The digested DNA products showed the right size of 2.3 kb and 1.35 kb (the size of *laz* gene + *chl*' gene is 3.65 kb) and 3.5 kb (pCR-Blunt II TOPO plasmid) (Figure 4.33). Then MC58 strain was transformed by TOPO plasmid

containing disrupted *laz* gene. The transformants were plated and selected on tetracycline Blood Agar plate. Colonies selectively grown were screened for disrupted *laz* gene by colony PCR (Figure 4.34).

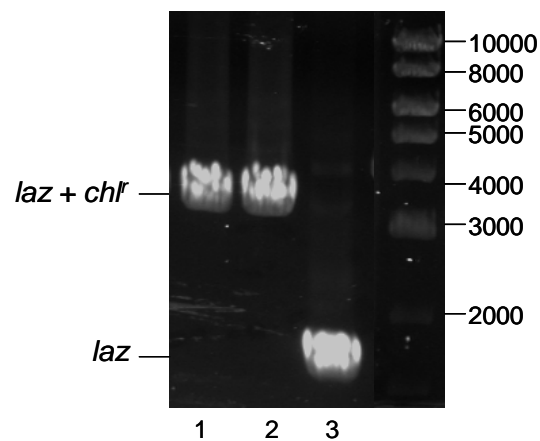


Figure 4.32 Colony PCR screen of *laz* gene with *chl^r* cassette insert. The *laz + chl^r* fragments (3.6 kb) were found in lane 1 and 2 while *laz* fragment (1.7 kb) without insert was found in lane 3.

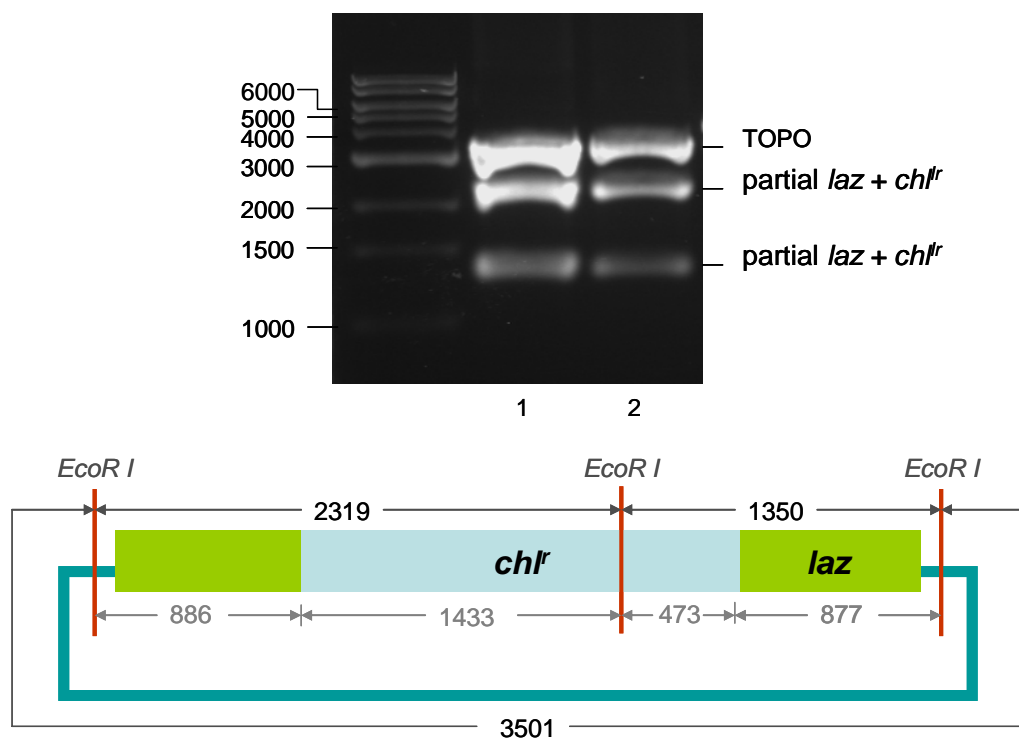


Figure 4.33 *EcoRI* digest screen of *laz* gene with *chl^r* insert. In both lanes 1 and 2, there are 3 fragments corresponding to restriction map on recombinant plasmid.

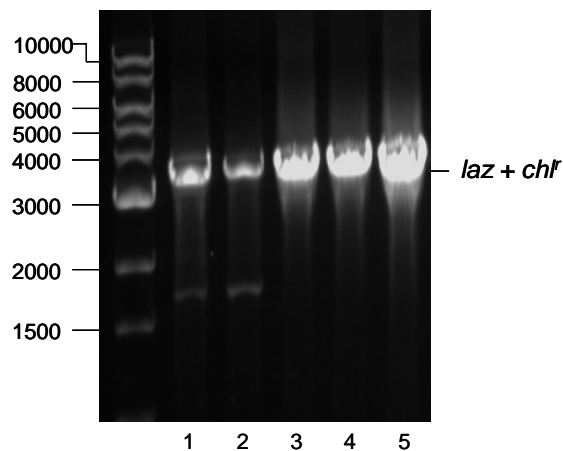


Figure 4.34 Colony PCR screen of disrupted and partially deleted *laz* gene in MC58 transformants. The disrupted *laz* gene was found in every lane.

4.7 Construction of *nsrR* / *laz* double mutant

N. meningitidis nsrR mutant strain was transformed by pCR-Blunt II TOPO + *laz* + *chl'* plasmid. Transformants were plated and selected on combined spectinomycin and chloramphenicol Blood Agar plate. Colonies grown on the selective agar plate were screened for disrupted *nsrR* and *laz* genes by colony PCR (Figure 4.35). Colonies containing combined disrupted *nsrR* and *laz* gene were found. Forward primer (20 nucleotides) and reverse primer (20 nucleotides) for disrupted *nsrR* gene are as shown respectively.

Forward primer (*nsrRF*) 5'-CCC GAC GGA CAG GGT TTC AA-3'

Reverse primer (*nsrRR*) 5'-CGC TCG GTC GGA ATA TCC GT-3'

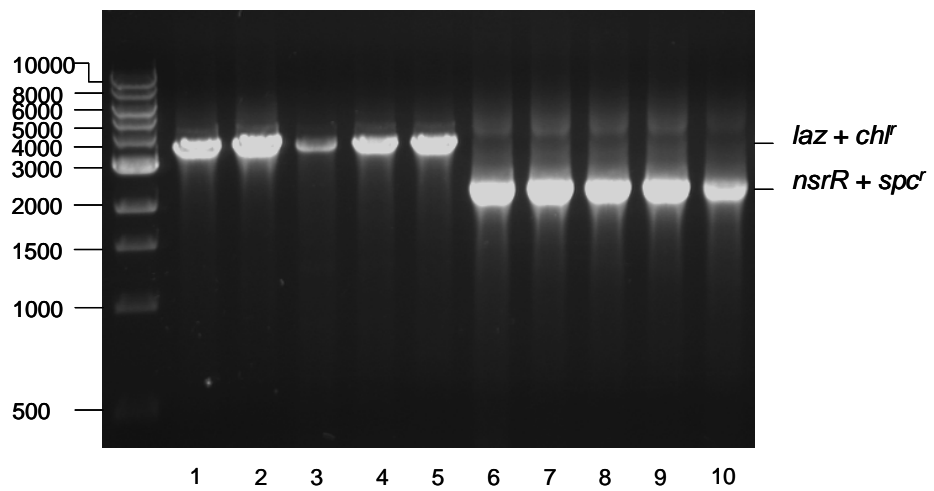


Figure 4.35 Colony PCR screen for combined disrupted *nsrR* gene and *laz* gene in MC58 transformants. Lane 1 and lane 6 are same colony and likewise other lane pair. The fragments of both *laz + chl* and *nsrR + spc'* were found in all colonies shown.

Chapter 5

Cytochromes *c2* and *c4* are major electron donors to *cbb₃* oxidase

5.1 Introduction

N. meningitidis has a choice of three respiratory electron acceptors which are oxygen, nitrite, and nitric oxide. Genome analysis shows one reductase encoded for each terminal electron acceptor. These three terminal reductases include cytochrome *cbb₃* oxidase, AniA nitrite reductase, and NorB nitric oxide reductase. The *cbb₃* oxidase reduces oxygen whereas AniA nitrite reductase reduces nitrite, and NorB nitric oxide reductase reduces nitric oxide. Oxidase and nitrite reductase are predicted to oxidize *c*-type cytochromes whilst nitric oxide reductase is predicted to oxidize quinol. It has been shown that electron flow to the *cbb₃* oxidase and AniA are dependent on *bc₁* complex whereas the flow to NorB is predicted to be independent from *bc₁* complex (Deeudom *et al*, 2006). There is more diversity of small periplasmic *c*-type cytochromes than there are reductases. There are three *c*-type cytochromes predicted to function as electron transfer proteins that carry electrons in the periplasm from the *bc₁* complex to terminal reductases. These include cytochrome *c2*, *c4*, and *c5*. It is possible that some of these periplasmic cytochromes could have similar roles or overlapping functions. The differences in their biophysical and biochemical properties may give them advantage to function most effectively under different conditions.

The electron transfer proteins that are responsible for carrying electrons from the *bc₁* complex to the terminal reductases have not been identified and characterized in the meningococcus. The aim of this chapter is to characterize the involvement of

cytochrome *c2* and *c4* in particular respiratory pathways. This chapter shows investigation and evidence regarding the role of cytochrome *c2* and cytochrome *c4* in electron transport, respiration and growth of *N. meningitidis*.

5.1.1 Structure of cytochrome *c2*

NMB0717 is predicted to encode a small *c*-type cytochrome with similar structure of cytochrome *c₅₅₂* in other bacteria. Protein sequence comparison shows that cytochrome *c2* of serogroup B is very similar to that in serogroup C, whereas cytochrome *c2* of serogroup A is different at its C-terminus. Its apoprotein has 138 amino acids with predicted MW of 14,715 Da. The sequence contains a predicted signal peptide of 26 residues to be cleaved off and give rise of mature protein with a predicted MW of 12,034.8 Da. It is predicted to be monohaem cytochrome and localized in periplasm (Figure 5.1). Molecular mass of haem is 616.4 Da. Therefore, the association of haem gives rise to the mature cytochrome *c2* with predicted mass of 12,651.2 Da.

The protein sequence is quite similar to that in *N. gonorrhoeae* but with differences in N- and C-terminal region. C-terminus of cytochrome *c2* of serogroup A contains an extra 30 residues and that of gonococcus contains extra 22 residues longer than that of serogroup B (Figure 5.2) but these extra sequence residues are also different from each other. The haem-binding site is conserved near the N-terminus suggesting that cytochrome *c2* could be a low spin cytochrome with the sixth ligand, hexacoordinate, provided by a methionine residue further on towards the C-terminus (Figure 5.3). There are homologs of cytochrome *c2* in other β -proteobacteria, including *Methylobacillus*, *Nitrosomonas*, *Polaromonas*, *Rhodoferrax*, *Burkholderia*, and *Ralstonia*. One of the homologs, cytochrome *c₅₅₂* in *Thermus thermophilus* transfers

electrons from bc_1 complex to ba_3 oxidase (Muresanu *et al*, 2006). The crystal structure of cytochrome c_{552} from this organism shows haem being hexacoordinate with conserved Met residue as the sixth ligand. This conserved Met residue is also found in the meningococcus cytochrome c_2 protein sequence (Figure 5.3).

```

MKETPMNTRLPTALVLGCFCAAASAADNSIMTKGQKVYESNCVACHGKKGGE
GRGTMFPPLYRSDFIMKKPQVLLHSMVKGINGTIKVNKTYNGFMPATAISDAD
IAAVATYIMNAFDNGGGSVTEKDVKQAKSKKN

```

Figure 5.1 Primary sequence of cytochrome c_2 from *N. meningitidis* strain MC58. The predicted signal peptide (pink highlight) has cleavage site at ASA-AD. The haem-binding site (yellow highlight) is near N-terminus. This might suggest low spin property of the cytochrome with hexacoordinate by methionine (green highlight) toward C-terminus. This Met residue is conserved among c_{552} homologs.

```

NMB0717      MKETPMNTRLPTALVLGCFCAAASAADNSIMTKGQKVYESNCVACHGKKGEGRGTMFPP
NMC0668      -----MNTTRLPTALVLGCLCAAASAADNSIMTKGQKVYESNCVACHGKKGEGRGTMFPP
NMA0925      -----MNTTRLPTALVLGCLCAAASAADNSIMTKGQKVYESNCVACHGKKGEGRGTMFPP
NGO0292      -----MNTTRLPTAFILCCLCAAASAADNSIMTKGQKVYESNCIACHGKKGEGRGTAFFPP
TTHA1423     -----MKRTLMAFLLLGGLALAQADGAK-----IYAQCAGCHQONGQIPGAFFP
              *: *  :.  :.      * *..*.          ::* .** :*:**   ***

NMB0717      LYRSDFIMKKPQ----VLLHSMVKGINGTIKVNKTYNGFMPATAIS--DADIAAVATYIM
NMC0668      LYRSDFIMKKPQ----VLLHSMVKGINGTIKVNKTYNGFMPATAIS--DADIAAVATYIM
NMA0925      LYRSDFIMKKPQ----VLLHSMVKGINGTIKVNKTYNGFMPATAIS--DADIAAVATYIM
NGO0292      LFRSDYIMNKPQ----VLLHSMVKGINGTIKVNKTYNGFMPATAIS--DADIAAVATYIM
TTHA1423     LAGHVAEILAKEGREYLILVLLYGLQGQIEVKGMYNGVMSSFAQLKDEEIAAVLNHIA
              *      :      .      *:      ::  *:* *:* * .***.*: *      * :**** .:*

NMB0717      NAFD-----NGGGSVTEKDVKQAKSKKN-----
NMC0668      NAFD-----NGGGSVTEKDVKQAKGKKN-----
NMA0925      NAFD-----NGGGSVTEKDVKQAKNKKTKQTKCRLKPAIRLQTAFKSNLSNAVLSAP
NGO0292      NAFD-----NGGGSVTEKDVKQAKGKKNQTDKMPSETGNPASDGIQIKPF-----
TTHA1423     TAWGDAKKVKGFKPFTAEEVKKLRAKKLTQQVLAERKKLGLK-----
              .*:.      :*  .*  :*: * : *

```

Figure 5.2 Multiple alignment of cytochrome c_2 homologs. Cytochrome c_2 of serogroup B (NMB0717) has 30 residues shorter than that of serogroup A (NMA0925) and of the gonococcus (NGO0292) at C-terminus (blue highlight). However, the structure of mature cytochrome of serogroup B and C should be identical after the signal peptide is cleaved off. They all are monohaem cytochromes and share the same haem-binding site (yellow highlight). The hexacoordinate by methionine (green highlight) toward C-terminus is conserved among

5.1.2 Structure of cytochrome *c4*

Gene NMB1805 is predicted to encode for a *c*-type cytochrome. We refer to the NMB1805 gene product as cytochrome *c4* due to the similarity to cytochrome *c4* of *Pseudomonas stutzeri* (Template PDB Code 1m70A). Cytochrome *c4* (NMB1805) of serogroup B is identical to that in serogroup A and C. There is only one amino acid residue that is different from that in *N. gonorrhoeae*. Its apoprotein has 207 amino acids with predicted MW of 21,989 Da. It is predicted to contain dihaem and be localised in periplasm as it has predicted signal peptide with cleavage site between position 18 and 19 (VSA-SP) (Figure 5.4). The predicted molecular mass of holoprotein is 20,175 Da. The molecular mass of each haem is 616 Da. This will give rise to molecular mass of 21,407 Da of mature dihaem cytochrome *c4*. As there are two haem-binding sites, this might suggest that this cytochrome might contain two domains that with different functions. The crystal structure of cytochrome *c4* from *Pseudomonas stutzeri* shows that both haems are hexacoordinate with Met residue as the sixth ligand. Generally, this Met ligand is downstream of C-XX-CH motif about 45-50 residues. In both the meningococci and the gonococcus, there are consensus of these Met residues, downstream of both haem-binding sites (Figure 5.5). In *P.stutzeri*, however, the position of Met ligand for haem 1 is slightly different from those in *Neisseria*. So, this haem 1 of cytochrome *c4* in *Neisseria* might not be hexacoordinate. As the protein sequences are identical among the meningococcus and the gonococcus, this might indicate similar function of this cytochrome in both species. There are homologs of cytochrome *c4* in other bacteria, mainly β -proteobacteria, including *Nitrospira*, *Nitrosomonas*, *Methylibium*, *Polaromonas*, *Rhodospirillum rubrum*, *Ralstonia*, *Burkholderia*, *Xanthomonas*, *Nitrosococcus*, *Legionella*, and *Vibrio*. However, functions of cytochrome *c₅₅₄* in other organisms have not been identified.

```
MKRLTLLAFVLAAGAVSASPKADVEKGKQVAATVCAACHAADGNSGI  
AMYPRLAAQHTAYIYHQTIGIRDGKRTHGSAAVMKPVVMNLSDQDILN  
VSAFYAKQPKSGEANPKENPELGAKIYRGGLSDKKVPACMSCHGPSG  
AGMPGGGSEIQAYPRLGGQHQAYIVEQMNAYKSGQRKNTIMEDIANR  
MSEEDLKAVANFIQGLR
```

Figure 5.4 Primary sequence of cytochrome *c4*. The predicted signal peptide (pink highlight) has cleavage site at VSA-SP. There are two haem-binding sites (yellow highlight). There are two methionines predicted to be the sixth ligand of each haem. The first haem is predicted to have methionine (green highlight), 47 residues downstream of C-XX-CH, as the sixth ligand. The second haem is predicted to have another methionine (red highlight), 45 residues downstream of C-XX-CH, as the sixth ligand. It is likely that both haem are hexacoordinate and might have low spin property.

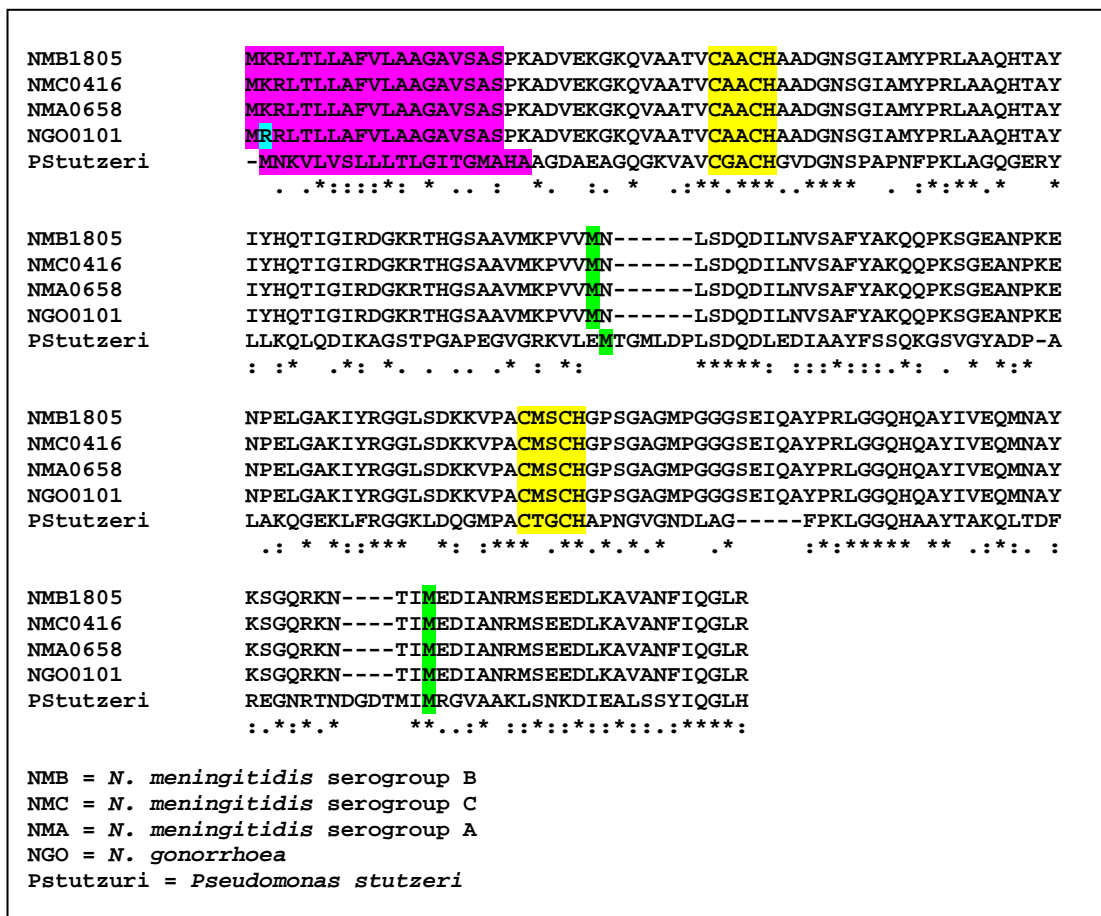


Figure 5.5 Cytochrome *c4* is extremely conserved among *N. meningitidis* serogroup A, B and C and *N. gonorrhoeae*. They have two haem-binding site (yellow highlight) and are predicted to be dihaem cytochromes. The homologs among those in meningococcus are identical while there is only one single amino acid that different in gonococcus which is in the signal peptide region (blue highlight). Basically, the mature cytochromes of the meningococci and the gonococcus are identical. The crystal structure of cytochrome *c4* from *Pseudomonas stutzeri* shows that both haems are hexacoordinate with Met residue as the sixth ligand. Generally, this Met ligand is downstream of C-XX-CH motif about 45-50 residues. In both the meningococci and the gonococcus, there are consensus of these Met residues, downstream of both haem-binding sites (green highlight).

5.2 Results

5.2.1 Visualization of cytochromes by western blot and ECL chemiluminescence.

In this investigation, soluble fraction of cell extracts were prepared and solubilized in 25 mM HEPES pH 7.0 with 1% dodecyl maltoside to give better resolution of cytochrome profiles. After solubilization, soluble fraction was collected for cytochrome detection. The haem group of *c*-type cytochromes is covalently linked to the protein polypeptide. *c*-type cytochromes can be visualized using chemiluminescence staining (Vargas *et al*, 1993) as described earlier in Chapter 3, section 3.2.1. A strain defect in any *c*-type cytochromes should be detected by this method with a missing signal band corresponding to predicted molecular weight of that cytochrome.

Haem stain of soluble and membrane protein from whole cell extract of *c2* , *c4* and *c2/c4* mutants, separated by SDS-PAGE, and blotted onto nitrocellulose membrane, are shown in Figure 5.6. The strain of *c2* mutant lane did not show any difference from WT strain. Cytochrome *c2* can not be characterized by this method of staining and visualization. The cytochrome *c2* might not have peroxidase activity and make it not possible to be detected by this method. There is a cytochrome missing from the lane of *c4* mutant and *c2/c4* double mutant while this protein is present in other mutant strains and in wild type strain. This cytochrome has approximate MW of 21-22 kDa which corresponds to the predicted molecular mass of cytochrome *c4* (21415 Da). It is likely that this cytochrome is the mature periplasmic cytochrome *c4*.

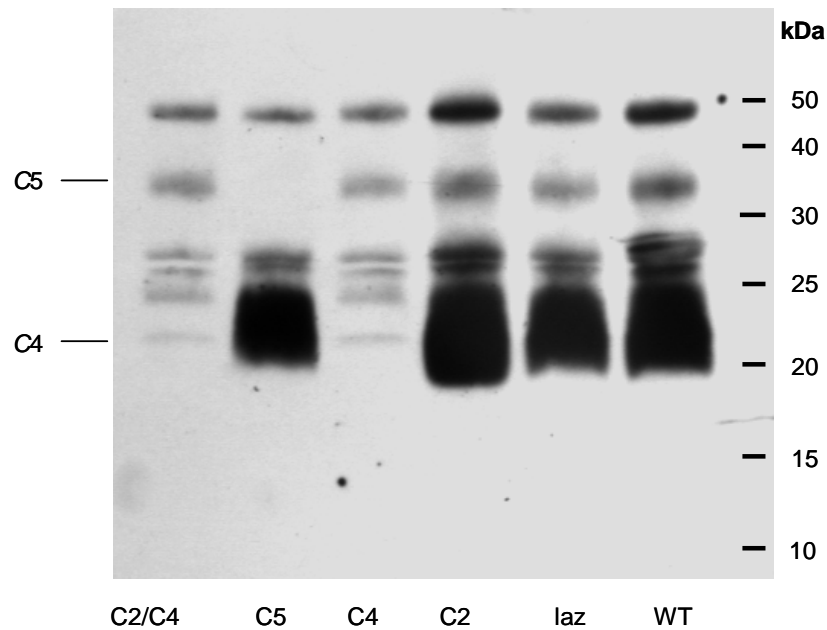


Figure 5.6 Cytochrome profiles of respiratory mutants. Soluble fraction of cell extracts were prepared in 25 mM HEPES buffer with 1% dodecyl maltoside. Equal amount of 13 μ g total protein was loaded in each lane. Mature cytochrome *c2* has predicted MW of 12651.2 Da. Cytochrome *c4* has predicted MW of 21,407.8 Da. Cytochrome *c5* has predicted MW of 29,987.8 Da. Lane 1 = *c2/c4* mutant, lane 2 = *c5* mutant, lane 3 = *c4* mutant, lane 4 = *c2* mutant, lane5 = *laz* mutant, lane 6 = WT. Cytochrome *c4* were not detected in *c4* and *c2/c4* mutant while cytochrome *c2* cannot be visualized by this method. Cytochrome *c5* was not detected in *c5* mutant but were detected in other strains appearing on SDS-PAGE at 35 kDa.

5.2.2 Growth under aerobic conditions

The purpose was to investigate the role of cytochrome *c2* and *c4* on growth of the meningococcus under high level of oxygen as terminal electron acceptor. The *c2*, *c4*, and *c2/c4* double mutant strains were grown in MHB under aerobic conditions. All mutant strains and WT strain were grown aerobically by shaking 6 ml of culture in 25 ml plastic MacCartney tube at 200 rpm. In this experiment, oxygen is the only terminal electron acceptor for respiration. The aerobic cultures were sampled and two fold diluted for

measuring optical density at 600 nm. The growth characteristics of the mutants are shown in Figure 5.7. In general, all the strains with cytochrome *c2*, *c4*, or *c2/c4* defect showed growth defect under high level of oxygen. The WT strain entered exponential growth after 2 hr and reached maximum optical density of 2.8 at 8 hr and quickly entered death phase. The *c2* mutant entered exponential growth at the same time as WT but it exhibited lower growth. It entered stationary phase after reaching optical density of 1.0 at 5 hr . The *c4* mutant grew slower than the *c2* mutant and it did not enter exponential growth. However, it still grew to optical density of 1.0 at 8 hr then quickly entered death phase. The *c2/c4* double mutant grew extremely slowly and only reached optical density of 0.5 after 10 hr. Doubling time for WT is 43 minutes, *c2* is 63 minutes, *c4* is 130 minutes, and *c2/c4* is 174 minutes.

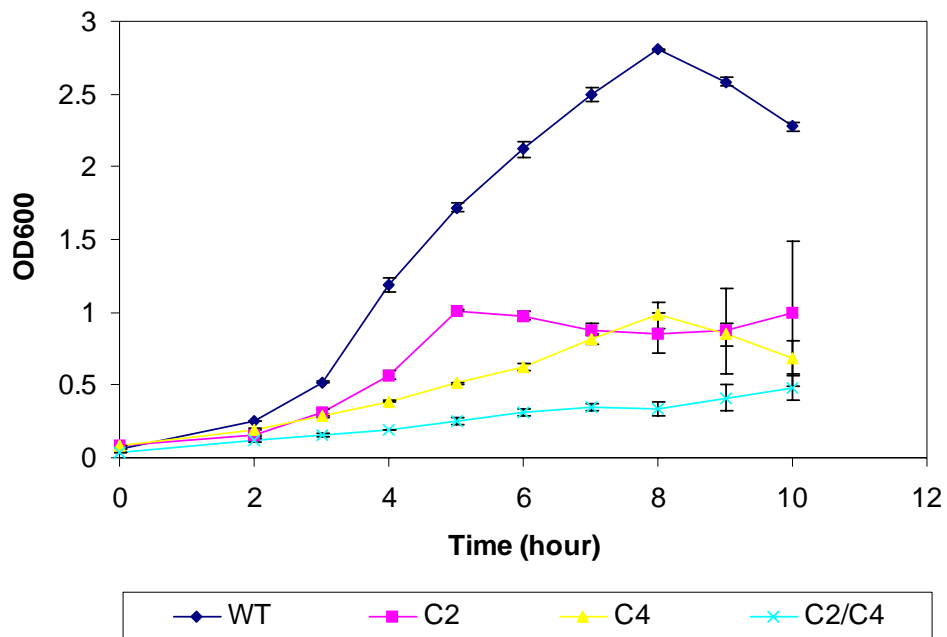


Figure 5.7 Growth of *c*-type cytochrome mutants under aerobic conditions. *c2* and *c4* mutant grew poorly and reached maximum optical density of 1.0. The *c2/c4* double mutant grew much more slower than single mutants. Doubling time for WT = 43 minutes, *c2* = 66 minutes, *c4* = 130 minutes, and *c2/c4* = 174 minutes.

5.2.3 Growth under microaerobic conditions

The purpose was to investigate the role of cytochrome *c2* and *c4* on growth of the meningococcus under very low level of oxygen. Cells were grown in 20 ml of MHB in plastic McCartney tube with 90rpm shaking. Growth of *c2* and *c4* under microaerobic conditions are poorer than WT strain (Figure 5.8). The maximum optical density of WT strain grown under microaerobic conditions was 0.2 whereas those of *c2* and *c4* are 0.16 and 0.14 respectively. Generally, the *c2* and *c4* mutant grew poorer than WT under low level of oxygen.

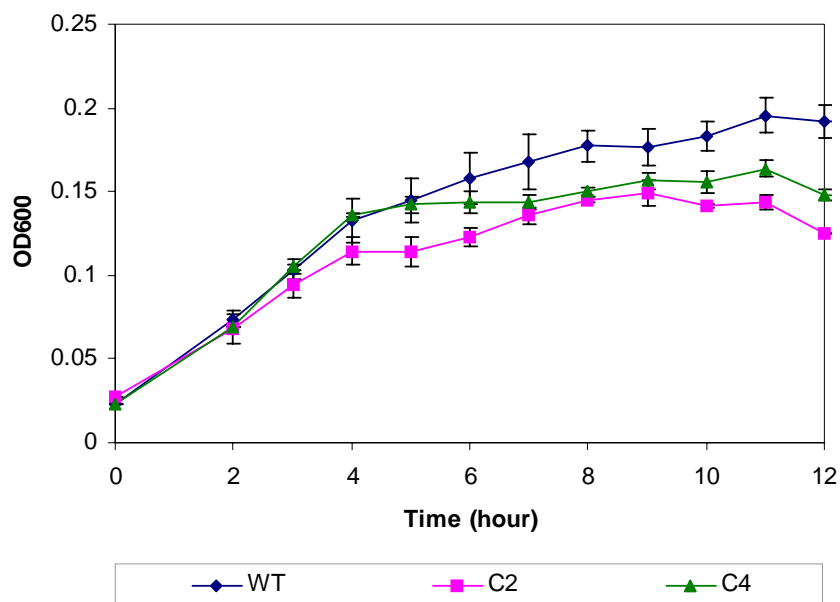


Figure 5.8 Microaerobic growth of *c2* and *c4* mutant. Both mutants grew poorer than wild type. The growth of *c2* mutant was most affected under low level of oxygen.

5.2.4 Growth under microaerobic conditions with nitrite

The purpose was to investigate the role of cytochrome *c2* and *c4* on growth of the meningococcus under very low level of oxygen with presence of nitrite as an alternative terminal electron acceptor. The growth conditions were similar to that under microaerobic conditions but 5 mM nitrite were present. All strains can grow under microaerobic conditions with nitrite supplement. The growth of all strains are better than those under microaerobic conditions without nitrite. The WT strain grew to a higher maximum optical density of 0.4. The *c2* mutant reached maximum optical density at 0.35 while those of *c4* and *c2/c4* at 0.25 (Figure 5.9). The *c2* mutant and the *c2/c4* double mutant grew faster than other strains during first six hour, then entered stationary phase. The *c2/c4* double mutant reached maximum growth at hour 6, earliest among all strains, then entered stationary phase. The *c2* mutant grew better than the others until reaching maximum optical density at hour 7, then entered stationary phase. Since all mutants grew under microaerobic condition with nitrite supplement better than under microaerobic conditions without nitrite, it is possible that all the mutants can still use nitrite as alternative terminal electron acceptor to supplement growth under low level of oxygen.

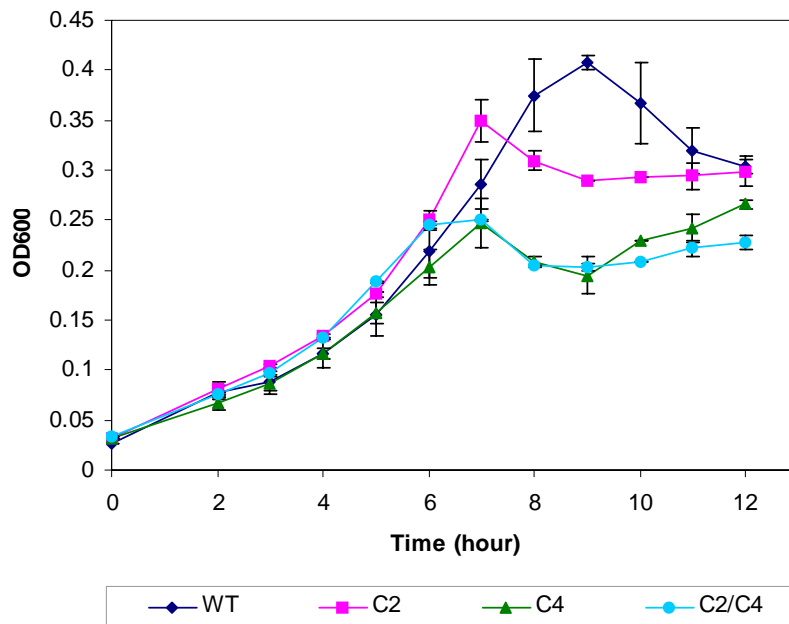


Figure 5.9 Growth of *c2*, *c4*, and *c2/c4* mutants under denitrifying conditions. All strains grew better than they were grown under microaerobic conditions without nitrite. However, the mutants grew poorer than WT, especially the *c4* mutant and the *c2/c4* double mutant.

5.2.5 Oxygen reduction rate in cytochromes *c2*, *c4*, and *c2/c4* mutants

The cytochrome *c2*, *c4*, and *c2/c4* double mutant grew poorly under aerobic conditions. It is hypothesized that this might be related to a decreased rate of oxygen consumption. As previously described the cytochrome *c2* and *c4* might be electron donors to *cbb₃* oxidase in the meningococcus, so the strains defective in one of these cytochromes might have decreased rate of oxygen reduction. The purpose was to measure oxygen reduction rate in intact cells of mutants compared to WT. This could help to explain if the growth defect under aerobic and microaerobic conditions are linked with an impairment of oxygen reduction. Cells were grown in MHB under aerobic conditions for 4 hours. Then, cells were harvested and resuspended in MHB to optical density (600 nm) around 1.3 -1.5. For the *c2/c4* double mutant strain, cells were grown under denitrifying conditions instead of aerobic conditions to get enough cells for oxygen reduction measurement. Oxygen consumption rates were measured using Clark-

type oxygen electrode. The measurements were done in total 3 ml of MHB with 5mM glucose at 37°C. First, 2.7 ml of MHB with glucose was added into the electrode chamber. Then, 0.3 ml of cell suspension was added into the chamber. Therefore, the final optical density of cell would be around 0.13-0.15. The disappearance of oxygen was recorded for the period of 10 to 15 minutes on chart recorder. The rate of oxygen reduction was calculated in the unit of nmole/min/mg protein. In this experiment, glucose was used for supplying electrons through generation of NADH by TCA cycle. The oxygen reduction rate is higher in the presence of glucose than in its absence (data not shown). Since the measurement was done in such a very short time, the cell density should not be significantly increased. Under aerobic growth, the oxygen reduction rate of WT was 145 nmole/min/mg. The *c2* mutant has 130 nmole/min/mg (10% decrease) and the *c4* mutant has 90 nmole/min/mg (37% decrease) (Figure 5.10). Under microaerobic growth with nitrite, WT has 77 nmole/min/mg while *c2/c4* mutant has 35 nmole/min/mg (55% decrease)(Figure 5.11). In WT strain, the oxygen reduction rate of microaerobic preculture cell was nearly half of aerobic preculture cell.

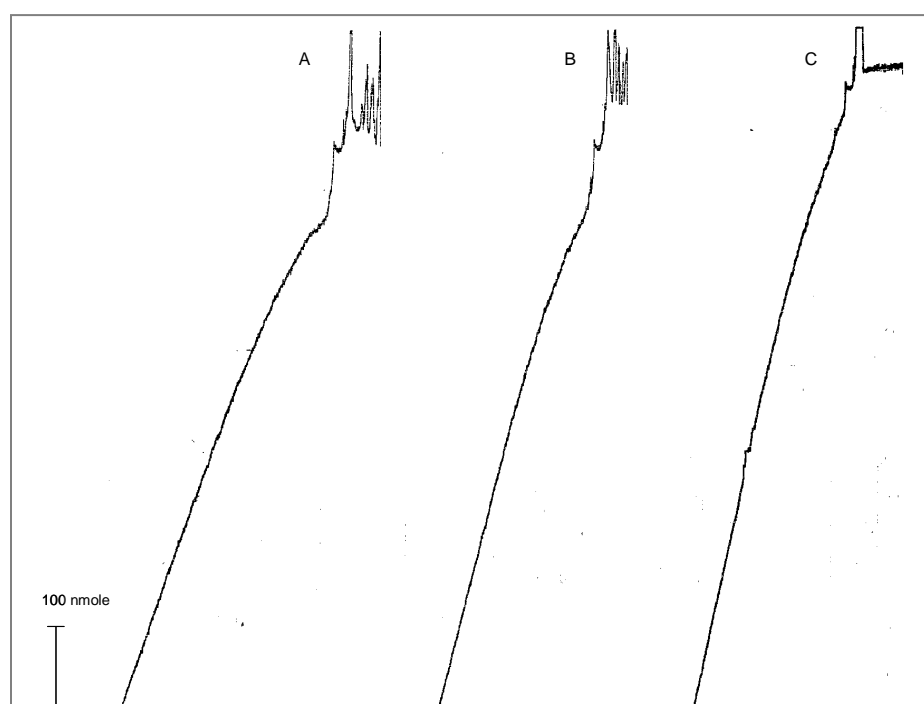


Figure 5.10 oxygen reduction rate of *c4* mutant, *c2* mutant, and WT. Cells were grown under aerobic conditions. The *c4* mutant has oxygen reduction rate of 90 nmole/min/mg (A) while the *c2* has 130 nmole/min/mg (B) and WT has 145 nmole/min/mg (C). The *c4* mutant has 37 % decreased rate of oxygen reduction while the *c2* mutant has 10 % consistent with both cytochromes being electron donors to *cbb₃* oxidase whilst *c4* is the major electron donor under this aerobic conditions.

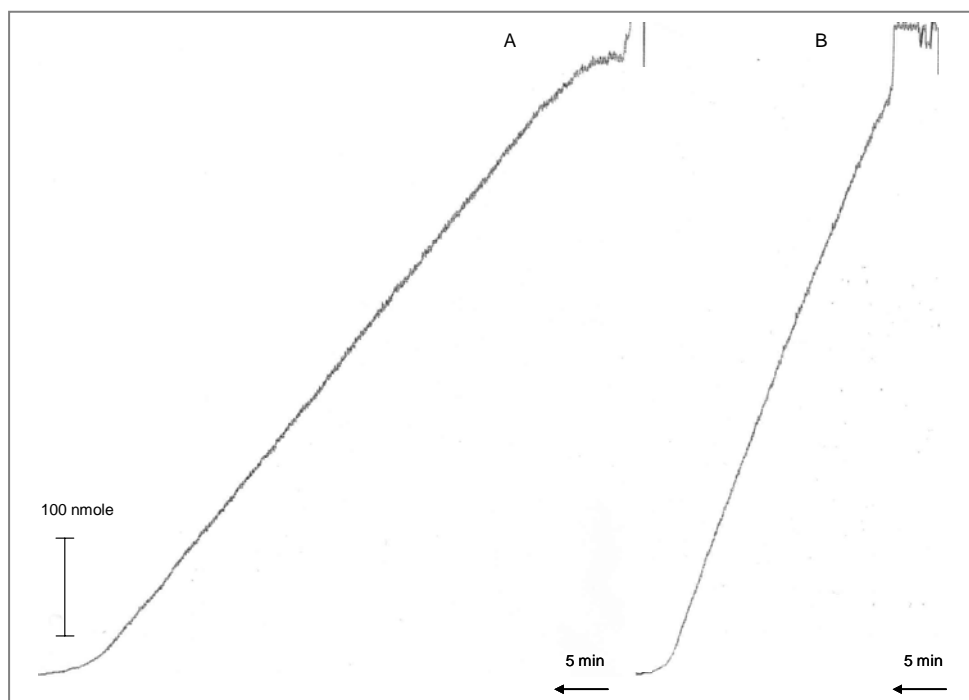


Figure 5.11 Oxygen reduction rate of *c2/c4* double mutant (A) compared to WT (B). Cells were grown under microaerobic condition with 5 mM nitrite as *c2/c4* poorly grows under aerobic

conditions. Content of cells were equal in each assay. The *c2/c4* mutant has oxygen reduction rate of 35 nmole/min/mg whereas the WT has 77 nmole/min/mg. The *c2/c4* mutant has 55% decreased rate of oxygen reduction suggesting that cytochrome *c2* and *c4* are electron donors to *cbb₃* oxidase.

5.2.6 Nitrite reduction of cytochromes *c2*, *c4*, and *c2/c4* mutant

Since *c2*, *c4*, and *c2/c4* mutant can grow under denitrifying conditions better than microaerobic conditions, it is likely that they can use nitrite as respiratory substrate to support growth under low level of oxygen. However, the denitrifying growth yields of mutants are still poorer than that of WT. The purpose was to measure the utilization of nitrite during microaerobic growth to see if poor growth yield is related to the decreased ability to reduce nitrite. The meningococci were grown under microaerobic conditions with 5 mM nitrite supplement. Levels of nitrite were measured by nitrite assay every hour of growth. It has been found that all mutants can reduce nitrite during growth under microaerobic conditions. All mutants utilized nitrite better than WT (Figure 5.12). The *c2/c4* double mutant started reducing nitrite quicker than other strains. The level of nitrite was decreased faster than other strains. Nitrite disappearance by *c2* and *c2/c4* double mutants occurred at the same time, at hour 8, while that by WT at hour 9. However, after 6 hours the *c4* mutant had slower nitrite reduction than other strains and nitrite completely disappeared at hour 12.

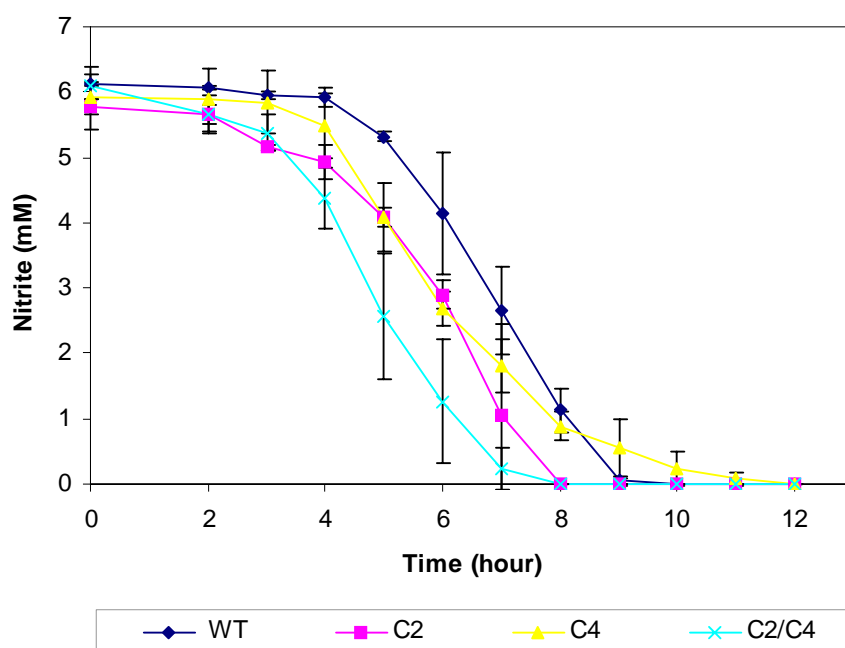


Figure 5.12 The *c2* mutant, *c4* mutant, and *c2/c4* double mutant can reduce nitrite during microaerobic growth. *c2/c4* double mutant reduced nitrite earlier than other strains including WT. However, its growth is similar to *c4* but poorer than other strains.

5.2.7 Production of nitric oxide by *c2/c4* mutant

Since *c2* and *c2/c4* consumed nitrite faster than WT strain, it was of interest to investigate if the mutant is able to reduce nitrite and generate nitric oxide faster than WT. Intact cells of *c2/c4* mutant strains were used for measuring the rate of nitric oxide accumulation compared to WT.

5.2.7.1 Cell preparations for nitric oxide accumulation assay

N. meningitidis were grown under conditions that allow expression of AniA but not NorB in order to determine the rate of nitric oxide production without removal of nitric oxide. It is shown that the direct inducer of NorB is nitric oxide, not nitrite (Rock *et al*, 2007). However, nitrite can indirectly induce expression of NorB via nitric oxide generated by AniA. This cell preparation is based on the implication that under

microaerobic conditions without nitrite, FNR can induce expression of AniA but not NorB. On the other hand, the presence of nitrite can induce expression of both AniA and NorB. Preliminary study shown in Figure 5.13 supports the supposition here. NO accumulation between cells grown under denitrifying conditions and cells grown under microaerobic conditions were different. It was found that cells grown under denitrifying condition shows much lower NO accumulation than cells grown under microaerobic conditions.

In this experiment, *N. meningitidis* were grown on Columbia-Blood Agar for over night. Then colonies at the end of streaking plane were scraped and inoculated into 20 ml of MHB in plastic McCartney tube to OD600 of 0.5. Cells were grown under microaerobic conditions without nitrite for 3 hours. Then, cells were centrifuged at 4000xg for 10 minutes and resuspended in MHB to OD600 of 1.5.

5.2.7.2 Nitric oxide accumulation assay

The assay for nitric oxide generation were done using Clark-type electrode with nitric oxide electrode. First, 2.7 ml of MHB with 5 mM glucose was added to the electrode chamber and level of oxygen and nitric oxide were recorded by chart recorder. Then, 0.3 ml of cell suspension was added to the chamber. The chamber was capped and nitric oxide electrode was submerged into the suspension. After the level of oxygen decreased to zero percent, nitrite was added to final concentration of 5 mM. The level of nitric oxide generated from nitrite reduction, supposedly by AniA, and accumulated in the electrode chamber was monitored and recorded over time course.

It has been found that the *c2/c4* mutant can generate nitric oxide almost at the same rate as that of WT (Figure 5.14). These experiments are not really usefully quantitative as AniA expression is suboptimal under microaerobic growth in the

absence of nitrite. Nitrite reduction rates were shown to be at least as high in *c2*, *c4*, and *c2/c4* mutant compared to wild type in denitrifying growth conditions.

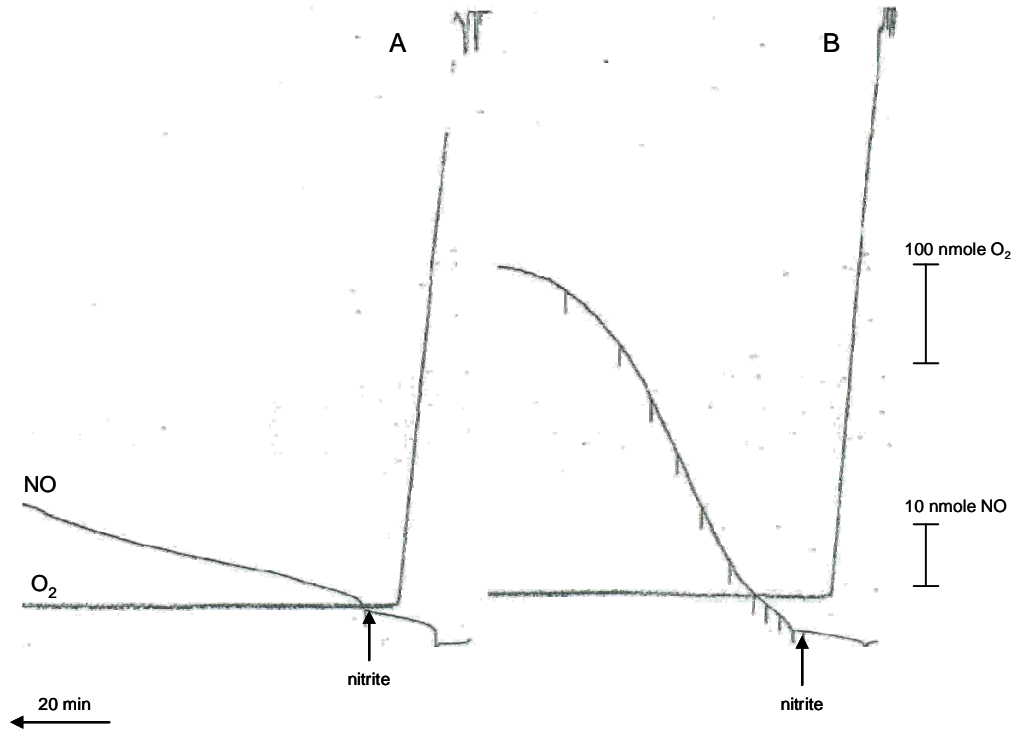


Figure 5.13 NO accumulation between WT cell grown under denitrifying conditions and WT cells grown under microaerobic conditions. (A) WT cells grown under denitrifying condition shows lower NO accumulation presumably due to higher expression of NorB. (B) WT cells grown under microaerobic conditions show higher NO accumulation presumably due to lower expression of NorB. Therefore, cells grown under microaerobic conditions have been used for investigation of capability of NO generation in respiratory mutants.

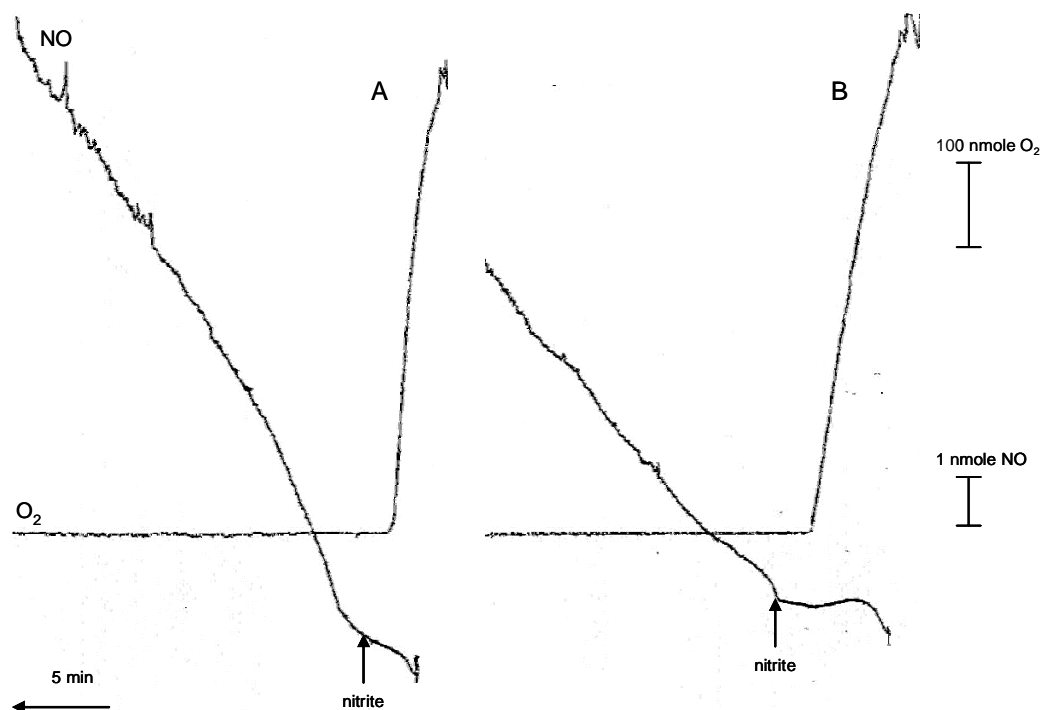


Figure 5.14 NO production in WT (A) and *c2/c4* double mutant (B) demonstrated that the cytochrome *c2* and cytochrome *c4* may be not electron donors to AniA. The mutant can reduce nitrite to NO. It shows NO accumulation at the rate of 0.7 nmole/min/mg whereas WT at the rate of 1 nmole/min/mg. Cells were grown under microaerobic conditions without nitrite in order to induce expression of AniA without expression of NorB. It is assumed that NorB is induced by the presence of NO. The expression of AniA under microaerobic conditions without nitrite might be much lower than that with nitrite and cause the slower rate of NO accumulation. The background NorB expression under microaerobic conditions without nitrite has not been investigated. The background rate of NO removal and degradation has also not been investigated.

5.2.8 Nitrite inhibits aerobic growth of *N. meningitidis*.

As *c2/c4* mutant utilized oxygen poorly for aerobic respiration and utilized nitrite earlier than WT when cultured for denitrification growth, this raised the question if this mutant is able to reduce nitrite before oxygen has become depleted. Nitrite is an alternative terminal electron acceptor for the meningococcus but little is known about the interplay between oxygen and nitrite in control of respiratory metabolism. The purpose of this experiment was to investigate if the meningococcus can utilize nitrite as respiratory substrate under high level of oxygen. Another question is if the rate of aerobic respiration is low, would the meningococcus utilize nitrite under high level of oxygen. Nitrite is well known for its toxicity to bacterial cell, but the mechanism of toxicity is not well understood. It was found that the *c2/c4* mutant did not grow at all under aerobic conditions with 3 mM nitrite. The WT strain poorly grew in the presence of nitrite. Nitrite inhibited growth of both WT and the *c2/c4* mutant (Figure 5.15).

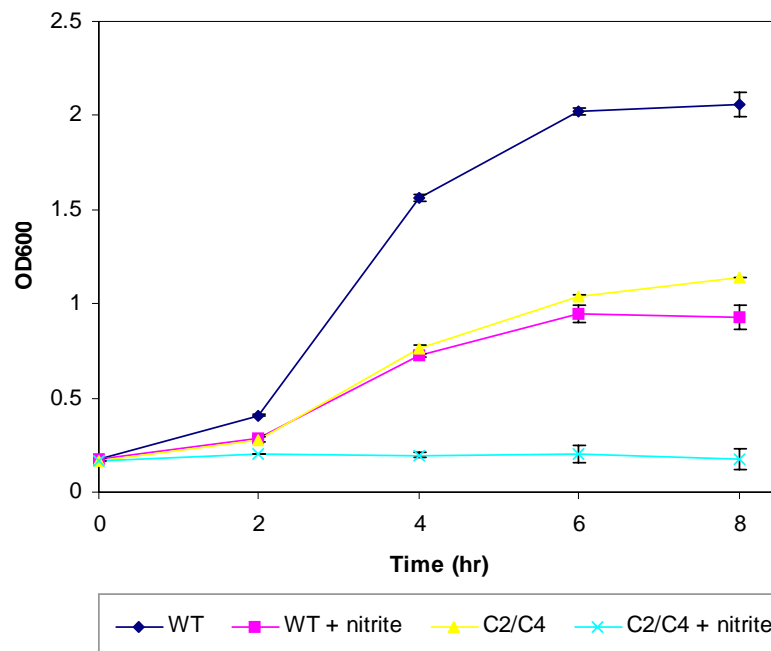


Figure 5.15 Nitrite inhibits aerobic growth of WT and *c2/c4* double mutant. The *c2/c4* is highly sensitive to nitrite. It is not known if AniA was expressed in the mutant under this growth conditions. The expression of AniA might lead to accumulation of NO and cell death.

5.2.9 Nitrite reduction does not occur under aerobic conditions

WT strain and *c2/c4* mutant were grown under aerobic conditions in the presence of nitrite. Both strains cannot reduce nitrite under aerobic conditions (Figure 5.16). The level of nitrite was not changed over the time course of 8 hours. The expression of AniA and NorB were not investigated in this experiment.

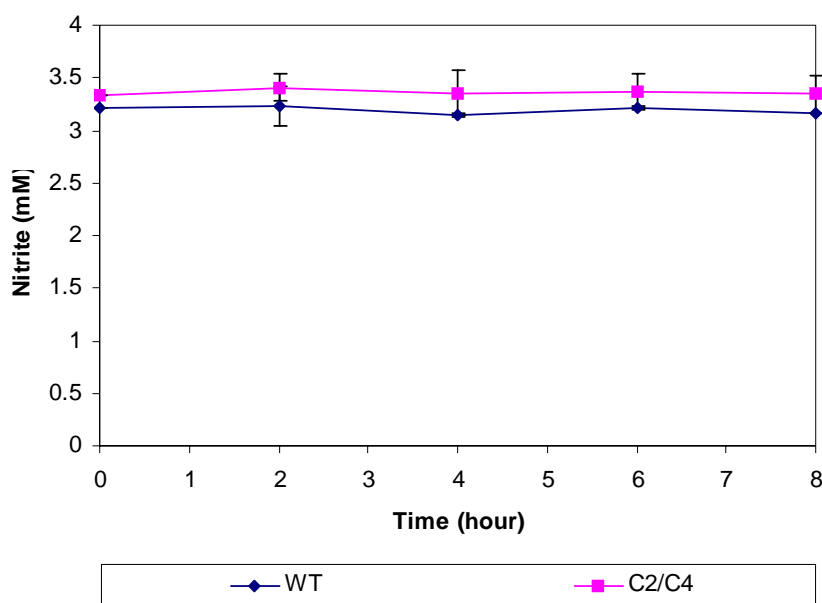


Figure 5.16 WT strain and *c2/c4* mutant did not utilize nitrite under aerobic conditions.

5.2.10 Spectra of *c2*, *c4*, and *c2/c4* mutants

Intact cells of *c2*, *c4* and *c2/c4* mutants show different visible light spectra when oxidized by oxygen. The double derivatives of the oxidized minus reduced difference spectra are shown in Figure 5.17A. Each mutant showed different pattern of spectra. All mutants showed decreased absorption at Soret band. The absorption at alpha band is of interest (Figure 5.17 B). The WT strain exhibited alpha peak at 554 nm whereas *c2* mutant exhibited alpha peak at 552.5 nm and *c4* mutant exhibited alpha peak at 555 nm. WT minus mutant difference spectra showed the lost absorption in

mutants (Figure 5.18A). At alpha peak, *c2* mutant lost absorption at 555 nm while *c4* mutant lost absorption at 551 nm. The *c2/c4* double mutant lost absorption at 554 nm (Figure 5.18B). Interestingly, *c2* mutant also lost Soret peak absorption at higher wavelength than that of *c4* mutant.

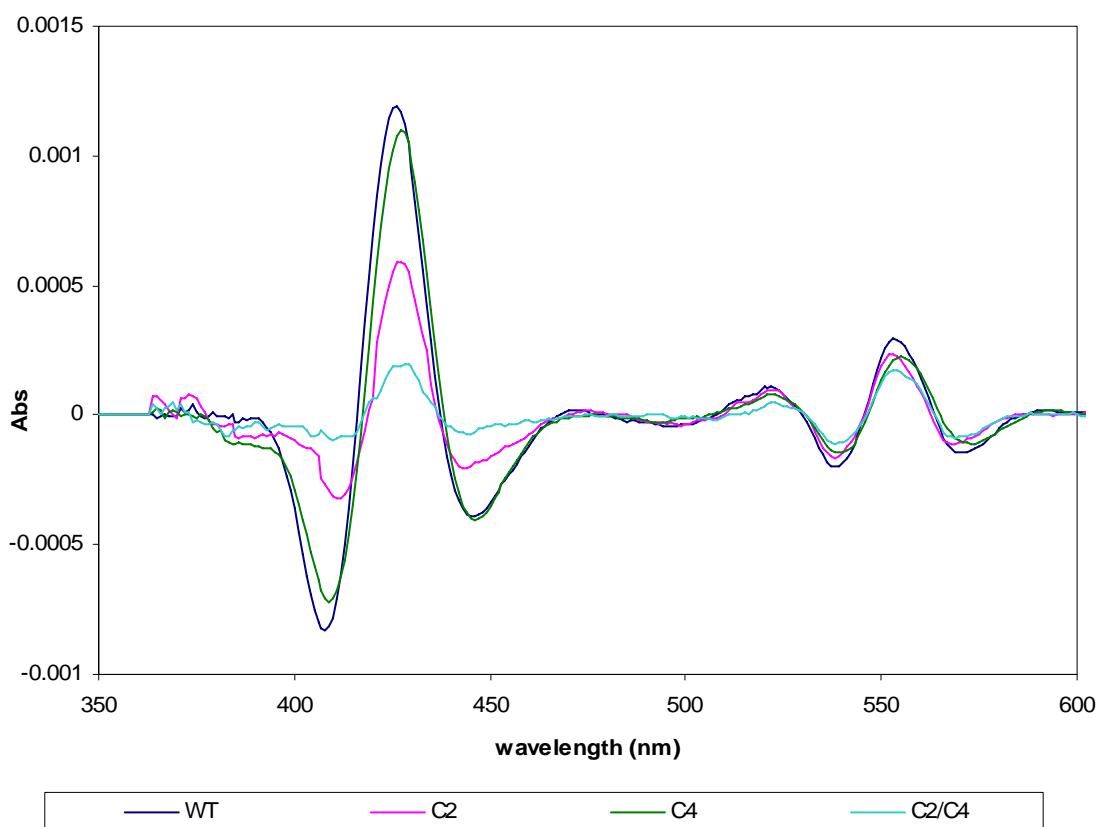


Figure 5.17A Double derivatives of oxidized minus reduced difference spectra of mutants. *c4* mutant still exhibited strong absorption change at Soret band while *c2* mutant exhibited weaker change at Soret band. The *c2/c4* double mutant exhibited very little change at Soret band. The absorption change at α band is also unique in each mutant.

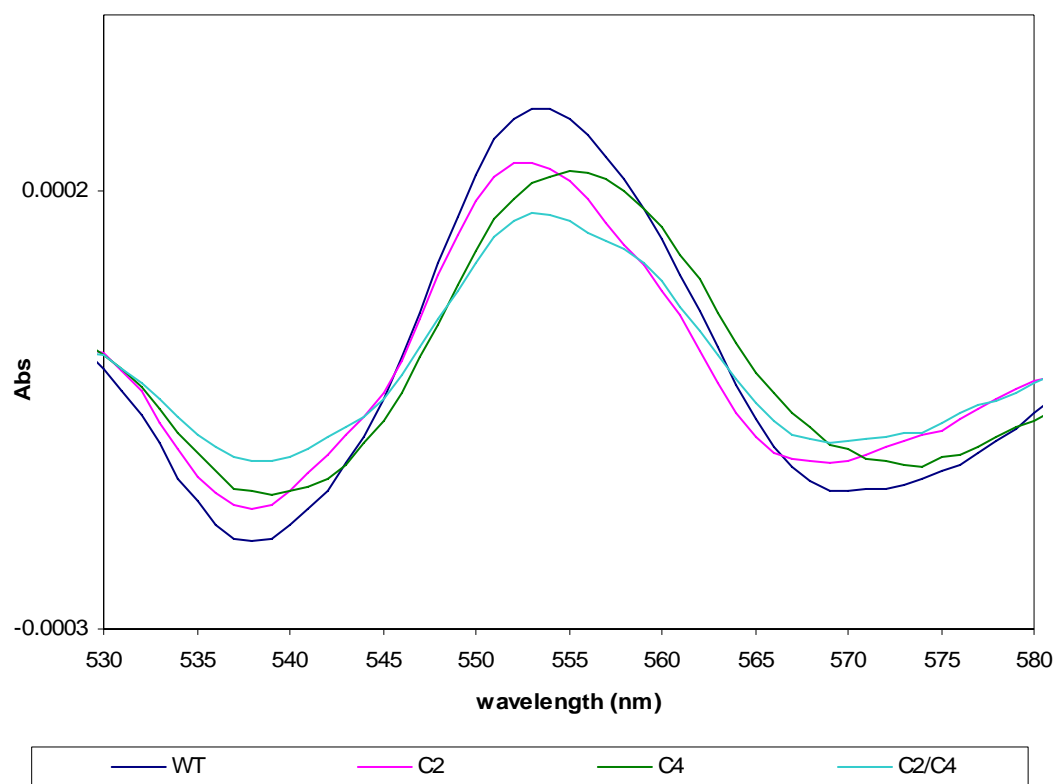


Figure 5.17B Mutant strains exhibited different absorption at α band. *c2* mutant exhibited α peak at 552 nm whereas *c4* mutant exhibited α peak at 555 nm. The *c2/c4* mutant exhibited α peak at 553 nm with weaker absorption than other strains. WT strain exhibited α peak at 553 nm.

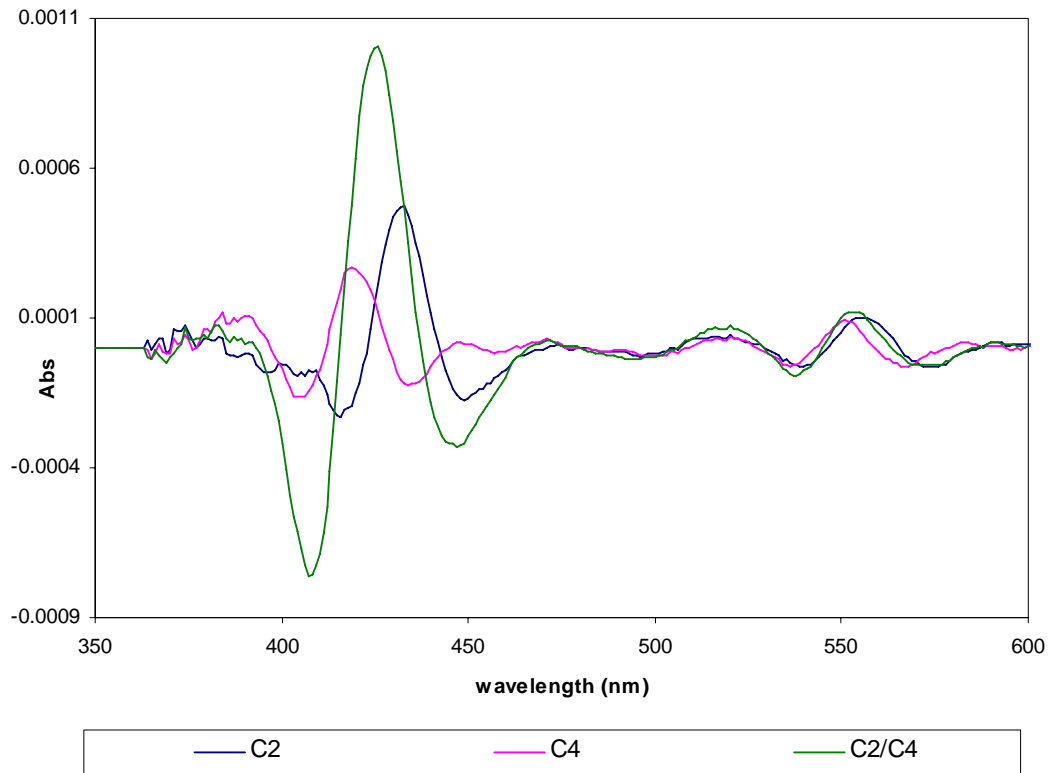


Figure 5.18A Lost peaks of respiratory mutants. Light absorption at Soret and α peak can distinguish different *c*-type cytochrome. The *c2* mutant shows that the cytochrome *c2* absorbs lower wavelength both at Soret and α peak. The *c4* mutant shows that the cytochrome *c4* absorbs higher wavelength at Soret and α peak. The composite absorption of cytochrome *c2* and *c4* probably looks similar to that of *c2/c4* double mutant.

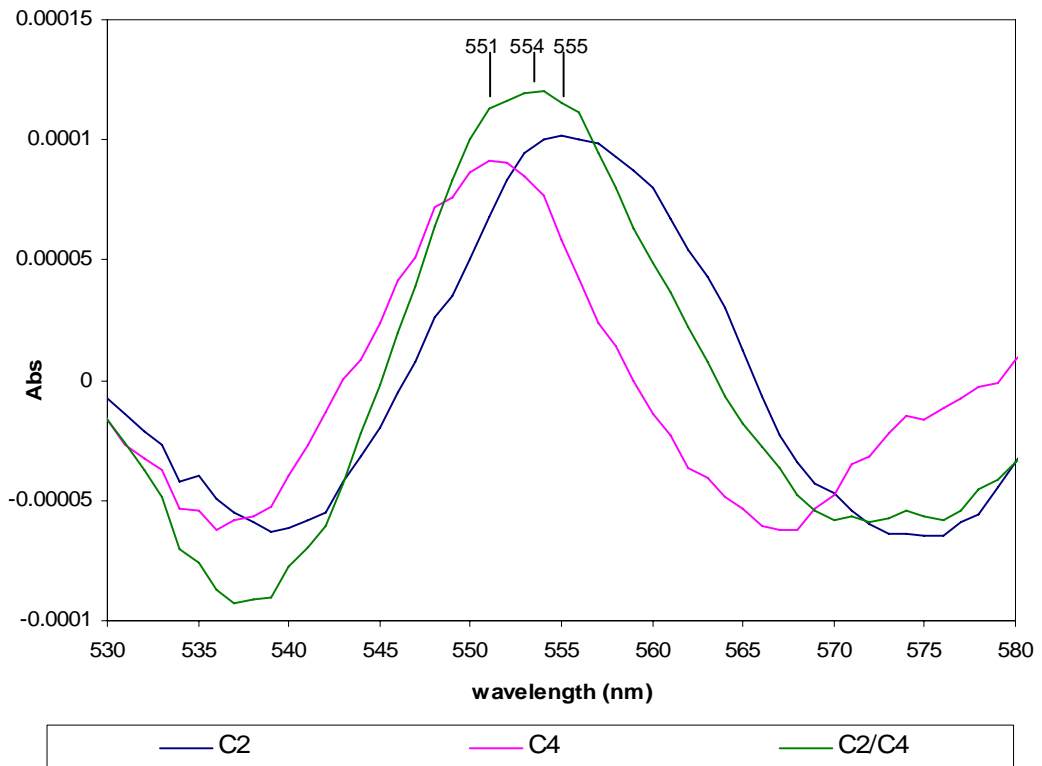


Figure 5.18B Lost peak at α band of cytochrome mutant represents actual absorption of that cytochrome. The α peak of cytochrome *c2*, *c4*, and composite peak of *c2* + *c4* are shown. The cytochrome *c2* has α peak around 554-555 nm whereas the cytochrome *c4* has around 551-552 nm. Composite peak of cytochrome *c2* + *c4* is around 554 nm.

5.3 Discussion

ECL haem staining comparison of WT and *c4* mutant strain showed that the cytochrome *c4* exhibits molecular mass of 21-22 kDa on SDS-PAGE . It has very strong peroxidase activity. The signal intensity from cytochrome *c4* is strongest among *c*-type cytochromes in *N. meningitidis*. It is not clear whether the signal intensity is due to a large amount of cytochrome or whether the cytochrome *c4* itself has a very high peroxidase activity. The cytochrome *c2* can not be detected by peroxidase activity maybe due to its haem structure being six coordinate and that H_2O_2 can not bind and

interact with iron center. It is likely that cytochromes with pentacoordinate haem confer peroxidase activity. However, the absence of cytochrome *c2* in *c2* mutant can be demonstrated spectrophotoscopically as *c2* mutant showed distinct spectra from WT and other cytochrome mutants. Generally, haem proteins owe most of their intense absorption to the conjugated haem group rather than the iron metal center. Reduced cytochrome *c2* absorbed lower energy (longer wavelengths) than cytochrome *c4*, both in Soret band and α band. The spectral differences between mutant and WT absorption give can be used to get an idea of the spectral features of the missing cytochromes. The lost absorption in mutant cells may represent the actual absorption by that *c*-type cytochrome although this assumes that levels of other cytochromes remain equal, an assumption that appears reasonable on the basis of banding pattern in Figure 5.6. *c2* mutant lost absorption peak at 554-555 nm in α band, suggesting that cytochrome *c2* has α peak at 554-555 nm. Meanwhile, *c4* mutant lost absorption peak at 551 nm in α band, suggesting that cytochrome *c4* has α peak at 551 nm. *c2* mutant lost absorption peak at 435 in Soret band, suggesting that cytochrome *c2* has Soret peak at 435 nm. *c4* mutant lost absorption peak at 420 in Soret band, suggesting that cytochrome *c4* has Soret peak at 420 nm.

As it is hypothesized that cytochrome *c2* and *c4* accept electrons from *bc₁* complex, the defect in either cytochrome *c2* or *c4* may cause less oxidation of the *bc₁* complex and, possibly, results in higher ratio of reduced:oxidized quinone pool. Mutating cytochrome *c2* or *c2* resulted in a growth defect under aerobic and microaerobic conditions though defect in *c4* was manifestly more severe in the former case while defect in *c2* more severe in the latter. These growth defects are linked to the decreased oxygen consumption rate. *c4* mutant has 40% decreased rate while *c2* mutant has 10% decreased rate and *c2/c4* double mutant has 55% decreased rate. In

general, oxygen reduction rate is a major factor that directly affects growth, regarding the energy-transducing aspect. The oxygen reduction rate showed that cytochrome *c4* defect leads to much lower oxygen reduction rate than that of cytochrome *c2* defect suggesting that electron transfer to oxygen via cytochrome *c4* is more than via cytochrome *c2*. It is interesting that although oxygen reduction rate in cytochrome *c2* mutant is decreased only 10%, the aerobic growth is much more affected. It might be possible that the defect in cytochrome *c2* decreases oxidation of the *bc₁* and increase the chance of direct interaction between oxygen and *bc₁* complex generating more superoxide radical. The increased superoxide radical may kill more cells and decrease total growth though the oxygen reduction rate is only slightly decreased. The growth of mutants under microaerobic conditions were poorer than WT, suggesting that these cytochromes are also important for growth under low level of oxygen. The *c2* mutant had poorer growth than *c4* mutant, suggesting that the cytochrome *c2* might play important role during microaerobic growth. It is very interesting that all mutants can begin reducing nitrite quicker than WT during microaerobic growth but their growth yields were poorer than WT. The mutants entered stationary phase faster than WT. The entering to stationary phase correlates exactly to the time of nitrite disappearance from culture. WT started reducing nitrite later than mutants and entered stationary phase later than mutant because nitrite has completely disappeared later than mutants. This suggests that WT is able to use oxygen to support microaerobic growth during early phase whilst the mutants started nitrite reduction earlier in the growth phase. Since the mutant strains have lower capability to use oxygen to support microaerobic growth than WT, they probably turn to use nitrite earlier to support microaerobic growth though oxygen remains present in low level. The mutants used up nitrite earlier than WT and, hence, entered stationary phase earlier than WT. The rates of nitrite reduction

are similar among all strains including WT. The ability to reduce nitrite in *c2*, *c4*, and *c2/c4* mutant were not altered, indicating that the cytochrome *c2* and *c4* are not involved in nitrite reduction. The nitric oxide accumulation assay also confirmed this. The *c2/c4* mutant can generate and accumulate nitric oxide from nitrite reduction similarly to WT. The rate of nitric oxide generation in WT is 1.0 nmoles/min/mg while that in *c2/c4* mutant is 0.7 nmole/min/mg. Both strains were grown under microaerobic conditions without nitrite. The low activity relative to other nitrite reduction activity measurement of 20 nmole/min/mg (Rock *et al*, 2005) may be due to the activity of AniA being very low under growth condition without nitrite. There might also be background of NorB expression as well. The *norB* mutant could have been used as control to check NorB background in this experiment. Though *c2/c4* mutant is impaired in utilizing oxygen and it prefers nitrite under microaerobic conditions, it can not reduce nitrite under aerobic conditions. Under aerobic condition, *c2/c4* was killed by nitrite toxicity. It is of interest why the *c2/c4* mutant is highly sensitive to nitrite. It is possible that the *c2/c4* mutant may express genes involved in anaerobiosis, including AniA under aerobic conditions. Nitrite might instantly get reduced to nitric oxide and killed most of *c2/c4* cells from the beginning of aerobic culture. A small change in nitrite reduced relates to a large enough product of nitric oxide to be toxic. The expression of AniA nitrite reductase of *c2/c4* mutant under aerobic growth should be further investigated. Another possibility is that *c2/c4* mutant can not express AniA nitrite reductase under aerobic conditions. Nitrite might also directly interacts with *cbb₃* oxidase and partially inhibit aerobic respiration that carry on by other electron transfer proteins in periplasm.

Both cytochrome *c2* and cytochrome *c4* are important but not critical for growth of *N. meningitidis*, both under high level and low level of oxygen. The 37%

decreased oxygen reduction rate in *c4* mutant suggests that this *c*-type cytochrome might dominate the electron transfer to *cbb₃* oxidase. However, the cytochrome *c2* might also play a role in electron transfer to *cbb₃* oxidase. The *c2* mutant exhibits 10% decreased rate of oxygen reduction. Defect in both cytochrome *c2* and *c4* exhibited 55% decreased rate oxygen reduction and greatly affects growth. Combined data of growth defect and decreased oxygen reduction suggest that cytochromes *c4* and *c2* are major electron donors to *cbb₃* oxidase. There might be other proteins that function as electron donors, to a lesser extent, to *cbb₃* oxidase. This might include another periplasmic *c*-type cytochrome *c5* and cupredoxin Laz, or indeed *bc₁* complex might directly transfer electrons to *cbb₃*.

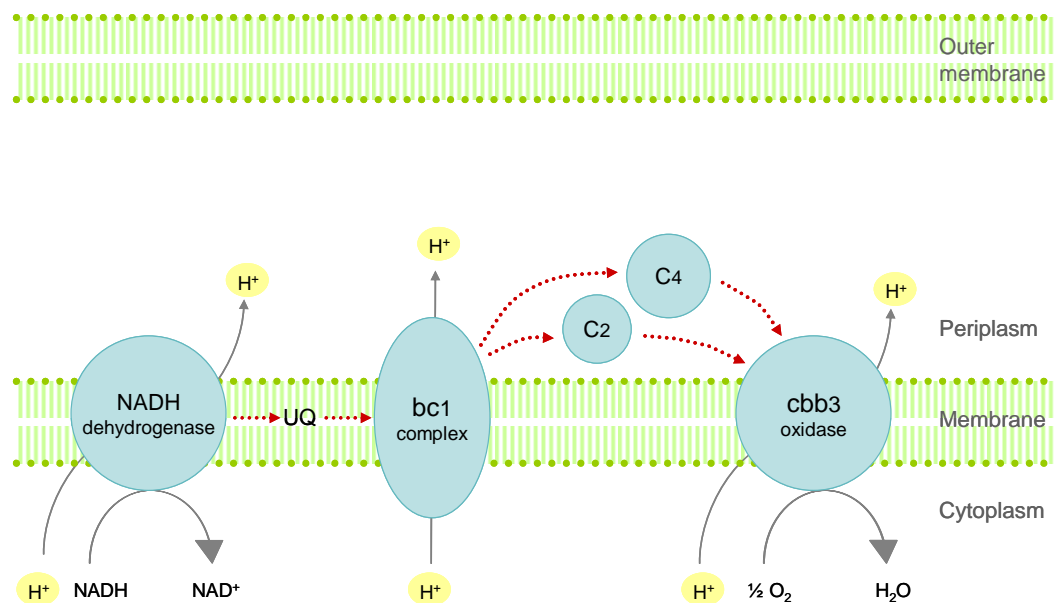


Figure 5.19 In *N. meningitidis*, electron flow from *bc₁* complex to *cbb₃* oxidase depends on periplasmic *c*-type cytochromes. Two major electron donors to *cbb₃* oxidase are cytochrome *c4* and *c2*, respectively. The electron flow to oxygen generate more energy than that to nitrite as it translocate more protons to periplasm and generate more proton gradient and proton motive force. Aerobic respiration is, therefore, more favorable than anaerobic respiration in terms of energy conservation.

Chapter 6

Cytochrome *c5* is an electron donor to AniA nitrite reductase

6.1 Introduction

Nitrite is an important respiratory substrate for *N. meningitidis*. The organism can reduce nitrite to support growth under low level of oxygen. It is hypothesized that nitrite reduction might be crucial for the meningococcus in colonization of nasopharynx. Genome analysis reveals that the meningococcus has only one gene, the *aniA* gene, encoding for a protein predicted to function as a nitrite reductase. The copper protein AniA nitrite reductase is predicted to be localized in the outer membrane with globular domain exposed in periplasm. The putative electron donors to AniA are predicted to be a cupredoxin Laz and some periplasmic *c*-type cytochromes. These cytochromes include *c2*, *c4*, and *c5*. The aim of this chapter is to characterize the involvement of cytochrome *c5* in particular respiratory pathways. This chapter shows investigation and evidence regarding the role of cytochrome *c5* in electron transport, respiration and growth of *N. meningitidis*.

6.1.1 Structure of cytochrome *c5*

Gene NMB1677 of *N. meningitidis* is predicted to encode a periplasmic cytochrome *c5*. Cytochrome *c5* is very similar to that in *N. gonorrhoeae*. Its apoprotein has 279 amino acids with predicted MW of 28,755 Da. It is predicted to contain 2 haem domains and to be localised in cytoplasmic membrane. The amino acid residue 1-12 are predicted to be exposed in cytoplasm while the residue 13-32 are predicted to be localized in cytoplasmic membrane. The two haem-containing domains (residue 33-

279) are predicted to be exposed in periplasm (Figure 6.1). The mature cytochrome with association of two haems has predicted molecular mass of 29,987 Da. Though there is a possible signal peptidase cleavage site at KLA-GS (between residue Ala35 and Gly36), the prediction is very weak. It is more likely that cytochrome *c5* is a membrane protein. Protein sequence comparison shows that cytochrome *c5* is identical to that of the gonococcus and among the serogroups of the meningococci (Figure 6.2). There are homologs of cytochrome *c5* in other bacteria including *Vibrio*, *Chromobacterium*, *Thiobacillus*, *Burkholderia*, *Ralstonia*, and *Polaromonas*. The crystal structure of cytochrome *c5* from *Azotobacter* shows hexacoordination with Met as the sixth ligand of haem. However, the crystal structure of cytochrome *c5* from *Shewanella* does not show Met as the sixth ligand though both protein sequences are quite similar and share a consensus of Met residue as haem ligand. The cytochrome *c5* of *Azotobacter* and *Shewanella* contain only one haem domain similar to the haem 1 domain of cytochrome *c5* from *N. meningitidis* (Figure 6.3). Interestingly, the haem-containing domain of *c5* in the meningococci shows high similarity of sequence to each other (Figure 6.4). It is possible that this cytochrome has evolved by domain duplication.

```

MKQLRDNKAQGSALFTLVSGIVIVIAVLYFLIKLAGSGSFGDVDATEAATQTRIQPVGQLTMGDGIPVGER
QGEQIFGKICIQCHAAASNVPNAPKLEHNGDWAPRIAQGFDTLQHALNGFNAMPAKGGAADLTDQELKR
AITYMANKSGGSFPNPDEAAPADNAASGTASAPADSAAPAEAKAEDKGAAAPAVGVGDKKVFPEATCQVC
HGG SIPGIPGIGKKDDWAPRIKKGKETLHKHALEGFNAMPAKGGNAGLSDDDEVKAAVDYMANQSGAKF

```

Figure 6.1 Primary structure of cytochrome *c5*. The first twelve amino acid residues are exposed in cytoplasm (blue highlight) while the next twenty amino acid residues are localized in cytoplasmic membrane (pink highlight) and two haem domains with haem-binding sites (yellow highlight) are exposed in periplasm.

NMB1677	MKQLRDNKAQGSALFTLVSGIVIVIAVLYFLIKLAGSGSFGDV DATTEAATQTRI QPVGQ
NGO1328	MKQLRDNKAQGSALFTLVSGIVIVIAVLYFLIKLAGSGSFGDV DATTEAATQTRI QPVGQ
NMC1595	MKQLRDNKAQGSALFTLVSGIVIVIAVLYFLIKLAGSGSFGDV DATTEAATQTRI QPVGQ
NMA1936	MKQLRDNKAQGSALFTLVSGIVIVIAVLYFLIKLAGSGSFGDV DATTEAATQTRI QPVGQ *****
NMB1677	LTMGDGIPVGERQGEQIFGKI CIQCHAADSNVPNAPKLEHNGDWAPRIAQGFDTL FQHAL
NGO1328	LTMGDGIPVGERQGEQIFGKI CIQCHAADSNVPNAPKLEHNGDWAPRIAQGFDTL FQHAL
NMC1595	LTMGDGIPVGERQGEQIFGKI CIQCHAADSNVPNAPKLEHNGDWAPRIAQGFDTL FQHAL
NMA1936	LTMGDGIPVGERQGEQIFGKI CIQCHAADSNVPNAPKLEHNGDWAPRIAQGFDTL FQHAL *****
NMB1677	NGFNAMPAKGGAADLTDQELKRAITYMANKSGGSFPNPDEAAPADNAASGTASAPADSAA
NGO1328	NGFNAMPAKGGAADLTDQELKRAITYMANKSGGSFPNPDEAAPADNAASGTASAPADSAA
NMC1595	NGFNAMPAKGGAADLTDQELKRAITYMANKSGGSFPNPDEAAPADNAASGTASAPADSAA
NMA1936	NGFNAMPAKGGAVDLTDQELKRAITYMANKSGGSFPNPDEAAPADNAASGTASAPADSAA *****
NMB1677	PAEAKAEDKGAAAPAVGVDGKKVFEAT CQVCHGGSIPGIPGIGKKDDWAPRIKKGKETLH
NGO1328	PAEAKAEDKGAAAPAVGVDGKKVFEAT CQVCHGGSIPGIPGIGKKDDWAPRIKKGKETLH
NMC1595	PAEAKAEDKGAAAPAVGVDGKKVFEAT CQVCHGGSIPGIPGIGKKDDWAPRIKKGKETLH
NMA1936	PAEAKAEDKGAAAPAVGVDGKKVFEAT CQVCHGGSIPGIPGIGKKDDWAPRIKKGKETLH *****
NMB1677	KHALEGFNAMPAKGGNAGLSDDEVKAAVDYMANQSGAKF
NGO1328	KHALEGFNAMPAKGGNAGLSDDEVKAAVDYMANQSGAKF
NMC1595	KHALEGFNAMPAKGGNAGLSDDEVKAAVDYMANQSGAKF
NMA1936	KHALEGFNAMPAKGGNAGLSDDEVKAAVDYMANQSGAKF *****

Figure 6.2 Primary structure comparison of cytochrome *c5* (NMB1677) of serogroup B and its homologs in serogroup C (NMC1595), serogroup A (NMA1936), and *N. gonorrhoeae* (NGO1328). The primary protein sequences show they are identical, except that of serogroup A has one amino acid different. The cytochrome *c5* are extremely conserved among the meningococci and the gonococcus. Transmembrane section is highlighted in pink and haem-binding site in yellow.

NMB1677 Chromobacterium Azotobacter Shewanella	-----MKQLRDNKAQGSALFTLVSGIVIVIAVLYFLIKLAGSGSFGDVDATTEAATQ MSFFQARLGMSNENGMAPGQIVKVLVSI VVFLVVAIWLLAKLATSGFNVDAEVMTEAVA -----
NMB1677 Chromobacterium Azotobacter Shewanella	TRIQPVGQLTMGDGIPVGERQGEQIFGKICIQCHAADSNVPNAPKLEHNGDWAPR-IAQG ARLKPVGESKASD-APPGMRTGEQVYKGI CMSCHATG--LAGSPKFGDAGAWGPR-IAKG -----GGGARSDDVVAKYCNACHGTG--LLNAPKVGDSA AWKTRADAKG -----ADLQDAEAIYNKACTVCHSMG--VAGAPKSHNTADWEPR-LAKG . : .: : * ** . . : .:** . . * . * **
NMB1677 Chromobacterium Azotobacter Shewanella	-FDTLFQHALNGFNAMPAKGGAADLTDQELKRAITYMANKSGGSFPNPDEAAPADNAASG -WDMLVNHALHGFNAMPKGGATDLSDEVKRAVAYMGNAGGAKFTEPPVGGAAAG----- GLDGLLAQSL SGLNAMPKGT CADCSDELKAAIGKMSGL----- -VDNLVKS VKTGLNAMP PGMCTDCTDEYKAAIEFMSKAK----- * * . * :****. * .:* :*:: * * : *
NMB1677 Chromobacterium Azotobacter Shewanella	TASAPADSAAPAEAKAEDKGAAPAVGVDGKKVFEATCQVCHGGSSIPGIPGIGKDDWAP -----AAAADPAVVGKKIYDSV CVACHGAGVAGAPKFGDKAAWAA -----
NMB1677 Chromobacterium Azotobacter Shewanella	RIKKGKETLHKHALEGFNAMPKGGNAGLSDDEVKAAVDYMANQSGAKF RLKPGMDEVVKIATKGLNAMPKGGYTGS-DAEFRSAIEYMVNNSK--- -----

Figure 6.3 Methionine as the sixth haem ligand of cytochrome *c5*. The crystal structure of cytochrome *c5* from *Azotobacter* shows Met as the sixth ligand of haem. However, the crystal structure of cytochrome *c5* from *Shewanella* does not show the sixth ligand in spite of its similar protein sequence and a consensus of Met residue (green highlight). The second haem domain of cytochrome *c5* from *N. meningitidis* is not found in both cytochrome *c5* of *Azotobacter* and *Shewanella*.

first haem second haem	GDGIPVGERQGEQIFGKICIQCHAADSNVPNAPKLEHNGDWAPRIAQGFDTLF GAAAPAVGVDGKKVFEATCQVCHG--GSIPGIPGIGKDDWAPRIKKGKETLH * . * . :*::* * ** . .:* . * : :*.***** :* :***.
first haem second haem	QHALNGFNAMPKGGAADLTDQELKRAITYMANKSGGSF KHALEGFNAMPKGGNAGLSDDEVKAAVDYMANQSGAKF :***:***** * .:*:*:* * * : *****:***.

Figure 6.4. Domain repeats in cytochrome *c5* structure. Based on the intramolecular repeat of protein structure, the second haem is also predicted to have hexacoordinate with Met as the sixth ligand (green highlight). These two haem domains share 50% sequence identity. It is possible that these two domains are result of domain duplication.

6.2. Results

6.2.1 Visualization of cytochrome *c5* by western blot and ECL chemiluminescence

The purpose was to identify and characterize properties of cytochrome *c5* on the SDS-PAGE gel and to confirm the defect of this cytochrome in respiratory mutant strains. The mutant strain construct was described in Chapter 4, section 4.4. Detailed methods of sample preparation and cytochrome staining were previously described in Chapter 5, section 5.2.1. Briefly, lysed cells were solubilized in 25 mM HEPES with 1% dodecyl maltoside. Soluble fractions were used for SDS-PAGE. After blotting gels onto nitrocellulose membrane, cytochromes were stained by ECL chemiluminescence and visualized on X-ray film. Cytochrome *c5* has been shown to have approximate MW of 33-35 kDa inspite of the predicted molecular mass of 29,987 Da. The cytochrome was present in every strain but the *c5* mutant strain (Chapter 5, Figure 5.6).

6.2.2 Growth under aerobic conditions

The purpose was to investigate the role of cytochrome *c5* on growth of the meningococcus under high level of oxygen as terminal electron acceptor. The *c5* mutant and wild type strains were grown in MHB under aerobic conditions. All strains were grown aerobically by shaking 6 ml of culture in 25 ml plastic McCartney tube at 200 rpm. In this experiment, oxygen is the only terminal electron acceptor for respiration. The aerobic cultures were sampled and two fold diluted for measuring optical density at 600 nm. The growth characteristics of wild type strain and the mutant strain are shown in Figure 6.5. The WT strain entered exponential growth after 2 hr and reached maximum optical density of 2.8 at 8 hr and quickly entered death phase. The mutant strain with cytochrome *c5* defect showed normal growth from lag phase to mid-exponential phase. It entered exponential growth at the same time as WT but after the

growth reached high optical density around 1.2 the mutant grew slower under this decreased level of oxygen. Upon reaching optical density of 1.4-1.5 the mutant stopped growing for 3-4 hours. After that, the *c5* mutant returned to fast growth and reached high growth yield similarly to wild type strain. Doubling time for *c5* mutant during fast growth is similar to that for WT, which is 43 minutes. Growth pattern of *c5* mutant is similar to *laz* mutant.

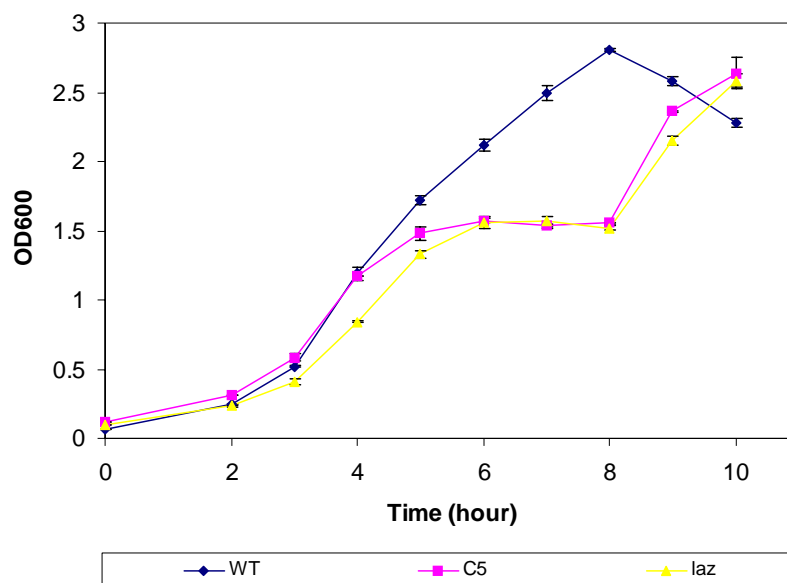


Figure 6.5 Growth of *c5* mutant under aerobic conditions. The *c5* mutant grew as well as wild type strain until reaching optical density around 1.2. At this high cell density the mutant grew slower and stop growing at optical density of 1.5 for about three hours then returned to fast growth after that. Interestingly, the growth pattern of *laz* mutant is similar to *c5* mutant.

6.2.3 Growth under microaerobic conditions

The purpose was to investigate the role of cytochrome *c5* on growth of the meningococcus under very low level of oxygen. Cells were grown in 20 ml of MHB in plastic McCartney tubes with 90 rpm shaking. Growth pattern of *c5* under microaerobic conditions was not different from WT strain (Figure 6.6) The maximum optical density of WT strain and the mutant were not different.

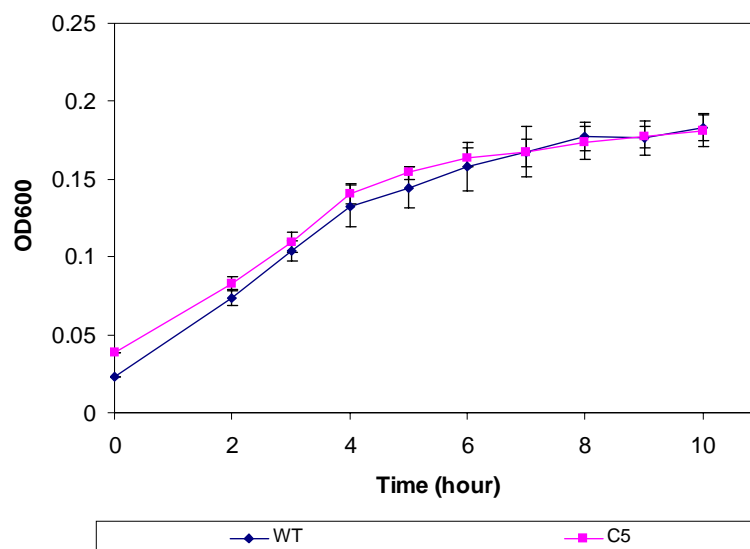


Figure 6.6 Growth of *c5* mutant under microaerobic conditions without nitrite. Growth of *c5* mutant under microaerobic conditions was not different from wild type.

6.2.4 Growth under microaerobic conditions with nitrite

The purpose was to investigate the role of cytochrome *c5* on growth of the meningococcus under very low level of oxygen with presence of nitrite as an alternative terminal electron acceptor. The growth conditions were similar to that under microaerobic conditions but 5 mM nitrite was present. The *c5* mutant can grow in the presence of nitrite marginally better than without nitrite. The wild type strain grew to a higher maximum optical density of 0.4 at hour 9 and then enter death phase. The growth of *c5* under denitrifying conditions seemed to be linear. Though at slow rate, the mutant can grow to optical density of 0.33 at hour 12 (Figure 6.7). Since the *c5* mutant grew under microaerobic conditions with nitrite supplement slower than WT, it is possible that the mutant has a defect in utilizing nitrite as an alternative terminal electron acceptor in order to supplement growth under low level of oxygen. It is of interest to

further investigate if this growth defect is linked to the decreased ability of the mutant to reduce nitrite.

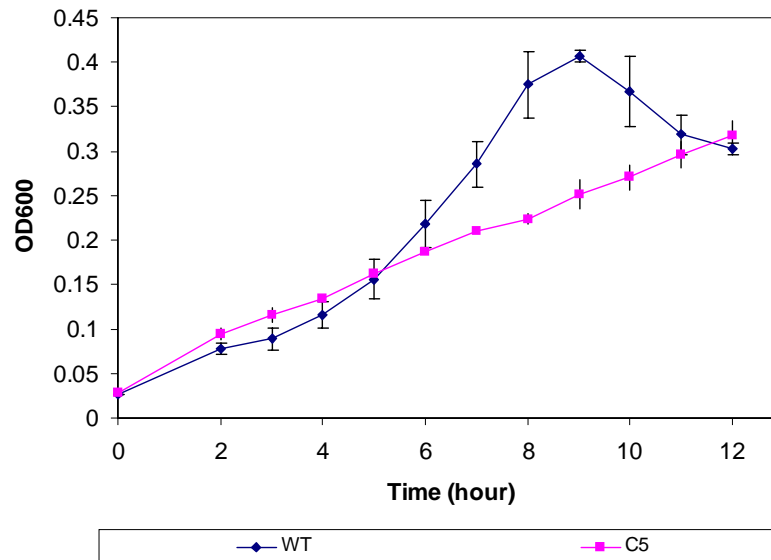


Figure 6.7 Growth of *c5* mutant under microaerobic conditions with 5 mM nitrite. The *c5* mutant showed growth defect under microaerobic conditions in the presence of nitrite.

6.2.5 Nitrite reduction

Since the *c5* mutant grew much poorer than wild type under denitrifying conditions, it is likely that the mutant has decreased ability to use nitrite as respiratory substrate to support growth under low level of oxygen. The purpose was to measure the utilization of nitrite during microaerobic growth to see if poor growth is related to the decreased ability to reduce nitrite. The meningococci were grown under microaerobic conditions with 5 mM nitrite supplement. Levels of nitrite were measured by nitrite assay every hour of growth. It was found that the *c5* mutants has a decreased ability to reduce nitrite during growth under microaerobic conditions (Figure 6.8). Nitrite disappearance by wild type occurred at hour 9 while the nitrite level in *c5* was still not much changed. However, some nitrite disappearance started to occur after 10 hours.

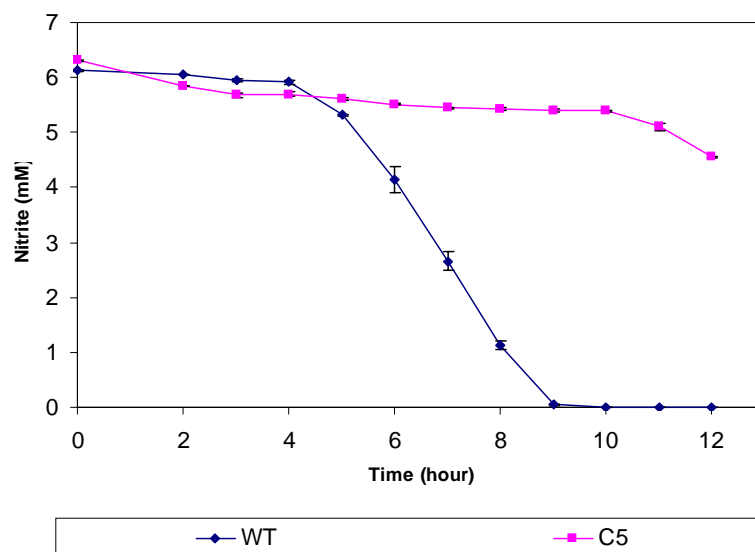


Figure 6.8 The *c5* mutant showed decreased ability to utilize nitrite under microaerobic growth conditions. However, some nitrite disappearance started to occur after 10 hours. It might be possible that there are other periplasmic protein(s), such as cupredoxin, that can transfer electrons to AniA nitrite reductase.

6.2.6 Production of nitric oxide by *c5* mutant

Since *c5* mutant grew poorer and showed decreased ability to utilize nitrite under microaerobic conditions, it was of interest to investigate if the mutant is able to reduce nitrite and generate nitric oxide. Intact cells of *c5* mutant strain were used for measuring the rate of nitric oxide accumulation compared to WT.

6.2.6.1 Nitric oxide accumulation assay

Cell preparation for the assay of nitric oxide accumulation was previously described in Chapter 5, section 5.2.7.1. Briefly, cells were grown under microaerobic conditions without nitrite to induce the expression of AniA but not NorB. Then, cells were harvested and resuspended in MHB to an optical density around 1.3-1.5. The assay for nitric oxide generation was done using Clark-type electrode with nitric oxide electrode. First, 2.7 ml of MHB with 5 mM glucose was added to the electrode chamber and level of oxygen and nitric oxide were recorded by chart recorder. Then,

0.3 ml of cell suspension was added to the chamber. The chamber was capped and nitric oxide electrode was submerged into the suspension. After the level of oxygen decreased to zero percent, nitrite was added to final concentration of 5 mM. The level of nitric oxide generated from nitrite reduction, supposedly by AniA, and accumulated in the electrode chamber was monitored and recorded over time course. It has been found that the *c5* mutant can not generate nitric oxide while the wild type strain generate and accumulate nitric oxide at the rate of 1.0 nmole/min/mg (Figure 6.9).

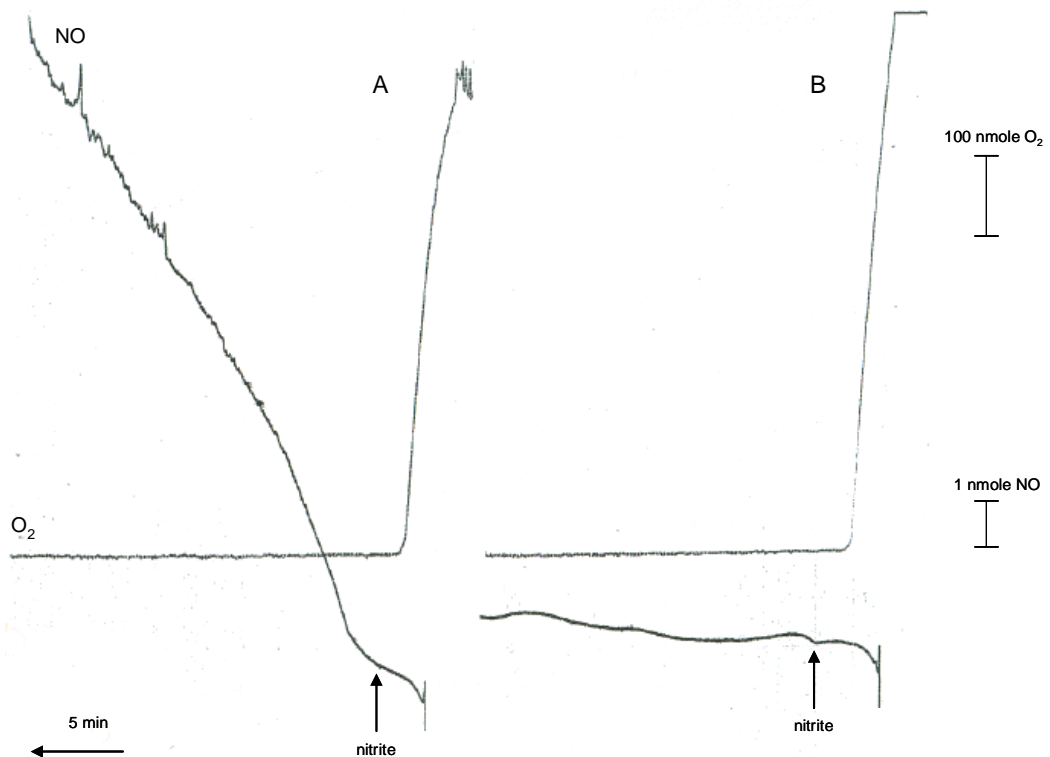


Figure 6.9 The *c5* mutant can not generate and accumulate NO. The wild type strain showed accumulation rate of nitric oxide at 1.0 nmole/min/mg. This suggest the involvement of cytochrome *c5* in nitrite reduction.

6.2.8 Expression of AniA nitrite reductase in *c5* mutant

Based on genome sequence analysis, it is likely that the capability of the meningococcus to reduce nitrite is dependent solely on nitrite reductase activity of AniA protein. There is no other protein predicted to be nitrite reductase in this organism. As the *c5* mutant loses the ability to reduce nitrite and grow under microaerobic conditions in the presence of nitrite, it is interesting to investigate if these altered characteristics are linked to a defect in expression of AniA or it is direct effect of the cytochrome *c5* itself. The expression of AniA in *c5* mutant and other respiratory mutants was detected using western blot with primary antibody against the meningococcal AniA. The other mutants includes *laz* mutant, cytochrome *c2* mutant, cytochrome *c4* mutant, and cytochrome *c2/c4* double mutant. All strains were grown in MHB under microaerobic conditions with 5mM nitrite for 6 hours. After that, cultures were centrifuged to separate cells and whole cell extract were prepared. It is found that all strains can express AniA, including *c5* mutant, under microaerobic conditions with nitrite supplement (Figure 6.10) The weaker signal of AniA in *c4* mutant may be due to lower total protein loading.

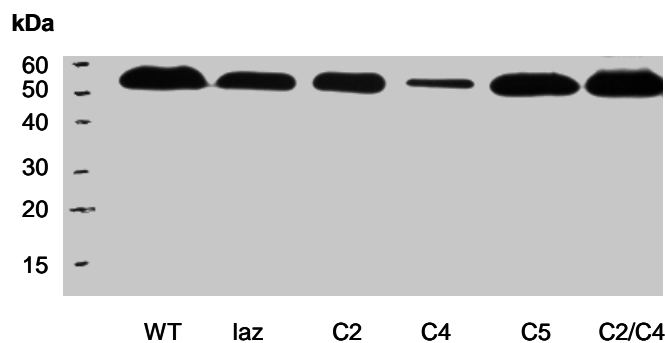


Figure 6.10 AniA expressions in respiratory mutants. Expression of AniA nitrite reductase is not altered in strains defected in *Laz* and *c*-type cytochromes. The *c5* mutant can expressed AniA normally, suggesting that the decreased ability to reduce nitrite is due to a defect in cytochrome *c5*, not repression of AniA. Equal amount of 10 μ g total protein was loaded in each lane.

6.2.9 Spectra of *c5* mutant

6.2.9.1 Cell oxidation by oxygen

Intact cells of *c5* mutants show different visible light spectra when oxidized by oxygen. The double derivatives of the oxidized minus reduced difference spectra are shown in Figure 6.11A. The *c5* mutant showed different pattern of spectra, decreased absorption at both Soret and α band. The absorption at alpha band is of interest (Figure 6.11B). The WT strain exhibited α peak at 554 nm whereas the *c5* and *c2* mutant exhibited α peak similarly at 552.5 nm and *c4* mutant exhibited α peak at 555 nm. WT minus mutant difference spectra showed the lost absorption in mutants (Figure 6.12A). At α peak, *c5* and *c2* mutant similarly lost absorption at 555 nm while *c4* mutant lost absorption at 551 nm (Figure 6.12B). However, the lost α peak of *c5* mutant is sharper than that of *c2* mutant. Interestingly, *c5* mutant also lost Soret peak absorption at longer wavelength than that of *c4* mutant but shorter wavelength than that of *c2* mutant.

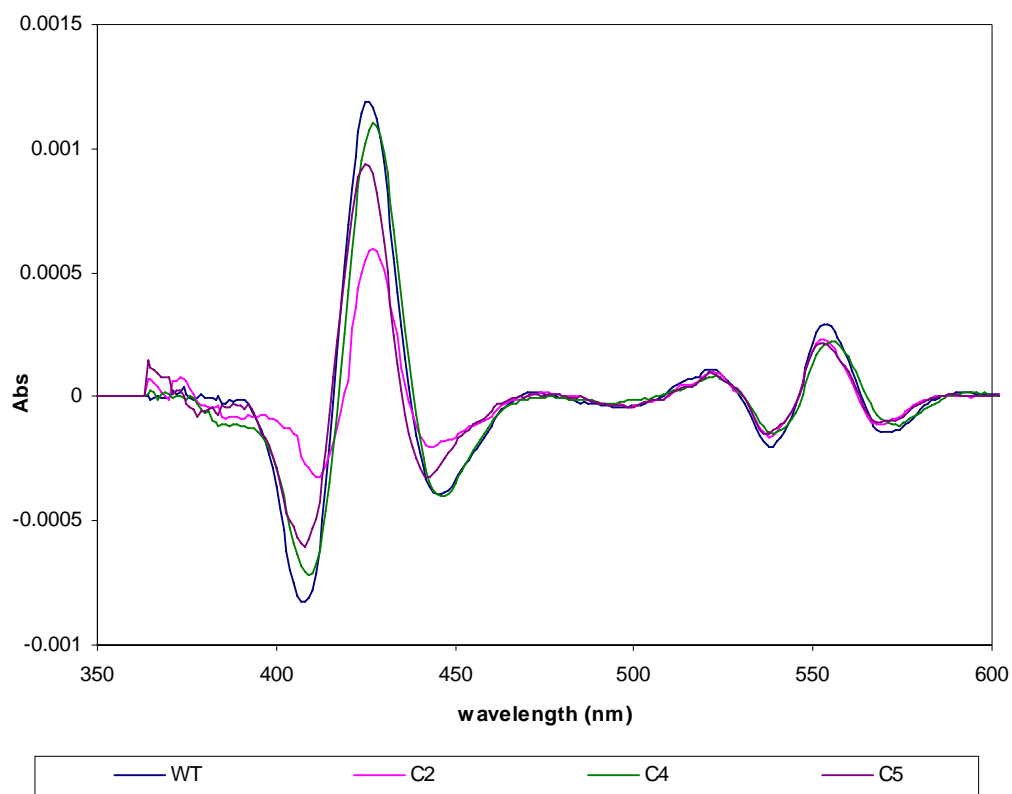


Figure 6.11A Double derivatives of oxidized minus reduced difference spectra of mutants. The *c5* mutant exhibited stronger absorption change at Soret band than that of *c2* mutant but a bit weaker than that of *c4* mutant. The absorption change at α band are quite similar between those of *c5* and *c2* mutants.

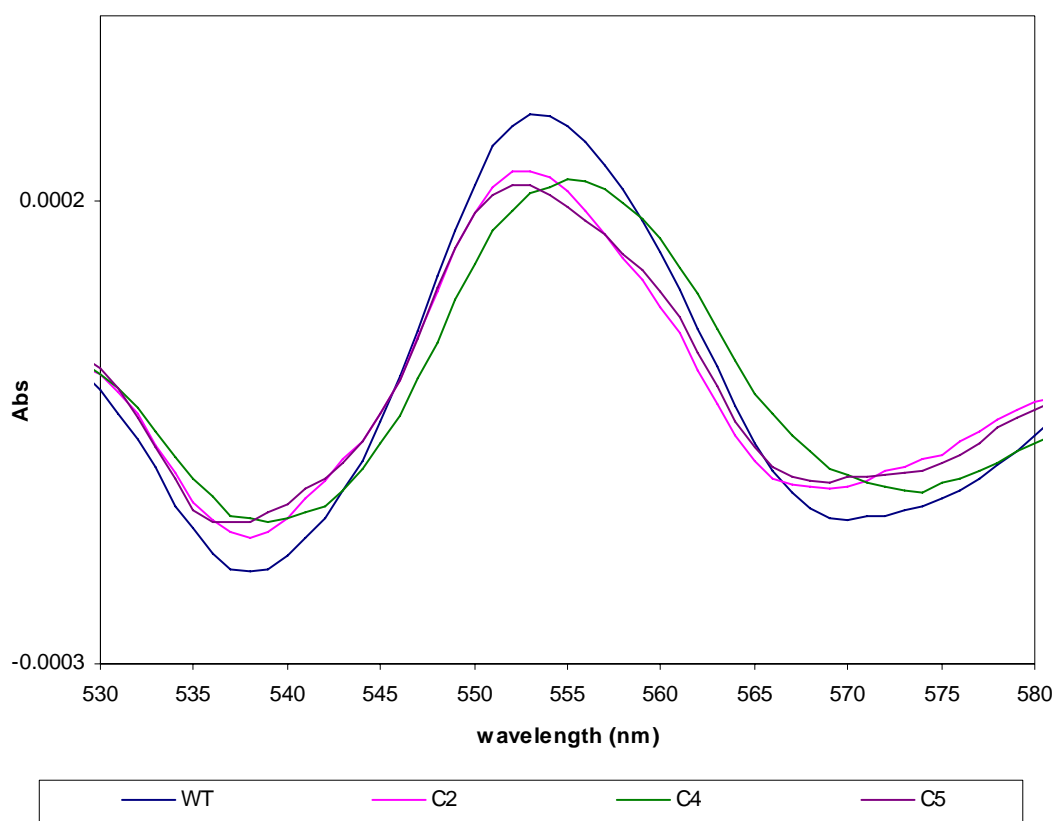


Figure 6.11B Mutant strains exhibited different absorption at α band. The *c5* and *c2* mutant exhibited α peak at 552 nm whereas the *c4* mutant exhibited α peak at 555 nm. WT strain exhibited alpha peak at 553 nm.

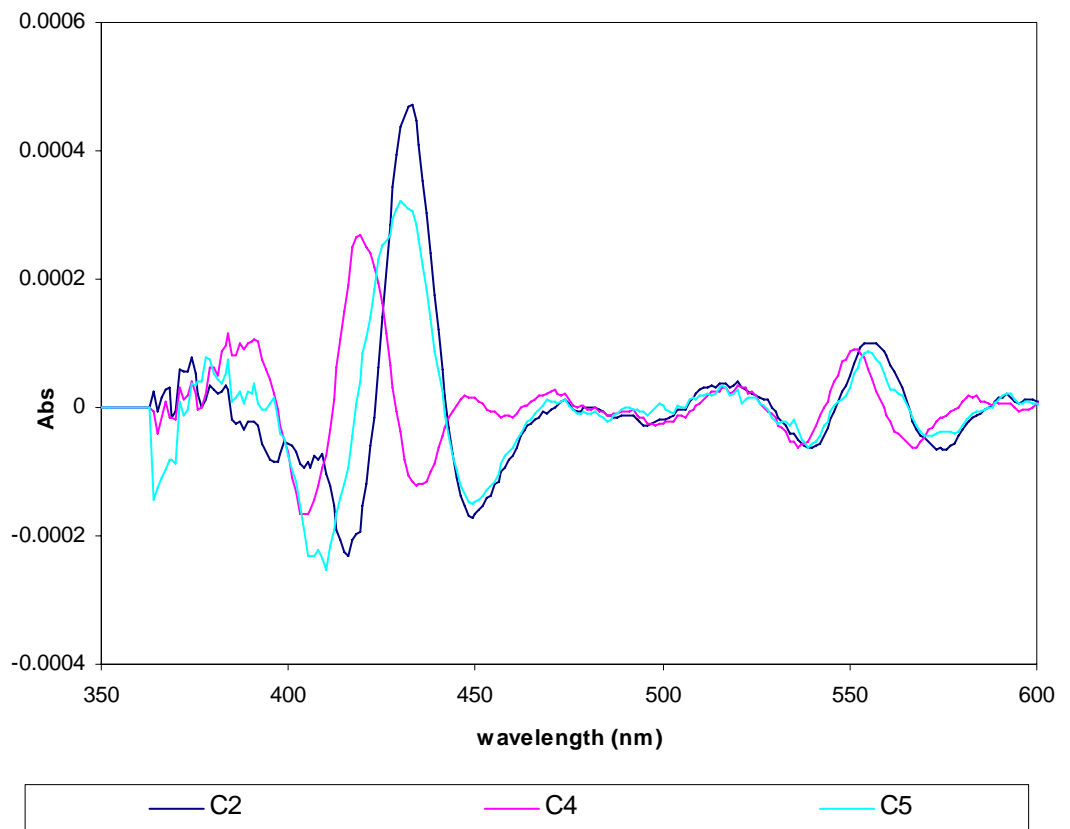


Figure 6.12A Lost absorptions of respiratory mutants. Light absorption at Soret and α peak can distinguish different *c*-type cytochrome. The *c5* mutant shows that the cytochrome *c5* absorbs lower wavelength both at Soret and α peak than cytochrome *c4*. However, cytochrome *c5* absorbs a bit higher wavelength at Soret peak than cytochrome *c2* and the α peak is also sharper.

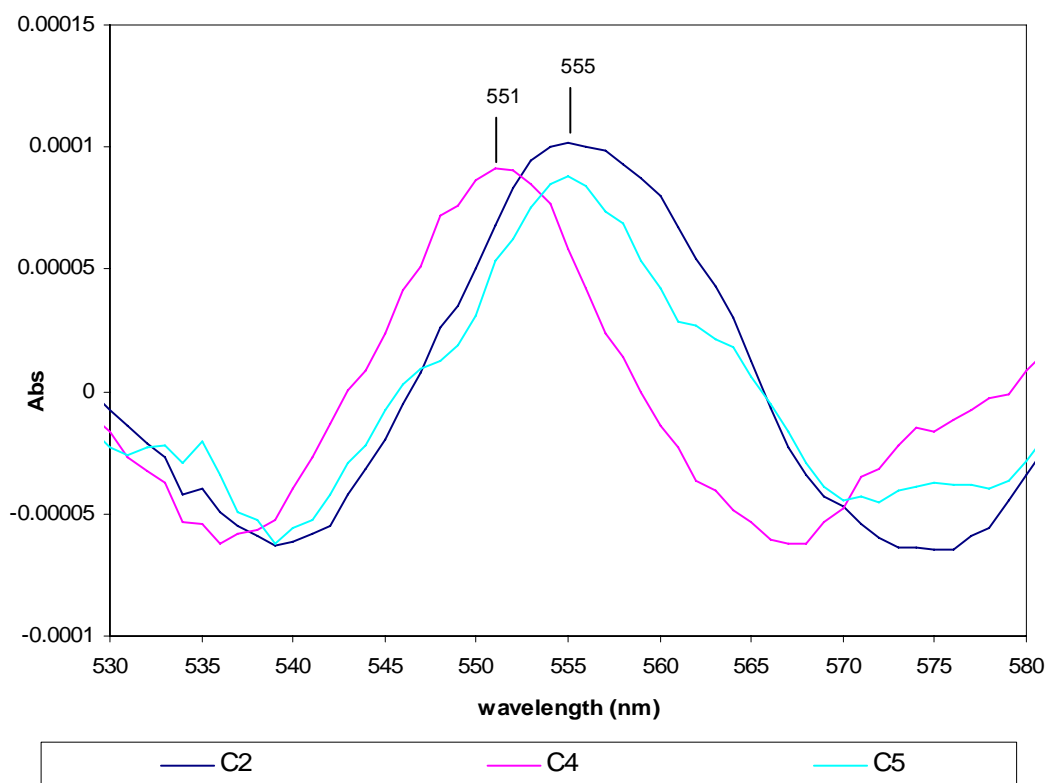


Figure 6.12B Lost peak at α band of cytochrome mutant represents actual absorption of that cytochrome. The cytochrome *c5* has α peak at 555 nm. The cytochrome *c2* has α peak around 554-555 nm whereas the cytochrome *c4* has around 551-552 nm.

6.2.9.2 Cell oxidation by nitrite

Intact cells of *c5* mutant show different visible light spectra when oxidized by nitrite. The double derivatives of the oxidized minus reduced difference spectra are shown in Figure 6.13A. Oxidation of wild type cells by nitrite give rise to α peak at 560 nm while oxidation of *c5* mutant cell did not alter the absorption at all (Figure 6.13B). Generally, the α peak at 560 nm is a typical spectral feature of *b*-haem. It is clear that the defect in cytochrome *c5* prevented the oxidation of this *b*-haem.

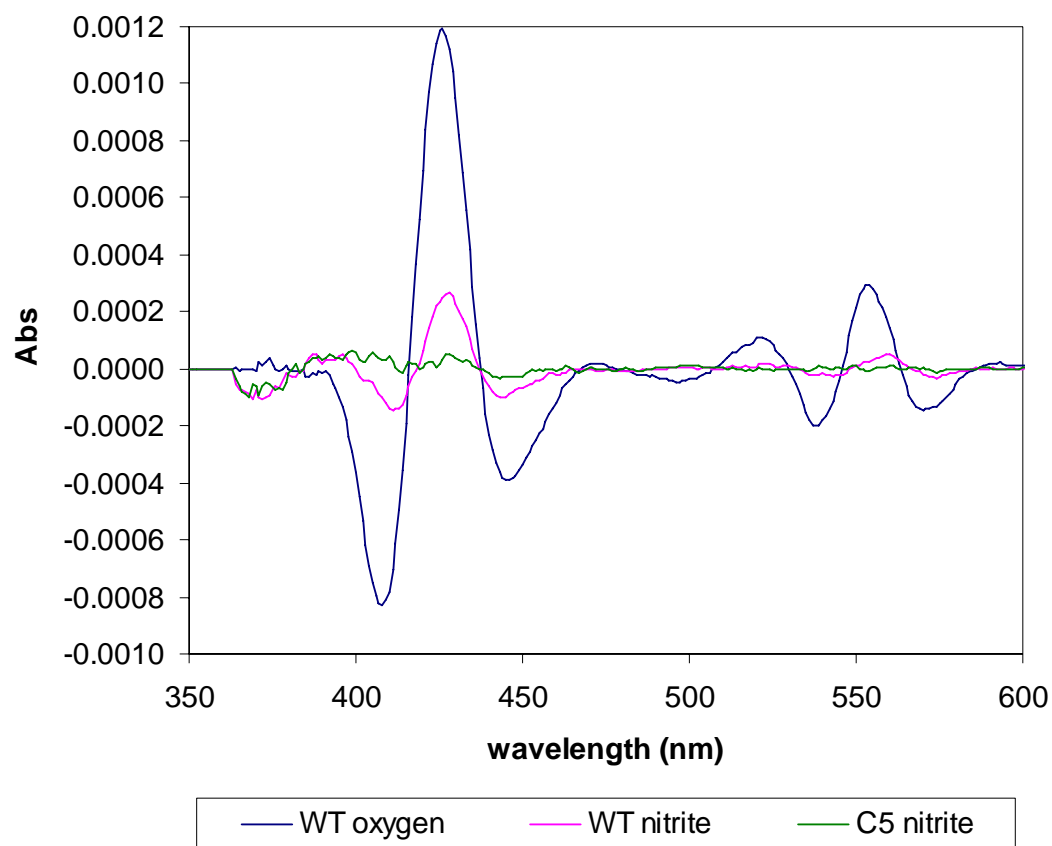


Figure 6.13A Nitrite can not oxidize cytochromes in *c5* mutant. In wild type this cytochrome can be oxidized when cells were exposed to nitrite.

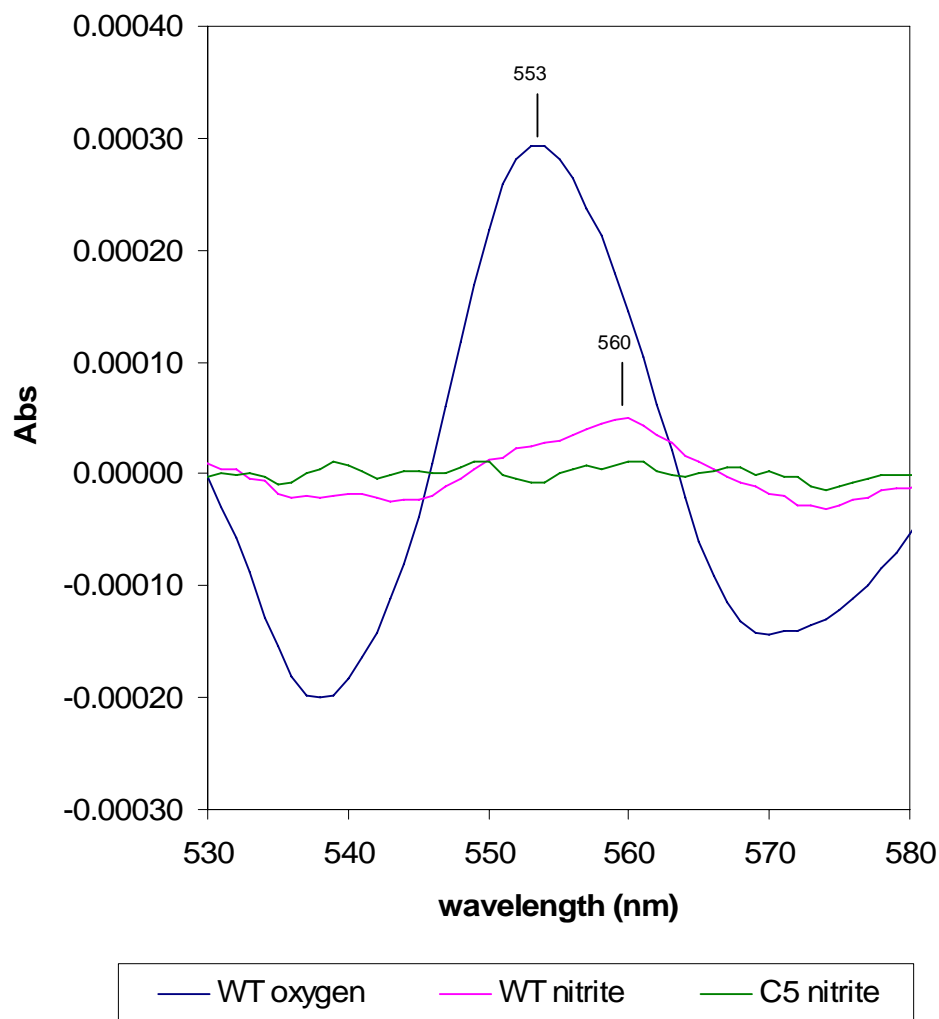


Figure 6.13B Difference spectra of wild type oxidized by nitrite gives α peak at 560 nm indicating oxidation of *b*-haem or *b*-type cytochrome. It has been demonstrated in Chapter 3 that oxidation by nitric oxide gave the same result. This spectral feature possibly represent the oxidation of *b*-haem in NorB by nitric oxide generated from nitrite reduction. The loss of this spectral feature indirectly suggest the decreased ability to reduce nitrite in *c5* mutant though AniA is normally expressed. This suggests an important role of cytochrome *c5* in generation of nitric oxide and oxidation of NorB.

6.2.9.3 H₂O₂ can oxidize *c*-type cytochromes directly, not via AniA

The *c5* mutant stop growing temporarily during growth at high cell density and entered stationary phase for 4 hours (Figure 6.5). It is hypothesized that this might be the result from the decreased level of oxygen, nutrient availability, or pH change. Moreover, this might be involved with the ability to cope with reactive oxygen radicals, such as hydrogen peroxide. The purpose was to investigate the involvement of cytochrome *c5* in response to oxidation by hydrogen peroxide. Cells were grown under aerobic conditions to optical density about 1.0 and harvested for spectral measurement. A high concentration of 2 mM hydrogen peroxide was used for the oxidation of cytochromes in the intact cells in order to maintain oxidized state of cytochromes during the spectral measurement. It was found that the oxidation by hydrogen peroxide gave spectral features that are different from that by oxygen (Figure 6.14A). In wild type, the oxidation by hydrogen peroxide gave α peak at 555 nm whereas oxidation by oxygen gave α peak at 553 nm. In the *c5* mutant, oxidation by hydrogen peroxide gave alpha peak at 560 nm and also a Soret band at longer wavelength (Figure 6.14B). It is not clear if the α peak at 555 nm is a spectral feature of cytochrome *c5* but the α peak at 560 nm is likely to be that of *b*-type cytochrome. As previously shown that cytochrome *c5* could possibly be an electron donor to AniA, it is of interest to investigate if the oxidation of cytochrome *c5* by hydrogen peroxide is AniA dependent. The *aniA* mutant cells were oxidized by hydrogen peroxide at the same concentration of hydrogen peroxide, 2 mM. It was found that the oxidation still gave α peak at 555 nm.

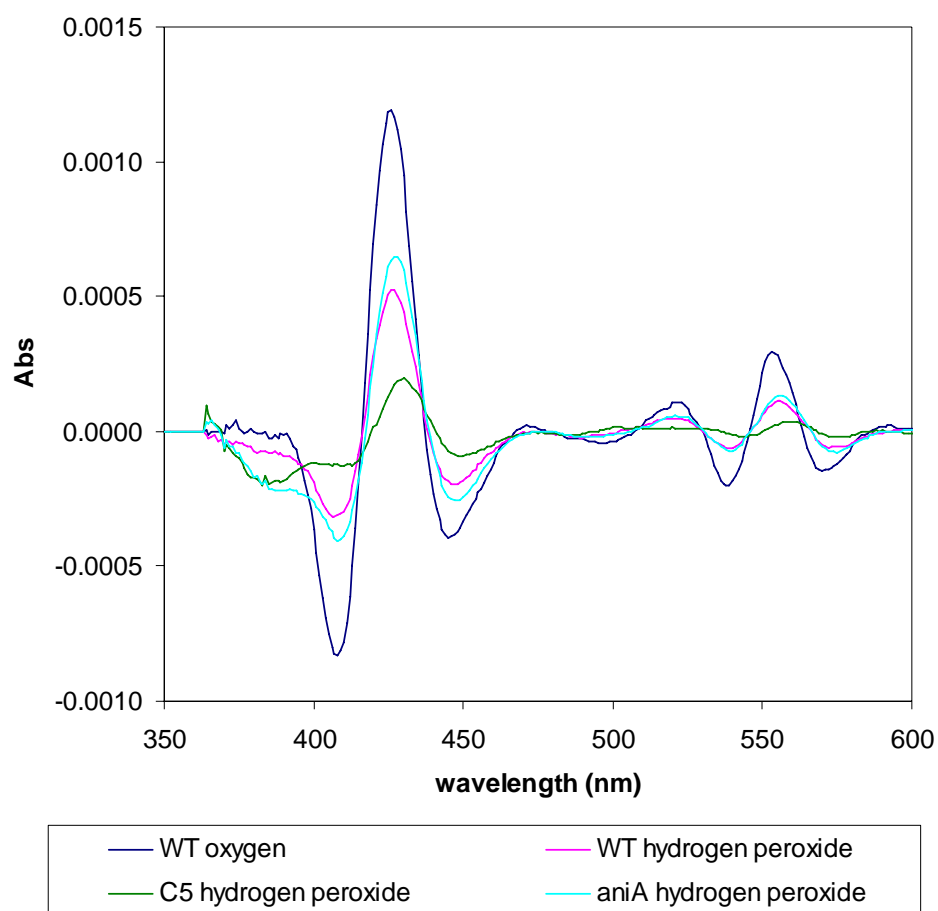


Figure 6.14A. Oxidation of *c5* mutant cells by hydrogen peroxide. Difference spectra of *c5* mutant cells oxidized by hydrogen peroxide gave α peak at 560 nm whereas oxidation of wild type cell gave α peak at 555 nm. The Soret band of the *c5* mutant was also less intense than that of wild type. It is not clear whether the α peak at 555 nm is a composite peak of many cytochromes or an individual peak of cytochrome *c5*. The defect in cytochrome *c5* affected this absorption and the α peak shifted to 560 nm, which is likely to be the absorption of *b*-type cytochrome.

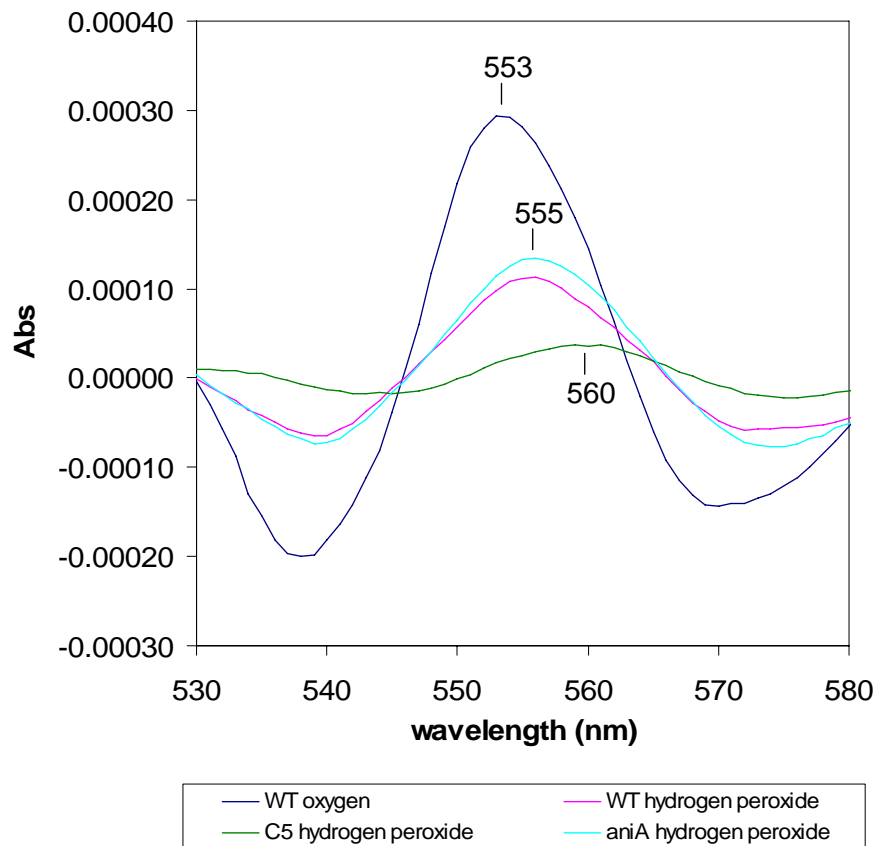


Figure 6.14B Difference spectra of wild type cells oxidized by hydrogen peroxide. The spectra showed α peak at 555 nm while that in *c5* mutant gave α peak at 560 nm. Oxidation of *AniA* mutant cells also showed α peak at 555 nm, suggesting that oxidation of cytochrome *c5* is *AniA* independent as *aniA* mutant still showed α peak at 555 nm. The *c5* mutant lose α peak absorption at 555 nm but exhibited peak at 560 nm instead. The α peak at 560 nm is likely to be the result of haem *b* oxidation.

6.3 Discussion

ECL haem staining comparison of WT, *c5* mutant and other *c*-type cytochrome mutant strains showed that the mature cytochrome *c5* exhibits molecular mass of 34-35 kDa on SDS-PAGE despite of the predicted mass of 29987 Da. There might be some post-translational modifications such as glycosylation on this cytochrome. The growth of *c5* mutant under aerobic conditions showed that it entered stationary phase once cell density was high above 1.0. At this point it is possible that the level of oxygen is much decreased. It is quite clear that cytochrome *c5* plays a role in maintaining growth during high cell density and possibly under depleted oxygen conditions. At high cell density, oxygen becomes depleted quickly and this may cause the respiratory chains become more reduced. The cytochrome *c5* may play an important role to maintain growth during highly reduced state of cell. Under the highly reduced state, the cytochrome *c4* and cytochrome *c2* might not be very effective in oxidizing *bc₁* complex and in reducing *cbb₃* oxidase.

Another factor that had been proposed to induce this early stationary growth of the *c5* mutant is pH change in growth medium. MHB is an amino acid based media. Depending on which amino acids are utilized during growth, the pH of the media may become altered (to great acidity or alkalinity). However, ammonia is usually generated from deamination of amino acid and excreted into culture media. It is assumed that the pH of bacterial periplasm is similar to the pH of culture media. As the organism grow to high cell density, the pH of culture media may increase or decrease and affect the performance of cytochromes *c2* and *c4* but not *c5*. The cytochrome *c5* might become more active under this situation. Thus, the defect in cytochrome *c5* may slow down the reduction of oxygen by *cbb₃* oxidase and halt the growth under this circumstance. After 4 hours the *c5* mutant returned to fast growth. It is possible that the mutant can

overcome the highly reduced state of cell and start utilizing oxygen again. This later fast growth might be the result of upregulation of Laz which is another proposed electron donor to *cbb₃* oxidase (see Chapter 7). The oxidation of wild type cells and *c5* mutant cells by oxygen showed different spectra. The *c5* mutant lost absorption of α peak at 555 nm. This might suggest cytochrome *c5* actual absorption of α peak is at 555nm. Combined data of growth characteristics and cytochrome spectra suggest the role of cytochrome *c5* as an electron donor to *cbb₃* oxidase.

The growth of *c5* mutant under microaerobic conditions was not different from wild type strain. Generally, both strains grew poorly compared to those under aerobic conditions. Under these growth conditions, the pH of culture media is likely to remain unchanged. The growth of both strains were clearly limited by a very low level of oxygen. However, the growth of *c5* mutant under microaerobic conditions in the presence of nitrite was much poorer than wild type. The mutant had decreased ability to utilize nitrite to support growth though the expression of AniA nitrite reductase was not altered. It is clear that the cytochrome *c5* is an important electron donor to AniA. This is confirmed by measuring the accumulation of nitric oxide generated by nitrite reduction. The *c5* mutant had decreased ability to generate and accumulate nitric oxide from nitrite reduction under anearobic conditions. The exposure of *c5* mutant cells to nitrite showed no oxidation of cytochromes at all while exposure of wild type cells to nitrite produced α peak at 560 nm. This absorption at 560 nm can be reproduced exactly by exposure cells to nitric oxide. It is likely that this α peak at 560 nm represents the oxidation of *b*-haem in NorB nitric oxide reductase. The *b*-haem in NorB is oxidized by nitric oxide generated from nitrite reduction by AniA. This stresses the important role of cytochrome *c5* in donating electrons to AniA. Interestingly, the oxidation of wild type cells by nitrite did not produce α peak at 555 nm, a proposed spectral feature of

cytochrome *c5*. This may be due to the relatively slow turnover rate of AniA (compared to cytochrome *cbb₃* oxidase). Cytochrome *c5* is probably re-reduced more quickly than it can be oxidized by AniA. Therefore, oxidized cytochrome *c5* is not seen in the presence of nitrite. The oxidation of wild type cells by oxygen exhibits the oxidation of cytochrome *c5* in a composite α peak. The difference spectra between spectra of wild type and *c5* mutant revealed oxidation of cytochrome *c5*. The oxidation of cytochrome *c5* showed α peak at 555 nm.

The oxidation of cells by hydrogen peroxide gave spectra different from that by oxygen. In wild type, the α peak is at 555 nm while in the *c5* mutant the α peak is at 560 nm. The α peak at 560 nm suggests the oxidation of *b*-type cytochrome. Interestingly, the α peaks of *c2/c4* mutant are also at 560 nm and even stronger than that in *c5* mutant. The difference in spectral features indicates a genuine effect of hydrogen peroxide, not from oxygen generated following dismutation of hydrogen peroxide by catalase on cytochrome oxidation. It is possible that the cytochrome *c5* can be oxidized directly by hydrogen peroxide. The oxidation of cytochrome *c5* by hydrogen peroxide is not AniA dependent as the oxidation of aniA mutant cells still gave α peak at 555 nm.

From combined data of growth pattern under denitrifying conditions, nitrite reduction assay, nitric oxide generation assays, and cytochrome spectra, there is good evidence that cytochrome *c5* is the major electron donor to AniA nitrite reductase.

The growth pattern under aerobic conditions and cytochrome spectra upon oxidation by oxygen suggests the role of cytochrome *c5* as an electron donor to *cbb₃* oxidase under the conditions with high cell density.

Chapter 7

Characterization of lipid-modified azurin

7.1 Introduction

The *laz* gene (NMB1533) of *N. meningitidis* strain MC58 is predicted to encode lipid-modified azurin (Laz). Laz is a predicted outer membrane protein or lipoprotein. It has 182 amino acids consisting of three domains (Figure 7.1). The N-terminal domain (residue 1-17) is a lipoprotein signal peptide which can be cleaved by the signal peptidase II between Ala17 and Cys18. The next domain (residue 18-62) is predicted to be a flexible linker region. The last domain (residue 63-182) is predicted to be a globular azurin domain. The predicted isoelectric point (pI) of Laz protein is 4.6. Protein sequence alignments reveals that the flexible linker region, approximately 40 amino acid residues, is unique and conserved among *Neisseria* species and not found in other species (Figure 7.2). Homologs of Laz with high similarity in the globular azurin domain are found in other β -proteobacteria including *Methylobacillus*, *Pseudomonas*, *Methylomonas*, *Burkholderia*, *Alcaligenes*, *Bordetella*, and *Vibrio*.

Laz protein is very similar to azurin, a periplasmic protein, which belongs to the copper-containing proteins in the cupredoxins superfamily. Other cupredoxins includes pseudoazurin, amicyanin, rusticyanin, plastocyanin, and stellacyanin. Cupredoxins are usually involved in electron transport and energy metabolism. Cupredoxins exhibit a strong blue colour at oxidized state, which can be detected by using visible spectrophotometry. They normally absorb visible light around 600 nm due to S \rightarrow Cu charge transfer. The site where copper incorporated consists of two histidines and one cysteine, resulting in trigonal planar structure, and sometimes one methionine as axial

ligands (Figure 7.2). The predicted copper binding site of Laz is within the Greek key β -barrel structure (Figure 7.3).

Since crystal structure of cupredoxin containing this linker region are not available for structure prediction from template, linker region tertiary structure prediction was attempted using de novo approach instead. The prediction of tertiary structure by Protinfo (University of Washington, Seattle), using de novo modelling, showed globular conformation of Laz linker region. The folded linker region may be a part of the globular domain and stabilize the dimer/trimer form of Laz.

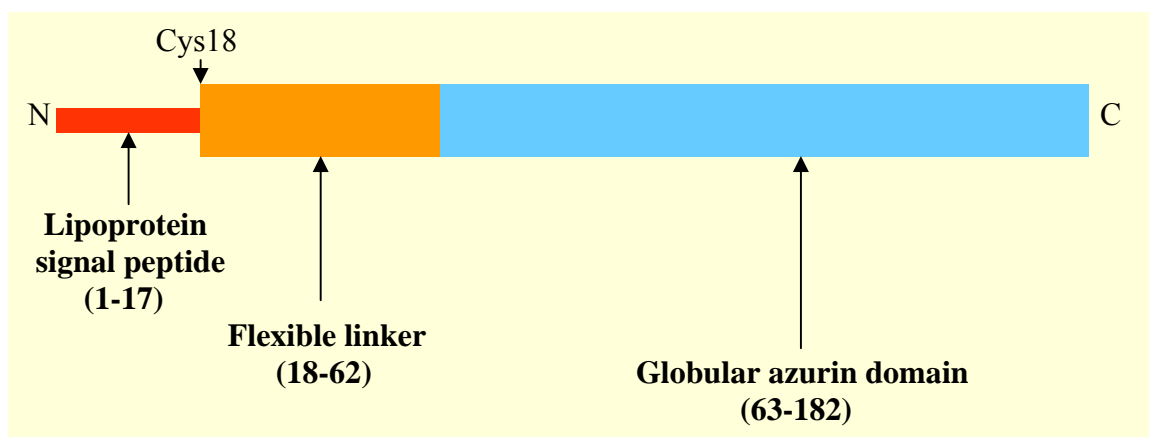


Figure 7.1 Predicted secondary structure of Laz protein with three domains. The first domain is a lipoprotein signal peptide domain which will be cleaved by signal peptidase II at Cys18. Then Cys18 will be acylated to phospholipid of outer membrane with flexible linker domain and globular azurin domain projected toward the periplasm.

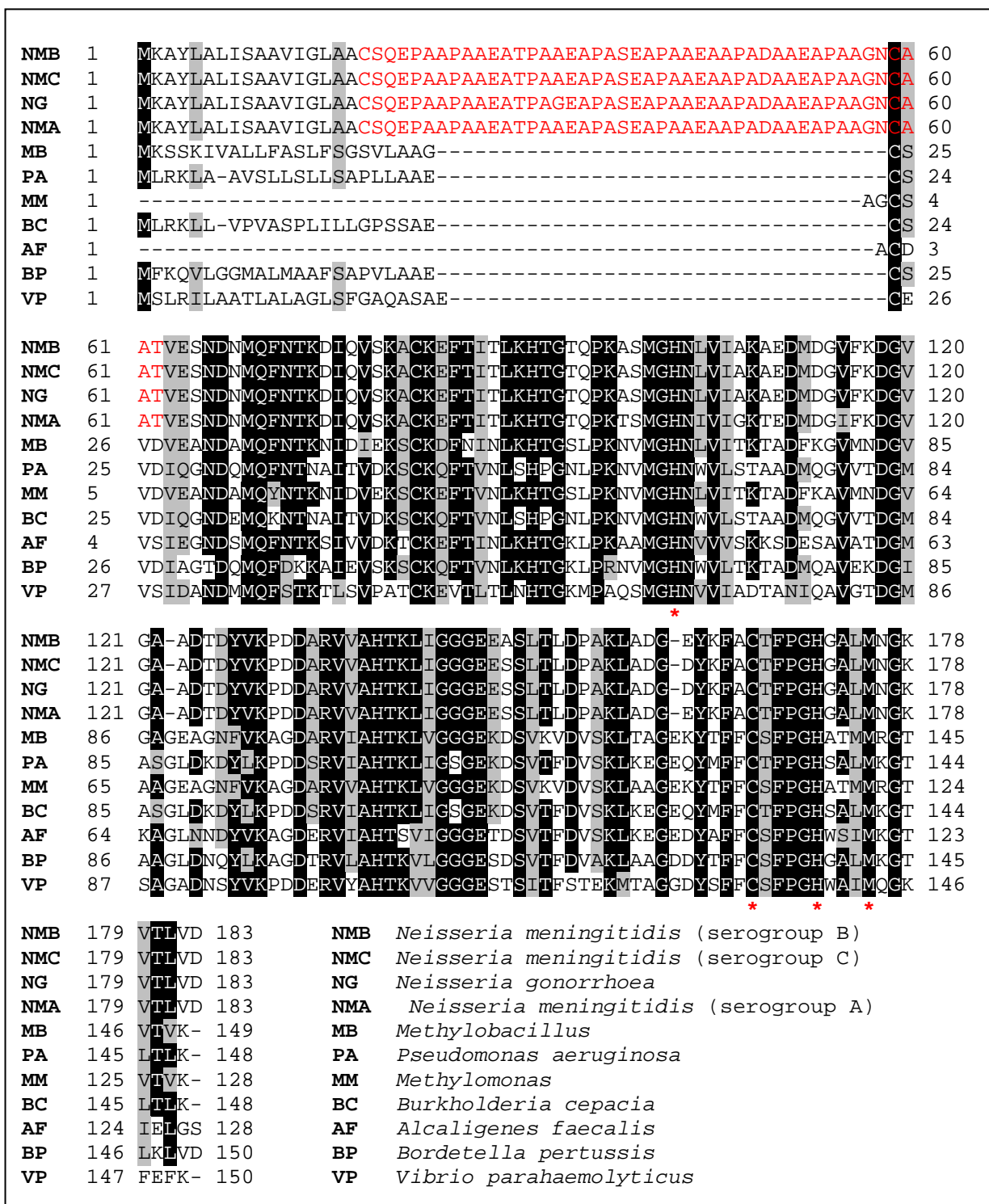


Figure 7.2 Homologs of Laz in other organisms. Multiple alignment of NMB Laz showing unique “flexible linker region” (red letters) from S19 to T62. This region is conserved among *Neisseria* species. The copper ligands (*) at His107, Cys166, His171 and Met175 are shown. These copper ligands are conserved among all bacterial blue copper proteins.

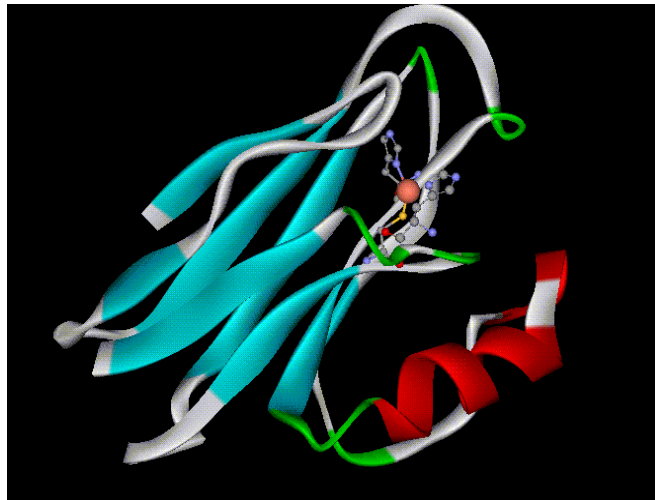


Figure 7.3 Predicted tertiary structure of Laz. Predicted structure of globular azurin domain of Laz with copper site. Copper is depicted in red sphere. The azurin domain contains copper site at His102, Cys166, His171 and Met175. The copper ligands are conserved among cupredoxin. The copper site is within the eight-stranded Greek key β -barrels structure (blue).

However, paralogous of Laz linker region are found in two other proteins, including Lip protein (NMB1523) and AniA protein (NMB 1623). The linker region of *Laz* contains 5 repeats of highly conserved AAEAP motif, though these repeats are not identical motifs. These 5 repeats are quite similar to 15 repeats in Lip protein (Figure 7.4 and Figure 7.5). The functions of these repeats are not known. In general, it is predicted that *Laz* linker region is anchored in the outer membrane while the globular azurin domain is exposed in periplasm (Figure 7.6). The linker region might aid the azurin domain to reach to *bc₁* complex and *cbb₃* oxidase during electron transfer. *Laz* might also be exposed on cell surface (Figure 7.6). If this case is true, the antibodies specific to *Laz* should be found in the patient sera contracted with meningococcal disease. In gonococcus, however, it was found that Lip protein contains surface antigen (H.8) which is highly immunogenic (Black *et al* 1985). This surface antigen is very common among pathogenic neisseria species, not nonpathogenic species (Cannon *et al* 1984, Tessier *et al*, 1985). H.8 epitope specific antibodies have been detected in

patients with local and disseminated meningococcal and gonococcal diseases (Black *et al* 1985). It might be possible that part of Laz linker region is exposed on cell surface and immunogenic similarly to that of Lip protein. This linker region may be looped through the outer membrane and expose the “H.8 epitope” on surface. Therefore, it might not allow the globular azurin domain to reach to and interact directly with the *bc₁* complex or *cbb₃* oxidase (Figure 7.6). There may be periplasmic *c*-type cytochrome(s) that transfers electron from the *bc₁* complex to Laz. Then, another *c*-type cytochrome(s) may pass electron from Laz to the *cbb₃* oxidase. Laz may be able to interact with and transfer electrons directly to AniA nitrite reductase as they both are predicted outer membrane proteins.

Another possibility is that the linker region might not have globular structure. It might exhibit linear structure that allows the globular azurin domain to move in the periplasm, to reach and receive electrons from the cytochrome *bc₁* complex in cytoplasmic membrane and transfer to the cytochrome *cbb₃* oxidase and AniA nitrite reductase (Figure 7.6).

<p>NMB1523 (Lip) MKKSLFAAALLSLVLAACGGGEKAAEAPAAEAPAAEAPATEAPAAEAPAAEAPAAEAPAAEAAATEAPA AAEAATEAPAAEAAATEAPAAEAPAAEAAK</p>
<p>NMB1533 (Laz) MKAYLALISA AVIGLAACSQEPAPAAAEATPAAEAPASEAPAAEAPADAAEAPPAAGNCAATVESNDN MQFNTKDIQVSKACKEFTITLKHTGTQPKASMGHNLVIAKAEDMDGVFKDGVGAADTDYVKPDDARVV AHTKLI GGEEASLTLDPAKLADGEYKFACTFP GHGALMNGKVTLVD</p>
<p>NMB1623 (AniA) MKRQALAAMIASLFAALACGGGEPAAQAPAE TPAAAEAASSAAQTAAETPSGELPVIDAVTTHAPEVP PAIDRDYPAKVRVKMETVEKTMEDGVEYRYWTFDGDVPGRMIRVREGDTVEVEFSNNPSSTVPHNV DFHAATGQGGGAAATFTAPGRSTFSFKALQPGLYIYHCAVAPVGMHIANGMYGLILVEPKGLPKVD KEFYIVQGDFYTKGKKAQGLQPFDMDKAVAEQPEYVVFNGHVGA IAGDNALKAKAGETVRMYVGNNG PNLVSSFHVIGE I FDKVYVEGGKLINE NVQSTIVPAGGSAIVEFKVDIPGSYTLVDHSIFRAFNGKAL GQLKVEGAENPEIMTQKLSDTAYAGNGAAPAASAPAAASAPAAASASEKSVY</p>

Figure 7.4 Paralogs of Laz linker region. The linker region of laz is similar to the sequence of Lip protein and the linker region of AniA nitrite reductase in the same organism.

NMB1533	MKAYLALISAAVIGLAACSQEPAAPA-----AEATPAAEAPASEAPAAE
NMB1523	MKKSLEFAAALLSLVLAACGGGEKAAEAPAAEAPAAEAPATEAPAAEAPAAEAPAAEAPAAE
	** * : : ****. * * * * * * : *****:*****
NMB1533	AAPADAAEAPAAGNCA-----
NMB1523	AAATEAPAAEAAAATEAPAAEAAAATEAPAAEAPAAEAAK
	**.:*: * * * . *

Figure 7.5 Alignment of Laz linker region (NMB1533) and Lip (NMB1523). NMB1523 is similar to H.8 antigen or Lip protein in *N. gonorrhoeae*. Lip contains lipoprotein signal peptide (blue highlight) and 15 repeats (yellow and pink highlight).

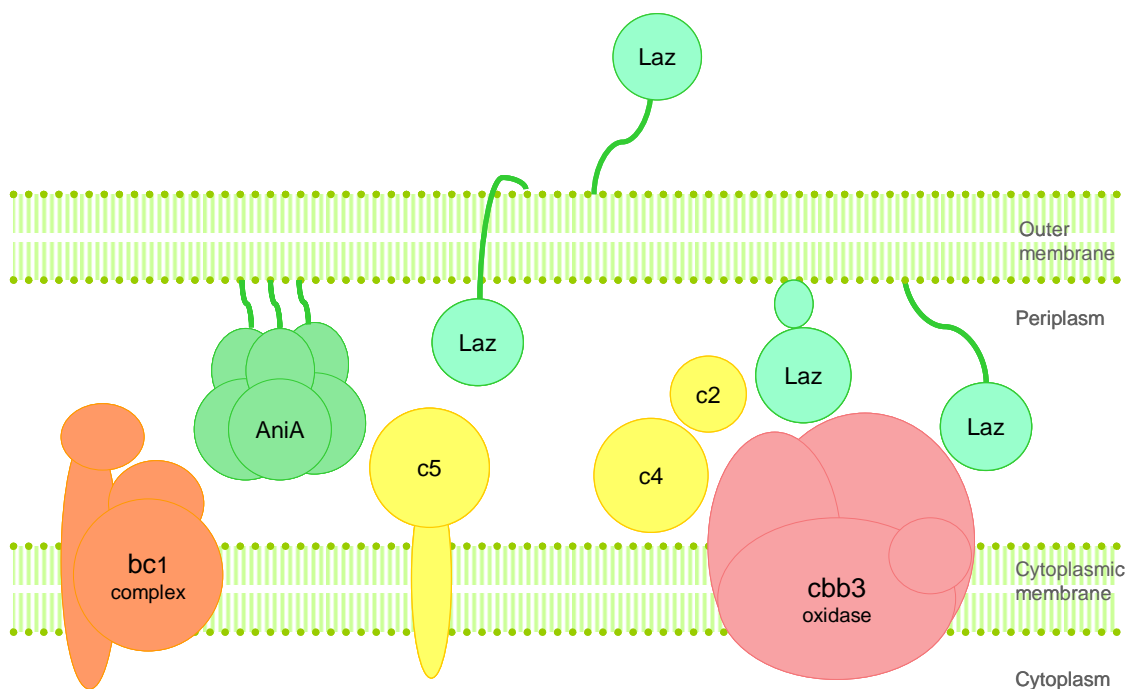


Figure 7.6 Predicted cellular localization of Laz. Laz is possibly localized **i**) in periplasm with N-terminal linker anchored in outer membrane **ii**) in periplasm with transmembrane N-terminal linker partially exposed on cell surface **iii**) in periplasm with globular linker anchored in outer membrane or **iv**) on cell surface with linker region anchored in outer membrane.

Azurin is also found to be an electron donor to nitrite reductase, an important enzyme in denitrifying process (Brittain *et al*, 1992; Silvestrini *et al*, 1994; Murphy *et al*, 2002; Pearson *et al*, 2003). Expression of many genes involved in denirification may be regulated by FNR (Fumarate / Nitrate Reduction) protein. In *P. denitrificans*, the expression of pseudoazurin is mainly controlled by the transcriptional activator FnrP

(Ferguson *et al.*, 2003). In *N. meningitidis*, it is not known whether *laz* expression is regulated by FNR as there is partial-FNR box upstream of *laz* gene centred 47 bases upstream of the translational start site (Figure 7.7). The role of Laz in aerobic and denitrifying respiration requires further investigation.

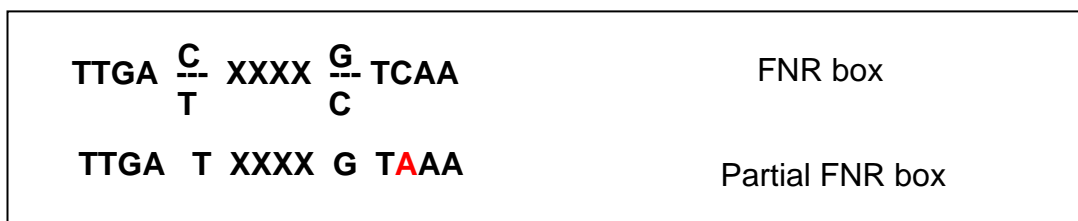


Figure 7.7 Partial FNR box upstream of *laz* gene compared to FNR box in *P. denitrificans*.

In this chapter, Laz protein will be overexpressed in *Escherichia coli*. Purified protein will be used for raising polyclonal antibodies. The anti-Laz antibodies will be used for quantifying the expression of *laz* gene under aerobic, microaerobic, and denitrifying conditions. Laz protein will be used in interaction with meningococcal membrane extract in order to identify the role of *Laz* as an electron donor of cytochrome *cbb₃* oxidase and/or nitrite reductase. Interruption of *laz* gene will be undertaken in order to investigate its importance on the meningococcal respiration and growth under different level of oxygen and nitrite. The cellular localization of Laz protein will be also investigated using cell fractionation and immunoblot.

7.2 Results

7.2.1 Overexpression and characterization of Laz

The initial purpose was to produce a large amount of soluble Laz protein for further functional studies. In order to get soluble Laz protein, cloning of *laz* gene and overexpression of Laz protein in *Escherichia coli* have been done. As previously described that predicted Laz protein has three domains consisting of the lipoprotein

signal peptide, the flexible linker peptide, and the globular azurin domain, at this initial period of study only complete globular azurin domain with flexible linker region was expressed. Laz protein was expressed in the periplasm in order to reduce time and steps of purification. The truncated *laz* gene encoding 165 amino acids of globular azurin domain was cloned and overexpressed in *E. coli* as follows. The *laz* gene from genomic DNA of *N. meningitidis* MC58 was amplified by PCR using Pfu polymerase. Forward primer with *Nco*I site (CCATGG) at 5' end and reverse primer with *Eco*RI site at 5' end have been used, the sequences as shown respectively.

Forward primer (manu1) 5' -CCA TGG CCT CTC AAG AAC CTG CCG CG- 3'

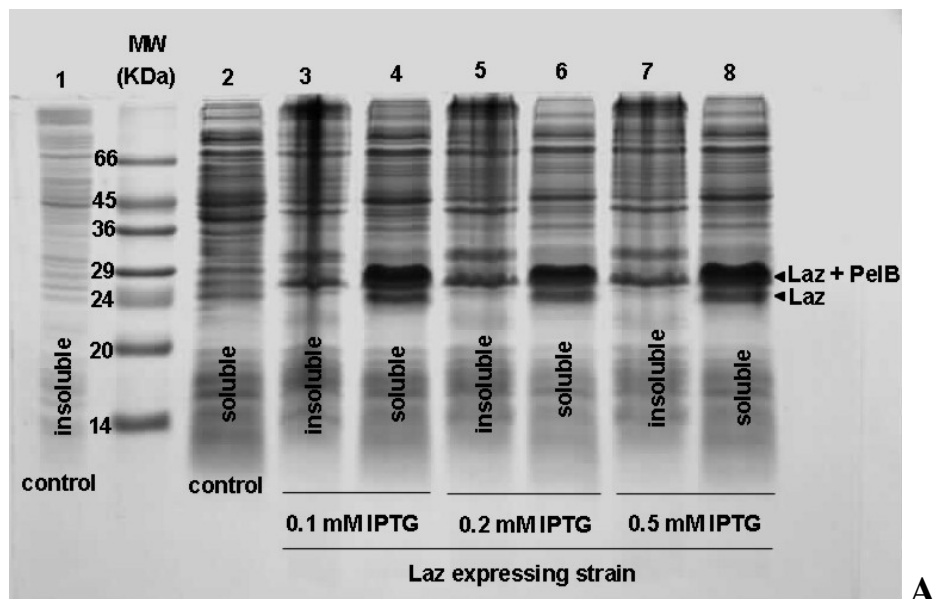
Reverse primer (manu2) 5' -GAA TTC CGG ATT AAT CGA CCA AAG TCA- 3'

The restriction sites were included in the ends of primers in order to get the PCR products compatible for later cloning into expression vector. However, this caused two extra amino acids, Met and Ala, to be included in the end of N-terminus of the protein and resulted in the protein with total 167 amino acids. The forward primer was designed for amplifying DNA sequence encoding the amino acids downstream of Cys18 (Figure 7.2) to prevent the attachment of Cys18 to the outer membrane. Then, blunt end cloning of truncated *laz* gene from PCR product was undertaken. The blunt end PCR product was inserted into pCR-Blunt II TOPO plasmid. Then, the plasmids were transformed into *E. coli* strain DH5- α by heat shock. The recombinant plasmid was purified for sequencing performed to check that insert is correct. Plasmid was digested with *Nco*I and *Eco*RI to generate a sticky end *laz* gene fragment for insertion into pET-22b(+) plasmid. The *laz* gene fragment was inserted next to the *pelB* leader sequence in order to direct the protein to the periplasm. Then pET-22b(+) plasmids with insert were transformed into *E. coli* strain DH5- α to check the plasmid stability. The plasmids were purified and transformed into the expression strain *E. coli* BL21 (λ DE3) by

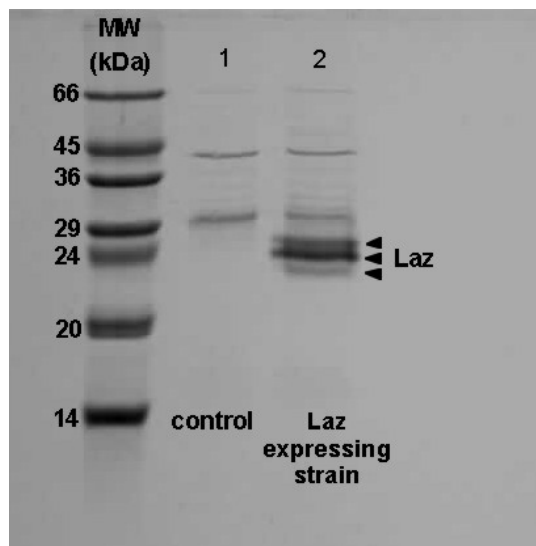
electroporation. The plasmids were purified for sequencing and PCR of *laz* gene. The *laz* gene has been successfully cloned into pET-22b(+) plasmid as confirmed by DNA sequencing.

The expression of Laz protein has been examined under various conditions in order to get highest yield of soluble protein. It has been induced by 0.1, 0.2, 0.5, 1.0, and 10 mM IPTG at 37°C and 25°C with 0.1, 0.3, 0.5 and 1 mM of CuCl₂. The induction by 0.1, 0.2 and 0.5 mM IPTG at 25°C with supplementation of 1mM CuCl₂ is shown in Figure 7.8. The larger portion of protein may be not cleaved and transported to periplasm, remained in cytoplasm with the pelB signal peptide (Figure 7.8). *Laz* protein was extracted from periplasm of expressing strain *E. coli* using osmotic shock. The profile of periplasmic proteins with Laz is shown (Figure 7.8). The periplasmic extract was then further purified for separating *Laz* using anion exchange column chromatography. The periplasmic extract was oxidized by APS to roughly check the amount of Laz protein as it exhibited blue colour in the presence of Laz. The static phase is DEAE sepharose while the mobile phases are Tris-HCl buffer pH 8 and HEPES buffer pH 7. The NaCl salt gradient is up to 500 mM. The purified *Laz* protein was shown in Figure 7.9. The predicted molecular mass of truncated Laz protein without copper is 16,984.9 Da. The expressed proteins were found with higher molecular masses, approximately 24 kDa, as analysed by SDS-PAGE. However, the electrospray mass spectrometry revealed that the protein has molecular mass of 16,983.5 Da analyzed in acidic conditions, 17,045.5 Da and 17,045.0 Da analyzed in non-acidic conditions with 20% methanol solvent and acetonitrile/water solvent respectively (Figure 7.10). It showed that copper was dissociated from the protein in acidic conditions while it was associated with the protein in non-acidic conditions of mass spectrometry. Those molecular masses corresponded correctly to the molecular

mass of Laz protein both without or with copper incorporated. Under non-acidic conditions, however, an adduct was found. This adduct with an increased molecular mass of 22.0 might be from either association of a sodium ion with a molecular weight of 23.0. The oxidized protein absorbs visible light at 626 nm and exhibits blue colour indicating that it has redox activity (Figure 7.11). Laz was treated with diethyldithiocarbamate (DDC), a copper chelating agent, to confirm the association of copper ion with the protein. Upon adding DDC into oxidized laz, the absorption around 626 was decreased rapidly and completely disappeared within 10 minutes (Figure 7.11).



A



B

Figure 7.8 Expression of meningococcal Laz protein in *E. coli*. (A) The expression of Laz induced by 0.1, 0.2, and 0.5 mM IPTG, grown with 1 mM CuCl_2 at 25 °C . (B) Periplasmic fraction containing Laz protein was expressed in Laz expressing strain BL21(λ DE3).

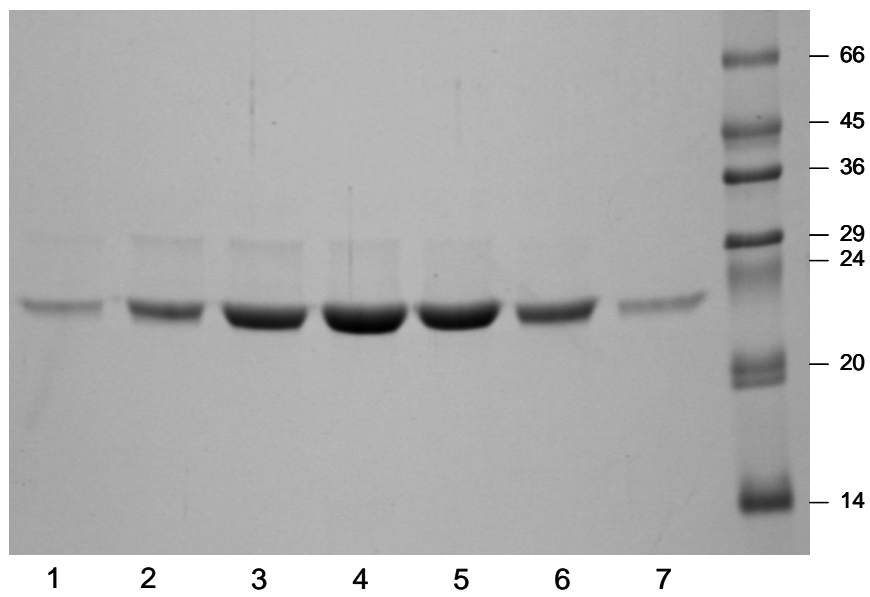


Figure 7.9 Purified Laz from DEAE-sepharose anion exchange chromatography. The purified protein was treated with β -mercaptoethanol to break disulphide bond and reduce the aggregation of protein. The soluble Laz protein exhibits molecular mass approximately at 24 kDa on SDS-PAGE. Lane 1-7 are protein fractions containing Laz.

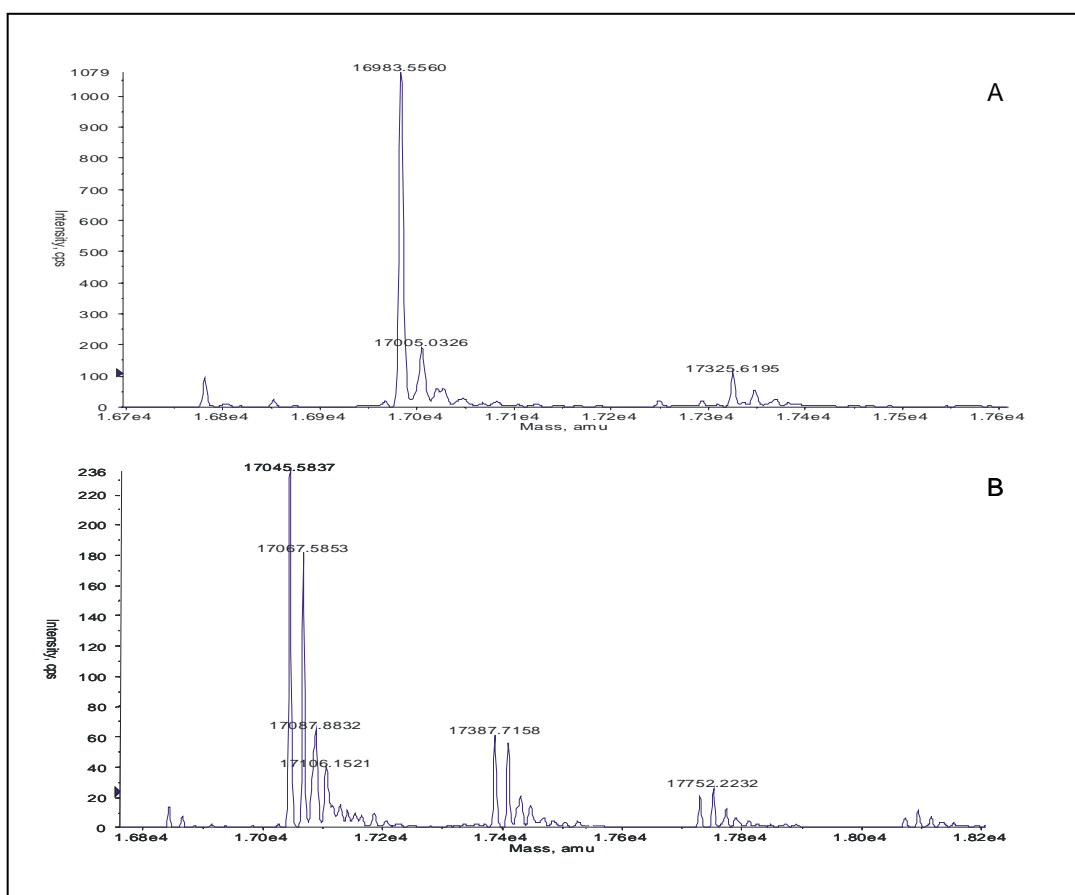


Figure 7.10 Molecular mass of Laz detected by electrospray mass spectroscopy. (A) Laz has a molecular mass of 16,983.5 Da analyzed in acidic conditions. (B) Laz has a molecular mass of 17,045.5 Da analyzed in non-acidic conditions with 20% methanol solvent. The copper ion has a molecular mass of 63.54 corresponding to the different mass between the two conditions, indicating that copper is dissociated from Laz under acidic conditions. The major adduct peak may be from an association of sodium ion with a molecular mass of 23.0.

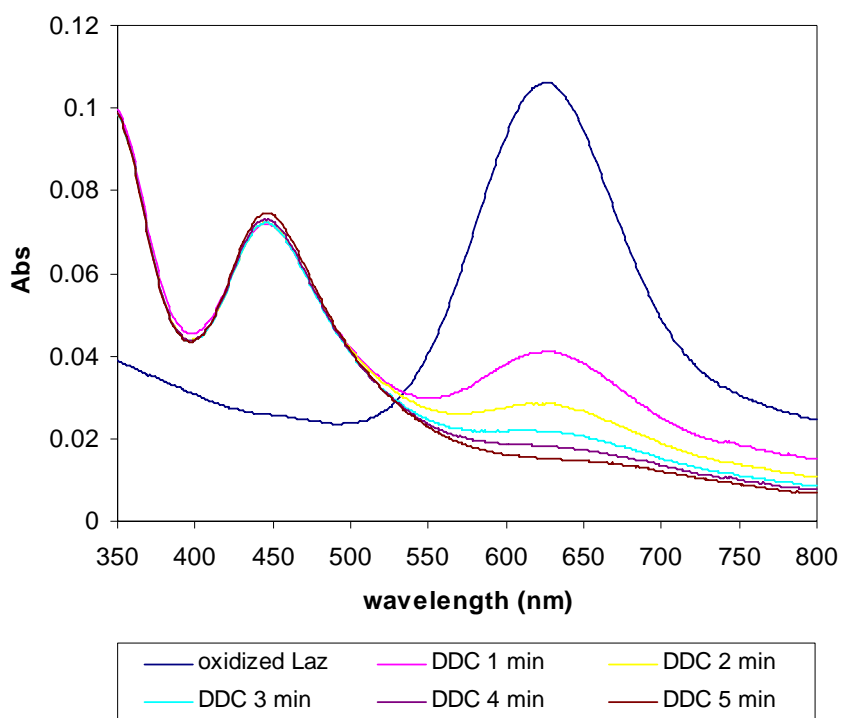
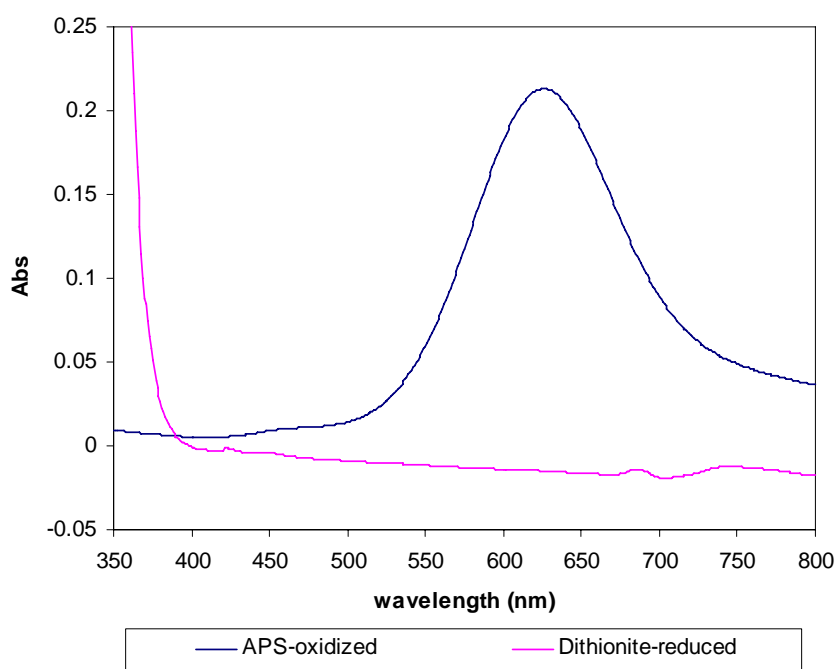


Figure 7.11 Spectral feature of oxidized Laz by UV-VIS spectroscopy and effect of copper chelating agent diethyldithiocarbamate (DDC). (A) Normally, blue copper proteins absorb visible light around 600 nm. Oxidized Laz exhibits broad absorption with maximum absorption at 626 nm (blue line). Reduced Laz exhibits very low absorption (pink line). (B) The removal of copper ion by DDC resulting in the loss of absorption at 626 nm.

7.2.2 Interaction of Laz with meningococcal membrane extract

The purpose was to identify the role of Laz as an electron donor to *cbb₃* oxidase and AniA nitrite reductase. Crude cytoplasmic membrane of NMB were isolated and interacted with purified reduced Laz. The oxidation of Laz by the membrane extract was observed in the presence of either oxygen or nitrite. Initially, the membrane extract was prepared from whole cell lysate after a series of freezing and thawing. The membrane fraction was separated and solubilized in a mild detergent dodecyl maltoside to generate small micelles of membrane and membrane proteins. It was found that *b*-type and *c*-type cytochromes were active as they exhibit recognizable spectra under different redox state (Figure 7.12), indicating that the cytochrome *bc₁* complex, the *cbb₃* oxidase, and maybe *c*-types cytochromes are still active in this extract. Oxidized Laz at concentration of 30 μ M was reduced by sodium dithionite. Then, the reduced Laz was transferred to a sealed cuvette and the measurement of light absorption at 626 nm over time course was started. In the presence of oxygen, by adding 5 μ l of water and shaking the cuvette, Laz can not be oxidized. Upon adding membrane extract, Laz was oxidized indicating by the increased absorption at 626 nm (Figure 7.13). In the presence of oxygen, Laz is oxidized by membrane extract at the rate of 4.08 nmole/min/mg protein. For oxidation of Laz in the presence of nitrite, the reduced Laz in a sealed cuvette was sparged with nitrogen gas to remove oxygen for 10 minutes. In the presence of nitrite, Laz was oxidized by membrane at the rate of 2.45 nmole/min/mg protein (Figure 7.13). Oxygen or nitrite itself can not oxidize Laz, directly. Oxidation of Laz either by oxygen or nitrite is membrane dependent (Figure 7.13).

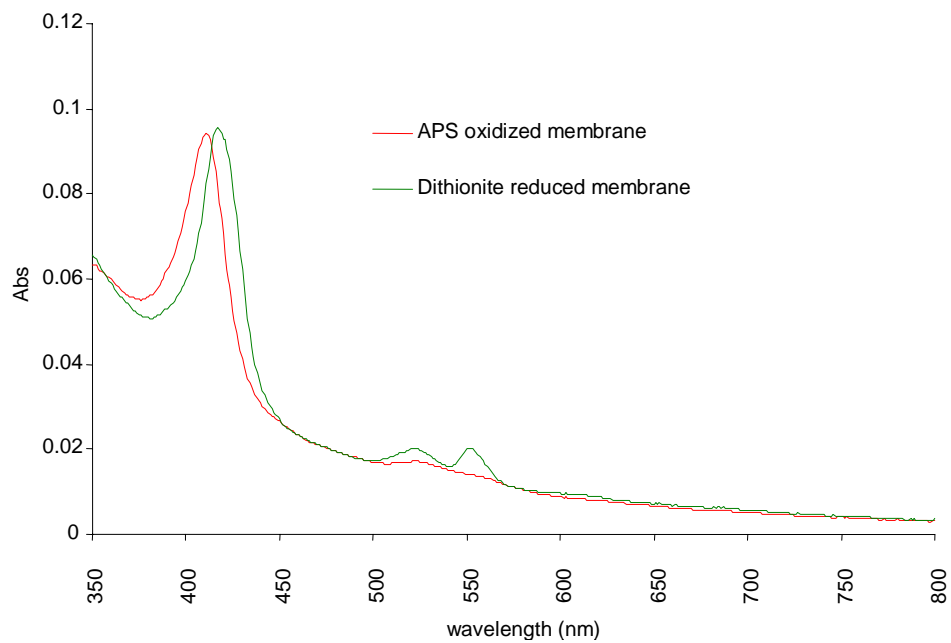


Figure 7.12 Difference spectra of the meningococcal membrane extract. Absorbance spectra of membrane extract in different redox state. The shift of Soret peak around 410-420 nm and the higher absorption at 520 and 552 nm is clearly observed in reduced state.

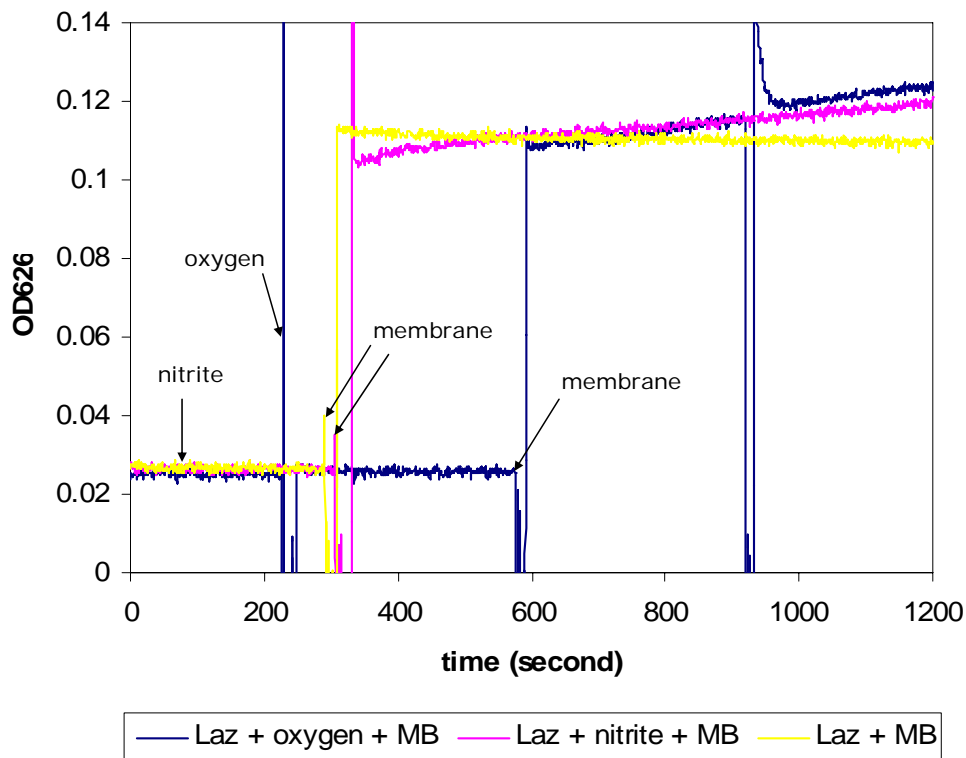


Figure 7.13 Interaction of Laz with meningococcal membrane extract. In the presence of oxygen, Laz is oxidized by membrane at the rate of 4.08 nmol/min/mg protein. In the presence of nitrite, Laz is oxidized by membrane at the rate of 2.45 nmol/min/mg protein. Oxygen or nitrite alone can not oxidize Laz, directly. Oxidation of Laz by oxygen or nitrite is membrane dependent.

7.2.3 Expression of Laz under different growth conditions

As mentioned earlier that Laz might be involved in denitrifying respiration in *N. meningitidis*, the expression of Laz in the meningococcus was investigated under three different growth conditions including aerobic conditions, microaerobic conditions, and denitrifying conditions to gain insight if it is influenced by the level of oxygen and nitrite. Since FNR is commonly known as regulator of anaerobiosis in many bacteria, *fnr* mutant strain was also investigated for its influence on Laz expression. Wild type and *fnr* mutant strains were grown in LB broth at 37 degree Celsius. Under aerobic

growth conditions the 5 ml culture was shaken at 200 rpm for 6 hour. Under microaerobic conditions the 20 ml culture was shaken at 90 rpm for 8 hours. Under denitrifying conditions, the 20 ml culture was shaken at 90 rpm for 8 hours where 5 mM nitrite was supplemented as terminal electron acceptor. Cells were harvested and resuspended in 30 mM Tris buffer. Then the cells were lysed by a series of freeze/thaw cycles. The total protein content of cell lysate from each growth conditions and strain were assayed by Bradford method to allow equal loading. Then Laz protein was detected by dot blotting and western blotting (Figure 7.14). From preliminary data, the expression of Laz protein was not different under all given growth conditions, suggesting that the level of oxygen and nitrite did not affect the expression.

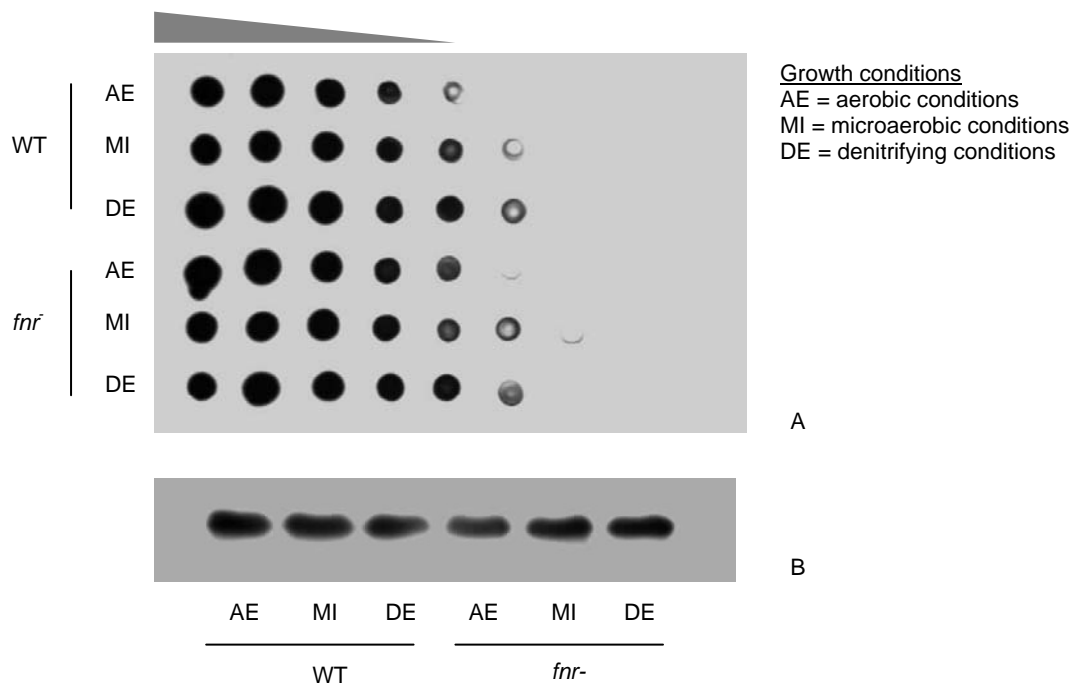


Figure 7.14 The expression of Laz under different growth conditions. The expression in wild type (WT) and *fnr* mutant (*fnr*⁻) were detected by dot blot (A) and western blot (B). Both wild type and *fnr* mutant strains expressed similar amounts of Laz under all given growth conditions, aerobic, microaerobic, and denitrifying conditions where nitrite is the terminal electron acceptor. The dot blot was done in a two fold serial dilution of total protein sample of whole cell lysate.

7.2.4 Laz expression in *c*-type cytochrome mutants

The purpose was to confirm the construction of *laz* mutant before further characterization and also to check the influence of periplasmic *c*-type cytochromes on the expression of Laz. Strains deficient in cytochrome *c2*, *c4*, *c5*, *c2/c4* and Laz were grown on Blood Agar plate for over night. Cells were suspended in 30 mM Tris buffer. Then the cells were lysed by a series of freeze/thaw cycles. The total protein content of cell lysate from each growth conditions and strain were assayed by Bradford method to allow equal loading. Then Laz protein was detected by western blotting (Figure 7.15). Laz expression was detected in all respiratory mutant strains except in *laz* mutant. It confirmed that *laz* mutant has been successfully constructed. The loss of cytochrome *c2*, *c4*, *c5*, or both *c2* and *c4* did not affect the expression of Laz.

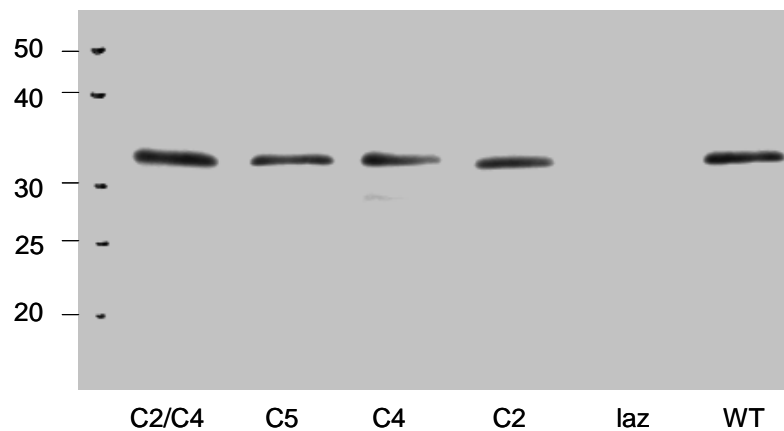


Figure 7.15 Laz expression in respiratory mutants. Laz was detected by western blot in all respiratory mutants except in *laz* mutant. Equal amount of 10 μ g total protein was loaded in each lane.

7.2.5 Growth of *laz* mutant under aerobic conditions

The purpose was to investigate the role of Laz on growth of the meningococcus under high level of oxygen as terminal electron acceptor. The *laz* mutant and wild type strains were grown in MHB under aerobic conditions. All strains were grown

aerobically by shaking 6 ml of culture in 25 ml plastic McCartney tube at 200 rpm. In this experiment, oxygen is the only terminal electron acceptor for respiration. The aerobic cultures were sampled and two fold diluted for measuring optical density at 600 nm. The growth characteristics of wild type strain and the mutant strain are shown in Chapter 6, Figure 6.5. The WT strain entered exponential growth after 2 hr and reached maximum optical density of 2.8 at 8 hr and quickly entered death phase. The mutant strain with Laz defect showed normal growth from lag phase to mid-exponential phase. It entered exponential growth at the same time as WT but after the growth reached high optical density around 1.2 the mutant grew slower under this decreased level of oxygen. Upon reaching optical density of 1.4-1.5 the mutant stopped growing for 3-4 hours. After that, the *laz* mutant returned to fast growth and reached high growth yield similarly to wild type strain. The growth pattern of *laz* mutant is similar to *c5* mutant. Doubling time for *laz* mutant during fast growth is similar to that for WT, which is 43 minutes. Laz mutant exhibits oxygen reduction rate similar to WT (data not shown).

7.2.6 Growth of *laz* mutant under microaerobic conditions

The purpose was to investigate the role of Laz on growth of the meningococcus under very low level of oxygen. Cells were grown in 20 ml of MHB in plastic McCartney tubes with 90 rpm shaking. Growth pattern of *laz* mutant under microaerobic conditions over 25 hour period was not different from WT strain (Figure 7.16). The maximum optical density of WT strain and the mutant were not different, which is about 0.2.

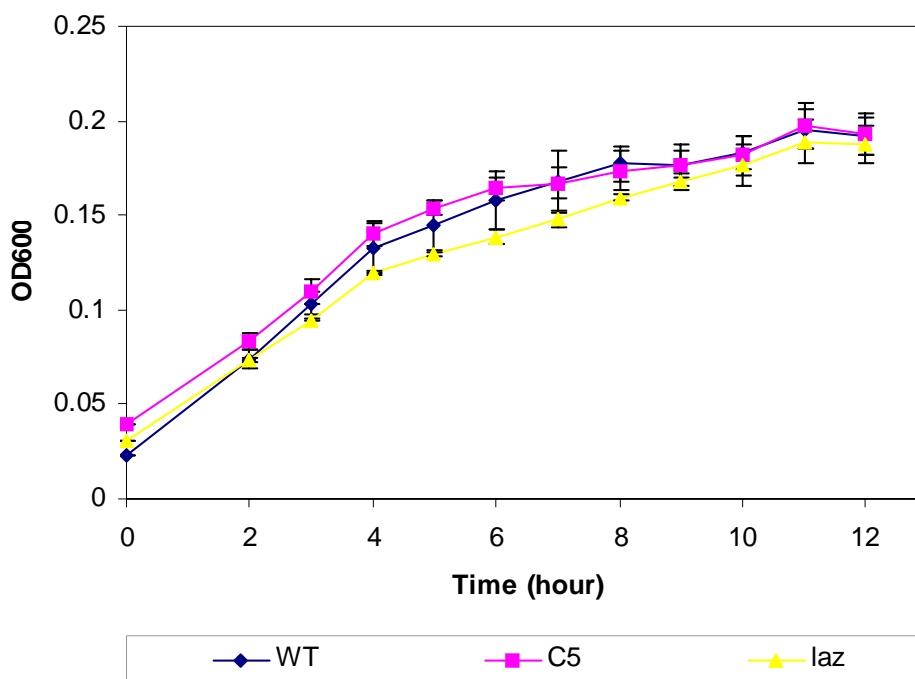


Figure 7.16 Growth of *laz* mutant under microaerobic conditions. *laz* mutant can grow similarly to WT and *c5* mutant under microaerobic conditions.

7.2.7 Growth of *laz* mutant under microaerobic conditions with nitrite

The purpose was to investigate the role of Laz on growth of the meningococcus under very low level of oxygen with presence of nitrite as an alternative terminal electron acceptor. The growth conditions were similar to that under microaerobic conditions but 5 mM nitrite was present. The *laz* mutant can grow in the presence of nitrite better than without nitrite. The wild type strain grew to a higher maximum optical density of 0.4 at hour 9 and then enter death phase. The growth of *laz* mutant under denitrifying conditions was slower than WT. It can enter log phase later than WT (shown as *laz* isolate 2, Figure 7.17). In some occasions the mutant hardly grew and did not enter log phase at all (shown as *laz* isolate 1, Figure 7.17). Since the *laz* mutant grew under microaerobic conditions with nitrite supplement slower than WT, it is possible that the mutant has a defect in utilizing nitrite as an alternative terminal

electron acceptor in order to supplement growth under low level of oxygen. It is of interest to further investigate if this growth defect is linked to the decreased ability of the mutant to reduce nitrite.

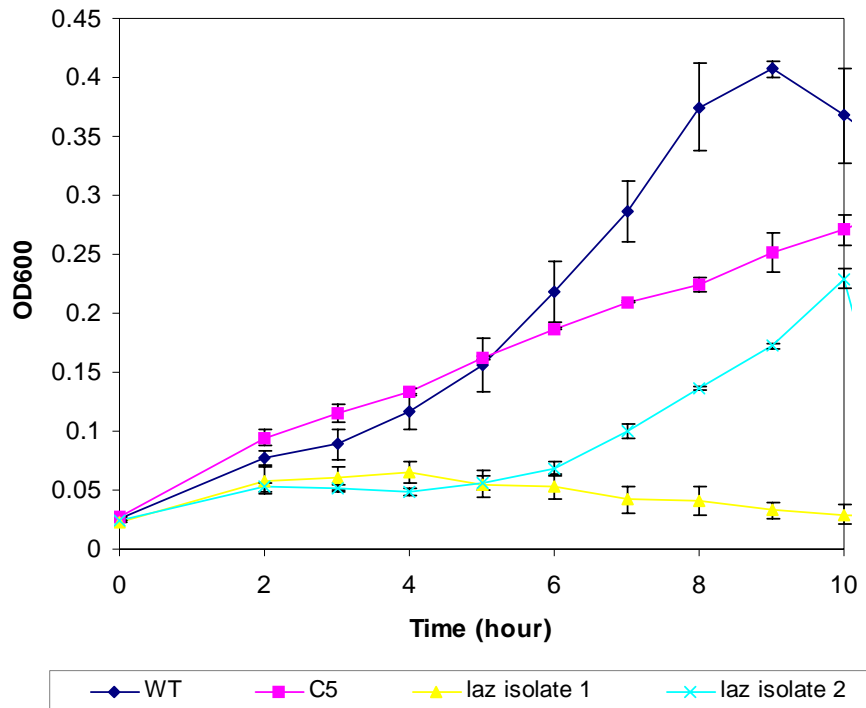


Figure 7.17 Growth of *laz* mutant under microaerobic conditions with nitrite. *laz* mutant showed growth defect under denitrifying conditions. In some occasions, *laz* mutant did not grow (*laz* isolate 1), but the other occasions it can grow after very long lag phase (*laz* isolate 2).

7.2.8 Nitrite reduction

Since the *laz* mutant starts growing and entering log phase later than wild type under denitrifying conditions and in some occasions the mutant cannot grow exponentially, it might be possible that the mutant has decreased ability to use nitrite as respiratory substrate to support growth under low level of oxygen. The purpose was to measure the utilization of nitrite during microaerobic growth to see if the delayed and poor growth were related to the decreased ability to reduce nitrite. The meningococci were grown under microaerobic conditions with 5 mM nitrite

supplement. Levels of nitrite were measured by nitrite assay every hour of growth. It was found that the level of nitrite was hardly changed in *laz* mutant (shown as *laz* isolate 1, Figure 7.18). However, in some occasions the level of nitrite was decreased during later hours (as shown in *laz* isolate 2, Figure 7.18). It is found that *laz* mutant reduced nitrite later than WT during growth under microaerobic conditions.

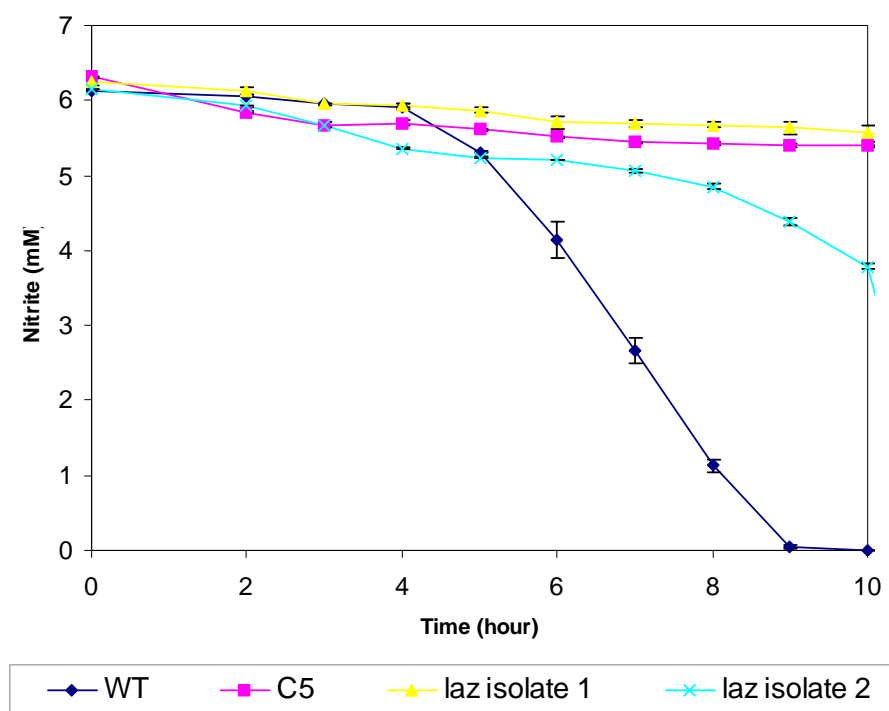


Figure 7.18 Nitrite reduction of *laz* mutant. *laz* mutant showed decreased ability to utilize nitrite to support growth under denitrifying conditions.

7.2.9 Expression of AniA nitrite reductase in *laz* mutant

Based on genome sequence analysis, it is likely that the capability of the meningococcus to reduce nitrite is dependent solely on nitrite reductase activity of AniA protein. There is no other protein predicted to be nitrite reductase in this organism. As the *laz* mutant showed decreased ability to reduce nitrite and grow under microaerobic conditions in the presence of nitrite, it is interesting to investigate if these altered characteristics are linked to a defect in expression of AniA or it is direct effect

of *laz* itself. The expression of AniA in *laz* mutant was detected using western blot with primary antibody against the meningococcal AniA. All strains were grown in MHB under microaerobic conditions with 5mM nitrite for 6 hours. After that, cultures were centrifuged to separate cells and whole cell extract were prepared. It is found that *laz* mutant can express AniA under microaerobic conditions with nitrite supplement (Figure 7.19).

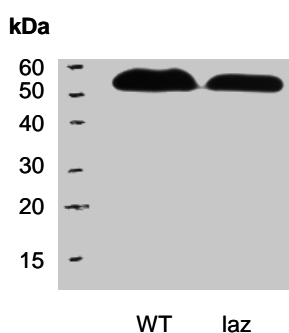


Figure 7.19 AniA expression in *laz* mutant. Equal amount of 10 μ g total protein was loaded in each lane. Detection by using western blot showed that *laz* mutant can normally express AniA.

7.2.10 Production of nitric oxide by *laz* mutant

Since *laz* mutant grew poorer than WT under microaerobic conditions with nitrite and somehow showed decreased ability to utilize nitrite as respiratory substrate, it was of interest to investigate if this is the direct effect of the *laz* mutant having decreased ability to reduce nitrite and to generate nitric oxide. Intact cells of *laz* mutant strain were used for measuring the rate of nitric oxide accumulation compared to WT.

7.2.10.1 Nitric oxide accumulation assay

Cell preparation for the assay of nitric oxide accumulation was previously described in Chapter 5, section 5.2.7.1. Briefly, cells were grown under microaerobic conditions without nitrite to induce the expression of AniA but not NorB. Then, cells were separated and resuspended in MHB to an optical density around 1.3-1.5. The assay for nitric oxide generation was done using Clark-type electrode with nitric oxide

electrode. First, 2.7 ml of MHB with 5 mM glucose was added to the electrode chamber and level of oxygen and nitric oxide were recorded by chart recorder. Then, 0.3 ml of cell suspension was added to the chamber. The chamber was capped and nitric oxide electrode was submerged into the suspension. After the level of oxygen decreased to zero percent, nitrite was added to final concentration of 5 mM. The level of nitric oxide generated from nitrite reduction, supposedly by AniA, and accumulated in the electrode chamber was monitored and recorded over time course. It has been found that the *laz* mutant can generate nitric oxide at faster rate than wild type strain. The WT accumulated nitric oxide at the rate of 1.0 nmole/min/mg while the *laz* mutant accumulated nitric oxide at the rate of 2 nmole/min/mg (Figure 7.20). The signal line from *laz* mutant was very smooth compared to that from WT strain.

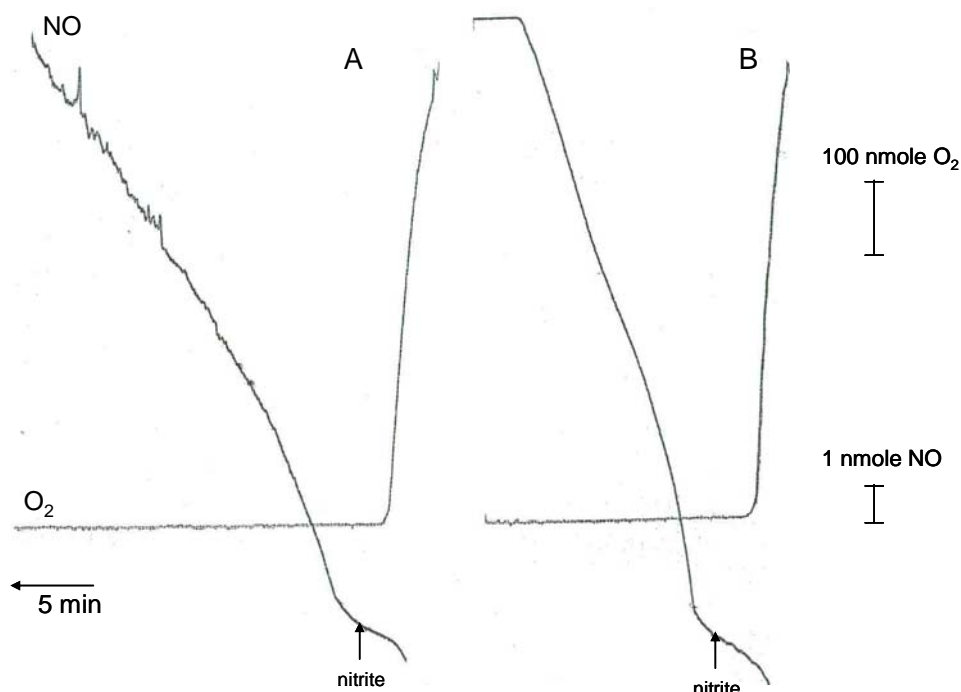


Figure 7.20 NO generation in *laz* mutant. The *laz* mutant can generate more NO than wild type strain. Wild type strain (A) accumulated nitric oxide at the rate of 1.0 nmole/min/mg while the *laz* mutant (B) accumulated nitric oxide at the rate of 2 nmole/min/mg.

7.2.11 Spectra of *laz* mutant

7.2.11.1 Cell oxidation by oxygen

Intact cells of *laz* mutants show different visible light spectra from WT and other respiratory mutant strains when oxidized by oxygen. The double derivatives of the oxidized minus reduced difference spectra are shown in Figure 7.21. Upon oxidation the Soret peak was normally shifted to shorter wavelengths. However, the Soret peak of *laz* mutant was not much altered compared to other strains. The *laz* mutant exhibited α peak similar to that of *c2* and *c5* mutant, the α peak shifted to shorter wavelength compared to WT. WT minus mutant difference spectra showed that *laz* mutant lost absorption at 558 and 562 nm in the α band. It is likely that the actual absorption peak is around 560 but it could be interfered by background signal. The absorption change at Soret was greatly lower from that of WT (Figure 7.22).

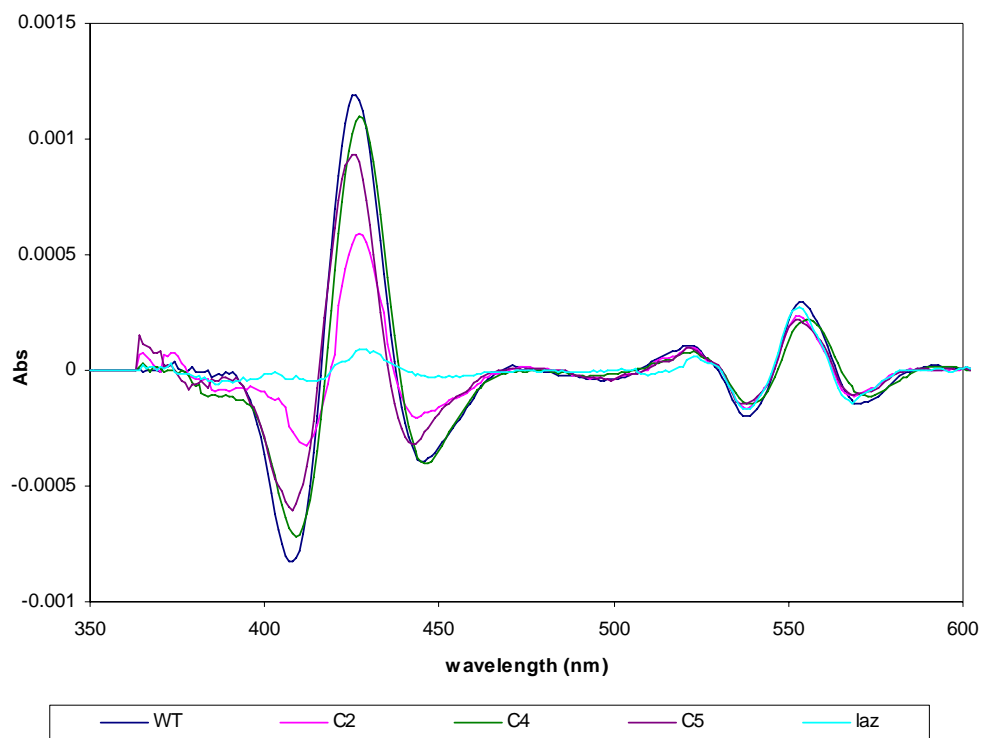


Figure 7.21A Spectra of *laz* mutant. Double derivatives of oxidized minus reduced difference spectra of mutants. The *laz* mutant exhibited very weak absorption change at Soret band than other strains. The absorption change at α band was quite similar to those of *c2* and *c5* mutants.

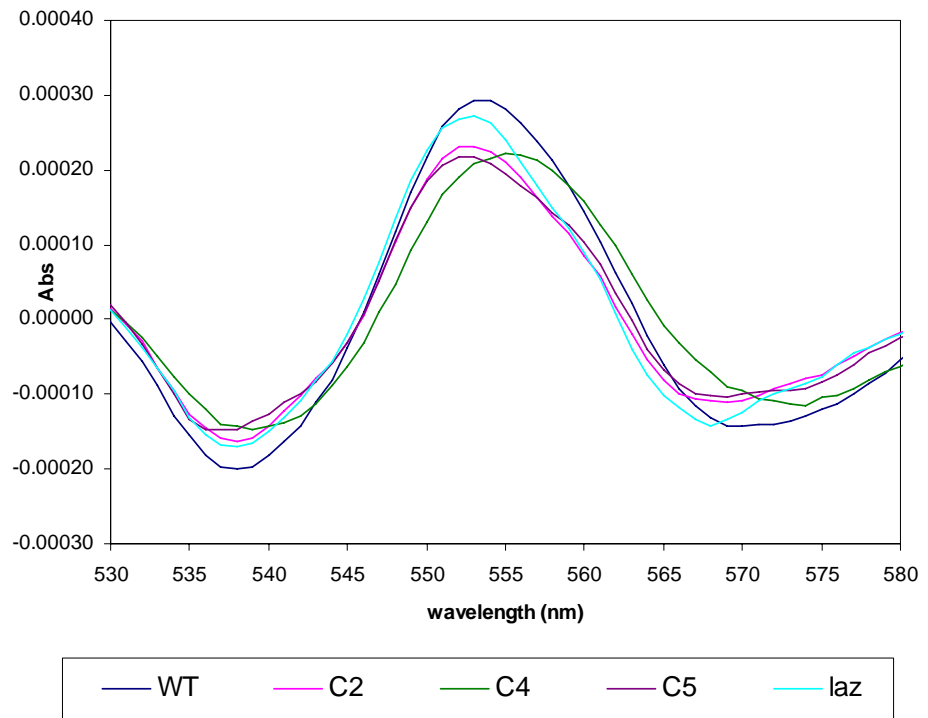


Figure 7.21B The α peak of *laz* mutant. The α peak of *laz* mutant is at 552 nm similarly to those from *c5* and *c2* mutant. *c4* mutant exhibited α peak at 555 nm. WT strain exhibited α peak at 553 nm.

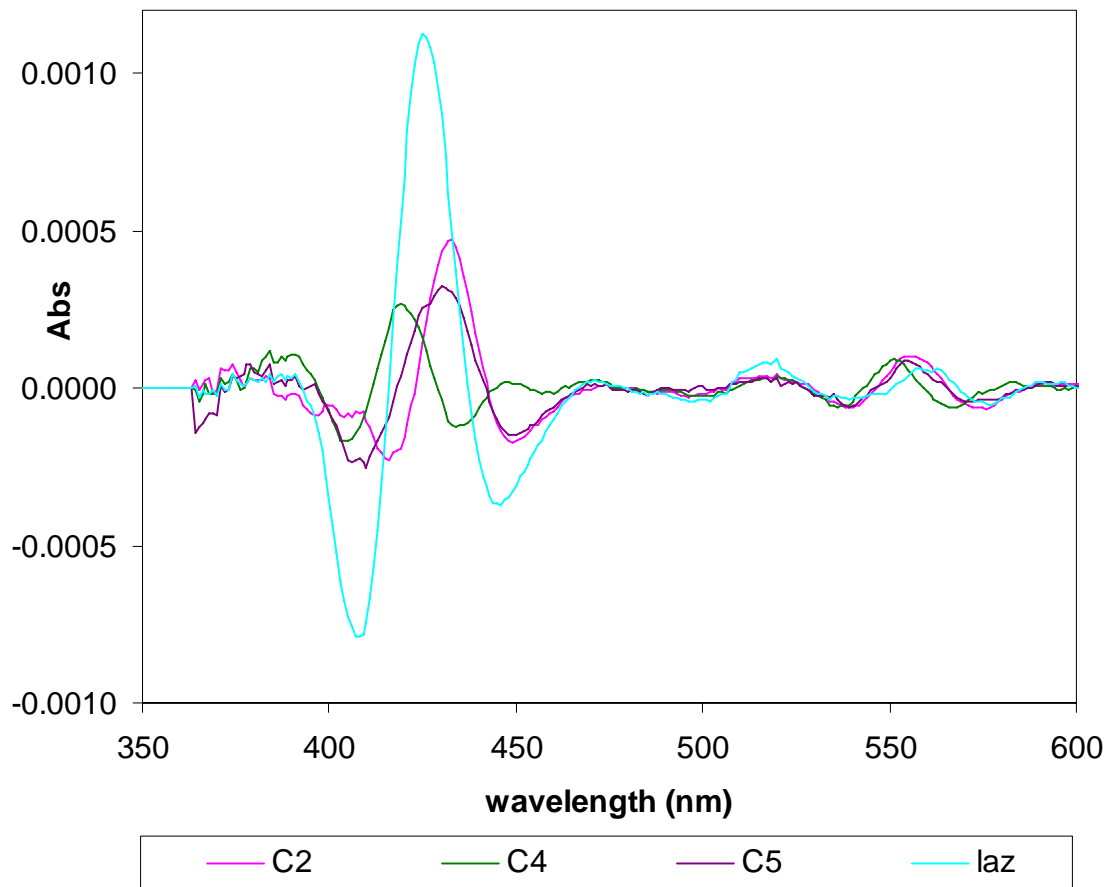


Figure 7.22A Lost absorptions of respiratory mutants. Light absorption at Soret and α peak can distinguish different *c*-type cytochrome. The lost absorption in each cytochrome mutant is proposed to be the actual absorption of that cytochrome. The *c5* mutant shows that the cytochrome *c5* absorbs lower wavelength both at Soret and α peak than cytochrome *c4*. However, cytochrome *c5* absorbs a bit higher wavelength at Soret peak than cytochrome *c2* and the α peak is also sharper.

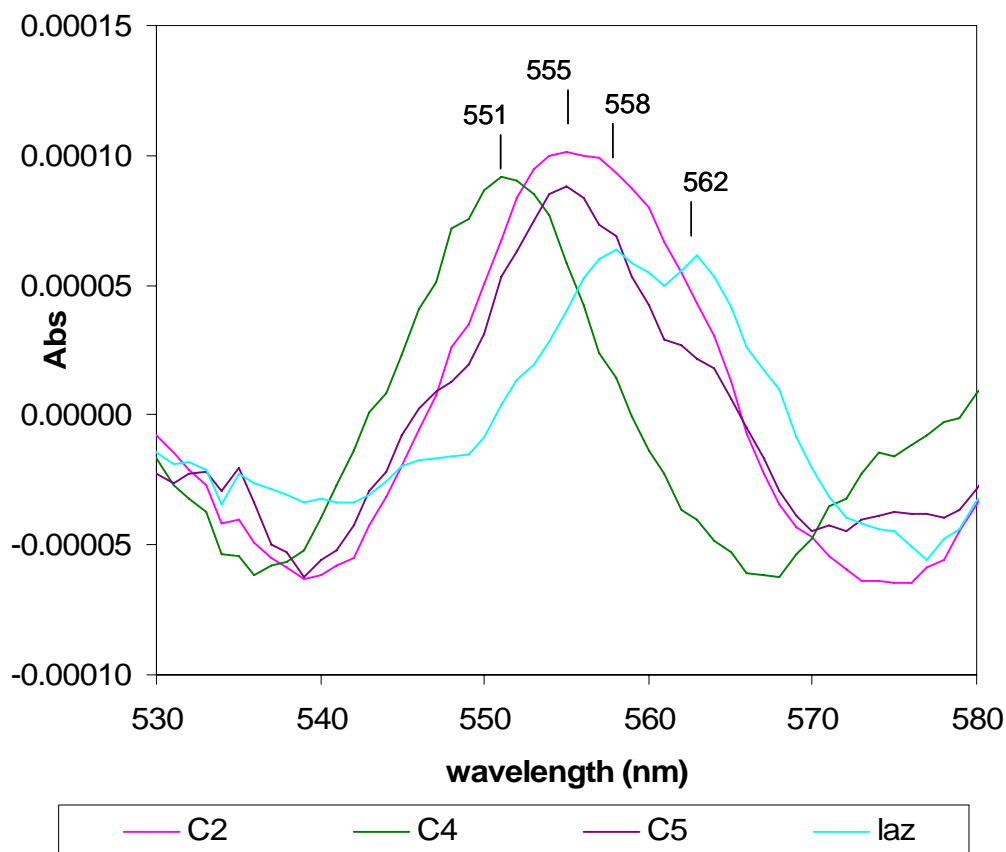


Figure 7.22B Lost peak at α band of *laz* mutant represents actual absorption of cytochromes. The absence of Laz resulted in the loss of absorption at 558 and 562 nm. This might be the effect of background signal and it is proposed that the actual absorption would be around 560 nm. This might suggest the lost absorption of some *b*-type cytochromes.

7.2.11.2 Cell oxidation by H₂O₂

The *laz* mutant stops growing temporarily during growth at high cell density and entered stationary phase for 4 hours (Chapter 6, Figure 6.5). It is hypothesized that this might be the result from the decreased level of oxygen, nutrient availability, or pH change. Moreover, this might be involved with the ability to cope with reactive oxygen radicals, such as hydrogen peroxide. The purpose was to investigate the involvement of Laz in response to oxidation by hydrogen peroxide and if this response is cytochrome-dependent. Cells were grown under aerobic conditions to optical density about 1.0 and

harvested for spectral measurement. A high concentration of 2 mM hydrogen peroxide was used for the oxidation of cytochromes in the intact cells in order to maintain oxidized state of cytochromes during the spectral measurement. It was found that the oxidation by hydrogen peroxide gave spectral features that are different from that by oxygen (Figure 7.23A). In wild type, the oxidation by hydrogen peroxide gave difference spectra with α peak at 555 nm whereas oxidation by oxygen gave α peak at 553 nm. In the *laz* mutant, oxidation by hydrogen peroxide also gave difference spectra with α peak at 555 nm (Figure 7.23B). The α peak and β peak are also similar to WT. It is not clear if the α peak at 555 nm is a spectral feature of cytochrome *c5*.

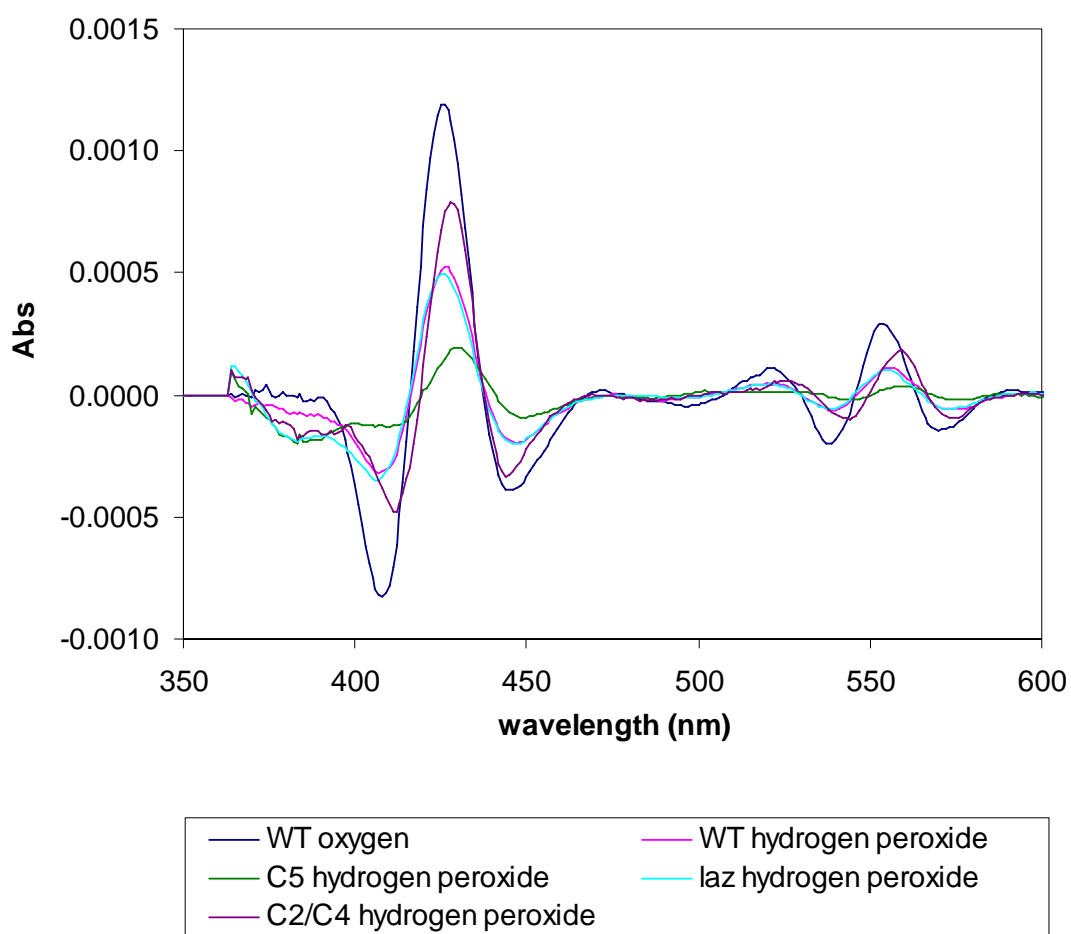


Figure 7.23A Difference spectra of *laz* mutant cells oxidized by hydrogen peroxide. The *laz* mutant gave spectra similar to that of WT indicating that Laz protein might not be involved in electron transfer to cytochrome(s) that reduce H₂O₂. Cytochrome that possesses peroxidase activity has not been identified yet in this organism.

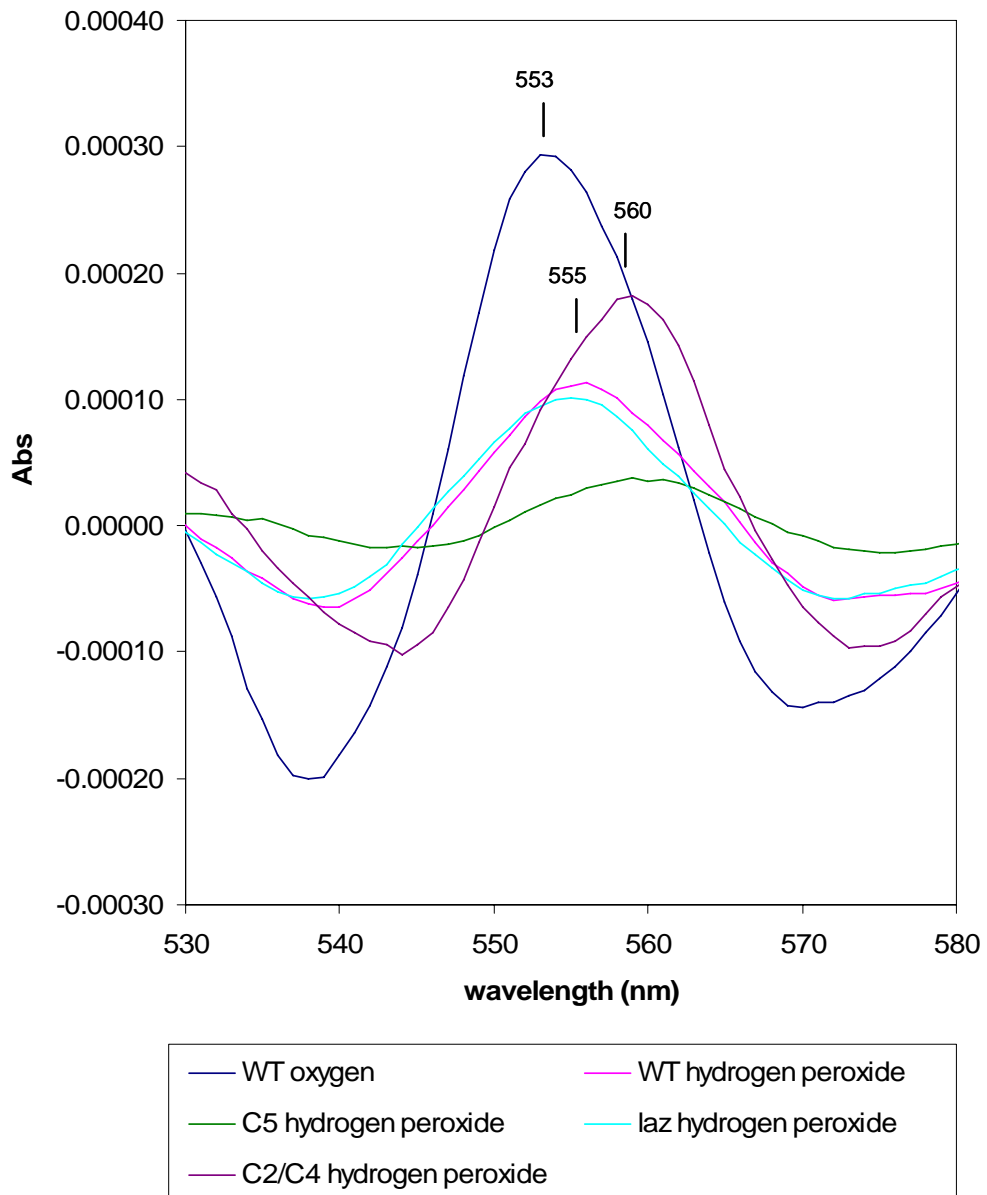


Figure 7.23B The α features of difference spectra of *laz* mutant cells oxidized by hydrogen peroxide. *Laz* may not be involved in detoxification of hydrogen peroxide as *laz* mutant exhibits cytochrome spectra when oxidized by hydrogen peroxide similar to that of WT. WT and *laz* mutant strains exhibit α peak at 555 nm. Interestingly, *c5* mutant and *c2/c4* double mutant exhibit α peak at 560 nm indicating that *b*-type cytochromes are predominantly oxidized.

7.2.12 Cellular localization of Laz

From protein sequence analysis, Laz is predicted to be an outer membrane protein. The localization of Laz has been investigated by determination of Laz in cell fractions and cell blebs. *N. meningitidis* was grown under denitrifying conditions to mid-log phase and cells were harvested. Then, cells were fractionated into membranes, periplasm, and cytoplasm. Briefly, cells were treated by hypertonic buffer, 20% sucrose in 30 mM Tris pH 8.0. Then, cells were treated by hypotonic solution, 0.5 mM MgCl₂ to cause osmotic shock and release of periplasm. The periplasmic fraction was separated from cells by centrifugation at 8000 g. Next, cells were lysed by lysozyme to released cytoplasm. Cell lysate, then, was centrifuged to separate membrane and cytoplasm. Membrane pellet was resuspended in 30 mM Tris. To achieve membrane blebs, a culture was centrifuged at 8000 g for 20 minute to remove all possible remaining cells. Then, the culture supernatant was centrifuged at 100,000 g for 1 hour to cause membrane blebs to form a pellet. The bleb fraction was obtained by resuspending of bleb pellet in 30 mM Tris. Immunoblot of cell fractions showed that amount of Laz in the membrane blebs and membrane fractions was much higher than that in the periplasm and cytoplasm (Figure 7.24). There are 5 major proteins from membrane bleb fraction. These were sequenced and identified by MALDI mass spectroscopy. Analysis of the sequences revealed that 3 of them are outer membrane porin protein homologs, including Porin A (NMB 1429), Porin B (NMB 2039), and RmpM (Figure 7.27). The RmpM is an outer membrane protein which belongs to OmpA family. Another protein is a putative cell-binding factor (NMB 0345) which is also a predicted parvulin-like outer membrane proteins. This protein is predicted to have peptidyl-prolyl cis-trans isomerase (PPI) activity that facilitates protein folding in periplasm. This protein may catalyze the cis-trans isomerization of proline bonds in linker region of Laz and those in

Lip protein. Another identified protein is chaperonin (NMB 1972) or GroEL protein. In general, chaperonin proteins are usually found in cytoplasm but can also be found associated with outer membrane (Ge and Rikihisa, 2007). GroEL has been detected on the *Helicobacter pylori* cell surfaces (Li *et al*, 2001), *Haemophilus ducreyi* (Frisk *et al*, 1998), *Legionella pneumophila* (Gardauno *et al*, 1998), and *Clostridium difficile* (Hennequin *et al*, 2001). In *H. pylori*, it was found that GroEL release is related to specific secretion rather than autolysis GroEL (Vanet and Labinge, 1998). In *H. ducreyi*, GroEL mediates the binding of the bacterium to host carbohydrate receptors (Pantzar *et al*, 2006). The GroEL homolog is predicted to have signal peptidase site at C-terminus.

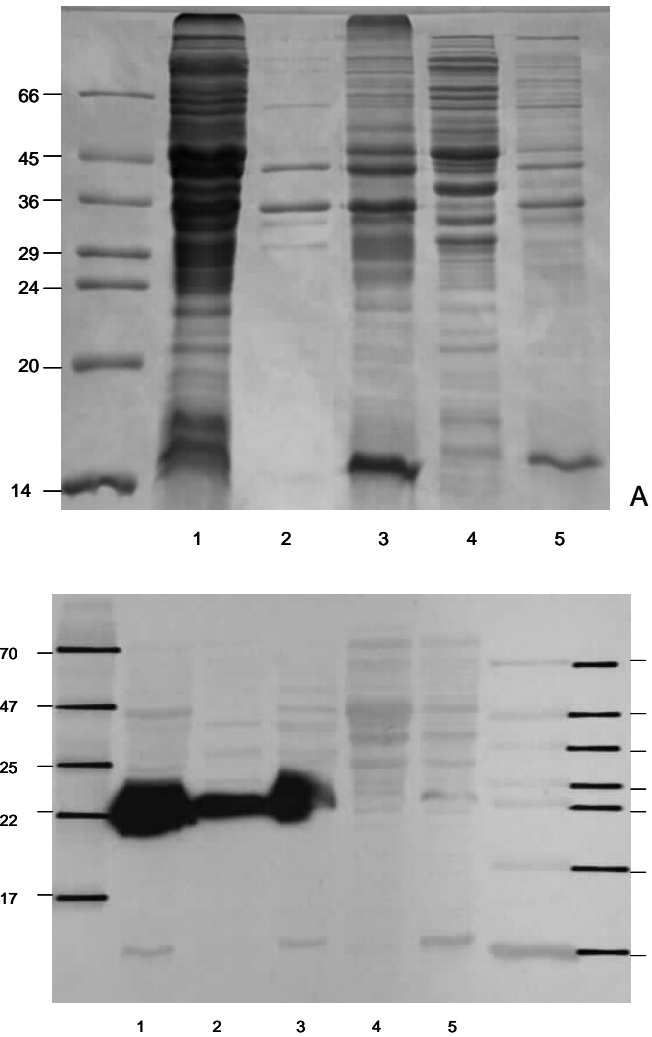


Figure 7.24 Localization of Laz in the outer membrane. Equal amount of 13 μg total protein was loaded in each lane except lane 2 which is less than the others. (A) Protein profile in cell fractions. (B) Amount of Laz in cell fractions by immunoblot developed using enhanced chemiluminescence (ECL). The background proteins were developed by Ponceau S staining. lane 1 = whole cell lysate ; lane 2 = outer membrane blebs ; lane 3 = total membrane ; lane 4 = cytoplasm ; lane 5 = periplasm

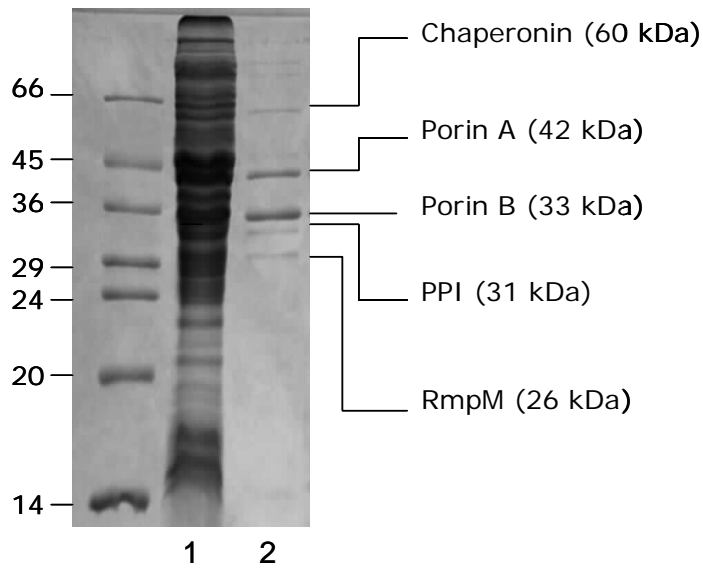


Figure 7.25 Outer membrane bleb proteins. The two major proteins are Porin A (42 kDa and Porin B (33 kDa). RmpM and PPI are also predicted to be outer membrane proteins. Chaperonin (GroEL) is generally found in cytoplasm but can also be found associated with outer membrane. lane 1 = whole cell lysate and lane 2 = outer membrane blebs.

7.3 Discussion

Laz protein of *N. meningitidis* has been successfully cloned and heterologously expressed in *E. coli*. The incubation temperature is very important for increasing soluble protein in periplasm. It was found that incubation at lower temperature, 25°C, increased much higher yield of soluble protein compared to incubation at 37 degree Celcius. In order to obtain Laz protein with bound copper ion, the culture must have been supplemented with CuCl₂. It was found that Laz protein from culture without CuCl₂ supplement did not show spectral absorption typical to azurin even oxidized by APS. The high concentration of CuCl₂ at 1 mM was used successfully to produce Laz protein that exhibit light absorption around 626 nm when oxidized by APS and decreased absorption when reduced by sodium dithionite.

The extraction of *E. coli* periplasm relied on using osmotic shock. The periplasmic extract showed high amount of soluble Laz protein with few other periplasmic proteins. Laz purification by column chromatography was very effective. As the predicted isoelectric point of Laz is 4.6, 100 mM Tris buffer pH 8.0 was used as mobile phase in a consecutive in order to make Laz protein become negatively charged and bind DEAE-sepharose matrix. A gradient of 0-500 mM NaCl was used to elute protein. Laz was further purified using 25 mM HEPES buffer pH 7 and the same salt gradient. After two session of running with different buffers, first Tris buffer and second HEPES buffer, the protein was clean enough for further characterization.

Laz protein exhibits molecular mass of 24 kDa analyzed by SDS-PAGE. The predicted molecular mass is 17 kDa. This may be due to high proline content (about 20%) distributed in the linker region. However, electrospray mass spectrometry showed that Laz actually has molecular mass of 16,983.5 Da analyzed in acidic conditions , and 17,045.5 Da analyzed in non-acidic conditions with 20% methanol solvent. The difference is due to the mass of copper ion. It remains bound under non-acidic conditions whereas it is dissociated from Laz under acidic conditions. This technique was demonstrated to be very useful for analyzing cupredoxin such as Laz protein.

The role of Laz in electron transport and respiration has been investigated. Laz can be oxidized by either oxygen or nitrite in the presence of meningococcal membrane extract. This is likely to be the activity of *cbb₃* oxidase and AniA nitrite reductase in each case respectively. However, the rate of oxygen reduction and nitrite reduction were very low suggesting that Laz may be sluggish in electron donating to those terminal reductases under these experimental conditions. In the presence of oxygen, Laz is oxidized by membrane at the rate of 4.08 nmol/min/mg protein. In the presence of nitrite, Laz is oxidized by membrane at the rate of 2.45 nmol/min/mg protein. The

oxygen reduction rate in intact cells of *N. meningitidis* measured by Clark-type electrode in the presence of 5 mM glucose is 145 nmole/min/mg protein. It might be possible that the concentration of Laz used in this experiment, 20-30 uM, might still be suboptimal for the reaction. The enzyme activity of *cbb₃* oxidase and AniA may also be suboptimal. Further studies and more evidences are required to investigate the notion that Laz is an electron donor to such terminal reductases.

Laz expression under aerobic, microaerobic, and denitrifying condition are not different suggesting that level of oxygen and nitrite do not influence the expression. The expression is also similar between WT and *fnr* mutant suggesting that FNR does not regulate the expression of Laz despite the presence of partial FNR box upstream of *laz* gene. This implies that Laz might not play important role in denitrification in this organism. In *P. aeruginosa*, azurin also does not play an obligatory role in denitrification (Vijgenboom *et al*, 1997).

Under aerobic conditions, *laz* mutant grew normally until it reached mid-log phase. Upon reaching high cell density, around 1.2 -1.5, it stopped growing for about 4 hours then returned to fast growth. This growth pattern is very similar to that of *c5* mutant. The delayed growth during mid-log phase were occasionally observed in WT strain but less prominent than those of *c5* and *laz* mutant. The oxygen reduction rate in *laz* mutant, measured during aerobic growth at hour 4, was not different from WT suggesting that during early log phase Laz is not important for aerobic respiration. However, it is hypothesized that Laz might be important for aerobic respiration once the culture is approaching high cell density. As mentioned in earlier chapter that once the culture reaches high cell density, the oxygen level may be decreased. Cells may become more reduced and the pH in periplasm may be altered. Under these circumstances, Laz together with cytochrome *c5* may become crucial for aerobic respiration and growth.

The comparison of oxygen consumption rate between *laz* mutant and WT at mid log phase, where growth of *laz* mutant started to delay, might be required to provide supportive evidence to this hypothesis. Growth pattern of *c5/laz* double mutant under aerobic condition might also provide evidence for better understanding. Increasing aeration for *laz* mutant during mid-log phase is another proposed experiment to support or refute the hypothesis.

Under denitrifying conditions, *laz* mutant hardly grew. This is linked with nitrite not being utilized to support growth when oxygen becomes limited. However, in some occasions it was found that *laz* mutant can grow following an extended lag phase and the level of nitrite was also decreased. Initially, it was proposed that *laz* mutant has decreased ability to reduce nitrite but this is not the case. Under microaerobic conditions conditions, *laz* mutant can reduce nitrite and generate nitric oxide at the rate faster than WT. The interruption of *laz* gene might have polar effect on the other gene(s) nearby, such as NMB1532 which is predicted to encode for hemerythrin. The function of this di-iron protein is unknown in this organism but in *Ralstonia eutropa* two hemerythrins domains are found in NorA protein which can bind nitric oxide and possibly act as a regulator of response to nitric oxide (Büsch *et al*, 2005 and Strube *et al*, 2007). Complementation of *laz* gene or deletion of hemerythrin should be undertaken to provide more understanding. In *laz* mutant, the response to nitric oxide might be disrupted and result in the decrease in removal of nitric oxide. However, in some occasions, *laz* mutant possibly overcome nitric oxide toxicity and strive to grow.

Interestingly, *laz* mutant exhibited cytochrome spectra different from WT and other cytochrome mutants upon cell oxidation by oxygen. When oxidized by oxygen, the absorption at Soret peak was not shifted to shorter wavelengths. It might be possible that the absence of Laz protein prevent oxidation of some cytochrome(s) by oxygen.

Laz might actually interact with some cytochromes during aerobic respiration. The spectra of *laz* mutant upon oxidation by hydrogen peroxide was similar to that of WT. It exhibited α peak at 555 nm. It is not known whether this is the absorption by cytochrome *c5*. The spectra did not provide relevant evidence regarding the role of Laz in response to hydrogen peroxide. Laz protein itself can not be oxidized directly by hydrogen peroxide. Recently it has been reported that *laz* mutant is more sensitive to hydrogen peroxide killing (Wu *et al*, 2005). However, the mechanism by which Laz involvement in resistance to hydrogen peroxide is not known.

Laz has been shown to be associated with outer membrane by determination of Laz amount in cell fractions. There is no definite evidence whether Laz is exposed in periplasm but the spectra of *laz* mutant might suggest that Laz can interact with cytochrome(s). Based on the slow rate of oxygen reduction and nitrite reduction and the characterization of *laz* mutant, it is clear that Laz does not play any crucial roles in respiration and growth of the meningococcus.

Chapter 8

General Discussion and Conclusions

From data generated in this work, it is proposed that cytochrome *c4* and cytochrome *c2* are major electron donors to *cbb*₃ oxidase while cytochrome *c5* is a major electron donor to AniA nitrite reductase. However, cytochrome *c5* may also be an electron donor to *cbb*₃ but to a lesser extent. Laz is proposed to be an electron donor to both *cbb*₃ oxidase and AniA nitrite reductase. New proposed electron transport chains in *N. meningitidis* is shown in Figure 8.1.

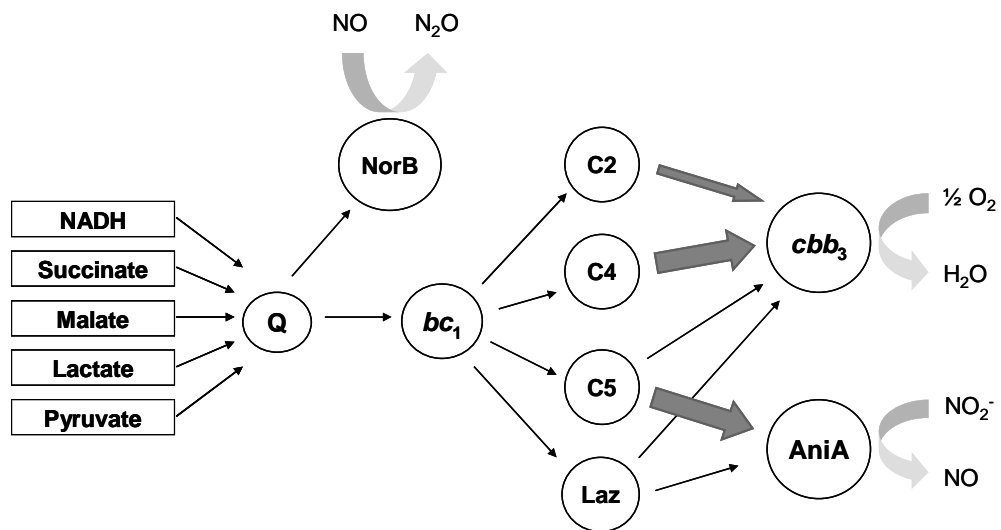


Figure 8.1 New proposed electron transport chains in *N. meningitidis*.

N. meningitidis is a microaerophilic bacterium that can utilize oxygen, nitrite, and nitric oxide as terminal electron acceptors in respiratory chains. Genome analysis revealed that there is a large number of proteins involved in electron transport and respiration. This work provided some evidence regarding the organization of the respiratory chains in this organism. The genome of *N. meningitidis* contains only *c*-type and *b*-type cytochromes. The spectroscopic studies of intact cells provided evidence to

support this prediction. Oxidation of intact cells by these respiratory substrates has shown spectral features corresponded to typical *c*-type and *b*-type cytochromes. Oxygen can predominantly oxidize *c*-type cytochromes while nitrite can predominantly oxidize *b*-type cytochrome(s), suggesting the involvement of certain cytochromes in specific branch of the respiratory chains. It is thought that the interplay between respiratory substrates may regulate respiration at metabolic level. From spectroscopic studies, nitrite has been shown to inhibit oxygen respiration directly as well as via the denitrification intermediate nitric oxide. It is likely that both nitric oxide and nitrite itself bind the cytochrome *cbb*₃ oxidase which is the only oxidase in this organism. In *Bradyrhizobium japonicum*, this cytochrome has been shown to have a very high affinity to oxygen. Interestingly, cytochrome oxidation by oxygen was only partially, but not completely, inhibited by nitrite and nitric oxide generated from nitrite reduction. This might suggest that under high level of oxygen, oxygen respiration still carry on despite the fact that the other two respiratory substrates are present and possess inhibitory power. It is not known whether the *cbb*₃ has higher affinity to oxygen than to nitric oxide. However, it is hypothesized that when the organism is exposed to different respiratory substrates simultaneously, it might favour oxygen respiration than the others. FNR-dependent activation of AniA nitrite reductase supports this notion as NarQ/P activation of AniA in the presence of nitrite depends on FNR (Rock *et al*, 2005). In this organism, nitrite will not be utilized if oxygen is not low enough. When oxygen becomes limited, AniA expression is activated by both FNR and NarQ/P leading to nitrite reduction for supporting growth. *N. meningitidis* possesses many periplasmic *c*-type cytochromes. This work provided some evidence regarding a role of these cytochromes in particular respiratory chains. The cytochrome *c4* and cytochrome *c2* are shown to be major electron donors to cytochrome *cbb*₃ oxidase while the

cytochrome *c5* is a major electron donor to AniA nitrite reductase. However, it is thought that cytochrome *c5* is also an electron donor to *cbb₃* oxidase to a lesser extent. Cytochrome *c5* might play a role in electron transfer to *cbb₃* oxidase under depleted level of oxygen when cell becomes highly reduced. It is of interest to monitor the change in oxygen level and pH during aerobic growth of *N. meningitidis* in MHB and to determine whether this is related to changes in the utilization of carbon sources, such as amino acids. It is observed that the *c5* mutant and *laz* mutant exhibited similar growth defect at late log phase when cell density in liquid culture is high. Both cytochrome *c5* and Laz have low pI, 6.2 and 4.6 respectively while cytochrome *c2* and *c4* have high pI, 9.5 and 9.8 respectively. Under depleted level of oxygen, periplasmic pH might change. Under these circumstances cytochrome *c2* and *c4* might not function effectively in donating electrons to *cbb₃* oxidase while cytochrome *c5* and Laz may still function effectively. Hence, cytochrome *c5* and Laz might play a role in donating electrons to *cbb₃* oxidase under depleted oxygen level while cytochrome *c2* and *c4* play the same role under higher level of oxygen. Interestingly, FixP subunit of *cbb₃* oxidase also has low pI 6.1. The function of FixP is unknown as the CcoNO subcomplex purified from *B. japonicum* (Zufferey *et al*, 1996) and *P. denitrificans* (de Gier *et al*, 1996) are catalytically active in oxygen reduction. It is not known under what circumstances FixP or CcoP is required for respiration. It might be possible that FixP plays a role in accepting electrons from cytochrome *c5* and Laz while FixO accepts electrons from cytochrome *c2* and *c4*. Cytochrome *c5* shares high identity with a truncated haem domain protein sequence from a pseudogene (NMB 1722) downstream of *fixP* gene. This truncated haem protein used to be a part of FixP but it was terminated during microevolution. This haem domain is still attached to the gonococcus CcoP, counterpart of the meningococcus FixP. This truncated haem protein shows very high identity

(75%) to the second haem domain of cytochrome *c5* (Figure 1.12 in Chapter 1). It might be possible that the second haem domain of cytochrome *c5* can bind FixP and transfer electrons to FixP similarly to that the third haem domain of CcoP transfers electrons to another haem center within its molecule.

It is hypothesized that *N. meningitidis* has evolved to live a microaerophilic lifestyle in human nasopharynx. It contains a cytochrome *cbb₃* oxidase which exhibits high affinity to oxygen. This gives them the ability to utilize a wide range of physiological oxygen.

The diversity of cytochromes with different biophysical properties might give the organism flexibility to maintain aerobic respiration under a wide range of physiological oxygen. This work showed that the expression of cytochromes were constitutive under aerobic and microaerobic conditions. Expression of the meningococcus cytochromes are not affected by level of oxygen. Maybe because the meningococcus adapts to live in a habitat where the level of oxygen and nitrite fluctuate often, the organism might exploit the difference in biophysical properties of cytochromes to gain quick response to maintain aerobic respiration to changing level of oxygen. This flexibility in aerobic respiration is regulated at metabolic level rather than at the level of cytochrome gene expression. Once the oxygen becomes limited, the organism activates AniA nitrite reductase and starts reducing nitrite. It was shown that cytochrome *c5* is an important electron donor to AniA nitrite reductase. The *c5* mutant has decreased ability to utilize nitrite to support growth and can not generate nitric oxide in the presence of nitrite. It will be of interest to reconstitute interaction between cytochrome *c5* and AniA nitrite reductase as part of future work on this system. The roles of NarQ/P and NsrR in regulation of cytochrome expression require further investigation. The expression of cytochromes in *narQ/P* mutant and in *nsrR* mutant

might provide evidence regarding the regulatory roles of these proteins. Currently, the effect of the meningococcus NarQ/P on cytochromes is still not known. Transcriptome analysis revealed that NsrR might not be involved in cytochrome expression (Heurlier *et al*, 2008-unpublished data). DNA microarray showed that NsrR only regulates a small set of genes, namely *norB* (encoding nitric oxide reductase), *dnrN* (encoding a protein putatively involved in repair of nitrosative damage to Fe-S cluster, *aniA* (encoding nitrite reductase), and *nirV* (encoding a putative nitrite reductase assembly protein). NsrR acts as a repressor in all case. NsrR does not seem to regulate cytochrome *c5* although this cytochrome is involved in electron transfer to AniA nitrite reductase.

References

- Bartolini E, Frigimelica E, Giovinazzi S, Galli G, Shaik Y, Genco C, Welsch JA, Granoff DM, Grandi G, Grifantini R (2006). Role of FNR and FNR-regulated, sugar fermentation genes in *Neisseria meningitidis* infection. *Molecular Microbiology* 60:963-972.
- Beaumont HJ, Lens SI, Reijnders WN, Westerhoff HV, van Spanning RJ (2004). Expression of nitrite reductase in *Nitrosomonas europaea* involves NsrR, a novel nitrite-sensitive transcription repressor. *Molecular Microbiology* 54:148-158.
- Bentley SD, Vernikos GS, Snyder LA, Churcher C, Arrowsmith C, Chillingworth T, Cronin A, Davis PH, Holroyd NE, Jagels K, Maddison M, Moule S, Rabinowitsch E, Sharp S, Unwin L, Whitehead S, Quail MA, Achtman M, Barrell B, Saunders NJ, Parkhill J (2007). Meningococcal genetic variation mechanisms viewed through comparative analysis of serogroup C strain FAM18. *PLoS Genetics* 3:e23.
- Berks BC, Ferguson SJ, Moir JWB and Richardson DJ (1995). Enzymes and associated electron transport systems that catalyse the respiratory reduction of nitrogen oxides and oxyanions. *Biochimica et Biophysica Acta – Bioenergetics* 1232: 97-173.
- Berry EA, Guergova-Kuras M, Huang LS, Crofts AR (2000). Structure and function of cytochrome *bc₁* complexes. *Annual Reviews of Biochemistry*. 69:1005-1075.
- Bhatnagar RK, Hendry AT, Shanmugam KT, Jensen RA (1989). The broad-specificity, membrane-bound lactate dehydrogenase of *Neisseria gonorrhoeae*: ties to aromatic metabolism. *Journal of General Microbiology* 135:353-360.
- Black JR, Black WJ, Cannon JG (1985). Neisserial antigen H.8 is immunogenic in patients with disseminated gonococcal and meningococcal infections. *Journal of Infectious Diseases* 151:650-657.

Blake RC 2nd , White KJ, Shute EA (1991). Effect of diverse anions on the electron-transfer reaction between iron and rusticyanin from *Thiobacillus ferrooxidans*. *Biochemistry* 30:9443-9449.

Bodenmiller DM and Spiro S (2006). The yjeB (nsrR) gene of *Escherichia coli* encodes a nitric oxide-sensitive transcriptional regulator. *Journal of Bacteriology* 188:874-881.

Bogdan JA, Minetti CA, Blake MS (2002). A one step method for genetic transformation of non-piliated *Neisseria meningitidis*. *Journal of Microbiological Methods* 49:97-101.

Bott M and Niebisch A (2003). The respiratory chain of *Corynebacterium glutamicum*. *Journal of Biotechnology* 104:129-153.

Boulangier MJ and Murphy ME (2002). Crystal structure of the soluble domain of the major anaerobically induced outer membrane protein (AniA) from pathogenic *Neisseria*: a new class of copper-containing nitrite reductases. *Journal of Molecular Biology* 315:1111-1127.

Bradford MM. (1976). A rapid and sensitive method for quantitation of microgram quantities of protein utilizing the principle of protein-dye-binding. *Analytical Biochemistry* 72:248-254.

Brittain T, Blackmore R, Greenwood C, Thomson AJ (1992). Bacterial nitrite-reducing enzymes. *European Journal of Biochemistry* 209:793-802.

Büsch A, Strube K, Friedrich B, Cramm R (2005). Transcriptional regulation of nitric oxide reduction in *Ralstonia eutropha* H16. *Biochemical Society Transactions* 33:193-194.

Cannon JG, Black W J, Nachamkin I, Stewart P W (1984). Monoclonal antibody that recognizes an outer membrane antigen common to the pathogenic *Neisseria* species but not to most nonpathogenic *Neisseria* species. *Infection and Immunity* 43(3): 994–999.

Cannon JG, Kawula TH, Spinola SM, Klapper DG (1987). Localization of a conserved epitope of an azurin-like domain in the H.8 protein of pathogenic *Neisseria*. *Molecular Microbiology* 1(2): 179-185.

Cannon JG (1989). Conserved lipoprotein of pathogenic *Neisseria* species bearing the H.8 epitope: lipid modified azurin and H.8 outer membrane protein. *Clinical Microbiology Reviews* 2:S1-S4.

Cannon JG, Woods JP, Dempsey JH, Kawula TH, Barritt DS (1989). Characterization of neisserial lipid-modified azurin bearing H.8 epitope. *Molecular Microbiology* 3: 583-591.

Carroll J, Fearnley IM, Shannon RJ, Hirst J, Walker JE (2003). Analysis of the subunit composition of complex I from bovine heart mitochondria. *Molecular and Cellular Proteomics* 2:117-126.

Castresana J, Lübben M, Saraste M (1995). New archaeobacterial genes coding for redox proteins: implications for the evolution of aerobic metabolism. *Journal of Molecular Biology* 250:202-210.

Castresana J (2001). Comparative genomics and bioenergetics. *Biochimica et Biophysica Acta* 1506:147-162.

Castresana J (2004). Chapter 1 Evolution of respiration. *Respiration in archaea and bacteria: diversity of prokaryotic electron transport carriers. Advance in Photosynthesis and Respiration* 15: 1-14.

Cecchini G, Schroder I, Gunsalus RP and Maklashina E (2002). Succinate dehydrogenase and fumarate reductase from *Escherichia coli*. *Biochimica et Biophysica Acta* 1553:140-157.

Cecchini G, Maklashina E, Yankovskaya V, Iverson TM and Iwata S (2003). Variation in proton donor/acceptor pathways in succinate:quinone oxidoreductases. *FEBS Letters*. 545:31-38.

Chen WP and Kuo TT (1993). A simple and rapid method for the preparation of gram-negative bacterial genomic DNA. *Nucleic Acids Research* 21: 2260.

Chiang RC, Cavicchioli R, Gunsalus RP (1997). 'Locked-on' and 'locked-off' signal transduction mutations in the periplasmic domain of the *Escherichia coli* NarQ and NarX sensors affect nitrate- and nitrite-dependent regulation by NarL and NarP. *Molecular Microbiology* 24:1049-1060.

Clark VL, Campbell LA, Palermo DA, Evans TM, Klimpel KW (1987). Induction and repression of outer membrane proteins by anaerobic growth of *Neisseria gonorrhoeae*. *Infection and Immunity* 55:1359-1364.

Cobley JG and Haddock BA (1975). The respiratory chain of *Thiobacillus ferrooxidans*: the reduction of cytochromes by Fe^{2+} and the preliminary characterization of rusticyanin a novel "blue" copper protein. *FEBS Letter* 60:29-33.

Constantinidou C, Hobman JL, Griffiths L, Patel MD, Penn CW, Cole JA, Overton TW (2006). A reassessment of the FNR regulon and transcriptomic analysis of the effects of nitrate, nitrite, NarXL, and NarQP as *Escherichia coli* K12 adapts from aerobic to anaerobic growth. *Journal of Biological Chemistry* 281:4802-4815.

Crack J, Green J, and Thomson AJ (2004). Mechanism of Oxygen Sensing by the Bacterial Transcription Factor Fumarate-Nitrate Reduction (FNR). *Journal of Biological Chemistry* 279: 9278-9286.

Cramm R, Pohlmann A, Friedrich B (1999). Purification and characterization of the single-component nitric oxide reductase from *Ralstonia eutropha* H16. *FEBS Letters* 460:6-10.

Crofts AR (2004). The cytochrome *bc₁* complex: function in the context of structure. *Annual Reviews of Physiology* 66:689-733.

Deeudom M, Rock J, Moir J (2006). Organization of the respiratory chain of *Neisseria meningitidis*. *Biochemical Society Transactions* 34:139-42.

Deghmane AE, Giorgini D, Larribe M, Alonso JM, Taha MK (2002). Down-regulation of pili and capsule of *Neisseria meningitidis* upon contact with epithelial cells is mediated by CrgA regulatory protein. *Molecular Microbiology* 43:1555-1564.

Devoe IW and Gilchrist JE (1973). Release of endotoxin in the form of cell wall blebs during in vitro growth of *Neisseria meningitidis*. *The Journal of Experimental Medicine*. 138:1156-1167.

Dinarieva T and Netrusov A (1989). Cupredoxins of obligate methylotroph. *FEBS Letters* 259:47-49.

Dougherty JM and Roth RM (1986). Cerebral spinal fluid. *Emergency Medicine Clinics of North America* 4:281-297.

Dove JE, Yasukawa K, Tinsley CR, Nassif X (2003). Production of the signalling molecule, autoinducer-2, by *Neisseria meningitidis*: lack of evidence for a concerted transcriptional response. *Microbiology* 149:1859-1869.

Doyle RJ, Zhou L, Srisatjalak R, Justus DE (1998). On the origin of membrane vesicles in Gram-negative bacteria. *FEMS Microbiology* 163:223-228.

Elsen S, Swem LR, Swem DL, Bauer CE (2004). RegB/RegA, a highly conserved redox-responding global two-component regulatory system. *Microbiology and Molecular Biology Reviews* 68:263-279.

Erwin AL, Gotschlich EC (1996). Cloning of a *Neisseria meningitidis* gene for L-lactate dehydrogenase (L-LDH):evidence for a second meningococcal L-LDH with different regulation. *Journal of Bacteriology* 178:4807-4813.

Erwin AL and Gotschlich EC (1993). Oxidation of D-lactate and L-lactate by *Neisseria meningitidis*: purification and cloning of meningococcal D-lactate dehydrogenase. *Journal of Bacteriology* 175:6382-6391.

Exley RM, Goodwin L, Mowe E, Shaw J, Smith H, Read RC, Tang CM (2005a). *Neisseria meningitidis* lactate permease is required for nasopharyngeal colonization. *Infection and Immunity* 73:5762-5766.

Exley RM, Shaw J, Mowe E, Sun YH, West NP, Williamson M, Botto M, Smith H, Tang CM (2005b). Available carbon source influences the resistance of *Neisseria meningitidis* against complement. *Journal of Experimental Medicine* 201:1637-1645.

Ferguson SJ, Pearson IV, Page MD, van Spanning RJ (2003). A mutant of *Paracoccus denitrificans* with disrupted genes coding for cytochrome *c₅₅₀* and pseudoazurin establishes these two proteins as the in vivo electron donors to cytochrome *cd₁* nitrite reductase. *Journal of Bacteriology* 185:6308-6315.

Fink RC, Evans MR, Porwollik S, Vazquez-Torres A, Jones-Carson J, Troxell B, Libby SJ, McClelland M, Hassan HM (2007). FNR is a global regulator of virulence and anaerobic metabolism in *Salmonella enterica* serovar Typhimurium (ATCC 14028s). *Journal of Bacteriology* 189:2262-2273.

Fischer RS, Martin GC, Rao P, Jensen RA (1994). *Neisseria gonorrhoeae* possesses two nicotinamide adenine dinucleotide-independent lactate dehydrogenases. *FEMS Microbiology Letters* 115:39-44.

Frasch C and Pollard AJ (2001). Development of natural immunity to *Neisseria meningitidis*. *Vaccine* 19:1327-1346.

Frisk A, Ison CA, Lagergard T (1998). GroEL heat shock protein of *Haemophilus ducreyi*: association with cell surface and capacity to bind to eukaryotic cells. *Infection and Immunity*. 66:1252-1257.

Frosch M and Vogel U (1999). Mechanisms of neisserial serum resistance. *Molecular Microbiology* 32:1133-1139.

Garduno RA, Faulkner G, Trevors MA, Vats N, Hoffman PS (1998). Immunolocalization of Hsp60 in *Legionella pneumophila*. *Journal of Bacteriology* 180:505-513.

Garrity GM, Bell JA, Lilburn TG (2004). Taxonomic outline of prokaryotes. *Bergey's manual of systematic bacteriology*, Second edition, Release 5.0, Springer-Verlag, New York. Pages DOI:10.1007/bergeysoutline200405

Ge Y and Rikihisa Y (2007). Surface-Exposed Proteins of *Ehrlichia chaffeensis*. *Infection and Immunity* 75:3833-3841.

de Gier JW, Shepper M, Reijnders WN, van Dyck SJ, Slotboom DJ, Warne A, Saraste M, Krab K, Stouthamer AH, van Spanning RJ, van der Oost J (1996). Structural and functional analysis of *aa₃* -type and *cbb₃* -type cytochrome c oxidases of *Paracoccus denitrificans* reveals significant differences in proton-pump design. *Molecular Microbiology* 20:1247-1260.

Goodhew CF, Brown KR, and Pettigew GW (1986). Haem staining in gels, a useful tool in study of bacterial *c*-type cytochromes. *Biochimica et Biophysica Acta* 852:288-294.

Grainger DC, Aiba H, Hurd D, Browning DF, Busby SJ (2007). Transcription factor distribution in *Escherichia coli*: studies with FNR protein. *Nucleic Acids Research* 35:269-278.

Gray KA, Grooms M, Myllykallio H, Moomaw C, Slaughter C, Daldal F (1994). *Rhodobacter capsulatus* contains a novel *cb*-type cytochrome *c* oxidase without a CuA center. *Biochemistry* 33:3120-3127.

Haehnel W, Jansen T, Gause K, Klösgen RB, Stahl B, Michl D, Huvermann B, Karas M, Herrmann RG (1994). Electron transfer from plastocyanin to photosystem I. *EMBO Journal* 13:1028-1238.

Hasegawa N, Arai H, Igarashi Y (2003). Need for cytochrome *bc₁* complex for dissimilatory nitrite reduction of *Pseudomonas aeruginosa*. *Bioscience, Biotechnology and Biochemistry* 67:121-126.

Hendriks J, Oubrie A, Castresana J, Urbani A, Gemeinhardt S, Saraste M (2000). Nitric oxide reductases in bacteria. *Biochimica et Biophysica Acta* 1459:266-273.

Hendry AT, Bhatnagar RK, Shanmugam KT, Jensen RA (1990). Exploitation of the broad specificity of the membrane-bound isoenzyme of lactate dehydrogenase for direct selection of null mutants in *Neisseria gonorrhoeae*. *Journal of General Microbiology*. 136:45-50.

Hennequin C, Porcheray F, Waligora-Dupriet A, Collignon A, Barc M, Bourlioux P, and Karjalainen T (2001). GroEL (Hsp60) of *Clostridium difficile* is involved in cell adherence. *Microbiology* 147:87-96.

Hippler M, Reichert J, Sutter M, Zak E, Altschmied L, Schröer U, Herrmann RG, Haehnel W (1996). The plastocyanin binding domain of photosystem I. *EMBO Journal* 15:6374-6384.

Hirst J (2003). The dichotomy of complex I: A sodium ion pump or a proton pump. *Proceedings of the National Academy of Sciences of the United States of America*. 100:773-775.

Huesca M, Borgia S, Hoffman P, Lingwood CA (1996). Acidic pH changes receptor binding specificity of *Helicobacter pylori*: a binary adhesion model in which surface heat shock (stress) proteins mediate sulfatide recognition in gastric colonization. *Infection and Immunity* 64:2643-2648.

Huston WM, Lowe EC, Butler CS, Moir JW (2005). Purification and characterization of cytochrome *c'* from *Neisseria meningitidis*. *Biochemical Society Transactions* 33:187-189.

Huber H, William T, Huber D, Trincone A, Burggraf S, Konig H, Rachel R, Rockinger I, Fricke H, and Stetter KO (1992). *Aquifex pyrophilus*gen nov.sp.nov., represents a novel group of marine hyperthermic hydrogen-oxidizing bacteria. *Systematic and Applied Microbiology* 15:340-351.

Hutchesson A, Preece MA, Gray G, Green A (1997). Measurement of lactate in cerebrospinal fluid in investigation of inherited metabolic disease. *Clinical Chemistry* 43:158-161.

Imrey PB, Jackson LA, Ludwinski PH, England AC 3rd, Fella GA, Fox BC, Isdale LB, Reeves MW, Wenger JD (1996). Outbreak of serogroup C meningococcal disease associated with campus bar patronage. *American Journal of Epidemiology* 143:624-630.

Imrey PB, Jackson LA, Ludwinski PH, England AC 3rd, Fella GA, Fox BC, Isdale LB, Reeves MW, Wenger JD (1995). Meningococcal carriage, alcohol consumption, and campus bar patronage in a serogroup C meningococcal disease outbreak. *Journal of Clinical Microbiology* 33:3133-3137.

IngledeW WJ and Poole RK (1984). The respiratory chains of *Escherichia coli*. *Microbiological Reviews* 48:222-271.

Johnston M, Zakharov A, Papaiconomou C, Salmasi G, Armstrong D (2004). Evidence of connections between cerebrospinal fluid and nasal lymphatic vessels in humans, non-human primates and other mammalian species. *Cerebrospinal Fluid Research* 1:2.

Jones CW, Poole RK (1985). The analysis of cytochromes. *Methods in Microbiology*. 18:285-328.

Jünemann S (1997). Cytochrome *bd* terminal oxidase. *Biochimica et Biophysica Acta* 1321:107-127.

Jyssum K (1962). Dissimilation of C¹⁴ labelled glucose by *Neisseria meningitidis*. The incorporation of 1-C¹⁴ and 6-C¹⁴ into pyruvate. *Acta Pathologica, Microbiologica, et Immunologica Scandinavica* 55:335-341.

Keilin D and Hartree EF (1939). Cytochrome and cytochrome oxidase. Proceedings of the Royal Society of London. Series B, Biological Sciences 127:167-191.

Kiley PJ and Beinert H (1998). Oxygen sensing by the global regulator, FNR: the role of the iron-sulfur cluster. FEMS Microbiology Reviews 22:341-352.

Komorowski RA , Farmer SG, Hannson GA, Hause LL (1978). Cerebrospinal Fluid Lactic Acid in Diagnosis of Meningitis. Journal of Clinical Microbiology 8:89-92.

Kukimoto M, Nishiyama M, Murphy ME, Turley S, Adman ET, Horinouchi S, Beppu T (1994). X-ray structure and site-directed mutagenesis of a nitrite reductase from *Alcaligenes faecalis* S-6: roles of two copper atoms in nitrite reduction. Biochemistry 33:5246-5252.

Lappann M, Haagensen JA, Claus H, Vogel U, Molin S (2006). Meningococcal biofilm formation: structure, development and phenotypes in a standardized continuous flow system. Molecular Microbiology 62:1292-1309.

Larson DW, Devine LF, and Larson GL (1968). Identification of *Neisseria meningitidis* carbohydrate fermentation patterns in Mueller-Hinton broth. Journal of Bacteriology. 96:563.

Lazazzera BA, Bates DM, Kiley PJ (1993). The activity of the *Escherichia coli* transcription factor FNR is regulated by a change in oligomeric state. Genes and Development 7:1993-2005.

Lindquist L, Linné T, Hansson LO, Kalin M, Axelsson G (1988). Value of cerebrospinal fluid analysis in the differential diagnosis of meningitis: a study in 710 patients with suspected central nervous system infection. European Journal of Clinical Microbiology and Infectious Disease 7:374-380.

Lissenden S, Mohan S, Overton T, Regan T, Crooke H, Cardinale JA, Householder TC, Adams P, O'Conner CD, Clark VL, Smith H, Cole JA (2000). Identification of

transcription activators that regulate gonococcal adaptation from aerobic to anaerobic or oxygen-limited growth. *Molecular Microbiology* 37:839-855.

Ludwig RA (2004). Microaerophilic bacteria transduce energy via oxidative metabolic gearing. *Research in Microbiology* 155:61-70.

Madigan MT and Martinko JM (2006). *Brock Biology of Microorganism*. Eleventh Edition. Pearson Prentice Hall. Upper Saddle River, New Jersey, p992.

Martin WJ (1983). Rapid and reliable techniques for the laboratory detection of bacterial meningitis. *American Journal of Medicine* 75:119-23.

McGuinness BT, Clarke IN, Lambden PR, Barlow AK, Poolman JT, Jones DM, Heckels JE (1991). Point mutation in meningococcal *porA* gene associated with increased endemic disease. *Lancet* 337:514-517.

Mesa S, Hennecke H, Fischer HM (2006). A multitude of CRP/FNR-like transcription proteins in *Bradyrhizobium japonicum*. *Biochemical Society Transactions* 34:156-159.

Minarik P, Tomaskova N, Kollarova M, Antalík M (2002). Malate dehydrogenases-structure and function. *General Physiology and Biophysics* 21:257-265.

Molenaar D, van der Rest ME, Petrovic S (1998). Biochemical and genetic characterization of the membrane-associated malate dehydrogenase (acceptor) from *Corynebacterium glutamicum*. *European Journal of Biochemistry* 254:395-403.

Morse SA, Stein S, Hines J (1974). Glucose metabolism in *Neisseria gonorrhoeae*. *Journal of Bacteriology* 120:702-714.

Muresanu L, Pristovsek P, Löhr F, Maneg O, Mukrasch MD, Rüterjans H, Ludwig B, Lücke C (2006). The electron transfer complex between cytochrome *c*₅₅₂ and the CuA domain of the *Thermus thermophilus* *ba*₃ oxidase. A combined NMR and computational approach. *Journal of Biological Chemistry* 281:14503-14513.

Murphy ME, Lindley PF, Adman ET (1997). Structural comparison of cupredoxin domains: domain recycling to construct proteins with novel functions. *Protein Science* 6:761-770.

Murphy LM, Dodd FE, Yousafzai FK, Eady RR, Hasnain SS (2002). Electron donation between copper containing nitrite reductases and cupredoxins: the nature of protein-protein interaction in complex formation. *Journal of Molecular Biology* 315:859-871.

Muto M, Hitomi Y, Ohtsu A, Shimada H, Kashiwase Y, Sasaki H, Yoshida S, Esumi H (2000). Acetaldehyde production by non-pathogenic *Neisseria* in human oral microflora: implications for carcinogenesis in upper aerodigestive tract. *International Journal of Cancer* 88:342-350.

Nakano MM, Geng H, Nakano S, Kobayashi K (2006). The nitric oxide-responsive regulator NsrR controls ResDE-dependent gene expression. *Journal of Bacteriology* 188:5878-5887.

Neal KR, Nguyen-Van-Tam J, Monk P, O'Brien SJ, Stuart J, Ramsay M (1999). Invasive meningococcal disease among university undergraduates: association with universities providing relatively large amounts of catered hall accommodation. *Epidemiology and Infection* 122:351-357.

Neal KR, Nguyen-Van-Tam JS, Jeffrey N, Slack RC, Madeley RJ, Ait-Tahar K, Job K, Wale MC, Ala'Aldeen DA (2000). Changing carriage rate of *Neisseria meningitidis* among university students during the first week of term: cross sectional study. *British Medical Journal* 320:846-849.

Nicholas DJD and Nelson A (1957). *Methods in Enzymology* 3:981.

Ohmoto H (1996). Evidence in pre-2.2 Ga paleosols for the early evolution of atmospheric oxygen and terrestrial biota. *Geology* 24:1135-1138.

Otten MF, van der Oost J, Reijnders WN, Westerhoff HV, Ludwig B, Van Spanning RJ (2001). Cytochromes *c₅₅₀*, *c₅₅₂*, and *c₁* in the electron transport network of *Paracoccus*

denitrificans: redundant or subtly different in function? Journal of Bacteriology 183:7017-7026.

Overton TW, Whitehead R, Li Y, Snyder LA, Saunders NJ, Smith H, Cole JA (2006). Coordinated regulation of the *Neisseria gonorrhoeae* truncated denitrification pathway by the nitric oxide-sensitive repressor, NsrR, and nitrite-insensitive NarQ-NarP. Journal of Biological Chemistry 281:33115-33126.

Pantzar, M., S. Teneberg, and T. Lagergard (2006). Binding of *Haemophilus ducreyi* to carbohydrate receptors is mediated by the 58.5-kDa GroEL heat shock protein. Microbes and Infection 8:2452-2458.

Parkhill J, Achtman M, James KD, Bentley SD, Churcher C, Klee SR, Morelli G, Basham D, Brown D, Chillingworth T, Davies RM, Davis P, Devlin K, Feltwell T, Hamlin N, Holroyd S, Jagels K, Leather S, Moule S, Mungall K, Quail MA, Rajandream MA, Rutherford KM, Simmonds M, Skelton J, Whitehead S, Spratt BG, Barrell BG (2000). Complete DNA sequence of a serogroup A strain of *Neisseria meningitidis* Z2491. Nature 404:502-506.

Pearson IV, Page MD, van Spanning RJ, Ferguson SJ (2003). A mutant of *Paracoccus denitrificans* with disrupted genes coding for cytochrome *c₅₅₀* and pseudoazurin establishes these two proteins as the in vivo electron donors to cytochrome *cd₁* nitrite reductase. Journal of Bacteriology 185:6308-6315.

Poole RK and Ingledew WJ (1984). The respiratory chain of *Escherichia coli*. Microbiological Reviews 48: 221-271.

Preisig O, Anthamatten D, Hennecke H (1993). Genes for a microaerobically induced oxidase complex in *Bradyrhizobium japonicum* are essential for a nitrogen-fixing endosymbiosis. Proceedings of the National Academy of Sciences of the United States of America 90:3309-3313.

Preisig O, Zufferey R, Thony-Meyer L, Appleby CA, Hennecke H (1996a). A high-affinity *cbb₃* -type cytochrome oxidase terminates the symbiosis-specific respiratory chain of *Bradyrhizobium japonicum*. *Journal of Bacteriology* 178:1532-1538.

Preisig O, Zufferey R, Hennecke H. (1996b). The *Bradyrhizobium japonicum* fixGHIS genes are required for the formation of the high-affinity *cbb₃* -type cytochrome oxidase. *Archives of Microbiology* 165:297-305.

Prentki P and Krisch HM (1984). *In vitro* insertional mutagenesis with a selectable DNA fragment. *Gene* 29:303-313.

Que L Jr (1991). Oxygen activation at the diiron center of ribonucleotide reductase. *Science* 253:273-274.

Reysenbach AL and Shock E (2002). Merging genomes with geochemistry in hydrothermal ecosystems. *Science* 296:1077-1082.

Richardson DJ (2000). Bacterial respiration: a flexible process for a changing environment. *Microbiology* 146:551-571.

Rock JD, Mahnane MR, Anjum MF, Shaw JG, Read RC, Moir JW (2005). The pathogen *Neisseria meningitidis* requires oxygen, but supplements growth by denitrification. Nitrite, nitric oxide and oxygen control respiratory flux at genetic and metabolic levels. *Molecular Microbiology* 58:800-809.

Rock JD, Thomson MJ, Read RC, Moir JW (2007). Regulation of denitrification genes in *Neisseria meningitidis* by nitric oxide and the repressor NsrR. *Journal of Bacteriology* 189:1138-1144.

Sambrook J, Fritsch EF, Maniatis T (1989). *Molecular cloning: A laboratory manual*. Second edition. Cold spring harbor laboratory press. New York, USA.

Saraste M and Castresana J (1994). Cytochrome oxidase evolved by tinkering with denitrification enzymes. *FEBS Letters* 341:1-4.

Sarkola T, Iles MR, Kohlenberg-Mueller K, Eriksson CJ (2002). Ethanol, acetaldehyde, acetate, and lactate levels after alcohol intake in white men and women: effect of 4-methylpyrazole. *Alcoholism: Clinical and Experimental Research* 26:239-245.

Sazanov LA and Hinchliffe P (2006). Structure of the hydrophilic domain of respiratory complex I from *Thermus thermophilus*. *Science* 311:1430-1436.

Silvestrini MC, Falcinelli S, Ciabatti I, Cutruzzolà F, Brunori M (1994). *Pseudomonas aeruginosa* nitrite reductase (or cytochrome oxidase): an overview. *Biochimie* 76:641-654.

Spanos A, Harrell FE Jr, Durack DT. (1988) Differential diagnosis of acute meningitis. An analysis of the predictive value of initial observations. *Journal of the American Medical Association* 262:2700-2707.

Spinosa MR, Progida C, Tala A, Cogli L, Alifano P, Bucci C (2007). *Neisseria meningitidis* capsule is important for intracellular survival in human cells. *Infection and Immunity* 75:3594-3603.

Stephens DS and Farley MM (1991). Pathogenic events during infection of the human nasopharynx with *Neisseria meningitidis* and *Haemophilus influenzae*. *Reviews in Infectious Diseases* 13:22-33.

Steuber J, Gemperli AC, Dimroth P (2002). The respiratory complex I (NDH1) from *Klebsiella pneumoniae*, a sodium pump. *The Journal of Biological Chemistry* 277:33811-33817.

Stevanin TM, Moir JW, Read RC (2005). Nitric oxide detoxification systems enhance survival of *Neisseria meningitidis* in human macrophages and in nasopharyngeal mucosa. *Infection and Immunity* 73:3322-3329.

Stewart V (2003) Nitrate- and nitrite-responsive sensors NarX and NarQ of proteobacteria. *Biochemical Society Transactions* 31:1–10.

Stewart V, Chen LL, Hui-chung WHC (2003). Response to culture aeration mediated by the nitrate and nitrite sensor NarQ of *Escherichia coli* K-12. *Molecular Microbiology* 50:1391-1399.

Strube K, de Vries S, Cramm R (2007). Formation of a dinitrosyl iron complex by NorA, a nitric oxide-binding di-iron protein from *Ralstonia eutropha* H16. *Journal of Biological Chemistry* 282:20292-20300.

Sun F, Huo X, Zhai Y, Wang A, Xu J, Su D, Bartlam M and Rao Z (2005). Crystal Structure of Mitochondrial Respiratory Membrane Protein Complex II. *Cell* 121:1043-1057.

Sutton VR, Mettert EL, Beinert H, Kiley PJ (2004). Kinetic analysis of the oxidative conversion of the $[4\text{Fe-4S}]^{2+}$ cluster of FNR to a $[2\text{Fe-2S}]^{2+}$ Cluster. *Journal of Bacteriology* 186:8018-8025.

Tessier SL, Hitchcock PJ, Hayes SF, Mayer LW, Shafer WM (1985). Analyses of gonococcal H8 antigen. Surface location, inter- and intrastain electrophoretic heterogeneity, and unusual two-dimensional electrophoretic characteristics. *Journal of Experimental Medicine* 162:2017-2034.

Tetelin H, Saunders NJ, Heidelberg J, Jeffries AC, Nelson KE, Eisen JA, Ketchum KA, Hood DW, Peden JF, Dodson RJ, Nelson WC, Gwinn ML, DeBoy R, Peterson JD, Hickey EK, Haft DH, Salzberg SL, White O, Fleischmann RD, Dougherty BA, Mason T, Ciecko A, Parksey D, Blair E, Cittone H, Clark EB, Cotton MD, Utterback TR, Khouri H, Qin H, Vamathevan J, Gill J, Scarlato, Masignani D, Pizza M, Grandi G, Sun Li, Smith HO, Fraser CM, Moxon ER, Rappuoli R, and Venter JC (2000). Complete genome sequence of *Neisseria meningitidis* serogroup B strain MC58. *Science*. 287:1809-1815.

Thony-Meyer L, Beck C, Preisig O, Hennecke H. (1994). The *ccoNOQP* gene cluster codes for a *cb*-type cytochrome oxidase that functions in aerobic respiration of *Rhodobacter capsulatus*. *Molecular Microbiology* 14:705-716.

Tobari J and Harada Y (1981). Amicyanin—an electron acceptor of methylamine dehydrogenase. *Biochemical and Biophysical Research Communication* 101:502–508.

Toledo-Cuevas M, Barquera B, Gennis RB, Wikstrom M, Garcia-Horsman JA (1998). The *cbb₃* type cytochrome *c* oxidase from *Rhodobacter sphaeroides*, a proton-pumping heme-copper oxidase. *Biochimica et Biophysica Acta* 1365: 421-434.

Tunbridge AJ, Stevanin TM, Lee M, Marriott HM, Moir JW, Read RC, Dockrell DH (2006). Inhibition of macrophage apoptosis by *Neisseria meningitidis* requires nitric oxide detoxification mechanisms. *Infection and Immunity* 74:729-733.

Turner S, Reid E, Smith H, Cole J (2003). A novel cytochrome *c* peroxidase from *Neisseria gonorrhoeae*: a lipoprotein from a Gram-negative bacterium. *Biochemical Journal* 373:865-873.

Turner SM, Moir JWB, Griffiths L, Overton TW, Smith H, Cole JA (2005). Mutational and biochemical analysis of cytochrome *c'*, a nitric oxide-binding lipoprotein important for adaptation of *Neisseria gonorrhoeae* to oxygen-limited growth. *Biochemical Journal* 388:545–553.

Unkmeir A, Latsch K, Dietrich G, Wintermeyer E, Schinke B, Schwender S, Kim KS, Eigenthaler M, Frosch M (2002). Fibronectin mediates Opc-dependent internalization of *Neisseria meningitidis* in human brain microvascular endothelial cells. *Molecular Microbiology* 46:933-946.

Vanet A and Labigne A (1998). Evidence for specific secretion rather than autolysis in the release of some *Helicobacter pylori* proteins. *Infection and Immunity* 66:1023-1027.

Vargas C, McEwan AG, Downie JA (1993). Detection of *c*-type cytochromes using enhanced chemiluminescence. *Analytical Biochemistry* 209(2):323-326.

Vijgenboom E, Busch JE, Canters GW(1997). In vivo studies disprove an obligatory role of azurin in denitrification in *Pseudomonas aeruginosa* and show that *azu* expression is under control of RpoS and ANR. *Microbiology* 143 :2853-2863.

Virji M, Makepeace K, Ferguson DJ, Achtman M, Sarkari J, Moxon ER (1992). Expression of the Opc protein correlates with invasion of epithelial and endothelial cells by *Neisseria meningitidis*. *Molecular Microbiology* 6:2785-2795.

Virji M, makepeace K, Peak IRA, Ferguson DJP, Jennings MP (1995). Opc- and pilus-dependent interaction of meningococci with human endothelial cell: modulation by surface polysaccharides. *Molecular Microbiology* 18: 741-754.

de Vries FP, van Der Ende A, van Putten JP, Dankert J (1996). Invasion of primary nasopharyngeal epithelial cells by *Neisseria meningitidis* is controlled by phase variation of multiple surface antigens. *Infection and Immunity* 64:2998-3006.

de Vries S and Schröder I (2002). Comparison between the nitric oxide reductase family and its aerobic relatives, the cytochrome oxidases. *Biochemical Society Transactions* 30:662-667.

Watmough NJ and Pitcher RS (2004). The bacterial cytochrome *cbb₃* oxidases. *Biochimica et Biophysica Acta* 1655:388-399.

Weiss H, Friedrich T, Hofhaus G, Preis D (1991). The respiratory-chain NADH dehydrogenase (complex I) of mitochondria. *European Journal of Biochemistry* 197: 563–576.

Wellmer A, Prange J, Gerber J, Zysk G, Lange P, Michel U, Eiffert H, Nau R (2001). D- and L-lactate in rabbit and human bacterial meningitis. *Scandinavian Journal of Infectious Diseases* 33:909-913.

Whitehead RN, Overton TW, Snyder LA, McGowan SJ, Smith H, Cole JA, Saunders NJ (2007). The small FNR regulon of *Neisseria gonorrhoeae*: comparison with the larger *Escherichia coli* FNR regulon and interaction with the NarQ-NarP regulon. *BMC Genomics* 8:35.

Winzer K, Sun Y, Green A, Delory M, Blackley D, Hardie KR, Baldwin TJ, Tang CM. (2002). Role of *Neisseria meningitidis* luxS in cell-to-cell signaling and bacteremic infection. *Infection and Immunity* 70:2245–2248.

Woods JP, Aho EL, Barritt DS, Black JR, Connell TD, Kawula TH, Spinola SM and Cannon JG (1987). The H.8 antigen of pathogenic *Neisseria*. *Antonie Leeuwenhoek* 53: 533-536.

Yagi T (1991). Bacterial NADH-quinone oxidoreductase. *Journal of Bioenergetics and Biomembrane* 23:211-215.

Yazdankhah SP and Caugant DA (2004). *Neisseria meningitidis*: an overview of the carriage state. *Journal of Medical Microbiology* 53:821-832.

Yi K, Rasmussen AW, Gudlavalleti SK, Stephens DS, Stojiljkovic I (2004). Biofilm formation by *Neisseria meningitidis*. *Infection and Immunity* 72:6132-6138.

Yohannes E, Barnhart DM, Slonczewski JL (2004). pH-dependent catabolic protein expression during anaerobic growth of *Escherichia coli* K-12. *Journal of Bacteriology* 186:192-199.

Zigha A, Rosenfeld E, Schmitt P, Duport C (2007). The redox regulator Fnr is required for fermentative growth and enterotoxin synthesis in *Bacillus cereus* F4430/73. *Journal of Bacteriology* 189:2813-2824.

Zufferey R, Preisig O, Hennecke H, Thony-Meyer L (1996). Assembly and function of the cytochrome *cbb₃* oxidase subunits in *Bradyrhizobium japonicum*. *Journal of Biological Chemistry* 271:9114-9119.